



**HAL**  
open science

## **GANIL / SPIRAL - 2001-2007 - Achievements, Highlights and Perspectives**

F. Azaiez, D. Beaumel, Bertram Blank, W. Catford, F. Chautard, S. Galès,  
G. Gaubert, A. Görgen, S. Fortier, V. Lapoux, et al.

► **To cite this version:**

F. Azaiez, D. Beaumel, Bertram Blank, W. Catford, F. Chautard, et al.. GANIL / SPIRAL - 2001-2007 - Achievements, Highlights and Perspectives. [Research Report] GANIL. 2008, pp.1-225. in2p3-00336915

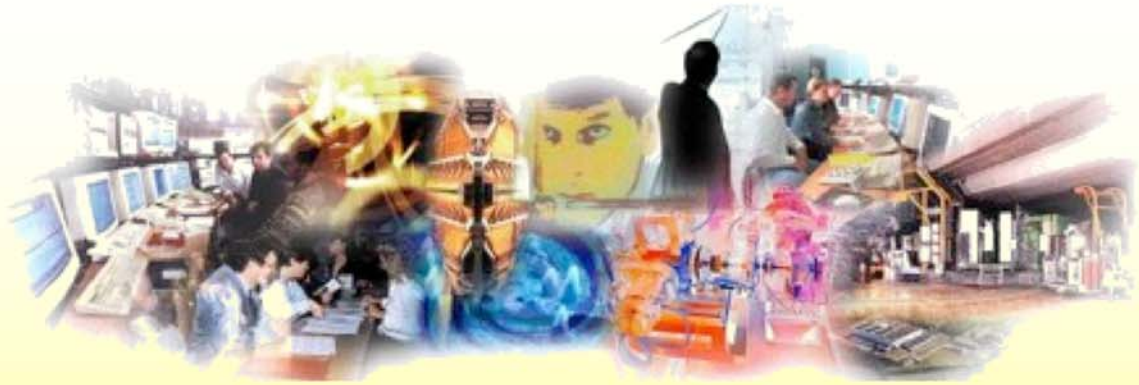
**HAL Id: in2p3-00336915**

**<https://hal.in2p3.fr/in2p3-00336915>**

Submitted on 5 Nov 2008

**HAL** is a multi-disciplinary open access archive for the deposit and dissemination of scientific research documents, whether they are published or not. The documents may come from teaching and research institutions in France or abroad, or from public or private research centers.

L'archive ouverte pluridisciplinaire **HAL**, est destinée au dépôt et à la diffusion de documents scientifiques de niveau recherche, publiés ou non, émanant des établissements d'enseignement et de recherche français ou étrangers, des laboratoires publics ou privés.



# **GANIL / SPIRAL**

## **2001-2007**

### **Achievements, Highlights and Perspectives**

Grand Accélérateur National d'Ions Lourds

**GANIL**  
Laboratoire commun CEA / DSM - CNRS / IN'P'

**GANIL R 08 01**



# Table of content

<b>Introduction - <i>S. Gales</i></b> .....	1
---	---

## **A. Topical review**

I. Production of exotic ions - <i>G. Gaubert</i> .....	7
II. Post acceleration and new lines - <i>F. Chautard</i> .....	17
III. Haloes and Clusters - <i>D. Beaumel</i> .....	27
IV. Magicity and Interactions: Transfer Reaction Spectroscopy at SPIRAL - <i>W. Catford</i> .....	41
V. Nuclear shapes and shape coexistence Gamma-ray spectroscopy at SPIRAL - <i>A. Görgen</i> .....	55
VI. Study of asymmetric nuclear matter at low energy - <i>O. Lopez</i> .....	69
VII. Astrophysics applications - <i>F. de Oliveira Santos</i> .....	77
VIII. Experiments at the LIRAT beam line of SPIRAL - <i>B. Blank</i> .....	85
IX. SPIRAL1 – Possible development strategies - <i>J.-C. Thomas</i> ....	97

## **B. Short description of SPIRAL experiments**

E342aS - Spectroscopic studies of $\beta$ -delayed multi-proton emission - <i>B. Blank et al.</i> .....	117
---	-----

E344aS - Shape coexistence near the N=Z line investigated by low-energy Coulomb excitation of secondary reaction products” and “Shape coexistence near the N=Z line and collective properties of Kr isotopes investigated by low-energy Coulomb excitation of radioactive ion beams emission - <i>A. Görgen et al.</i> .....	119
--	-----

E350aS - Isobaric analogue states of $^7\text{He}$ and $^9\text{He}$ - <i>W. Mittig et al.</i> .....	121
E400S - Study of $^{19}\text{Na}$ by Resonant Elastic Scattering - <i>F. de Oliveira Santos et al.</i> .....	127
E401S - Study of $^9\text{He}$ via the $d(^8\text{He},p)^9\text{He}$ reaction - <i>S. Fortier et al.</i> .....	131
E403S - Direct and compound reactions induced by unstable helium beams near the Coulomb barrier - <i>A. Navin et al.</i> .....	135
E403aS - Complete Reactions Studies with Borromean Nuclei near the Coulomb barrier - <i>A. Navin et al.</i> .....	139
E404aS - Identification of gamma rays in nuclei around the drip-line nucleus $^{130}\text{Sm}$ : probing the maximally deformed light rare- earth region - <i>P.J. Nolan et al.</i> .....	143
E405S - Structure of the exotic $^8\text{He}$ nucleus via the elastic and inelastic scattering on proton target - <i>V. Lapoux et al.</i> ...	147
E406S - Study of extremely neutron-rich light nuclei with a new technique - <i>H. Savajols et al.</i> .....	151
E408S - Competition between octupole and multi-particle excitations in $^{212}\text{Po}$ and $^{213}\text{At}$ - <i>P.M. Walker et al.</i> .....	159
E421S - Deep Inelastic collisions induced by neutron rich beams from SPIRAL and in beam gamma spectroscopy using EXOGRAM - <i>F. Azaiez et al.</i> .....	163
E422S, E465S - Study of the 4n system using the $^8\text{He}(d,^6\text{Li})$ transfer reaction - <i>D. Beaumel et al.</i> .....	165
E442S - Very High Resolution Spectroscopy of $^{19}\text{Ne}$ for Application to Astrophysics - <i>F. de Oliveira Santos et al.</i> .....	169
E443S - Study of $N = 16$ and the sd-fp shell gap far from stability - <i>A. Obertelli et al.</i> .....	173
E445S - Transfer Study of $^{23}\text{F}$ in Inverse Kinematics - <i>R.C. Lemmon et al.</i> .....	177

E456S	- Study of the N=28 shell closure via the $^{46}\text{Ar}(d,p)^{47}\text{Ar}$ reaction - <i>O. Sorlin et al.</i> .....	181
E473S	- Study of $^9\text{He}$ via the $d(^8\text{He},p)^9\text{He}$ reaction - <i>P. Roussel-Chomaz et al.</i> .....	185
E475S	- Isospin dependence in the emission of complex fragments from compound nuclei of mass=115 and N~Z - <i>J.-P. Wieleczko et al.</i> .....	189
E476aS	- Measurement of the $\beta$ - $\nu$ angular correlation coefficient in the $\beta$ decay of $^6\text{He}$ - <i>O. Naviliat-Cuncic et al.</i> .....	191
E493S	- Shell structure and shape coexistence in neutron-rich Ar isotopes - <i>A. Gorgen et al.</i> .....	195
E494S	- Level density parameter determination for different isotopes - <i>N. Le Neindre</i> .....	201
E498S	- High Spin States in the $T_z=-3/2$ Nucleus $^{37}\text{Ca}$ – Mirror Symmetry at the Largest Values of Isospin - <i>S.J. Williams et al.</i> .....	203
E512	- Laser Spectroscopic Determination of the $^8\text{He}$ Nuclear Charge Radius - <i>P. Mueller et al.</i> .....	205
E521S	- Measurement of $\text{H}(^{17}\text{Ne},p)^{17}\text{Ne}$ and $\text{H}(^{17}\text{Ne},3p)^{15}\text{O}$ reactions to study $^{18}\text{Na}$ , $^{17}\text{Ne}$ and $^{16}\text{F}$ - <i>F. de Oliveira Santos et al.</i> .....	209
E528S	- Study of the correlations in $^6\text{He}$ using nuclear break-up on $^{208}\text{Pb}$ - <i>J.-A. Scarpaci et al.</i> .....	211

## C. Publication list

I.	Experiment and theory.....	217
II.	Beam development.....	225



## Introduction

S. Gales\*

\* GANIL, CEA/DSM - CNRS/IN2P3, Bvd Henri Becquerel, BP 55027, F-14076 Caen Cedex 5, France

Contact: [gales@ganil.fr](mailto:gales@ganil.fr)

Since the early eighties, the intermediate energy ion beams of the GANIL facility and the associated equipments have played a pioneer role in the emergence of new fields in Nuclear Physics based on the production of exotic nuclei in unknown territories of the chart of nuclides. Fragmentation of high energy heavy ion beams on thin target, the so-called “in-flight” method, has allowed to create beams of “exotic” species with intensities ranging from a few to  $10^4$  pps. Associated to the LISE fragment separator the “in-flight” method has allowed the observation and measurements of mass and lifetime of very exotic nuclei in the light ( $A=4-40$ ) and medium ( $A=40-100$ ) mass regions. Additionally secondary reactions induced with these exotic fragments, such as Coulomb excitation and transfer, have been investigated. Such combination of intense heavy ion drivers at intermediate energy (50-1000 A.MeV) and powerful “fragment separators” have been then put into operation all around the world at MSU-NSCL, RIKEN, DUBNA and have produced a number of discoveries from “halo” nuclei like  $^{11}\text{Li}$  to drip-line nuclei  $^{24}\text{O}$ ,  $^{48}\text{Ni}$  and  $^{100}\text{Sn}$ .

Started a few decades before at the Niels Bohr institute (1957), another method to produce unstable species was employed. A beam of protons or light particles (d,He ) with energies ranging from 50 MeV to 2 GeV is stopped in thick heavy targets producing, by target fragmentation, fission or spallation a large number of exotic species. Target heating, effusion and diffusion with appropriate ion sources enable electrostatic extraction and acceleration up to few tenths of keV. A subsequent high-resolution mass spectrometer has been used to produce hundreds of new isotopes ranging from  $^{11}\text{Li}$  (few ms lifetime) to Fr isotopes. This ISOL technique or “thick target” method is well represented by the ISOLDE facility placed at the CERN accelerator complex.

In the beginning of the 90's, Louvain-La-Neuve was the first accelerator facility to introduce in the ISOL concept the so-called “two-step method”. A driver cyclotron was used to produce in a thick target light exotic beams of mainly noble gas (from He to Ne). After ionization and charge breeding in an ECR ion source, these species were injected and accelerated by a cyclotron, reaching energies of a few A.MeV in order to investigate reactions of astrophysical interest.

The origin of the ISOL-SPIRAL project is directly linked with the success of this new ISOL post-accelerated method to produce secondary Radioactive Ion Beams (RIB) at energies between 1 and 25 A.MeV, with excellent purity and optical quality, and intensities up to  $10^7$  pps.

The fundamental choices of the SPIRAL project were the following:

- The intense high energy heavy ion beams at GANIL associated to completely equipped experimental areas have established the facility as one of the leaders of “in-flight” facilities in the world.

- The high-power heavy-ion driver and the strong expertise in ECR ion sources were employed to produce a rich variety of exotic beams ranging from  ${}^6,8\text{He}$  to neutron deficient Kr isotopes in a thick carbon-heated target.
- The high charge state values of the ions extracted from an ECR source were well adapted to the choice of a cyclotron as a post-accelerator. The other advantage of the cyclotron, named CIME, is that it acts as a powerful mass separator, henceforth supplying rather pure beams of exotic nuclei.

The SPIRAL project has been officially approved by the French funding agencies, CEA, CNRS and the Region of Basse-Normandie, through an official financial agreement in October 1993. The first SPIRAL beam,  ${}^{18}\text{Ne}$ , was delivered in October 2001.

The present document reports on the SPIRAL science achievements since its beginning at the end of 2001. A few indicators, listed below and developed in the following sections of this report, assess the considerable success of the SPIRAL project at GANIL as well as the milestones and discoveries accomplished in less than six years. Up to 16 experiments have been achieved with He beams since 2001, establishing SPIRAL as the ISOL facility among those having the highest beam intensities worldwide for  ${}^6,8\text{He}$  isotopes. In addition more than 18 other experiments have been carried out with O, Ne, Ar, and Kr isotopes. 5000 hours of beam-time have been allocated with an efficiency of 85% (ratio of beam-time used by physicists to scheduled value).

The high reliability achieved over the years can be summarized as follows:” SPIRAL exotic beams are as “stable” as stable beams”. The life cycle of SPIRAL targets limited to 15 days until last year is now extended to much longer irradiation times. This in turn provides more beam time for users and reduces the operation cost of the facility and the produced nuclear waste.

Topics of physics investigated with the SPIRAL facility are rich in quality and variety. To give examples with post-accelerated beams, the search of neutron clusters, the study of “halo” nuclei, of fusion and transfer reactions with very neutron-rich beams, the discovery of super heavy  ${}^7\text{H}$ , the proof of shell gap weakening around magic neutron numbers  $N=20$  and  $28$ , the evolution of the spin-orbit splitting, the shape coexistence in the neutron-deficient Kr isotopes, the level densities measurements using  $N/Z$  dependence of evaporation residues associated to stringent tests of statistical model, the astrophysical reaction rates related with the physics of X-rays bursts or novae, are the main themes of physics where the SPIRAL facility has brought significant achievements.

In addition the low-energy LIRAT beam line has been built. Associated to a Paul trap the beta-neutrino angular correlation in the decay of  ${}^6\text{He}$  is being investigated.

All these results were obtained only because of a strong instrumentation program corresponding to the construction or adaptation of innovative and competitive spectrometers and detectors like the Si-strip arrays MUST2 and TIARA for light charged particles, INDRA for evaporation residues, the gamma array EXOGAM, the MAYA “3D” target-detector chamber, and the VAMOS, SPEG and LISE magnetic spectrometers. The combination of very efficient particle and/or gamma ray detectors, with the different spectrometers available at GANIL for recoil identification, was key ingredients in the success of SPIRAL experiments.

Since 2001 more than 30 publications on beam developments of SPIRAL have been released whereas the results of the SPIRAL experimental physics program have led to about 60 publications in refereed journals during the last six years. With such convincing results, the GANIL scientific council with the help of GANIL experts has developed since mid 2006 a strategy for the developments of SPIRAL beams at GANIL for the period 2007-2012, before the start of the new SPIRAL2 facility. This strategy has to take into account the limited manpower caused by the preparation of the upcoming major long term project SPIRAL2. It therefore concentrates for the moment on two mid-term projects:

- The developments of new radioactive beams using an alkali ion source (surface ionization) will provide new beams, extending the physics potential of SPIRAL. This ongoing project is expected to produce new exotic beams in 2010.
- The increase of SPIRAL beam intensities with the development of a general purpose 3kW target in combination with a  $^{26}\text{Mg}$  primary beam to increase the production of neutron-rich O and Ne isotopes.

With these main characteristics, and until 2012-2013 with the start of the new SPIRAL2 facility, GANIL-SPIRAL is and will continue to be an outstanding facility in the field of nuclear structure and reactions induced by RIB using both "in flight" and ISOL methods, serving an international community of about 600 users who carry research at the frontier of present knowledge in fundamental and applied physics, stemming from fundamental subatomic physics to radiobiology.



## A. Topical review



# I. Production of exotic ions

G. Gaubert\*

\* GANIL, CEA/DSM - CNRS/IN2P3, Bvd Henri Becquerel, BP 55027, F-14076 Caen Cedex 5, France

Contact: [gabriel.gaubert@pantchnik.com](mailto:gabriel.gaubert@pantchnik.com)

## Abstract

The SPIRAL1 Target Ion Source (TIS) is based on a 10 GHz permanent magnet ECR ion source coupled with a projectile fragmentation graphite target. Thus this design is optimised for gas production. On the other hand, the stable beam intensities available from the beginning allowed us to work with a maximum of 2 kW power on targets. Seven radioactive elements are now offered with 36 isotopes.

The first SPIRAL radioactive ion beam produced was delivered in 2001. Improvements of this system have been done constantly to reach better stability and reliability.

At the same time, the increasing primary beam intensities achieved have made it possible to develop a 3 kW target for helium beams in 2005. Up to now, 16 exotic He experiments have been done with 14 TIS units; 18 other (O, Ne, Ar, Kr) experiments have been achieved with 11 TIS units. Statistics show a fairly good ratio of available beam time to scheduled beam time.

Concerning new beams, a direct  $1^+$  to  $n^+$  system is under development to provide multi-charged alkali elements. The  $1^+$  device gave some competitive production yields in May 2006 on the SIRa test bench. Today the  $1^+$  to  $n^+$  coupling is studied with stable Na. An exotic  $n^+$  experiment could be done at the middle of 2007 and a new TIS should be available the following year for SPIRAL.

In this contribution we describe the technical achievements, the state of the art and statistics about TIS in SPIRAL 1. More details are given in the second part concerning the production of alkali elements. We finish with other possible developments and their safety/security and technical implications.

## 1. Present set-up

### 1.1. Description

The SPIRAL 1 Target Ion Source (TIS) is based on a 10 GHz permanent magnet ECR (Electron Cyclotron Resonance) ion source called Nanogan-3, coupled with a thick projectile fragmentation graphite target (see Fig. 1).

The high-energy beam delivered by the GANIL cyclotrons interacts with this target, where all the reaction products are stopped. The target is thereby heated by the primary beam up to 2000°C. Such a temperature is a challenge for the target in terms of reliability and duration. This high temperature is a major parameter for atoms to diffuse out of the matrix. Anyway, if the primary beam power is not sufficient to reach this temperature, one can have additional ohmic heating through the axis or with an oven.

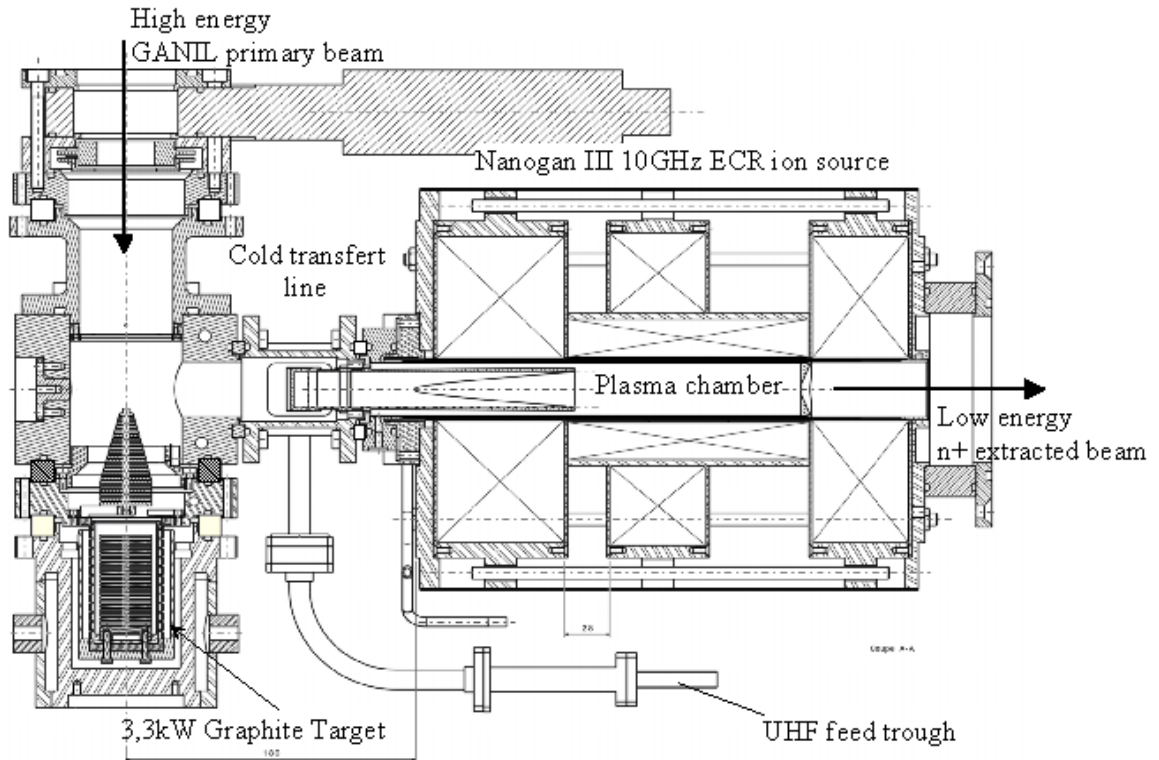
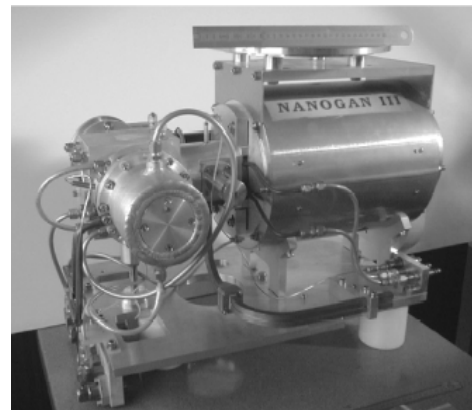


Figure 1: SPIRAL Target Ion Source system. The Nanogan-3 ion source and the target container are both mounted on a support plate, which can be remotely removed from the production cave.



After production and diffusion, the radioactive atoms effuse to the ion source through a cold transfer tube that makes a chemical selection, as the main part of the non-gaseous elements sticks on the walls of the tube. The atoms then enter into the ECR plasma chamber where they are ionised and then extracted to form the radioactive ion beam. The number of radioactive atoms created by this method depends on the primary beam intensity, and on the integrated fragmentation cross section. However the creation rate of nuclei of interest is always low, and the major problem of the method is to be as efficient as possible in order to maintain suitable

radioactive ion beam intensity. This means that the system of production of the radioactive ion beam has to take into account all the loss processes that can occur, like sticking on the walls, leaks, chemical reactions, etc. The production time, including diffusion out of the target, effusion, ionisation and confinement, has to be compatible with the lifetime of the nuclei of interest.

Concerning diffusion, different experiments permitted to determine the POCO 1 $\mu$ m grain size carbon graphite as the best grade for our targets. Today, two different kinds of targets are used to produce noble gases (see Fig. 2).

The first one presents a conical shape with respect to the primary beam power

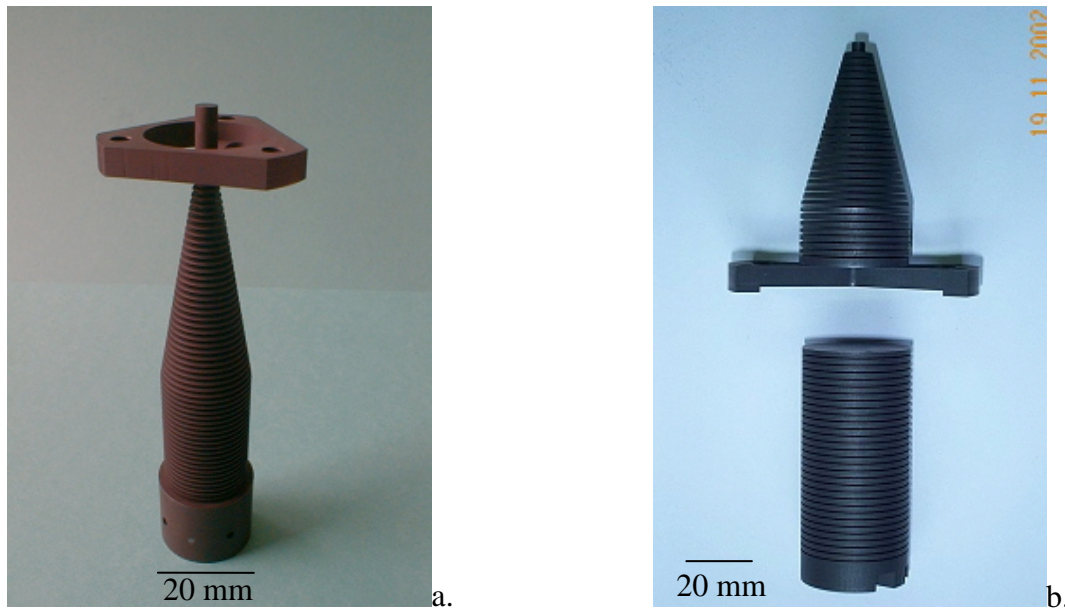


Figure 2: POCO 1 $\mu$ m grain size targets

a: production target in conical shape for Ne, Ar, Kr, N and O isotopes – max. of 1,5 kW  
b: production and diffusion target for He – max. 3 kW.

deposition and homogeneous temperature distribution. It is dedicated to produce Ne, Ar and Kr isotopes. Additional ohmic heating is possible by means of current trough the axis. This target is also suitable to produce O or N beams using the fact that those atoms can combine with the carbon and produce CO molecules that diffuse and effuse to the ion source.

The second one, divided in two parts because of the long range of He in carbon, is dedicated to  $^6\text{He}$  and  $^8\text{He}$ . The first part, the production target, induces fragmentation of the carbon primary beam and also the fragmentation of carbon atoms of the target. Helium produced by projectile fragmentation stops in the second part (called diffusion target) while the helium produced by target fragmentation stop in the production target. By this means, the production target is heated by the primary beam power while the diffusion target needs an additional ohmic heating to reach a suitable temperature for diffusion.

Talking about effusion, the mechanical design between the target chamber and the ion source is optimised to increase the gaseous conductance and to avoid losses especially with short live isotopes.

Finally, atoms of interest effuse to the Nanogan-3 ion source, which permits to produce multicharged ions. This 10 GHz ECR ion source, totally built with permanent magnets, produces ions with a charge state distribution (CSD) following the acceleration parameters of the CIME post-accelerator. For example, the Nanogan-3 CSD is optimised for  $\text{Ar}^{8+}$  ions with something like 10 to 15 % of particles in this charge state (see Fig. 3).

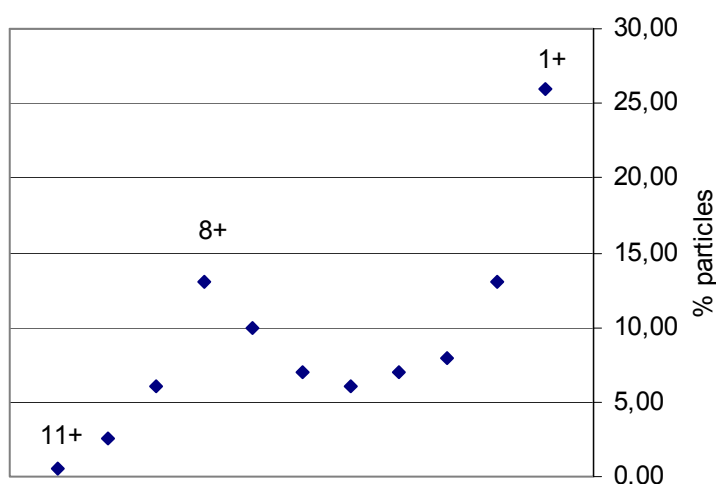


Figure 3: Argon CSD

Radiation risks, choice of materials and the reliability of the Target Ion Source system have been taken into account in the design of the production cave.

## 1.2. The life cycle of the TIS

The SPIRAL TIS is built at GANIL. Each Nanogan-3 ion source contains about 120 permanent magnets and up to now 18 ion sources have been constructed. The target in its chamber is connected to the ion source and both are mounted on the support plate, which allows the connections of all needed services in the production cave. Before irradiation, each TIS is tested on a dedicated bench. The continuity of connections is checked (vacuum, electrical and cooling feed-trough, etc.). The ion source performances are checked with stable gas, and the target is heated, thus insuring out-gassing. The remote-controlled unit manipulator withdraws the irradiated TIS after the last SPIRAL experiment (irradiation period of 15 days), and place the new TIS for the next one. One must store the irradiated TIS during 2 years in a lead container (or as far as the dose rate decreases to a convenient level) and then dismantle the target parts from the ion source in a dedicated glove box, in order to use once again the magnetic circuit which is more than 2/3 of the total TIS cost. A new target is then mounted with the “second-hand” ion source and support plate. All these operations constitute the life cycle of the TIS (see Fig. 4). They are managed and framed by a Quality Assurance system in order to guarantee traceability without fault of the irradiated sets.

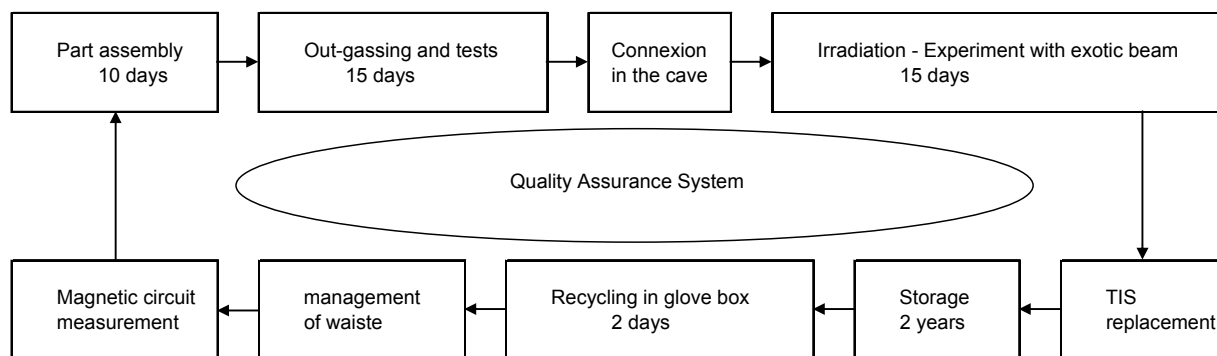


Figure 4: The life cycle of the TIS

## 2. Results of the first 5 years

### 2.1. Statistics and stability

The first SPIRAL beam was  $^{18}\text{Ne}$  in October 2001. Up to now, 16 He experiments have been done with 14 TIS units; 18 other (O, Ne, Ar and Kr) experiments have been achieved with 11 TIS. The intensities of all possible beams available at SPIRAL are updated in the GANIL web page<sup>1</sup> and the list of beams presently provided at SPIRAL is shown in Table 1.

Element	A											
Kr	72	73	74	75	76	77	79	81				
Ar	31	32	33	34	35	41	42	43	44	45	46	
Ne	17	18	19	23	24	25	26	27				
F	18											
O	14	15	19	20	21	22						
Ne	13	16										
He	6	8										

Table1: List of presently available beams at SPIRAL

Up to now, a cumulative time of about 5000 hours of exotic beam on the target of the physicist is achieved. More than 700 hours of stable beam have also been produce with TIS. The average ratio between the total beam time scheduled and the beam time actually furnished to the experiment is about 85%. Three experiments could not be done due to breaking of the production system and two of them were already re-scheduled (see Fig. 5).

<sup>1</sup> [http://www.ganil.fr/operation/available\\_beams/radioactive\\_beams.htm](http://www.ganil.fr/operation/available_beams/radioactive_beams.htm)

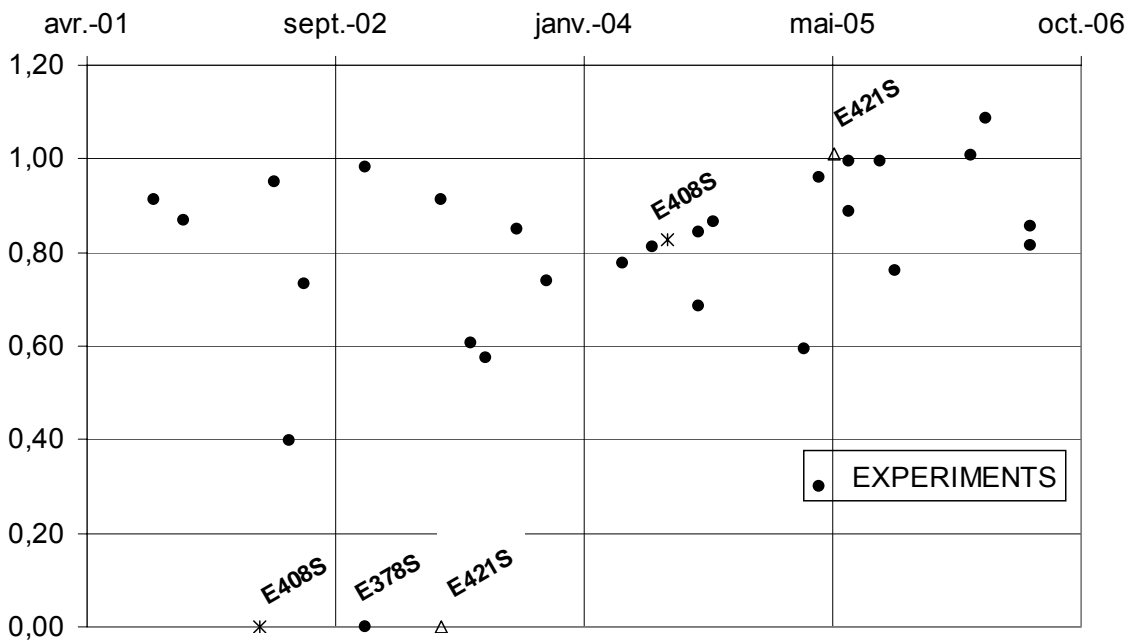


Figure 5: Ratio of available beam time to scheduled beam time

## 2.2. Improvements

The overall efficiency of the system varies with the lifetime of the isotope and the extraction voltage of the TIS.

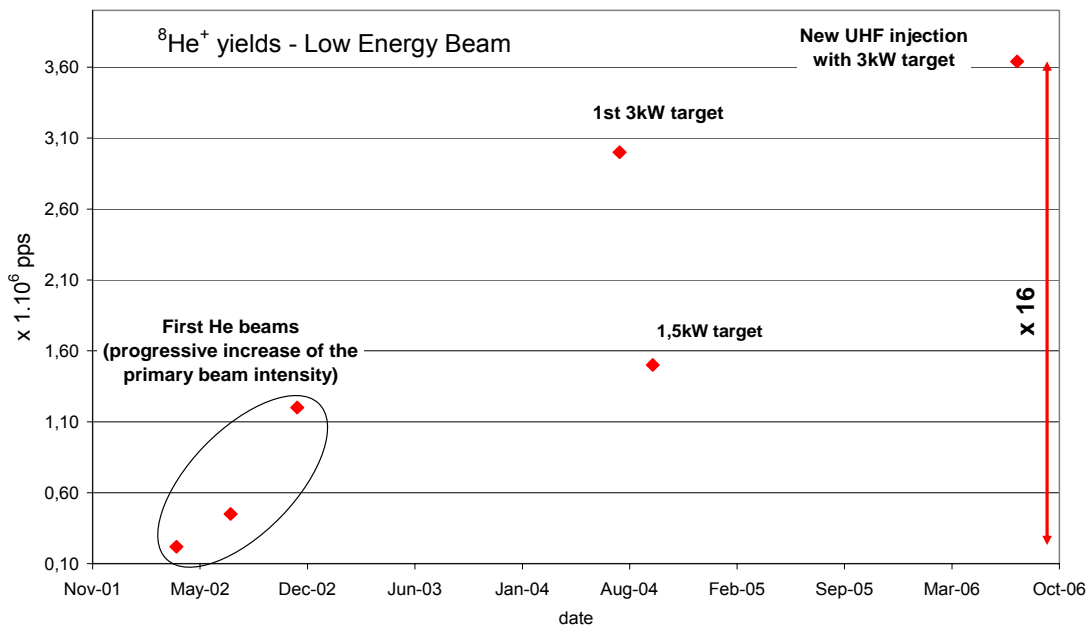


Figure 6: 2001 – 2006  $^8\text{He}^{1+}$  yields

From the beginning a lot of mechanical improvements of the system have been done. For example, the losses through the High-Energy Front-End of radioactive atom

by the pumping system have been reduced by the improvement of the first entrance tantalum window design and position. The UHF feed-trough has been changed from coaxial to direct injection system in order to improve and simplify the operation of the ion source. At the same time, the increasing primary beam intensities achieved have made it possible to develop a 3 kW target for helium beams. Figure 6, showing the  $^8\text{He}^{1+}$  yields obtained from 2001 to 2006, is a good illustration of all these improvements.

### **2.3. Neutron irradiation damages**

The Nanogan-3 ion sources associated to TIS N°1 to N°18 were totally built with brand new permanent magnets. TIS N°18 to 26 are built with second-hand magnetic circuits recycled from the first units. From the end of 2005, it appears that some He dedicated TIS units have been damaged by neutrons irradiation. Correlation between neutrons and damages is clear even if it is not easy to correlate the neutron doses to the demagnetisation level. In any case, the position of the target seems to be the most important criteria.

In the near future we will have to reconsider the cycle of life of the TIS. One must take into account this fact before further investigations for developments of new kind of targets or new TIS designs.

## **3. Possible developments**

As shown before, SPIRAL1 gets radioactive gas isotopes with efficient TIS. The other elements production developments were very limited during last years because of the activities related to the definition and the starting of the SPIRAL2 project. Concerning the production of new elements for SPIRAL1, a study is going on for the development of an exotic alkali ions production system.

### **3.1. The $1^+/n^+$ device for alkali elements: NanoNaKe**

The production principle is based on beam fragmentation on a graphite target. The target has approximately the same design as the previous one, for gaseous elements and compounds. The difference from the previous design is that a surface ionisation ion source is coupled directly to the target and serves for the production of  $1^+$  ions immediately after the radioactive atoms diffusion out of the target. After first ionisation, the  $1^+$  beam is accelerated and directed to the NANOGAN-3 ECRIS. The  $1^+$  beam is afterwards decelerated to very low energy (of the order of 5 eV) in order to be injected into the ECR plasma of the ECRIS. After that, the beam will be extracted as multi-charged ions from the ECRIS and conducted to CIME for further acceleration. In this process no heating of the transfer tube between the target container and the ion source, as well as the ion source chamber, is needed. Alkali elements are easily ionised by surface ionisation ion sources with excellent efficiencies.

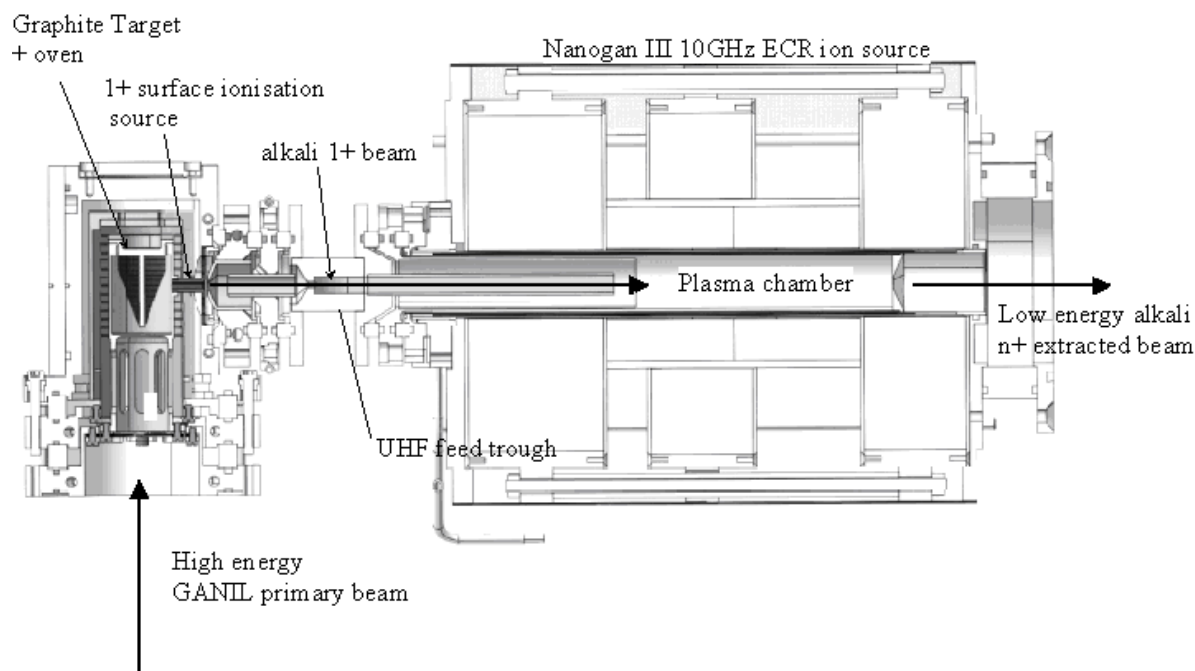


Figure 7: TIS for production of alkali at SPIRAL. In the left side a target is embedded in a surface ionisation ion source. The ECR ion source is Nanogan-3.

Preliminary tests of the surface ionisation ion source (the left part of Fig. 7) were performed at the SIRa test bench using a  $^{48}\text{Ca}$  primary beam at 60 A.MeV with an intensity of 70 pA. Table 2 presents the obtained yields as well as the overall efficiencies for Li, Na and K isotopes. The efficiencies obtained are in good agreement with estimated diffusion/effusion and ionisation performances using a carbon ioniser.

Beam	Lifetime (s)	Yields (pps)	Efficiency (%)
$^8\text{Li}$	0,84	$1.0 \cdot 10^6$	13
$^9\text{Li}$	0,18	$3,4 \cdot 10^4$	2,1
$^{25}\text{Na}$	59,1	$3.0 \cdot 10^7$	34
$^{26}\text{Na}$	1,07	$6,5 \cdot 10^6$	18
$^{27}\text{Na}$	0,3	$9,5 \cdot 10^5$	10
$^{29}\text{Al}$	394	$1,8 \cdot 10^6$	1,2
$^{37}\text{K}$	1,2	$7,5 \cdot 10^4$	31
$^{47}\text{K}$	17,5	$1,8 \cdot 10^8$	42

Table 2: Measured radioactive beam intensities for  $1^+$  alkali isotopes using a  $^{48}\text{Ca}$  primary beam at 60 A.MeV with intensities normalised to 0,14  $\mu\text{A}$  (400W).

Tests of the overall system, including injection and extraction of the beam out of Nanogan-3 are under progress with a stable element ( $^{23}\text{Na}$ ). We plan to perform an exotic experiment of this TIS in spring 2007.

Further investigations about neutron damages must be taken into account especially in this new design in which the target position is worst than with dedicated He TIS.

### **3.2. Other possible developments**

A large amount of possibilities about new beams or the increase of present exotic beam intensities have already been presented at the last GANIL colloquium (May-June 2006).

Most of them concern the development of new (size and materials) targets and/or the improvement of GANIL primary beams. That last item could be achieved by the improvement of the present ECR4 ion source intensities or by the implementation of the GTS ion source.

As shown before, alkali elements could be produced by the new direct  $1^+/n^+$  TIS called NanoNake.

Specific new  $1^+$  TIS could provide better intensities and/or condensable elements or short-lived isotopes.

On the other hand, one should study the possibility to develop a totally new radiation-hard ion source, taking into account the problem of the present TIS demagnetisation due to neutrons.

These developments will be discussed point-to-point and more in detail during this scientific council and the last contribution gives an exhaustive list of them, in order to be able to define a strategy of development.

### **3.3. Constrains**

The developments can lead to the multiplication of TIS units of different kinds. The impact on the management engineering of the TIS can be important and the planning of the SPIRAL beams will be more complicated.

In any case, it is obvious that a new TIS design, new materials and equipment certainly mean a modification of the SPIRAL cave, in some case a modification of the remote handling system, together with a safety report, and these changes will be subject to administrative authorisation.

## **4. Conclusion**

SPIRAL 1 provides more and more intense and stable beams. Five years of improvements of the TIS allowed to reach the present intensities. However, neutron

damages on Nanogan-3 ion sources change the life cycle of the TIS and this must be taken into account for further developments.

The development of a dedicated direct  $1^+/n^+$  TIS for alkali elements is already in progress. We plan to test its overall efficiency at the SIRa test bench in spring 2007. A new TIS could provide alkali beams for SPIRAL in 2008.

It is of course also possible to reach other elements and/or better intensities with present isotopes with some other developments: primary beam increase, other target materials or fast and efficient radiation-hard new TIS.

The modification of the cave, safety considerations and administrative authorisation must be taken into account.

Finally, because of the present stable beam and radioactive ion source operation, together with the large amount of commitments for SPIRAL2, it is clear that human resources is a major criterion if we want to go further with SPIRAL1 beam developments.

## II. Post acceleration and new lines

F. Chautard\*

\* GANIL, CEA/DSM - CNRS/IN2P3, Bvd Henri Becquerel, BP 55027, F-14076 Caen Cedex 5, France

Contact: [chautard@ganil.fr](mailto:chautard@ganil.fr)

### 1. Assessment the machine/SPIRAL operation

#### 1.1. GANIL operation

The first SPIRAL beam delivered to the physics was  $^{18}\text{Ne}$  in October 2001. Since, more than 30 radioactive beams were produced in 5000 h of SPIRAL operation over 12000 h of total operation of GANIL. SPIRAL also provided 700 h of stable beams to preset the experiments or for the development of detectors. The operation of the machine is distributed over 4 periods of approximately 8.5 weeks, separated by 4 periods from maintenance (16 weeks in total). Thus, in 2006, approximately 5700 h of operation was envisaged with physics with around 60% available for the physics experiments.

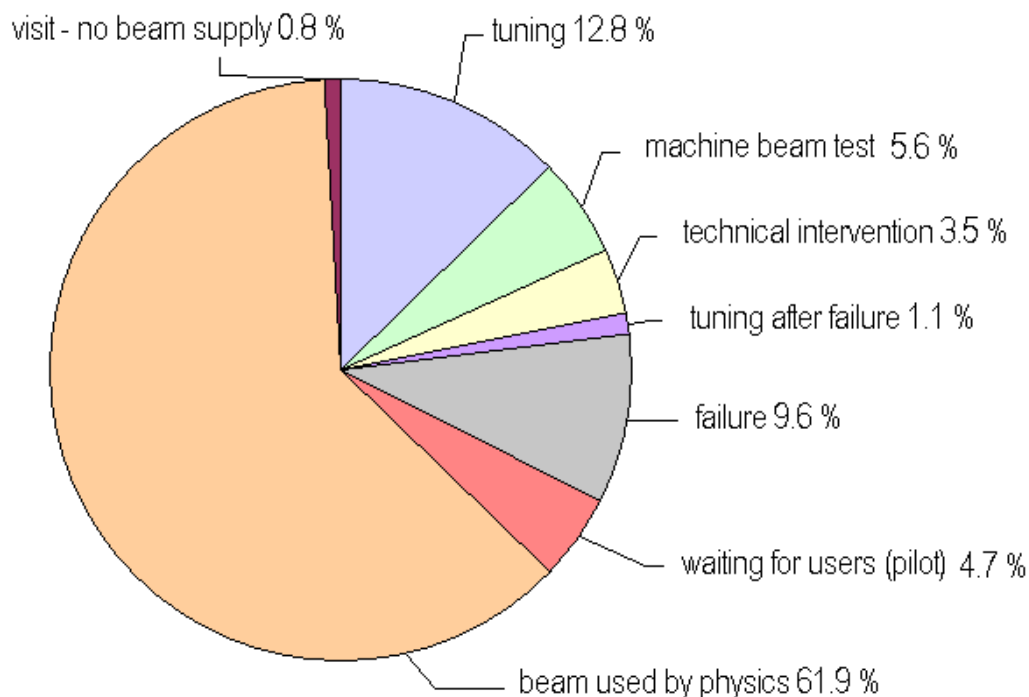


Figure 1: Cumulated statistics from 2001 to 2005.

The GANIL facility possesses a versatile combination of equipments, which permits the production of accelerated radioactive ion beams with two complementary methods: Isotope Separation On Line (SPIRAL) and In-Flight Separation techniques.

More than 10 beams are available at a power exceeding 1 kW (Table 1) (over 50 stable beams available from the GANIL sources)

([http://www.ganil.fr/operation/available\\_beams/available\\_beams\\_tabular.htm](http://www.ganil.fr/operation/available_beams/available_beams_tabular.htm)).

Beam	$I_{\max}$ [ $\mu\text{Ae}$ ]	[pps]	$E_{\max}$ [A.MeV]	$P_{\max}$ [W]	Used with Spiral
$^{12}\text{C}^{6+}$	18	$1.9 \cdot 10^{13}$	95	3 200	
$^{13}\text{C}^{6+}$	18	$2 \cdot 10^{13}$	80	3 000	X
$^{14}\text{N}^{7+}$	15	$1.4 \cdot 10^{13}$	95	3 000	
$^{16}\text{O}^{8+}$	16	$10^{13}$	95	3 000	X
$^{18}\text{O}^{8+}$	17	$10^{13}$	76	3 000	X
$^{20}\text{Ne}^{10+}$	17	$10^{13}$	95	3 000	X
$^{22}\text{Ne}^{10+}$	17	$10^{13}$	79	3 000	
$^{36}\text{S}^{16+}$	6.4	$2.5 \cdot 10^{12}$	77.5	1100	X
$^{36}\text{Ar}^{18+}$	16	$5.5 \cdot 10^{12}$	95	3 000	
$^{40}\text{Ar}^{18+}$	17	$6 \cdot 10^{12}$	77	3 000	
$^{48}\text{Ca}^{19+}$	4-5	$1.3 \cdot 10^{12}$	60	600-700	X
$^{58}\text{Ni}^{26+}$	5	$1.2 \cdot 10^{12}$	77	860	
$^{76}\text{Ge}^{30+}$	5	$1.2 \cdot 10^{12}$	60	760	
$^{78-86}\text{Kr}^{34+}$	7.5	$1.4 \cdot 10^{12}$	70	1200	X
$^{124}\text{Xe}^{46+}$	2	$2.7 \cdot 10^{11}$	53	300	

Table 1: Some of the GANIL highest stable beam intensities, the main limitation comes now from the target ability to sustain the high power density.

The beam losses detectors, beam transformers and control systems allow the transport of intense stable beams with power exceeding 3 kW in routine operation.

## 1.2. SPIRAL operation

In Fig. 2, the beam time repartition between GANIL and SPIRAL is shown from 2002. With an average of 3700 h of beam to the physics, the part of SPIRAL increased since 2002. In 2006, because of the unavailability of SISSI in 2005, a large number of experiments using this equipment were scheduled instead of SPIRAL experiments.

A list of the radioactive beams delivered is reported in Table 2: Radioactive beams produced from 2001 to 2006. Additionally, progress in the tuning time was observed (see Figure 3), from of about 20 % in the first years down to 7% today. This is mainly due to a better knowledge of the machine behaviour but also thank to the building of a parameter database in which initial theoretical figures are replaced by experimental figures.

([http://www.ganil.fr/operation/available\\_beams/radioactive\\_beams.htm](http://www.ganil.fr/operation/available_beams/radioactive_beams.htm))

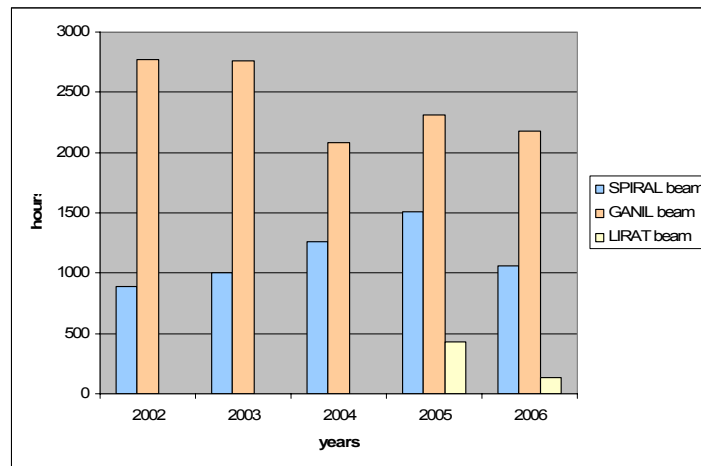


Figure 2: Beam time distribution between GANIL and SPIRAL from 2002 to 2006.

Ion	W [A.MeV]	[pps]	Year	Ion	W [A.MeV]	[pps]	Year
$^{18}\text{Ne}$	7	$10^6$	2001	$^{31}\text{Ar}$	1.45	$1.10^5$	2004
$^8\text{He}$	15.5	$10^4$	2001	$^6\text{He}$	3.2, 5	$3.10^7$	2004
$^8\text{He}$	3.5	$10^5$	2002	$^8\text{He}$	15.4	$2.10^4$	2005
$^{24}\text{Ne}$	4.7	$2 \cdot 10^5$	2002	$^8\text{He}$	3.4-3.9	$8.10^4$	2005
$^{74}\text{Kr}$	4.6	$1.5 \cdot 10^4$	2002	$^8\text{He}$	3.5	$6.10^5$	2005
$^8\text{He}$	15.4	$1.5 \cdot 10^4$	2002	$^{18}\text{Ne}$	7	$10^6$	2005
$^8\text{He}$	15.4	$9 \cdot 10^3$	2002	$^{24}\text{Ne}$	4.7-10	$2.10^5$	2005
$^{24}\text{Ne}$	10	$2 \cdot 10^5$	2002	$^{26}\text{Ne}$	10	$3.10^3$	2005
$^8\text{He}$	15.4	$2.5 \cdot 10^4$	2002	$^{44}\text{Ar}$	10.8	$2.10^5$	2005
$^{15}\text{O}$	1.2	$1.7 \cdot 10^7$	2003	$^{46}\text{Ar}$	10.3	$2.10^4$	2005
$^{24}\text{Ne}$	7.9	$1.4 \cdot 10^5$	2003	$^{74}\text{Kr}$	2.6	$1.510^4$	2005
$^{33}\text{Ar}$	6.5	$3 \cdot 10^3$	2003	$^{76}\text{Kr}$	2.6-4.4	$6.10^5$	2005
$^6\text{He}$	3.8	$2.8 \cdot 10^7$	2003	$^{75}\text{Kr}$	5.5	$2 \cdot 10^5$	2005
$^8\text{He}$	15.4	$2.5 \cdot 10^4$	2003	$^{44}\text{Ar}$	2.6-3.8	$3 \cdot 10^5$	2006
$^{35}\text{Ar}$	0.428	$4 \cdot 10^7$	2004	$^6\text{He}^{2+}$	20	$5 \cdot 10^6$	2006
$^6\text{He}$	2.5	$3.7 \cdot 10^7$	2004	$^6\text{He}^{1+}$	LIRAT	$2 \cdot 10^8$	2006

Table 2: Radioactive beams produced from 2001 to 2006.

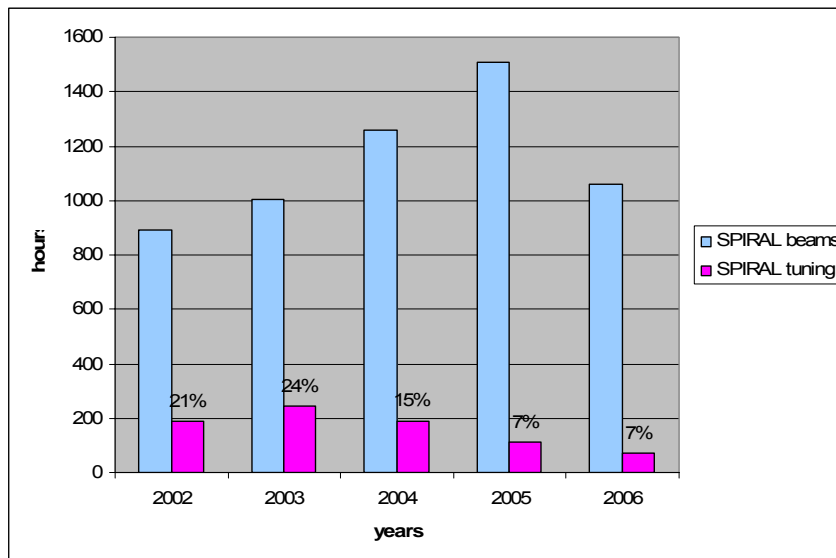


Figure 3: Distribution of the tuning time compared to the available SPIRAL beam time.

## 2. Developments

The Spiral strength can be described as follows:

- i) Large energy range of the post-accelerator: from 1.2 A.MeV to 16 A.MeV (for  $Q/A=0.25$ )
- ii) Mass purification of the cyclotron  $R = \text{few } 10^{-4}$
- iii) Good energy definition of the CIME beams  $\Delta E/E < 5 \cdot 10^{-3}$
- iv) Good transmission for such accelerator technology (20 % - 40 %)
- v) Great source selectivity + cyclotron purification giving a pure beam of most of the available ions
- vi) 40 isotopes available
- vii) Possibility to run detectors developments with stable beams of CIME in a standalone operation (users: LPC, groupe des aires experimentales)

But Spiral has also its limitations:

- i) Beam time limitation. A 15 days irradiation limit for each target-source ensemble
- ii) Still, few elements are available (He, O, N, Ne, Ar, Kr, F)
- iii) Intensity is a parameter of utmost importance; It is the main limitation for most of experiments.
- iv) The large turn number in CIME influence the Beam emittance:  $\Delta T_{FWHM} < 2\text{ns}$  and emittance  $\sim 16 \pi \text{ mm.mrad}$ , multiturn ejection.

Let us note that figures were predicted before construction (see the white book). In the experimental rooms the observed bunch length  $\Delta T_{FWHM} = 3-5\text{ns}$  is dominated by the effect of the very long beam line with low-energy ions, not by the CIME properties themselves.

In the following, the evolutions concerning the machine are reviewed, taking into account the previous limitations and more.

## 2.1. Working diagram extension

Even with a large range of energies, the interest of several physicists turned to lower energies, below the limits specified in the white book. Simulations and machine studies allowed reaching 1.2 A.MeV instead of 1.7 A.MeV (see Figure 4) by accelerating the beam on the harmonic 6 of the RF cavities. The yields out of CIME were acceptable and an experiment using  $^{15}\text{O}$  (F. de Oliveira et al.) was performed.

Lower energies might be reached but probably with poor yields.

Higher energies (16-25 A.MeV) are less demanded because of the source limitation and the difficulties to obtain  $Q/A > 0.25$ .

[http://www.ganil.fr/operation/available\\_beams/radioactive\\_beams.htm](http://www.ganil.fr/operation/available_beams/radioactive_beams.htm)

## 2.2. CIME Inflector

By conception, the whole range of energies is covered by using two different types of inflector to inject the beam into CIME:

- Muller inflector for the harmonic 3 and 2
- Spiral inflector for the harmonics 4 and 5 (and now 6)

Therefore, shifting from a high-energy experiment to a low-energy one may oblige to exchange the deflectors, which required about 2 days of intervention with an intervention on the RF cavity extremities. In order to avoid a waste of beam time, an extension of the inflector capabilities was studied. Currently, the Muller inflector covers the harmonic 4, 3 and 2, while the Spiral inflector covers the harmonics 6, 5, 4 and 3.

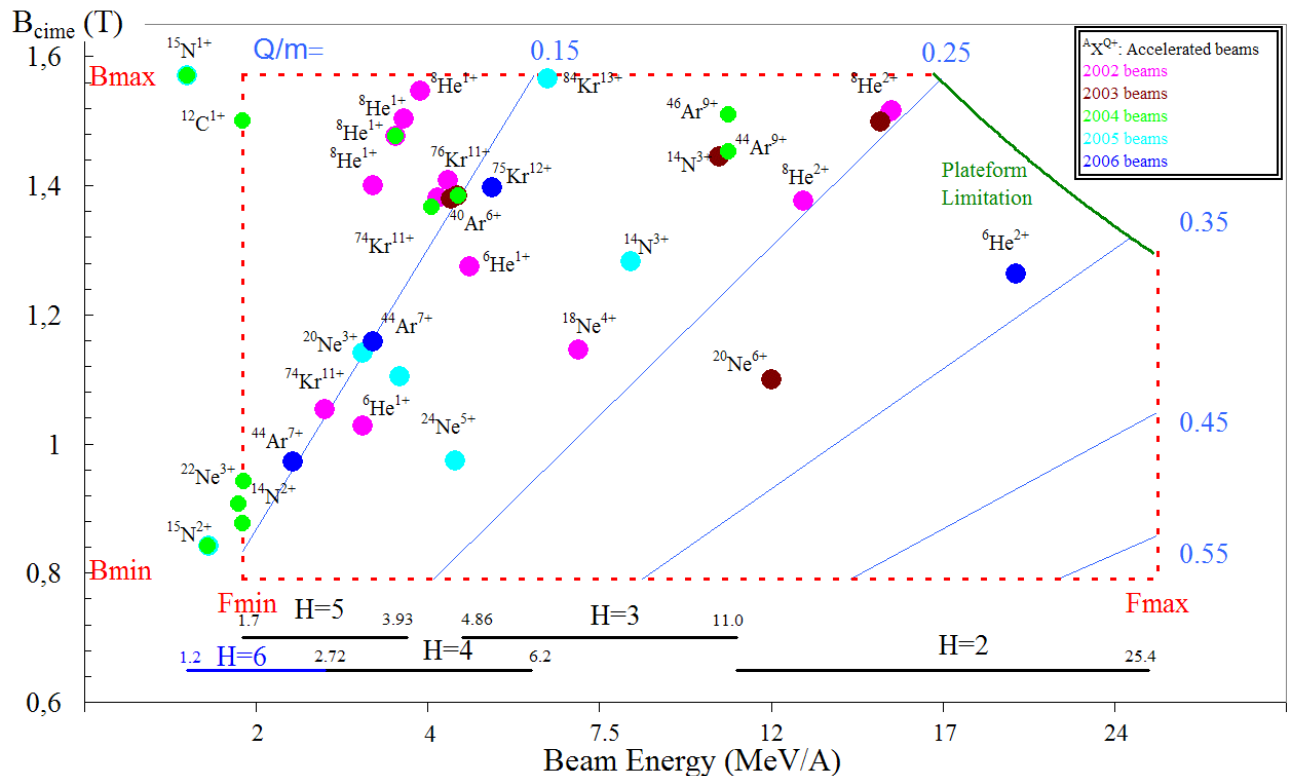


Figure 4: Working diagram of SPIRAL with accelerated beams since 2002.

### 2.3. Beam schedule

GANIL is increasingly a multi-user facility. In addition to GANIL beams, it is possible now possible to deliver simultaneously beams to:

- IRRSUD (low energy beam line)
- SME (medium energy beam line)
- 2 high-energy experiments (a main experiment and an auxiliary one)
- CIME or LIRAT for detector tests with stable beams

Thus, the beam planning becomes complicated because of the number of simultaneous experiments (Table 3). 2 or 3 months before the beginning of the run, the planning should be approved by the GANIL directorate, to be able to prepare SPIRAL target ion source ensembles, to tune beams ...

Buffers are inserted in the planning to anticipate technical failures of the machine. The amount of buffer is adapted to the experiment duration. Figure 5 shows the good agreement between scheduled and effective beam time delivered to the physics experiments. The buffers were totally used to compensate the technical interventions.

Date	hour	C01	C02	CSS1, CSS2	CIME	SME	SISSI	Auxiliary beam				
Saturday 29-Apr	2h00	ON LINE 48Ca		BEAM ON SPIRAL TARGET	E393S (Gorgen) 1UT							
	6h00				44Ar7+							
	10h00				2.6 MeV/A							
	14h00				H5 R45							
	18h00											
22h00												
Sunday 30-Apr	2h00								E393S (Gorgen) G2 6 UT			
	6h00											
	10h00											
	14h00											
	18h00											
Monday 1-May	2h00		IRRSUD 208Pb 0.66 MeV/A	BEAM ON SPIRAL TARGET	E393S (Gorgen) G2 6 UT							
	6h00											
	10h00											
	14h00											
	18h00											
Tuesday 2-May	2h00		P717-M-S Jurazsek	Tuning alpha	BUFFER				P695 muranaka 16UT			
	6h00											
	10h00											
	14h00											
	18h00											
Wednesday 3-May	2h00		S26 F. Studer	SIRA (M.G. St Laurent) D2 8UT	40Ar6+ 3.82 MeV/A H4 R45		Not Available	E457a (J. Giovinazzo) 8UT				
	6h00											
	10h00											
	14h00											
	18h00											
Thursday 4-May	2h00				Machine Study 9 E. Guéroult							
	6h00											
	10h00											
	14h00											
	18h00											
Friday 5-May	2h00											
	6h00											
	10h00											
	14h00											
	18h00											
	2h00											
	6h00											
	10h00											

Table 3: Beam planning example in a multi-user machine mode.  
<http://www.ganil.fr/user/experiments/planning.html>

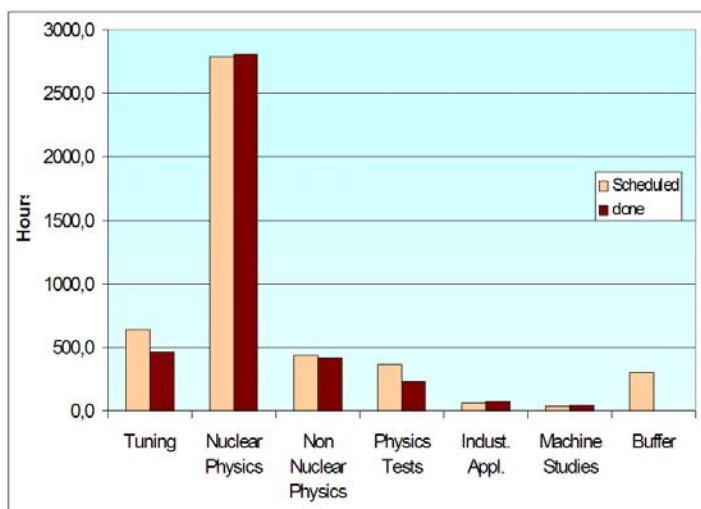


Figure 5: Scheduled and effective beam time.

## 2.4. LIRAT

The LIRAT beam line, initially foreseen to permit the delivery of all radioactive beams from SPIRAL to various experimental areas was reduced to a 15-meter long beam line coupled to a specific experimental apparatus: A RFQ gas cooler connected to a Paul trap. The beam line was built in 2003 and the first beam tests were realised in 2004. Two experiments to study  $\beta$ - $\nu$  correlations in the decay  ${}^6\text{He}$  have been performed in order to test the limits of the Standard Model in 2005 and 2006.

## 2.5. CICS Project

A new criterion aiming at limiting the target irradiation of a SPIRAL TIS, such as the maximum total number of incidental ions integrated by the target, makes it possible to decrease the volume of the waste, nuclear in particular. From an operation point of view, it makes it possible to optimise the availability of this device and decreases the frequency of the handling operations likely to generate radiological risks. It is proposed to limit the activity of the target by the fluence (the flux of ions integrated over the lifetime of the target). A dedicated device functioning permanently during the operation of SPIRAL ensures that the fluence does not exceed the maximum value.

## 2.6. R2 Rebuncher

A rebuncher installed before CSS2 (see Figure 6) was unavailable since 2002 because of defective RF contactors. The cavity is repaired and will be on line in 2007. The clear interest of such a rebuncher is to reduce the beam losses in the CSS2 deflector, which results in an improved beam stability, (especially for heavy ions such as Kr). A second advantage is the reduction of the bunch time width  $\Delta T$  with CSS1 beams:

- i) Without R2:  $\Delta T_{FWHM} = 2.0 - 1.5 \text{ ns}$
- ii) With R2:  $\Delta T_{FWHM} \sim 1.0 \text{ ns}$

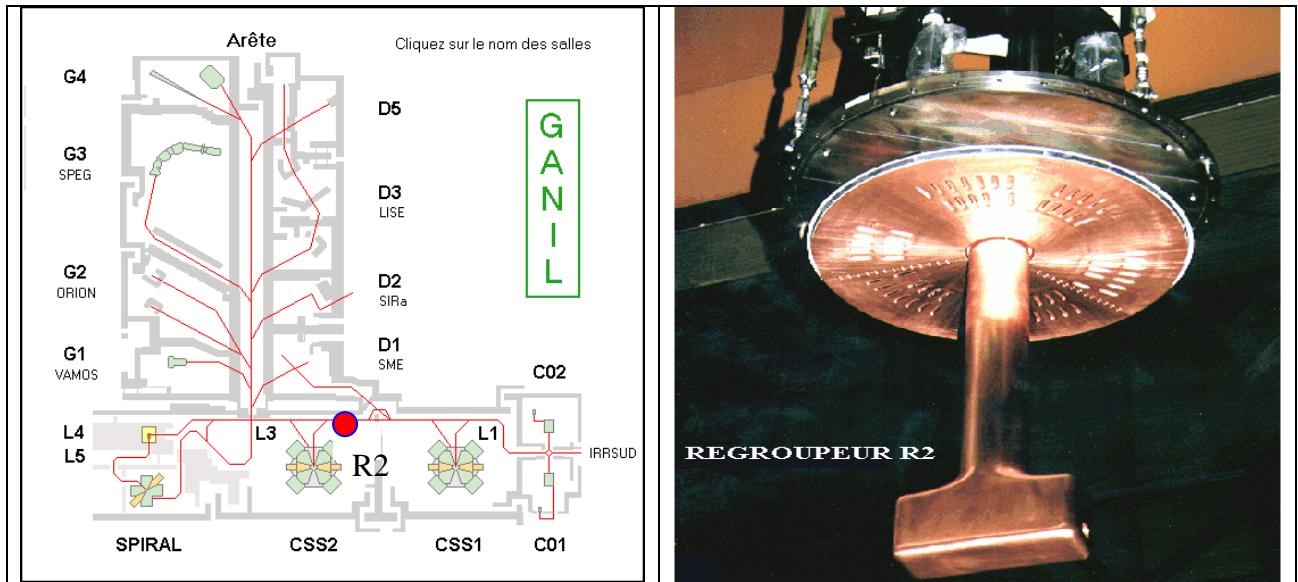


Figure 6: R2 rebuncher

## 2.7. Improvement of the identification station

The identification station of SPIRAL (IBE) is a powerful and flexible tool for the identification and counting of very low intensity radioactive beams. However in the case of routine intensity measurement of a radioactive beam dedicated to post acceleration ( $10^3$ - $10^6$  pps), which represents the main part of the activity of the station, the system was suffering with a lot of stability problems and was easy to use. These characteristics were very demanding in manpower.

An alternative acquisition system for germanium, silicon and plastic scintillator detectors, with its own software, has been developed which facilitates the use and the maintenance of the whole system. The developed software is integrated in the control system of the accelerator. The identification can be realised on-line with lifetime and intensity measurements. This system has been developed in the first part of 2006 (see Figure 7).

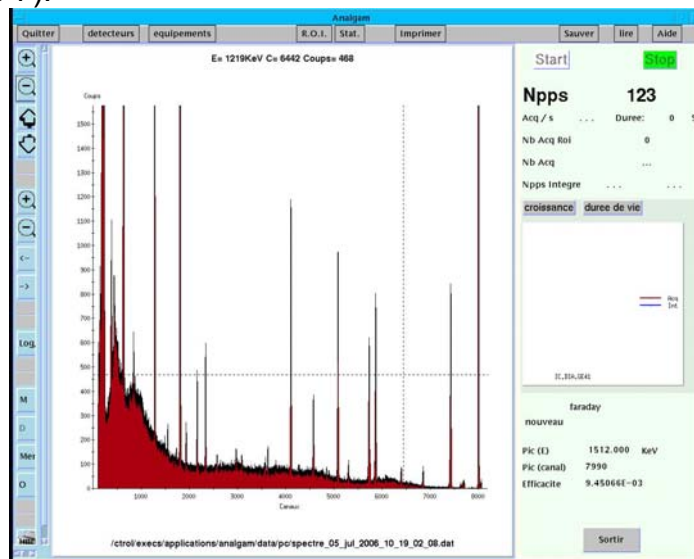


Figure 7: Gamma rays observed with the new software in the identification station. Efforts have been done in 2006 to make the station “user friendly”. The old system

relying on Labview+GANIL acquisition+ server developed from 2001 to 2006 is no longer available.

## 2.8. New source extraction

One of the technical limitations of SPIRAL is the current delivered by the ion source. The low voltage of the source extraction does not allow to transport more than 1 mA. This current is easily reached when the target is heated by a high-power primary beam. This reduces the transmission of the radioactive ions of interest. This space charge limitation could be overpass by:

- i) Replacing the electrostatic lenses by a magnetic solenoid, which performs a beam selection in  $M/Q$ , reducing the transported current (Ref: SDA/DIR/2006.204)
- ii) Increasing the source voltage 45 kV instead of 30 kV

These choices have been considered during the SPIRAL 1 design but has been rejected because of technical difficulties. Today it is still possible to reconsider theses choices.

## 2.9. LCG Project

Currently, the beams extracted from the cyclotron CIME that are sent to the experimental area go through the high-energy spectrometer configured in mode Z before they enter the fish-bone line. This situation prevents to send a beam from CIME to experimental area while providing other caves with CSS2 beams. This situation is currently already constraining because it prevents to use the stable ion beams of average energy from CIME without disturbing the normal operation of GANIL. It will be even worse when the SPIRAL 2 project will be operational because, by its principle, SPIRAL 2 will be able to operate independently of SSC, which would allow the simultaneous supply of 2 beams without this constraint.

The GANIL directorate thus proposed that a beam line joins the G1 and G2 rooms directly, starting from CIME without passing by the spectrometer (see Fig. 8). In order to allow the simultaneous supply of the beam from CIME in G1 or G2 (see Fig. 9) while another beam from SSC2 would be sent to other rooms. This project is now integrated to the SPIRAL 2 project and is waiting for collaboration with U.K. to be finalised.

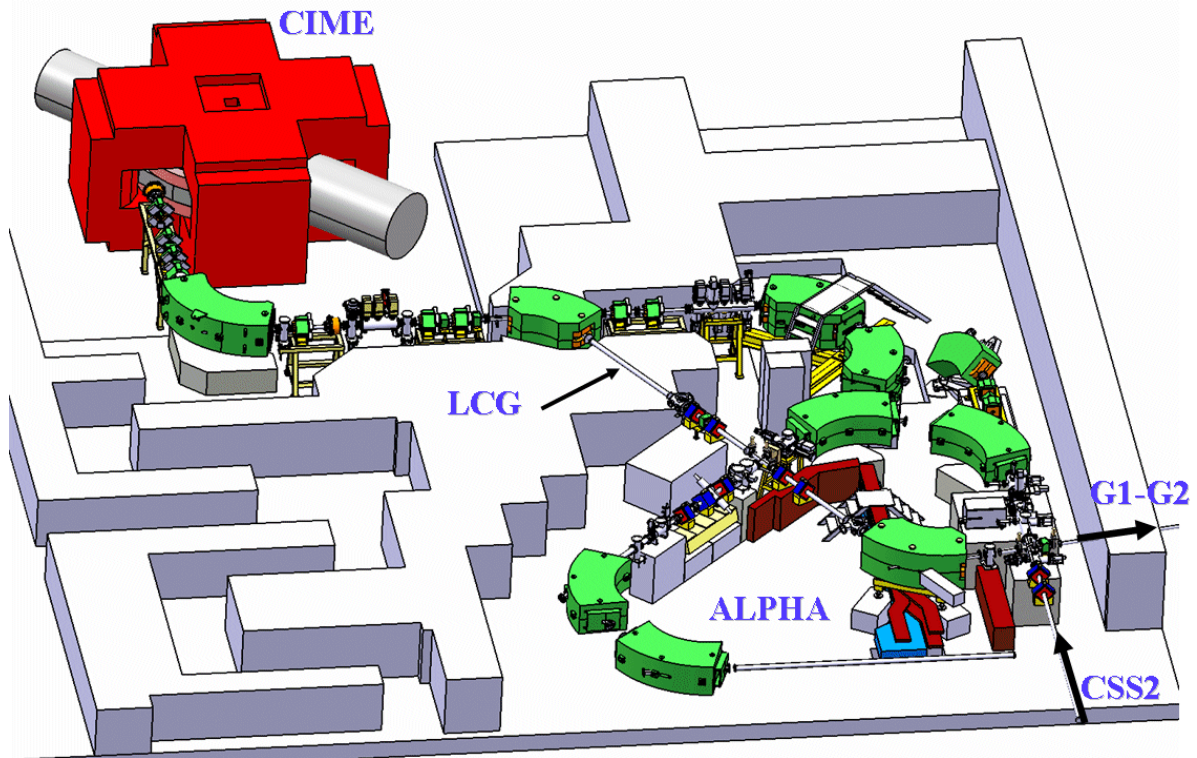


Figure 8: Layout of the beam line linking CIME to the G1 and G2 rooms and bypassing the ALPHA spectrometer.

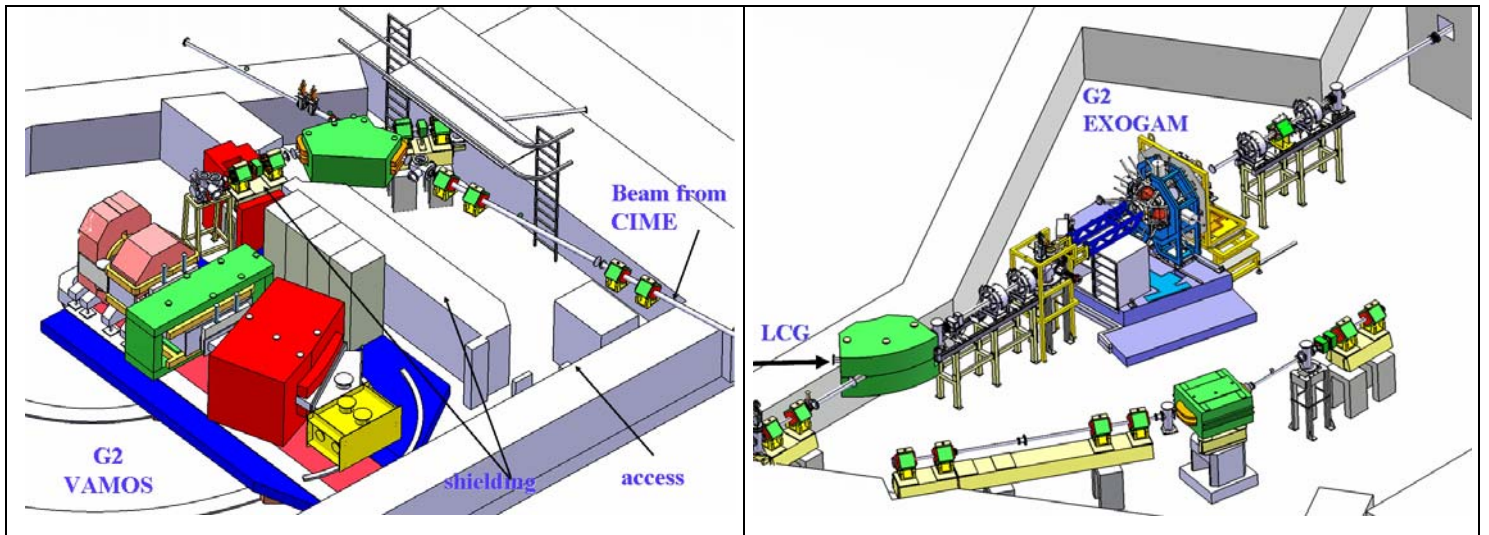


Figure 9: Details of the line in the G1 and G2 experimental area.

# III. HALOES AND CLUSTERS

D. Beaumel\*

\* IPN Orsay, IN2P3-CNRS, Université Paris-Sud, F-91406 Orsay, France

Report on SPIRAL experiments E350S, E401S, E403S, E403aS, E405S, E406S, E415S, E422S, E465S, E473S and E528S

Contact: [beaumel@ipno.in2p3.fr](mailto:beaumel@ipno.in2p3.fr)

## 1. Introduction

This report aims to review the work performed at SPIRAL centred on the theme “haloes and clusters”, and mention possible perspectives for the coming years. It is well known that haloes and clustering effects are specific features of light exotic systems. All the reported work has been done using the neutron-rich  $^{6,8}\text{He}$  SPIRAL beams.

The largest part of the reported studies consists in direct reactions experiments induced by the  $^8\text{He}$  SPIRAL beam.  $^8\text{He}$  itself, as well as the neighbouring  $^{7,9}\text{He}$  and  $^7\text{H}$  could be investigated through elastic/inelastic scattering and 1-nucleon transfer reactions, respectively. The search for 4-neutron clusters was performed using  $\alpha$ -transfer and break-up reactions. Another serie of experiments makes use of the low energy  $^{6,8}\text{He}$  SPIRAL beams to investigate the effect of the neutron halo on fusion cross-sections. Finally, we mention the recent experiment investigating correlations between the two neutrons of the halo of  $^6\text{He}$  through nuclear break-up.

For all these studies, a relatively large range of detectors has been used: recoil particle detectors (MUST, MAYA), neutron detectors (DEMON, NEUTRON WALL), spectrometers (SPEG, VAMOS) and gamma detectors (EXO GAM). For direct reaction experiments based on missing-mass method using MUST, beam-tracking detectors (CATS) had to be used to insure sufficient angular resolution.

In the following, we briefly describe the set-up and summarize the results of each experiment or serie of experiments related to haloes and clustering aspects of nuclei at SPIRAL. In each case we mention future prospectives and the related beam developments needed.

## 2. Experiments: scientific objective, results and perspectives

### Spectroscopy of $^{7,8}\text{He}$ (E405S)

#### Experiment with the MUST detector

With the first  $^8\text{He}$  beam of SPIRAL, a (p,p') experiment (E405S) was performed in November 2001 to investigate the properties of the expected four-neutron skin of this nucleus. The Si-strip detector array MUST [1] was used to detect the recoiling light particles and the beam was tracked with the CATS [2] detectors. The goal was to test the validity of microscopic few-body calculations and to deduce the features of the  $NN$  interaction inside a nucleus with very low nuclear-matter density. The

collaboration included physicists from GANIL, IPN-Orsay, the University of Ioannina (Greece), and from FLNR Dubna. Elastic, inelastic and transfer reaction cross-sections were extracted from the data and compared to theoretical calculations, yielding accurate results on the structure of the  ${}^8\text{He}$  [3-5]. Experimental differential cross-sections compared to theoretical calculations are presented in fig. 1 for elastic and  ${}^8\text{He}(p,d)$  transfer reactions.

From the  $(p,p')$  analysis, the characteristics of the excited states of  ${}^8\text{He}$  were extracted: the first  $2^+$  state is obtained at  $3.62 \pm 0.14$  MeV (width  $0.3 \pm 0.2$  MeV) and a second state was found at  $5.4 \pm 0.5$  MeV (width  $0.5 \pm 0.3$  MeV). Theories that include the coupling to the continuum states are in agreement with the location of these two resonant states, while other microscopic frameworks (like no-core shell model or cluster models) predict too high energies for the excited states.

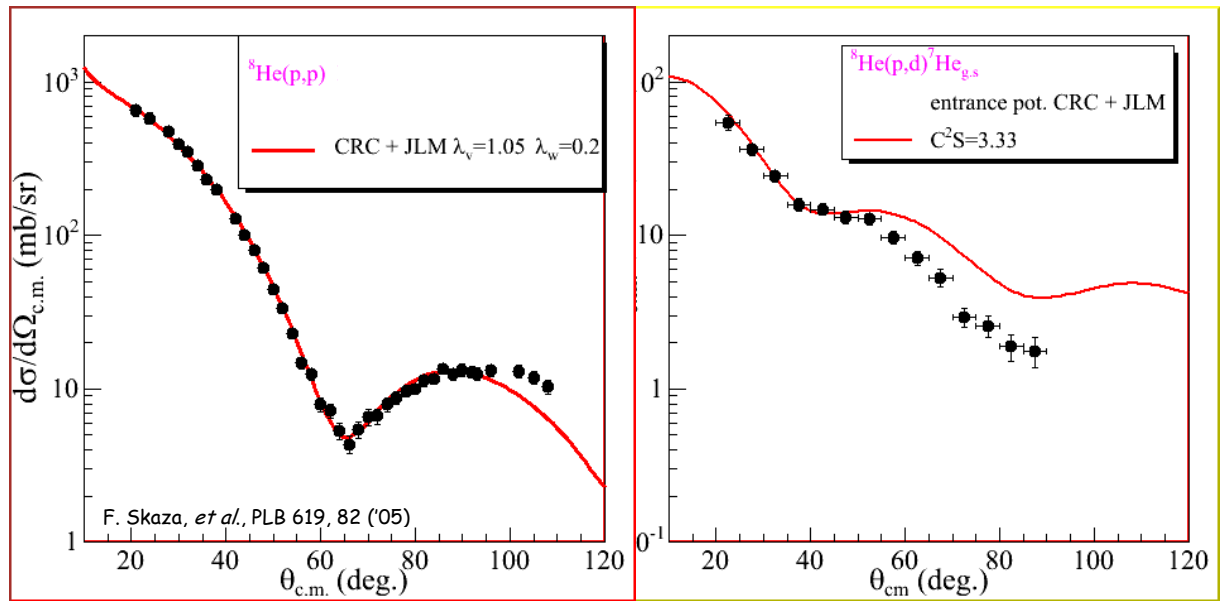


Figure 1:  ${}^8\text{He}(p,p)$  elastic and  ${}^8\text{He}(p,d){}^7\text{He}$  transfer reaction at 15.7 A.MeV.

In order to explore the few-body interaction in nuclear systems, the study of unbound neutron-rich nuclear states ( ${}^5\text{H}$ ,  ${}^7\text{He}$  and many-neutron clusters) can also be achieved through specific transfer reactions, for instance the resonances of  ${}^7\text{He}$  were studied via  ${}^8\text{He}(p,d)$  [5]. From the missing mass spectrum of  ${}^7\text{He}$ , a first excited resonant state at  $E^* = 0.9 \pm 0.5$  MeV (width  $\Gamma = 1.0$  (9) MeV) was indicated. Another resonance was also observed at  $2.9 \pm 0.1$  MeV ( $\Gamma = 2.1$  (8) MeV), consistent with the excited state pointed at RIKEN by A. Korshennikov et al., and assigned to be a  $5/2^-$ .

Strong coupling effects from the pick-up reaction  $(p,d)$  to the elastic scattering  ${}^8\text{He}(p,p)$  were observed. A coupled-channel analysis using microscopic potentials and explicit coupling to the  $(p,d)$  channel has demonstrated its ability to reproduce both elastic and  $(p,d)$  data. The same features can be expected throughout the nuclear chart, and particularly for neutron-rich nuclei with low particle threshold and continuum states close to the ground state. The results obtained in the case of  ${}^8\text{He}$  are important for future structure studies. They demonstrate the need for a complete data set of direct reactions in order to understand the coupled-channel effects between elastic, inelastic and transfer reactions. This is a necessary step to be able to investigate the structure of weakly bound nuclei.

## Experiment using the MAYA detector (E350S)

Resonances in  ${}^7\text{He}$  were also investigated in experiments at lower energies using another detection system, namely the MAYA active target [6]. Reactions induced on protons at low incident energy (3.5-3.9 A.MeV) were measured with a  ${}^8\text{He}$  and  ${}^6\text{He}$  beam accelerated by SPIRAL. The particles were detected in MAYA, filled with  $\text{C}_4\text{H}_{10}$  gas. The beam was stopped in the detector, so that energies ranging from the incident beam energy down to detector threshold were covered. Proton elastic scattering, one neutron pick-up (p,d) and (p,t) reactions were observed. In Fig. 2, we show an angular distribution of the  ${}^8\text{He}(p,d){}^7\text{He}$  reaction at an incident energy of 3 A.MeV. Figure 3 shows the angle integrated cross-sections, compared to theory with  $C^2S = 4$ .

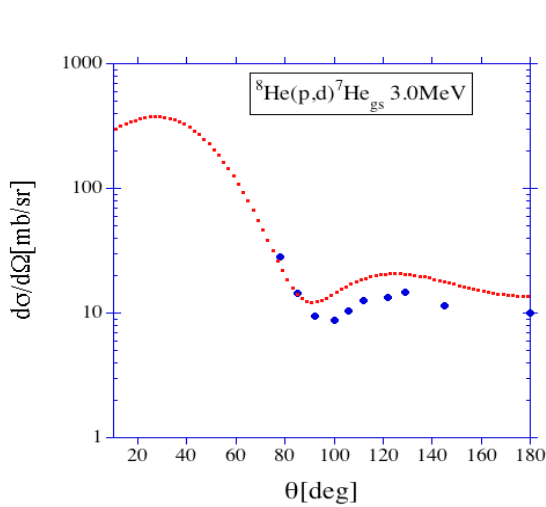


Figure 2: Experimental angular distributions compared to DWBA calculations with  $C^2S=4$ .

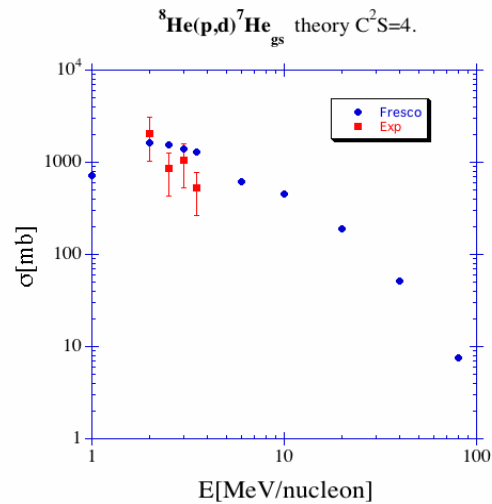


Figure 3: Experimental and theoretical cross-sections for the  ${}^8\text{He}(p,d){}^7\text{He}$  reaction

As can be seen, at low energy the cross-section reaches very high values, of the order of one barn. The origin of this very high cross-section is the good momentum matching at this low energy of the loosely bound neutron in the initial and final state. This is the first time that this strong increase of transfer reaction cross sections at very low energy predicted for loosely bound systems was observed. Spectroscopic factors are in agreement with a simple shell model configuration. Some of the results are published [6-9]. Due to the fact that the beam was stopped in the detector, an excitation function for the reactions with energies between the incident beam energy and essentially zero energy is obtained. The extraction of information on excited states in  ${}^7\text{He}$  from experimental spectra must take into account the fact that the widths of the populated states are large, and that both width and population cross-sections are energy dependent. The energy dependence of the decay width was treated in two ways: as given by R-matrix formalism, and calculated as single particle resonance width by the code FRESKO. The experimental energy resolution being much better than the observed structure, it was not necessary to take it into account in the simulation. Figure 4 shows a fit of the experimental energy spectrum with three resonances at  $E_R = 0.44, 1.0$  and  $3.3$  MeV, with arbitrary normalization. The final fit is shown as solid line. In this fit, the contribution relative to the ground state for the state at  $E_R = 1$  MeV was  $(-0.015 \pm 0.082)$ . This means no contribution of such a state is seen, in contradiction with the MUST experiment

above, and the upper limit is far below the contribution reported by Meitner et al [10]. The extracted spectroscopic factor for the ground state is  $C^2S = 3.6 \pm 0.4$ , in good agreement with the one obtained in the MUST experiment ( $C^2S = 3.3 \pm 0.4$ ).

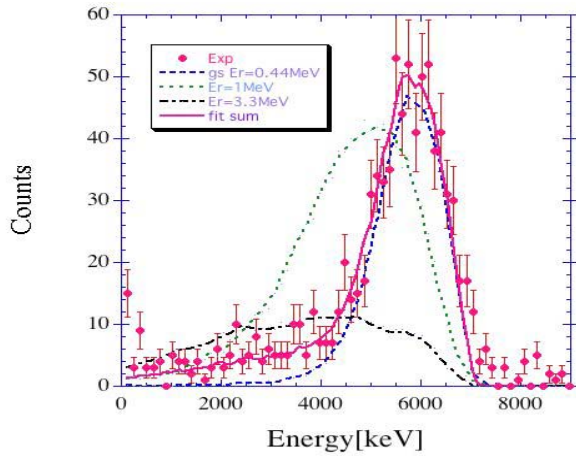


Figure 4: Projected deuteron energy spectrum for the (p,d) reaction. The experimental count rate/energy bin is compared to a Monte-Carlo simulation including the effect of the energy dependent decay width, recoil broadening, and energy dependence of the population cross-section. The individual contributions, with arbitrary normalisations, are shown for the ground state, and hypothetical states at 1 MeV and 3.3 MeV. The fitted sum of these contributions is shown, too.

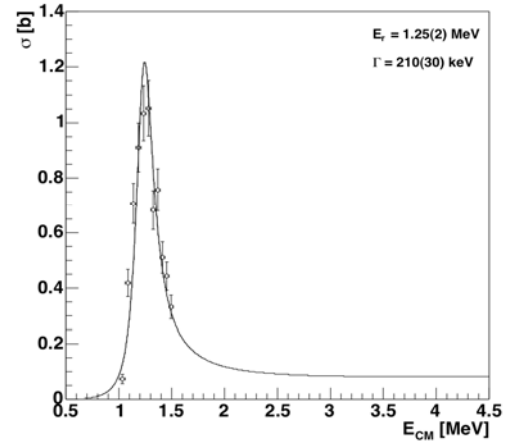


Figure 5: Isobaric analog resonance in the system  ${}^6\text{He}(p,n){}^6\text{Li}$  as obtained by the MAYA detector (L. Gaudefroy et al., preliminary).

A different way to study the  ${}^7\text{He}$  is via the *isobaric analogue resonance* in the  ${}^6\text{He}(p,n){}^6\text{Li}$  reaction. The efficiency of this method using the MAYA detector is illustrated by the fact that this result was obtained in some hours of parasitic beam. The result is shown on Fig. 5. The extracted spectroscopic factor is  $S = 0.69 \pm 0.1(\text{th}) \pm 0.13(\text{exp})$  is very compatible with the one deduced from the width of  ${}^7\text{He}$  ground state ( $S = 0.95 \pm 0.1(\text{th}) \pm 0.1(\text{exp})$ ). This indicates that  ${}^7\text{He}$  can be considered to a good degree as a core coupled to a neutron. We mention that in the  ${}^6\text{He}(d,p)$  study by Wuosmaa et al. [11], the deduced spectroscopic factor is significantly lower ( $S = 0.37 \pm 0.07$ ).

### 2.1.3. Near-future perspectives of the experimental program

With MUST2, the next experiment will be the search for the low-lying resonant states of  ${}^6\text{He}$  via the  ${}^8\text{He}(p,t)$  reaction at 15.7 A.MeV. A large angular coverage will be provided by 4 MUST2 telescopes which will be used to detect the He ejectiles at forward angles, in coincidence with the light particles (p,d,t) measured in the wall of MUST detectors. For a complete spectroscopy, MUST2 will be coupled to VAMOS and EXOGAM.

As we have seen, high cross-sections for transfer and resonant reactions are observed with MAYA in the energy domain of SPIRAL (and SPIRAL2). A unique possibility for studying drip-line nuclei therefore exists and IAS are particularly promising. Intensities needed with the MAYA detector are of the order of 1000 particles/s. With reasonable extraction efficiencies, most of the neutron rich Be, B, C, N, O, F and Ne isotopes should give such intensities. Be and B being very difficult, C, N, and O would provide very interesting isotopic chains to study single particle and collective properties.

## 2.2. Search for neutral clusters (tetraneutron) (E415S, E422S, E465S)

The search for neutron clusters at SPIRAL has been triggered by the very intriguing result obtained in an experiment performed at GANIL [12], studying the break-up of  $^{14}\text{Be}$ . In this experiment lead by the LPC group, break-up neutrons were detected using the DEMON array, in coincidence with charged fragments measured using a Si-CsI telescope placed around zero degrees. The analysis revealed the presence of “anomalous” events in neutron detectors, that is events for which the deposited energy exceeds by far the energy deduced from the time-of-flight, assuming that a single neutron is detected. Moreover, these events were found to be in coincidence with  $^{10}\text{Be}$  fragments. None were found in the other channels. A detailed study of free neutrons pileup leads to the conclusion that such process cannot be invoked to explain the data. It was then suggested that these events could be due to bound tetraneutrons.

At SPIRAL, the LPC group proposed to use the same approach to investigate the break-up of  $^8\text{He}$  (E415S), a good candidate for tetraneutron search. It was argued that strong clustering effect would imply a ground-state wave function of  $^8\text{He}$  containing a large fraction of the  $\alpha+4n$  component, which would favour the formation of a bound tetraneutron, and its observation after a break-up process. The experiment has been performed in November 2002 and results are detailed in the Ph.D. thesis of V. Bouchat (U.L. Bruxelles) with the 15 A.MeV SPIRAL beam. The presence of 13 “anomalous” events in neutron detectors is reported, as illustrated on Fig. 6. All these events are in coincidence with  $^4\text{He}$  fragments (that is, in the  $A_{\text{beam}}-4$  channel) and none in coincidence with  $^6\text{He}$ , providing another evidence in favour of tetraneutron observation. A very detailed analysis using 4 different methods shows that these events cannot be due to the pileup of free break-up neutrons. The analysis of the neutron-fragment relative angle spectrum built with these 13 events shows that these events cannot correspond to a *bound* tetraneutron. The situation is less clear concerning an eventual 4-neutron resonant state. The data are compatible with a resonance located below 1 MeV above the  $4n$  threshold, but the poor statistics do not allow a definite conclusion.

At nearly the same time, the Orsay-Dubna group investigated this issue using a different approach based on a missing mass measurement. Starting from the same 15 A.MeV  $^8\text{He}$  beam, the  $\alpha$ -transfer reaction  $^8\text{He}(d,^6\text{Li})$  was studied using the MUST array to which thin Silicon layers were added in order to provide an unambiguous identification of  $^6\text{Li}$  particles. Neutrons were also detected using thick plastic detectors so as to improve the reaction channel selection. After a first run performed in 2002 (E422S), a follow-up experiment was accepted by the GANIL PAC with the aim of increasing the statistics (E465S). This run was performed at the end of 2004 with a  $^8\text{He}$  peak intensity of 33 kcps. The excitation energy spectrum in the  $4n$  system deduced from the  $^6\text{Li}$  energy and angle is represented on Fig. 7. This spectrum is gated by the detection of at least one neutron in plastic detectors placed

in the forward direction to detect recoil neutrons. Counts observed below the  $\alpha+4n$  threshold can be accounted for the background originated from  $^{12}\text{C}$  in the  $\text{CD}_2$  target. Namely, no bound tetra-neutrons are observed in the limits of the statistics. Above the  $\alpha+4n$  threshold, a smooth increase of the cross-section is observed. The data cannot be satisfactorily reproduced by a pure 5-body phase-space calculation, which represents a clear evidence of correlations between the 4 neutrons in the exit channel. These correlations have been investigated using simple simulations of 2n-2n interaction in the final-state. More sophisticated analysis is to be done in the near future.

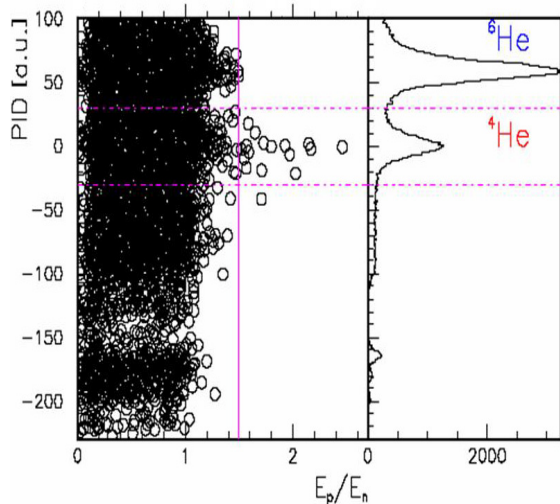


Figure 6: Scatter plot of the fragment identification parameter PID and  $E_p/E_n$  (ratio of the deposited energy in neutron counter vs energy deduced from time of flight).

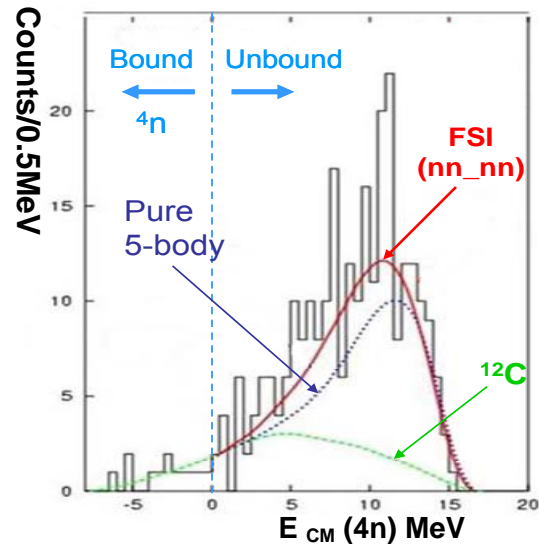


Figure 7: Excitation energy spectrum in the  $4n$  system reconstructed from the  $^6\text{Li}$  particles and gated by the plastic detectors.

On the theory side, state-of-the-art quantum Monte-Carlo calculations lead to the conclusion that a bound tetra-neutron would not be compatible with our present knowledge on nuclear forces [13]. These calculations however cannot yet make reliable predictions concerning the unbound case. Recently, Faddeev's method calculations could be achieved by Lazauskas and Carbonell [14] in which no resonant states were found.

In conclusion, both experiment and theory seem to agree at the present time that bound four-neutron clusters do not exist. The situation is less clear concerning resonances, such state being more difficult to observe especially in the case where it would be broad.

### Perspectives with SPIRAL:

Concerning the 4-neutron system, two-proton pickup on  $^6\text{He}$  nucleus could be performed using e.g. the intense  $^6\text{He}$  beam of SPIRAL. A test experiment aiming to establish the experimental method to measure this exotic reaction with a cryogenic helium target is already scheduled. The same reaction could be used to study the 6-neutron system with the  $^8\text{He}$  beam provided that the intensity would be 1 or 2 orders of magnitudes as it is presently.

Similarly, an intense  $^8\text{He}$  (and also  $^{11}\text{Li}$ ) beam could be used to search for  $^6\text{n}$  and  $^8\text{n}$  with the MAYA active target as was recently proposed by Roussel-Chomaz and Villari in a letter of intend submitted to the GANIL PAC.

### 2.3. The heavy hydrogen $^7\text{H}$ (E406S, E465S)

Search for resonant states in heavy unbound Hydrogen nuclei and subsequent determination of their energies and widths constitute an important challenge for the existing models of nuclear forces, as their properties may bring strong constraints on the poorly known neutron-neutron and 3- and 4-body interaction parameters. The heavy hydrogen  $^7\text{H}$  represents an extremely neutron rich system, with  $N/Z=6$ , comparable to neutron star case.

The first evidence for a low-lying resonance in the  $p+6n$  system was obtained at RIKEN using the  $p(^8\text{He},2p)^7\text{H}$  reaction at 61 A.MeV [15]. They observed a structure just above the  $t + 4n$  threshold superimposed on a large background. However the poor C.M. energy resolution (1.9 MeV) did not allow extracting accurate information on its energy and width.

Missing mass measurements using a secondary beam of  $^8\text{He}$  can provide experimental information on this very exotic  $^7\text{H}$  nucleus. The set-up of the “tetra-neutron” experiment (E465S) described above allowed a simultaneous investigation of the  $^7\text{H}$  production channel through the proton pick-up reaction ( $d, ^3\text{He}$ ), using the  $^8\text{He}$  SPIRAL beam at 15.3 A.MeV. Figure 8 displays the missing mass spectrum of  $^7\text{H}$ , obtained after subtracting contribution of Carbon atoms of the  $\text{CD}_2$  target. The dotted line shows the 6-body phase space convoluted with efficiency. The existence of a low-lying resonance in the  $^7\text{H}$  system above  $t + 4n$  threshold is clearly confirmed by the present data. The resonance energy  $1.56 \pm 0.27$  MeV and width  $\Gamma = 1.74 \pm 0.72$  MeV are deduced by fitting a Breit-Wigner curve to the experimental points.

A second SPIRAL experiment (E406S) has investigated  $^7\text{H}$  using a similar missing-mass method but with different experimental set-up. The one-proton transfer reaction  $^{12}\text{C}(^8\text{He}, ^{13}\text{N})^7\text{H}$  induced by the 15.4 A.MeV  $^8\text{He}$  beam of SPIRAL on a  $^{12}\text{C}$  gas target was measured. The main part of the experimental set-up was the Time-Charge Projection Chamber MAYA, used as a detector for the reaction products as well as a gas target cell. By detecting the recoiling  $^{13}\text{N}$  gated by tritons, the  $^7\text{H}$  spectrum could be obtained. The statistics is low (seven events), but the spectrum is very clean. A resonant state of  $^7\text{H}$  is observed (see Fig. 9), with an estimated resonance position at  $0.57^{+0.42}_{-0.21}$  MeV above the  $^3\text{H}+4n$  threshold, and a width  $\Gamma = 0.09^{+0.94}_{-0.06}$  MeV. The total cross-section associated to the process is  $40.1^{+58.0}_{-40.0}$   $\mu\text{b}/\text{sr}$ , obtained within the angular coverage of MAYA, calculated in  $\sim 10 - 45$  degrees in centre of mass frame.

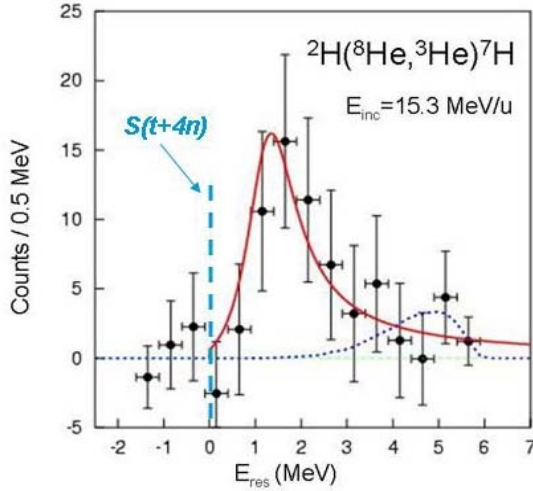


Figure 8: Excitation energy spectrum obtained from the recoiling  ${}^3\text{He}$ . Zero energy corresponds to the  ${}^3\text{H}+4n$  threshold. The resonance energy and width are deduced by fitting a Breit-Wigner curve (solid line) to the data (see text). The dotted line corresponds to a 6-body phase-space convoluted with the detection efficiency.

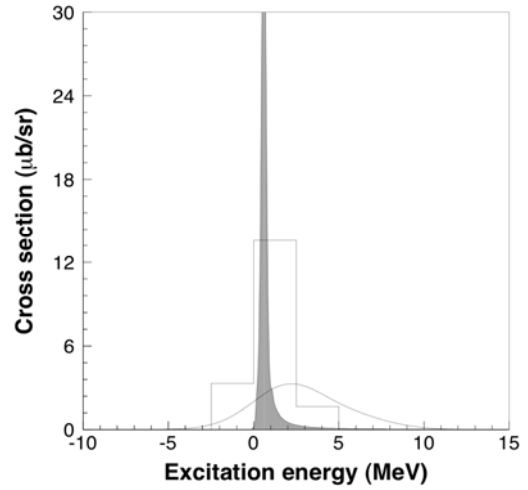


Figure 9: Excitation energy distribution of the events identified as  ${}^7\text{H}$  in the MAYA experiment. The mass of the  ${}^3\text{H}+4n$  system corresponds to the zero energy, and the distribution is normalized to the production cross section. The histogram corresponds to the experimental data with a 2.5 MeV binning, and the solid line represents the experimental distribution resulting from the contribution of the individual uncertainties. The full grey distribution is the modified Breit-Wigner function resulting from the fit of the experimental data.

## Conclusions and Perspectives:

The resonance characteristics found in the two SPIRAL experiments are somewhat different but, together with the early RIKEN experiment of Korshenninikov, all three point to the very important result that  ${}^7\text{H}$  exist as a resonance near the  $t+4n$  threshold.

The experimental approaches at SPIRAL have proven to be effective but we are clearly at the limit of the present  ${}^8\text{He}$  beam with respect to the cross-sections involved. Both experiments were already optimised in terms of efficiency so that only an increase of beam could significantly improve the statistical quality of the data.

### 2.4. Shell inversion in ${}^9\text{He}$ (E401S, E473S)

A spectacular evolution of shell structure as function of neutron-proton asymmetry is observed in  $N=7$  isotones. The shell energy gap  $E(s_{1/2})-E(p_{1/2})$  decreases from  ${}^{15}\text{O}$  to  ${}^{11}\text{B}$ , and becomes negative in  ${}^{11}\text{Be}$ , with ground state  $J^\pi$  being equal to  $1/2^+$  instead of the normally expected  $1/2^-$  value. The existence of neutron halo in  ${}^{11}\text{Be}$  and in  ${}^{11}\text{Li}$  is closely related to this “parity inversion” phenomenon, considering the small binding energy of the last neutron. A program investigating this issue started with two experiments (E259 and E319) using the  ${}^{11}\text{Be}$  beam produced by fragmentation at SISSI. The  ${}^{11}\text{Be}(p,d){}^{10}\text{Be}$  neutron-pickup reaction [16] performed

using SPEG and CHARISSA has shown that the wave function of  $^{11}\text{Be}$  ground state was predominantly  $s_{1/2}$ . The  $^{11}\text{Be}(d,^3\text{He})^{10}\text{Li}$  proton-pickup reaction [17] has demonstrated that the  $s_{1/2}$  single-particle state was located just above the  $^9\text{Li}+n$  emission threshold, thus being the  $^{10}\text{Li}$  ground state. The main motivation of E401s experiment, using the 15 MeV/u  $^8\text{He}$  beam from SPIRAL, was to search for a possible  $p_{1/2}$ - $s_{1/2}$  shell inversion in the next  $N=7$  nucleus  $^9\text{He}$ , as previously observed in  $^{11}\text{Be}$  and  $^{10}\text{Li}$ .

This very neutron-rich unstable nucleus was previously studied using  $(\pi^-\pi^+)$ ,  $(^{13}\text{C},^{13}\text{O})$  and  $(^{14}\text{C},^{14}\text{O})$  double-charge exchange reactions on  $^9\text{Be}$ . A narrow resonant state at about 1.3 MeV above neutron threshold was identified with  $^9\text{He}$  ground state. On the other hand, results of a  $^{11}\text{Be}$  fragmentation experiment [18] were found to be consistent with the existence of a  $s_{1/2}$  ground state at 0.1 MeV above threshold. The present experiment used the  $(d,p)$  reaction, which is the classical and powerful spectroscopic tool for studying single-particle neutron states. The  $d(^8\text{He},p)^9\text{He}$  reaction was studied at  $E=15.3$  MeV/u using the MUST array to detect recoil protons. Unfortunately, beam intensity was quite low during this experiment and achieved statistics was about 3-4 times poorer than expected.

The missing mass spectrum of  $^9\text{He}$  is presented in Fig. 10 (left). Proton angular distributions were compared with DWBA predictions for neutron transfer to unbound single-particle states (Fig. 10 (right)) in order to determine the transferred angular momentum and spectroscopic factor. Somewhat unexpected are the small natural widths (well below single-particle expectations) of  $^9\text{He}$  states previously observed in charge-exchange reactions [19,20] in contrast with neighbouring unbound nuclei which display very broad resonances. The present data confirms the existence of the two narrow low-energy resonant states ( $E = 1.34$  and  $2.38$  MeV) of refs [19, 20]. The measured  $l=1$  spectroscopic factor of the 1.34 MeV resonance is much lower than 1, indicating a strong fragmentation of the  $p_{1/2}$  single-particle state. As for the  $s_{1/2}$  neutron shell, the present  $(d,p)$  experiment also clearly establish that the  $^9\text{He}$  ground state is located just above neutron threshold ( $E = 0.1$  MeV) and has  $J^\pi=1/2^+$ , in agreement with the results of [18]. The  $^9\text{He}$  ground state is thus, like  $^{10}\text{Li}_{GS}$ , a “ $s_{1/2}$  virtual state”. A theoretical explanation can be found in ref. [21]. Such an inversion can be understood considering the properties of the spin-isospin dependent part of the nuclear interaction: the neutron  $p_{1/2}$  orbit becomes higher as the nucleus loses protons in its spin-flip partner  $p_{3/2}$  and dynamical correlations finally invert  $1/2^+$  and  $1/2^-$  states.

In a recent experiment, the  $^8\text{He}(d,p)^9\text{He}$  reaction was studied using the MUST2 array (E473S). The better resolution of about 100 keV in the centre of mass and the higher statistics should shed more light on the excitation energy spectrum of  $^9\text{He}$ .

## Conclusion and perspectives with SPIRAL:

The  $s_{1/2}$ - $p_{1/2}$  shell inversion observed in  $^{11}\text{Be}$  and  $^{10}\text{Li}$  also exists in the unbound nucleus  $^9\text{He}$ . The present experiment also gives information on distribution of  $p$  and  $d$  strengths in  $^9\text{He}$  and decay of resonant states, via proton angular distributions and detection of residual helium nuclei in plastics telescope. However a new experiment with more intense  $^8\text{He}$  beam and thinner  $\text{CD}_2$  targets is clearly needed to get additional data with better energy resolution and statistics about this very exotic nucleus.

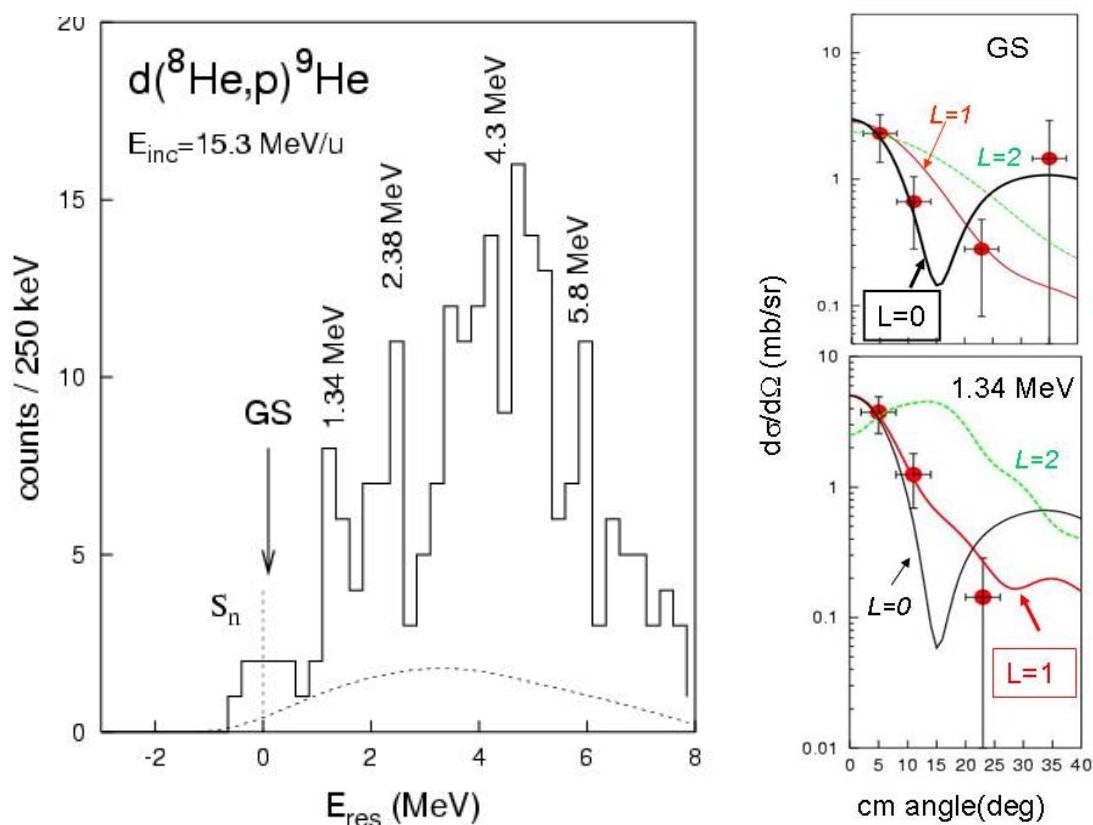


Figure 10: (left) Excitation energy spectrum of  ${}^9\text{He}$ . Zero energy corresponds to the  ${}^8\text{He}+n$  threshold. (right) Comparison of the measured angular distribution at  $E=0\text{MeV}$  and  $E=1.34\text{MeV}$  with calculated angular distribution

## 2.5. Fusion studies with halo nuclei (E403S, E403aS)

Fusion studies with radioactive ion beams are currently investigating the conflicting results/predictions of the influence of weak binding of the projectile. The origin of this is in the fundamentally different treatment of the role of the break-up channel, arising from the low binding of the neutron-rich isotopes. One approach treated the elastic and break-up channels incoherently (as a loss of flux) whereas in the other, the role of break-up was treated in coupled channels formalism as an inelastic excitation in the continuum, implying a coherent superposition of the elastic and break-up channels.

The weak binding of these projectiles leads to a significant cross section for both elastic break-up, transfer reactions and/or break-up followed by capture of a part of it by the target (incomplete fusion, massive transfer or stripping/stripping). Therefore, before interpreting results of fusion cross section measurements with weakly bound projectiles, it is of paramount importance to ensure that the quoted fusion cross section does not contain contributions from other mechanisms.

A first experiment (E403S) was performed using the very early stage of the EXOGAM array coupled with an annular strip detector. Reactions induced by radioactive  ${}^6,8\text{He}$  beams from the SPIRAL facility were studied on  ${}^{63,65}\text{Cu}$  and  ${}^{188,190,192}\text{Os}$  targets and compared to reactions with the stable  ${}^4\text{He}$  projectiles from the Mumbai Pelletron. In the case of the  ${}^6\text{He}$  beam, inclusive prompt  $\gamma$ -ray measurements have been performed in order to obtain residue cross sections (fusion and neutron transfer), and for the first time in a radioactive beam experiment, coincident measurements between  $\gamma$ -rays and light charged particles have been attempted to

address the separation of fusion and neutron transfer mechanisms. In the case of  $^8\text{He}$ , the weak beam intensity and the presence of large background from  $^8\text{He}$   $\beta$ -decay precluded a successful singles measurement; however, coincidences between the charged particles and characteristic  $\gamma$ -rays could be observed.

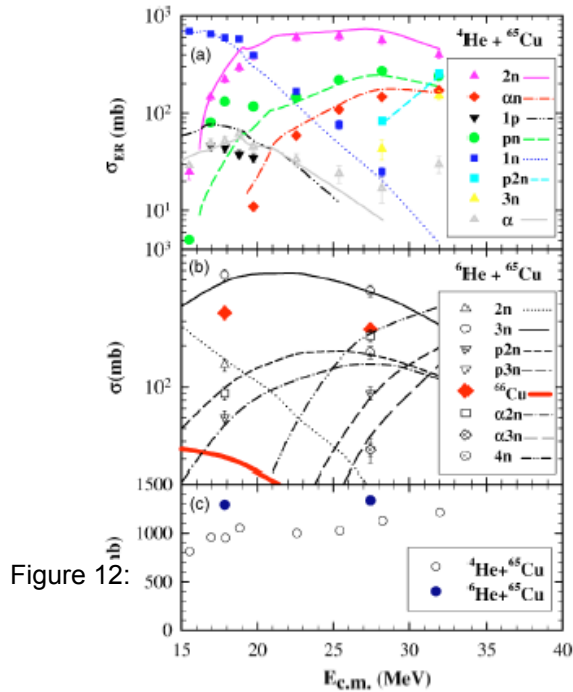


Figure 12:

FIG. (a) Measured partial residue cross sections indicated by different symbols for  $^4\text{He}+^{65}\text{Cu}$  system as a function of the center of mass energy. The lines are obtained using the statistical model code CASCADE (see text). (b) Same as in (a) for the  $^6\text{He}+^{65}\text{Cu}$  system. (c) Total residue cross section for  $^4\text{He}+^{65}\text{Cu}$  (open symbols) and  $^6\text{He}+^{65}\text{Cu}$  (filled symbols). Only statistical errors are shown.

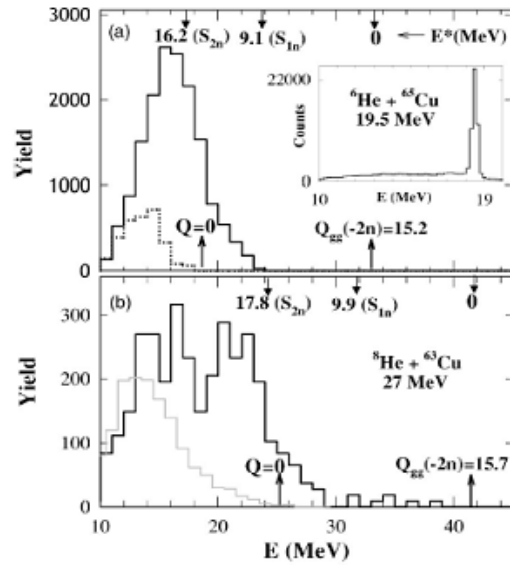


FIG. Charged particles measured in the annular Si detector. (a) In coincidence with the 185.9 keV  $\gamma$  transition in  $^{66}\text{Cu}$  (full line) and 1115.5 keV in  $^{65}\text{Cu}$  (dotted line) for  $^6\text{He}+^{65}\text{Cu}$  at 19.5 MeV at  $\theta_{lab}=35^\circ$ . The yields have been corrected for efficiency and branching of the gating transition. Inset shows the corresponding inclusive spectrum. (b)  $^8\text{He}+^{63}\text{Cu}$  at 27 MeV gated by the 159.1 keV transition in  $^{64}\text{Cu}$  at  $\theta_{lab}=37^\circ$ . The gray curve is a calculated  $\alpha$  evaporation spectrum using a statistical model. The ground state  $Q$  values ( $Q_{gs}$ ) and the neutron separation energies ( $S_n$ ) in the residual nucleus in a two-neutron stripping reaction are indicated.

In the case of the very tightly bound  $^4\text{He}$  projectiles, direct processes are expected to be weak in the energy range studied, and only  $\gamma$ -ray singles were measured to obtain the complete fusion cross sections. A similar measurement for the  $^6\text{He}+^{64}\text{Zn}$  system have been performed at Louvain-la-Neuve.

Partial residue cross sections for fusion and neutron transfer obtained from the measured intensities of characteristic in-beam  $\gamma$ -rays for the  $^6\text{He}+^{63,65}\text{Cu}$  systems are presented in Fig. 11. The large deviation of  $^{66}\text{Cu}$  production from statistical model prediction illustrates the large contribution of transfer. Coincidence measurements of heavy reaction products, identified by their characteristic  $\gamma$ -rays, with projectile like charged particles also provide direct evidence for a large transfer cross section with Borromean nuclei  $^6\text{He}$  at 19.5 and 30 MeV and  $^8\text{He}$  at 27 MeV (Fig. 12). Reaction cross sections were also obtained from measured elastic angular distributions for  $^{6,8}\text{He}+\text{Cu}$  systems. This work underlines the need to distinguish between various reaction mechanisms leading to the same products before drawing conclusions about the effect of weak binding on the fusion process. The feasibility of extracting small cross sections from inclusive in-beam  $\gamma$ -ray measurements for reaction studies near the Coulomb barrier with low intensity isotope separation on-line beams is highlighted. Results are reported in [22].

The purpose of the second experiment (E403aS) was to investigate triple coincidence events between particles, gammas, and also neutrons to allow the deconvolution between 1n and 2n transfer and break-up processes. Indeed, a beam

velocity-like neutron in the forward direction due to  $^5\text{He}$  decay accompanies  $1n$  transfer, while  $2n$  transfer to the target produces evaporation neutrons. The set-up used the EXOGAM gamma array, a  $\Delta E$ - $E$  annular Si telescope and the neutron wall. EXOGAM was optimised to minimize dead time and room background and was used with full Compton shields for the first time. Both the intensity ( $^6\text{He}$ :  $4.5 \cdot 10^7$  pps;  $^8\text{He}$ :  $1.1 \cdot 10^5$  pps) and beam spot size (3.5 mm FWHM) delivered in this experiment have no equivalent so far. The data are at an advanced stage of analysis. They represent the first successful triple coincidence experiments at energies near the Coulomb barrier with radioactive ion beams. The angular distribution measurement of  $1n$  and  $2n$  transfer and stripping will provide useful information on coupling to the continuum and its influence on fusion and elastic scattering. The correct treatment of continuum in coupled channels calculation is of current theoretical interest and the present experiment will provide a useful input for the theoretical models. Preliminary results have been presented at FUSION06 and NN06 conference.

### Perspectives with SPIRAL:

Based on the success of the present experiment with the  $^8\text{He}$  beam, we are attempting to measure lower cross sections at energies lower than the Coulomb barrier. Such studies would benefit of beam developments of  $^{15}\text{C}$ ,  $^{22}\text{O}$ , and  $^{14}\text{O}$  at the intensity level of  $10^5$  pps.

In view of SPIRAL2, the experience gained with these experiments will serve as a benchmark for future experiments, in particular in terms of handling the radioactivity of the beam.

### 2.6. Neutron correlations in the halo nucleus $^6\text{He}$ through nuclear break-up (E528S)

Nuclear break-up has been characterized in inelastic scattering experiment [23], both with stable nuclei and exotic nuclei. The emission of a light particle at large angle is described as due to its interaction with the nuclear potential of the perturbing target nucleus. The particle is diffracted by the nuclear potential and promptly emitted, as its velocity is relatively large compared to the other nucleus. A Time Dependent Schrödinger Equation (TDSE) model in which a one-nucleon wave function bound in a nucleus is perturbed by the nuclear potential of a second nucleus as it passes by has beautifully described this. This emission was first observed with protons in the  $^{40}\text{Ca}$ , then with neutrons in  $^{48}\text{Ca}$ ,  $^{90,94}\text{Zr}$  and  $^{58,62}\text{Ni}$ , and finally with alpha particles in a more complete experiment with  $^{40}\text{Ca}$  [24].

As the TDSE calculation predicted that the angular distribution and the energy of the emitted particle strongly depends on the initial angular momentum in the nucleus, nuclear break-up of the halo nucleus  $^{11}\text{Be}$  was measured in a previous SISSI experiment aiming to study its ground state. The energy distribution of the neutrons emitted at large angle were compared with the TDSE calculation and confirmed that the ground-state wave-function was a mixture of a  $2s_{1/2} \otimes 0^+$  and a  $1d_{5/2} \otimes 2^+$  wave function coupled to a  $2^+$  state of the  $^{10}\text{Be}$  core. Spectroscopic factors of both configurations were thus extracted [25].

The same method was applied to the study of  $^6\text{He}$  ground-state structure. Calculation by Zhukov et al. [26] has predicted that its ground-state was a mixture of di-neutron configuration and cigar configuration but previous experiments studying the Coulomb break-up, two-neutron transfer or radiative capture has lead to controversial results. A new experiment (E528S) aiming at the study of the nuclear

break-up was performed at GANIL in July 2006. Both neutrons of the halo were detected at large angles, in the Neutron Wall and the EDEN detectors positioned in the G2 line, whereas the  $^4\text{He}$  fragments energy and scattering angles were determined using an annular 500  $\mu\text{m}$  Silicon detector backed with a 3 mm Si(Li) detector. The data analysis is currently being performed in parallel to the development of a new TDSE calculation code which will be able to link the angular distribution of the two break-up neutrons to their initial spatial correlation in the ground-state of  $^6\text{He}$  (M. Assié, Ph.D. thesis).

### Perspectives at SPIRAL:

Nuclear break-up studies are of great interest at SPIRAL energies, in particular due to large cross-sections as predicted by our TDSE calculation (of the order of 0.1 barn around 10 to 20 MeV/u). A  $^{11}\text{Li}$  beam of  $10^5$  pps would allow the study of correlations between the halo neutrons.

### 3. [References](#)

- [1] Y. Blumenfeld et al., NIM A421, 471 (1999)
- [2] S. Ottini et al., NIM A431, 476 (1999)
- [3] F. Skaza, PHD thesis, University of Paris XI Orsay, DAPNIA-04-13-T, (2004)
- [4] F. Skaza et al., Phys. Lett. B619, 82 (2005)
- [5] F. Skaza et al., Phys. Rev. C73, 044301 (2006)
- [6] W. Mittig et al., Nucl. Phys. A722, 10c (2003)
- [7] W. Mittig et al, proceedings NENS (2003)
- [8] W. Mittig et al, Eur. Phys. J. A25, 263 (2005)
- [9] C.E. Demonchy et al, J. Phys. G31, S1831, (2005)
- [10] M. Meitner et al., Phys. Rev. Lett. 88, 102501 (2002)
- [11] A.H. Wuosmaa et al., Phys. Rev. C72, 061301 (R) (2005)
- [12] F.M. Marques et al., Phys. Rev. C65, 044006 (2002)
- [13] S. Pieper, Phys. Rev. Lett. 90, 252501 (2003)
- [14] R. Lazauskas and J. Carbonnel, Phys. Rev. C72, 034003 (2005)
- [15] A.A. Korshennikov et al., Phys. Rev. Lett. 90, 08251 (2003)
- [16] S. Fortier et al., Phys. Lett. B 461, 22 (1999); J.S. Winfield et al., Nucl. Phys. A683, 48 (2001)
- [17] S. Pita, Thèse Université Paris VI (2000), S. Pita et al., to be submitted
- [18] L. Chen et al., Phys. Lett. B505, 21 (2001)
- [19] K.K. Seth et al, Phys. Rev. Lett. 58, 19 (1987)
- [20] H.G. Bohlen et al., Z. Phys. A330, 227 (1988), H.G. Bohlen et al., Prog. Part. Nucl. Phys. 42, 17 (1999)
- [21] T. Otsuka et al., Phys. Rev. Lett. 87, 082502 (2001)
- [22] A. Navin et al., Phys. Rev. C70, 044601 (2004)
- [23] J.A. Scarpaci et al., Phys. Lett. B428, 241 (1998)
- [24] M. Fallot, Ph.D. thesis IPNO 2002 T-02-05, web address: <http://tel.ccsd.cnrs.fr/>
- [25] V. Lima, Ph.D. thesis IPNO 2004 T-04-16
- [26] M.V. Zhukov et al., Phys. Rep. 231, 151(1993)



# IV. Magicity and Interactions: Transfer Reaction Spectroscopy at SPIRAL

W. Catford

\* Department of Physics, University of Surrey, Surrey GU2 7XH, United Kingdom

Report on SPIRAL experiments E405S, E443S, E445S, E456S

Contact: [w.catford@surrey.ac.uk](mailto:w.catford@surrey.ac.uk)

## 1. Migration of the magic numbers

The SPIRAL White Book identified the use of transfer reactions with radioactive beams as a key tool to probe the evolution of nuclear orbital energies in exotic neutron-rich isotopes. It was recognized at that time, that the changing energies could affect the “magicity” of a shell closure and change the likelihood of shell breaking effects. At that time, it was not yet realized how dramatic these effects would be. A better understanding of the mechanism [1] for this monopole shift now allows us to understand how, for instance, the valence neutron energies can be very sensitive to the proton occupancies of certain orbitals. Other mechanisms, for example the effect of surface diffuseness, can also affect relative energies via a modified spin-orbit splitting [2]. The energy shifts, it is now realized, serve not only to reduce the magicity at traditional magic numbers of protons and neutrons, but also to cause a migration towards new magic numbers [3].

### A mechanism for monopole shift

Figure 1 illustrates an important feature of the spin-isospin structure on the NN force, which has as its origin the tensor force  $V_T$  that derives largely from the one-pion exchange process [1,4]. If we label the spin-orbit partners as  $j_>$  and  $j_<$  according to whether  $j = \ell + 1/2$  or  $j = \ell - 1/2$  respectively, then it is found that protons with  $j_>$  (or  $j_<$ ) attract neutrons with  $j_<$  (or  $j_>$ ), a result that can be understood by analogy with the structure of the deuteron [1]. This then implies [1,4] that as a  $j_>$  proton orbit is gradually emptied (to make a more neutron rich exotic nucleus) the effect will be to cause an interacting neutron  $j_<$  orbit to rise in energy, and its effective single-particle energy ESPE [5,6] to increase. This is illustrated in Fig. 2. In contrast, the interaction between like couplings such as  $j_<$  and  $j_<$  is of the opposite sign (repulsive). The magnitude of the effect also depends [1] on the angular momenta  $\ell$  and  $\ell'$  and the radial overlap.

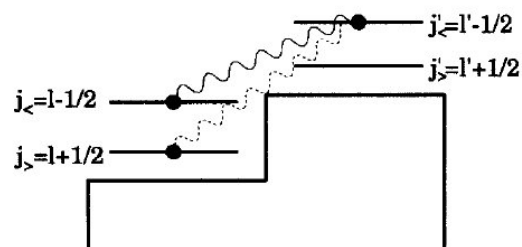


Figure 1: The protons and neutrons in the orbitals  $j_>$  and  $j_<$  exhibit an attractive interaction (dotted line) so that removing protons from orbital  $j_>$  causes  $j_<$  to rise in energy. Conversely, the interaction between protons in  $j_<$  with  $j_>$  is repulsive (solid line) and has the opposite effect. Most importantly, the level of filling of proton orbitals affects the spacings of the neutron orbital energies [1,4].

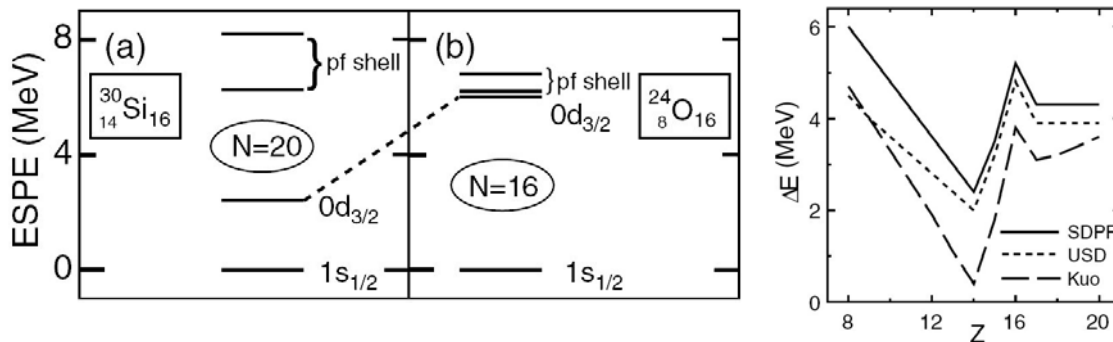


Figure 2: The tensor force between protons and neutrons produces a monopole contribution to the energies of single particle orbitals, and hence the energies depend on the occupancies. As the occupancy of the  $j_>$  orbit  $d_{5/2}$  is reduced in going from (a)  $^{30}\text{Si}$  to (b)  $^{24}\text{O}$ , then the attractive force on  $j_<$   $d_{3/2}$  neutrons is reduced, and the orbital rises relatively in energy. This is shown in the final panel by the  $s_{1/2}$  to  $d_{3/2}$  gap, calculated [7] using various interactions within the Monte-Carlo shell model [8].

### The key places to explore in the nuclear chart

The most accessible instances of monopole shift are those where the proton occupancy of a  $j_>$  orbit in an exotic nucleus can be made exceptionally low compared to the “normal” nuclei that shaped the original parameters of the shell model. In the lighter nuclei ( $A < 50$ ), this happens near closed proton shells since a closed shell is followed in energy by a  $j_>$  orbital. For example, compared to  $^{14}\text{C}$  the nuclei  $^{12}\text{Be}$  and  $^{11}\text{Li}$  (just above  $Z=2$ ) have a reduced  $\pi(0p_{3/2})$  occupancy, so the  $\nu(0p_{1/2})$  is raised and the  $N=8$  magic number is lost [9]. Similarly, compared to  $^{30}\text{Si}$ , the empty  $\pi(0d_{5/2})$  in  $^{24}\text{O}$  ( $Z=8$ ) leads to the breaking of the  $N=20$  magic number, as shown in Fig. 2. Another possible extreme is when a particular neutron orbital is much more complete than normal. Thus, in  $^{40,42}\text{Si}$  the  $\nu(0f_{7/2})$  is essentially filled, compared to stable  $^{30}\text{Si}$  where it is empty along with  $\nu(0d_{3/2})$ , and the attraction between the  $0f_{7/2}$  neutrons and any  $\pi(0d_{3/2})$  protons lowers this proton orbital to be close to the  $\pi(1s_{1/2})$ . This changes the collectivity in  $^{44}\text{S}$ , for example.

### Transfer as the experimental tool to study single particle levels

The key experimental measurement is to locate and identify states in real exotic nuclei that have a large overlap with pure single-particle states. An ideal tool for this is single-nucleon transfer, and in particular the (d,p) reaction that adds neutrons into empty valence orbitals. The strongly populated states will be those with substantial single particle character, and their energies can be compared with shell model calculations. The angular distributions for the transfer can also measure the orbital angular momenta  $\ell$  of the final states, and (with suitable interpretation) a distorted wave analysis can give a quantitative measure of the single particle nature (for example, via spectroscopic factors). If gamma-ray decay information is also measured then, via a comparison with systematics and models, this may allow the actual spin (rather than  $\ell$ ) to be deduced.

## Fitness of SPIRAL for transfer reaction studies

The quality of the beam optics from SPIRAL, plus its energy resolution and high isotopic purity, are all eminently suitable for the study of nucleon transfer [10]. The energy regime reached by SPIRAL is also very reasonably matched. In Fig. 3, the calculations are shown for transfer differential cross sections at several energies (plotted versus laboratory angle, assuming inverse kinematics) [11]. It is apparent that lower energies give higher cross sections and also have shapes that are more distinctive of the transferred  $\ell$  value. An energy of around 10 MeV/u is a good choice for (d,p) from these considerations.

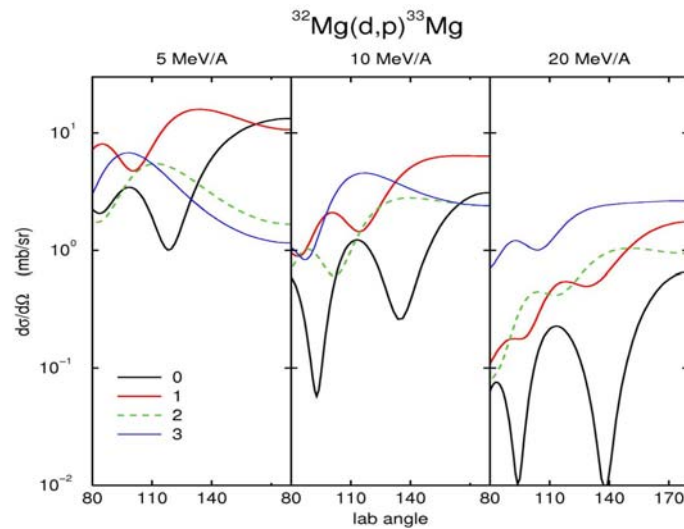


Figure 3: Differential cross sections for (d,p) at various energies, plotted versus laboratory angle for experiments using inverse kinematics with a radioactive beam incident on a deuteron target [11].

## 2. [The case of \${}^7\text{He}\$ : very neutron rich, at the \$Z=2\$ shell closure \(E405S\)](#)

An interesting case studied at SPIRAL concerns the effect on spin-orbit splitting due to the nucleus being very neutron rich [12]. In an experiment led by Saclay, using the MUST array [13] as shown in Fig. 4, the reaction  ${}^8\text{He}(p,d){}^7\text{He}$  was studied in inverse kinematics.

Rather than measuring a monopole shift effect, the question here is whether the diffuseness of the halo surface of  ${}^6\text{He}$  acts to reduce the spin-orbit splitting of the partner orbitals  $\nu(0p_{3/2})$  and  $\nu(0p_{1/2})$  [14]. The results show tentative evidence for a reduced splitting (Fig. 5), but finally conclude that further experimental work is required to improve the measurement [12]. The result is highly topical, especially since a recent (d,p) measurement using a  ${}^6\text{He}$  beam from an in-flight solenoid apparatus at Argonne [15] finds no evidence for a peak of the expected strength at the same low excitation energy. This challenges both the SPIRAL result and the earlier knockout result [14] (Fig. 6).

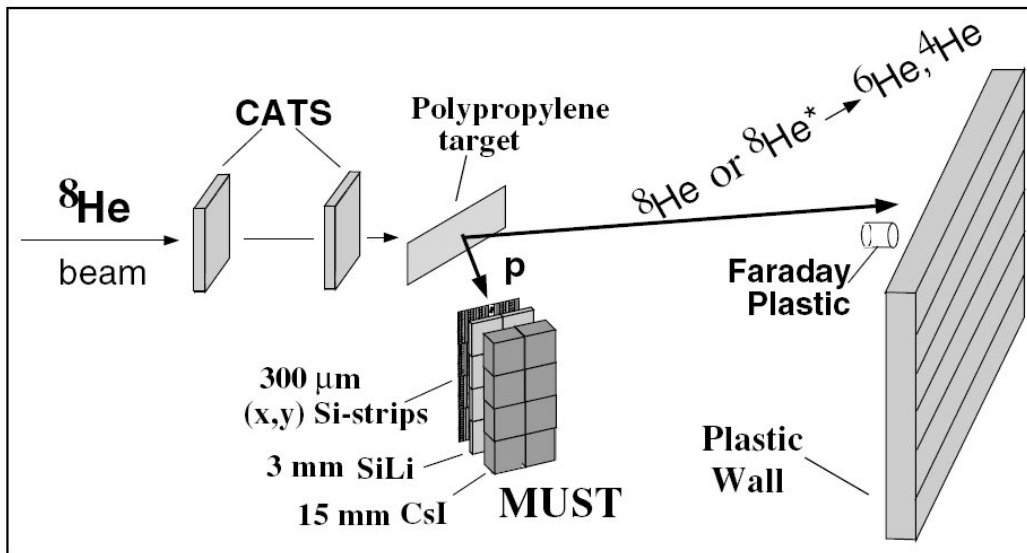


Figure 4: In a study of  ${}^7\text{He}$  [12] a beam of  ${}^8\text{He}$  was used to initiate the nucleon transfer reaction (p,d). A pure beam of up to 14000 particles per second at 15.7 A.MeV was incident on a  $(\text{CH}_2)_n$  target of thickness  $8.25 \text{ mg/cm}^2$ . (The reaction  $p({}^8\text{He}, {}^8\text{He}^*)p$  was also studied). Scattered target particles were recorded using the MUST detector array [13].

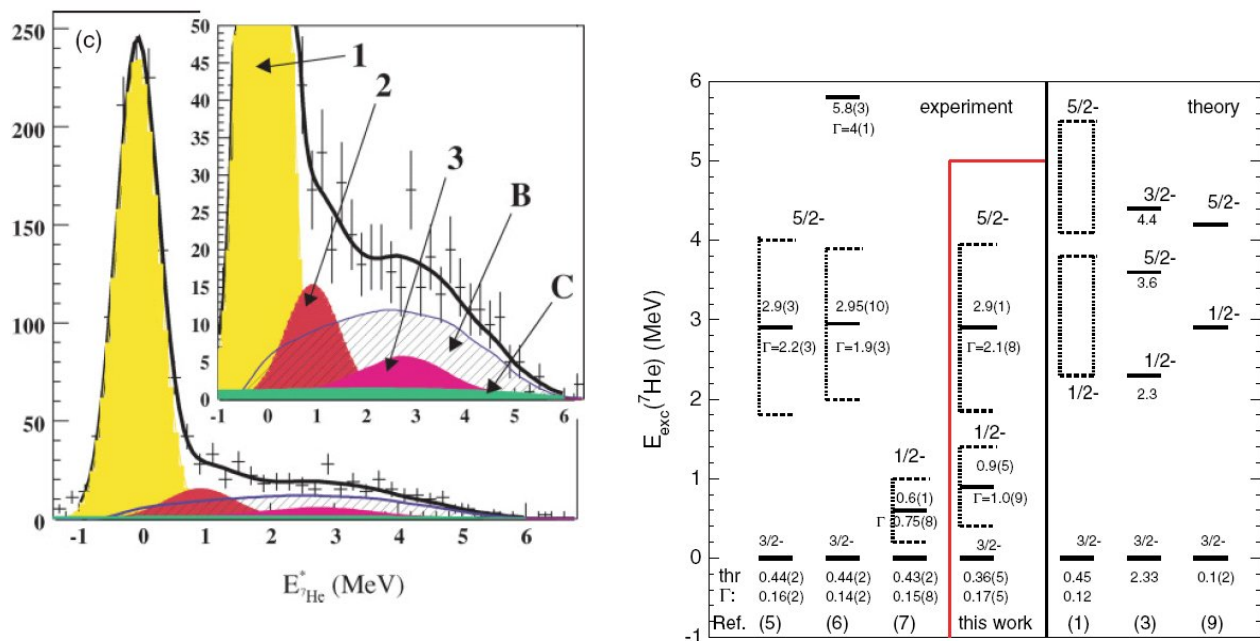


Figure 5: Results from a MUST experiment [12] to study spin-orbit splitting of neutron orbitals in  ${}^7\text{He}$ . The measured spectrum (left) shows: (1) a clear  $3/2^-$  ground state, (2) tentative evidence for a low-lying  $1/2^-$  state and (3) evidence for a higher state, possibly  $5/2^-$ . The level scheme (right) is consistent with the earlier work on high-energy knockout from  ${}^8\text{He}$  [14], which is also included in Fig. 6, but has limited support from other experiments and theory.

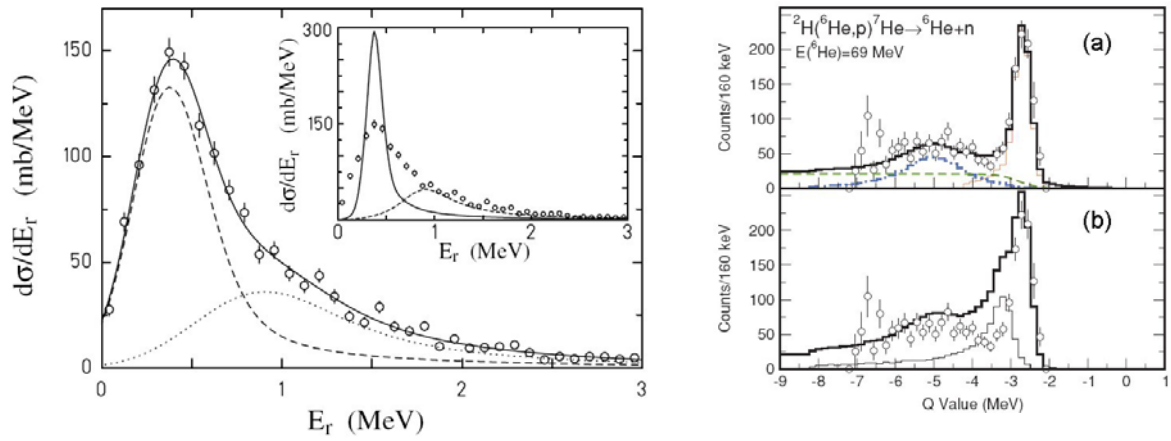


Figure 6: For comparison with the MUST results, the left panel shows the  $^8\text{He}$  knockout data [14], which includes the  $^7\text{He}$  ground state at a  $^6\text{He}+n$  energy of 0.43 MeV and a claimed  $1/2^-$  state at 0.57 MeV above. In contrast, the data from a (d,p) experiment [15] in the right panel show (a) a narrow ground state but (b) with no support for a  $1/2^-$  state of the expected strength, at the corresponding Q value which is 0.57 MeV more negative. (The thin histogram shows the expected  $1/2^-$  strength).

### 3. The cases of $^{25}\text{Ne}$ (E445S) and $^{27}\text{Ne}$ (E443S): very neutron rich, near the Z=8 closure

#### $^{25}\text{Ne}$ : results demonstrating migration from the N=20 to N=16 magic number

The experiments led by the UK TIARA collaboration implemented a highly efficient triple coincidence particle-particle-gamma technique that promises a unique way forward to studying transfer with high resolution. The results obtained [16,17] in the first TIARA experiment, studying  $^{24}\text{Ne}(d,p)^{25}\text{Ne}$ , also show clearly the power of transfer despite its limitation to beams of order  $10^4$  pps in intensity. Although producing the N=15 isotope of neon, the population of the higher single particle levels probes the spacing and migration of the same levels (up to  $0f_{7/2}$ ) as would be probed by the N=21 isotope  $^{31}\text{Ne}$  or similar, in a neutron knockout study. The main feature of the TIARA apparatus is the exceptionally high detection efficiency, which has already allowed a preliminary demonstration of gamma-gamma analysis in four-fold coincidence data (Fig. 9). The results for the energies, spins and spectroscopic factors of newly discovered states in  $^{25}\text{Ne}$  (Figs. 9 and 10) highlight the development of the new N=16 magic number below the  $\nu(0d_{3/2})$  orbital in this neutron rich region. The results have demonstrated deficiencies in the USD interaction and have provided key energy level information that has led, along with recent  $\beta$ -decay measurements, to a much improved version of the USD interaction for the very neutron rich O, F, Ne region [18].

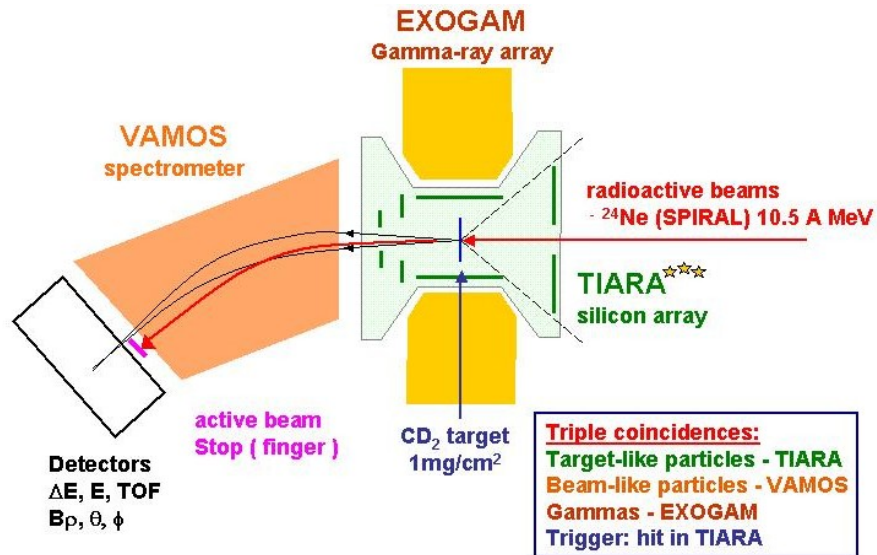


Figure 7: Schematic of the TIARA experimental set-up. A beam of  $10^5$  pps of  $^{24}\text{Ne}$  at 10.5 A.MeV was provided from SPIRAL, limited to  $8\pi$  mm.mrad to give a beam spot size of 1.5-2.0 mm. The target was  $1.0 \text{ mg/cm}^2$  of  $(\text{CD}_2)_n$  plastic. The TIARA array covered 90% of  $4\pi$  with active silicon [16].

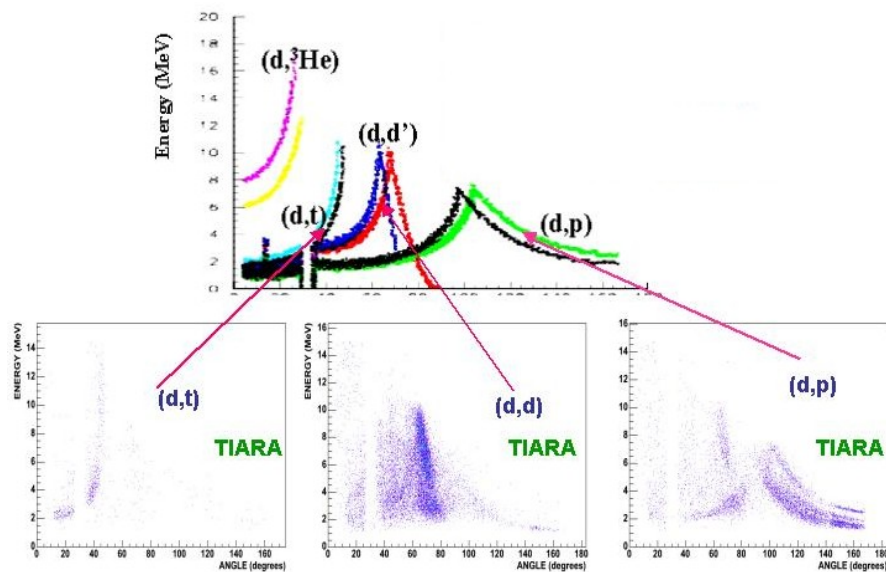


Figure 8: Measured energy-angle curves showing the population of various excited states in different reaction channels, measured simultaneously with TIARA [17]. The different channels were selected according to the identified particle in VAMOS, and are compared with Geant simulations. In this first version of TIARA, the more energetic particles passed through the detectors, depositing  $\Delta E$ .

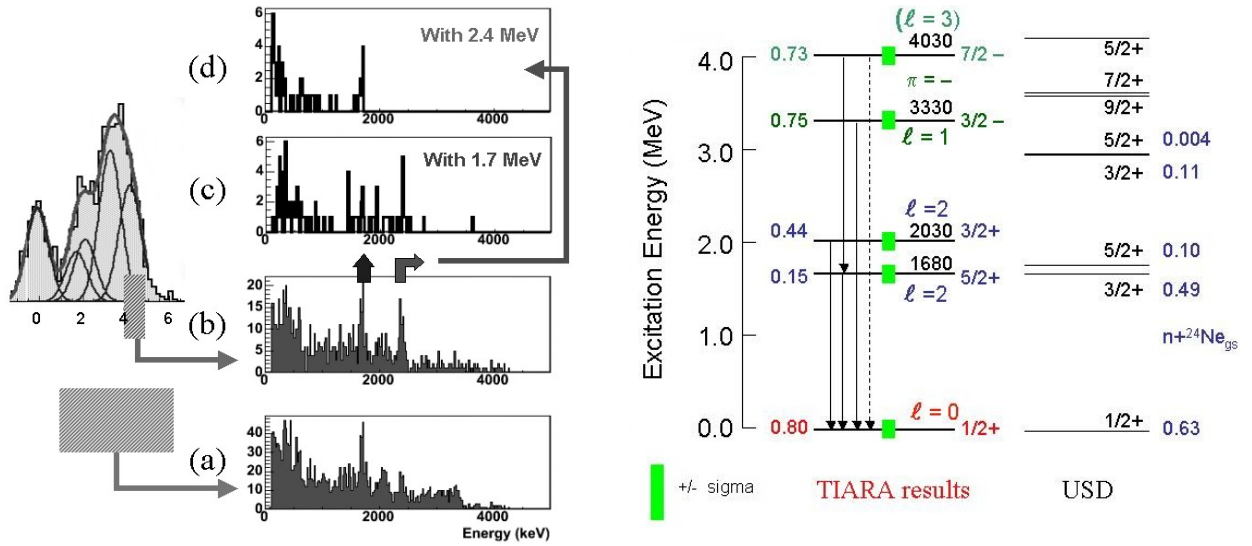


Figure 9: The left panel shows coincident gamma ray spectra from  $^{24}\text{Ne}(d,p\gamma)^{25}\text{Ne}$  studied in inverse kinematics. The spectra (a) and (b) are gated according to the indicated regions of excitation energy in  $^{25}\text{Ne}$  as plotted in the inset spectrum, derived using the measured proton energies and angles. The two prominent gamma peaks are shown by gamma-gamma gating in (c) and (d) to be in cascade. The right hand panel shows the levels identified in  $^{25}\text{Ne}$  and the measured spectroscopic factors, and also highlights the failure of the conventional USD shell model interaction for the raised  $3/2^+$  level [17].

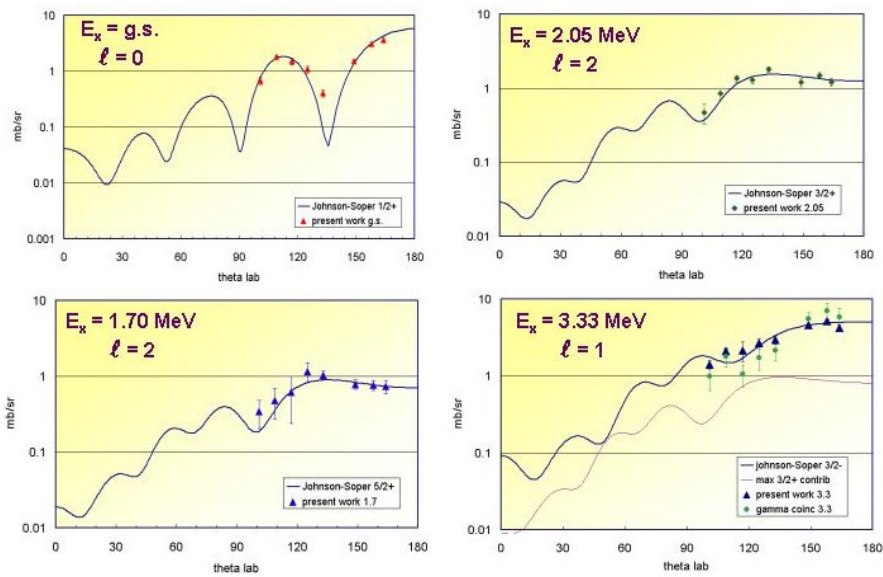


Figure 10: Measured angular distributions (in the laboratory frame) for various states in  $^{25}\text{Ne}$  produced by (d,p) with a  $^{24}\text{Ne}$  beam, with adiabatic reaction model (ADWA) fits [17].

The TIARA results for  $^{25}\text{Ne}$  also serve to demonstrate the utility of the coincident gamma-ray information. Firstly, the vastly superior energy resolution of the Doppler corrected gamma-rays (50 keV) allowed the resolution of states that could not be

resolved in the proton spectrum, and also when fitting the proton spectrum this allowed the centroid energies of states to be specified precisely. Secondly, the gamma-ray decay schemes of individual states could be used to deduce specific spin assignments.

### **<sup>27</sup>Ne: results to demonstrate the breakdown of N=20 as a magic number**

A SPIRAL experiment led by the Saclay group was able to extend transfer studies of neon to <sup>27</sup>Ne and gained the first direct evidence for intruder negative parity states at very low excitation energy in this region [19]. This allows a detailed study of the breakdown of the N=20 magic number, which in turn is responsible for the stability retained by extreme neutron rich F isotopes. The experiment exploited the unique cryogenic target technology developed at GANIL and the excellent Doppler correction provided by the highly efficient and segmented EXOGAM array (Fig. 12). This technique does not allow spin assignments except in principle by  $\gamma$ -particle and  $\gamma$ - $\gamma$  angular correlation techniques, but it does have an advantage in terms of the relatively thick and pure D<sub>2</sub> target.

The experiment observed the population of two low levels in <sup>27</sup>Ne, one of which was identified as the expected 1/2<sup>+</sup> state from the sd-shell  $\nu(0d_{3/2})^2\nu(1s_{1/2})^{-1}$  coupling and one of which is believed to be the intruder 3/2<sup>-</sup> level (Fig. 13). The systematics (Fig. 14) show clearly the developing N=20 breakdown. Extended shell model calculations to include the fp-shell (Fig. 14), along with neutron knockout data using <sup>28</sup>Ne, also support the existence of this low-lying negative parity structure [20]. The predicted 7/2<sup>-</sup> level is likely isomeric, so that its detection was precluded in these experiments.

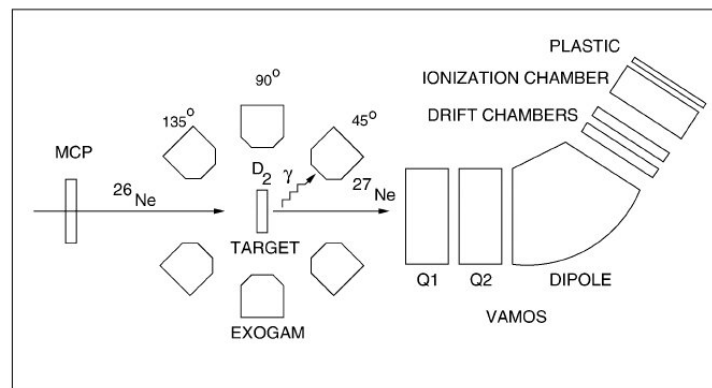


Figure 11: Schematic of the experimental set-up to study <sup>27</sup>Ne by the reaction (d,p) on <sup>26</sup>Ne in inverse kinematics, using a cryogenic deuterium target together with EXOGAM and VAMOS [19]. An isotopically pure beam of 3000 pps of <sup>26</sup>Ne at 9.7 A.MeV was provided from SPIRAL. The solid D<sub>2</sub> target was 17 mg/cm<sup>2</sup> thick, which prevented the detection of the proton reaction products. The clear separation and identification in Z and A for <sup>27</sup>Ne used ToF,  $\Delta E$  and B $\rho$  measurements in VAMOS.

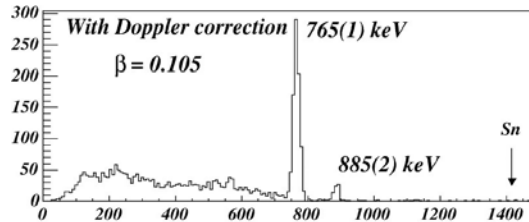


Figure 12: Energy spectrum of gamma rays in coincidence with  $^{27}\text{Ne}$ , for the  $^{26}\text{Ne} + d$  study [19].

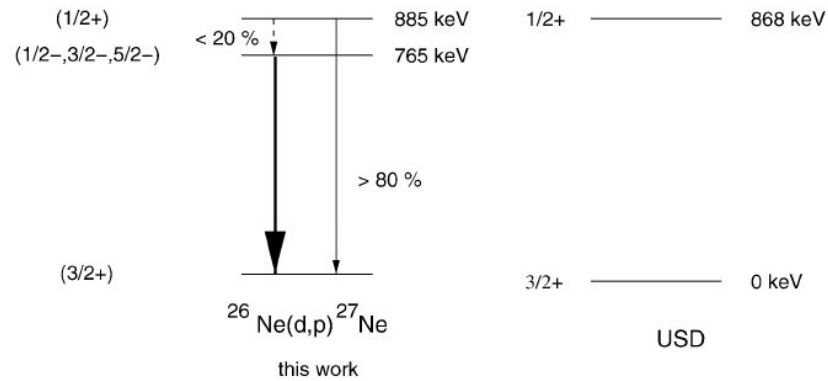


Figure 13: Energy levels in  $^{27}\text{Ne}$  deduced from the  $^{26}\text{Ne}+d$  experiment [19]. If the spectrum has two low-lying levels, this implies that one of them must have negative parity, by comparison with USD.

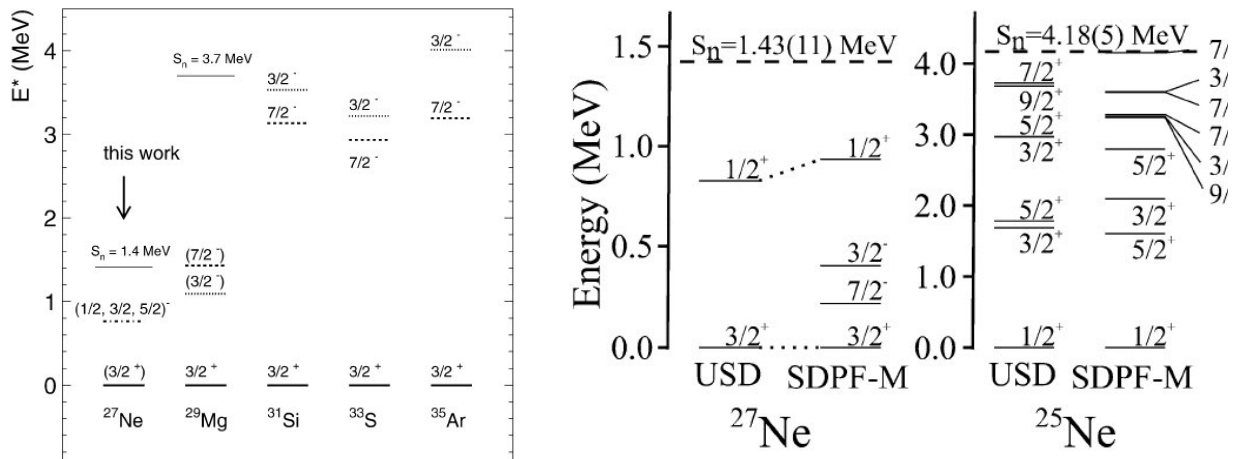


Figure 14: The level systematics of  $N=17$  isotones in the left panel [19] show the disappearance of the  $N=28$  magic number as protons are removed from the  $\pi(0d_{5/2})$  orbital, such that the energy of the  $\nu(0d_{3/2})$  energy rises to approach the  $\nu(0f_{7/2})$ . The right hand panel [20] shows that a very recent large basis shell model calculation can reproduce the observed intrusion of negative parity states from the  $fp$  shell, so that they come below the energy of the first excited  $sd$ -shell state.

#### 4. [The cases of \$^{47}\text{Ar}\$ : very neutron rich, near the \$Z=20\$ shell closure \(E456S\)](#)

An experiment led by an Orsay group used the MUST array (see Fig. 15) to study the changes in single particle energies in a nucleus with two fewer protons than  $^{48}\text{Ca}$ . The experiment used a beam of the N=28 isotone,  $^{46}\text{Ar}$ , to bombard a deuterated target. The SPEG spectrometer allowed detection and identification of the beam-like particles, both for  $^{47}\text{Ar}$  from the (d,p) reaction in inverse kinematics and for  $^{46}\text{Ar}$  from the sequential break-up of  $^{47}\text{Ar}$  unbound states. In fact, the angular acceptance of SPEG was not quite sufficient, especially in the case of the  $^{47}\text{Ar} \rightarrow ^{46}\text{Ar} + n$ , and it was necessary also to analyse data taken without the SPEG coincidence requirement. (The acceptance of VAMOS is increased by more than an order of magnitude, an improvement that is however accompanied by a poorer physical separation of different masses at the focal plane).

The energy resolution achieved for excited states in  $^{47}\text{Ar}$  (see Fig. 16) was 420 keV (FWHM), but this was limited by some detector degradation; in the same experiment an outstanding resolution of 280 keV was achieved for (d,p) with a beam of  $^{44}\text{Ar}$  [21].

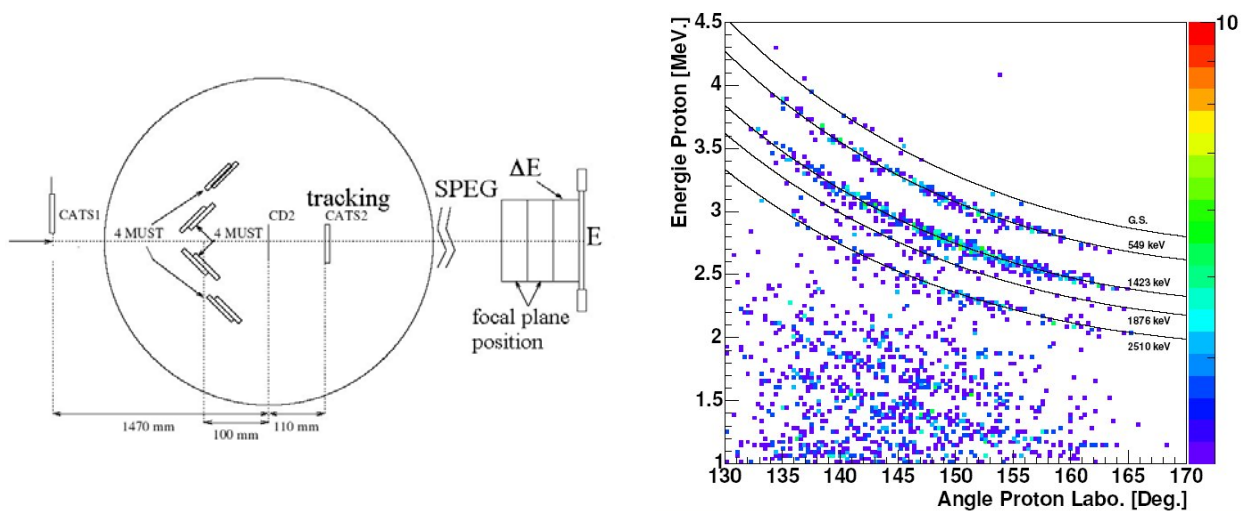


Figure 15: Schematic diagram of the experimental set-up for the (d,p) experiment with a beam of  $^{46}\text{Ar}$  [21]. A pure beam of  $2 \times 10^4$  pps of  $^{46}\text{Ar}$  at 10.2 A.MeV was obtained from SPIRAL and was focussed into SPEG with special parallel optics ( $\Delta\theta < 2$  mrad) so that the beam could be tracked using a single detector after the target. The target thickness was  $0.38 \text{ mg/cm}^2$  of  $(\text{CD}_2)_n$  plastic. The right hand panel shows data from  $^{44}\text{Ar}(d,p)^{45}\text{Ar}$ , taken in the same experiment, where the kinematic lines indicating the population of different states in  $^{45}\text{Ar}$  are clearly evident [21].

The measured differential cross sections for individual states (Fig. 17) gave angular momentum assignments as shown in Fig. 16. In addition, the absolute Q-value of the reaction gave an improved and corrected measurement of the mass of  $^{47}\text{Ar}$ . With this information, the spin-orbit splitting in  $^{47}\text{Ar}$  for the 0f and 1p orbital partners could be determined and compared to  $^{49}\text{Ca}$  (Fig. 18). A reduction in the splitting of 10% for 0f and 45% for 1p was measured. The reduction in the 0f orbital splitting can be explained by the monopole effect of the tensor force [22]. In contrast, the removal of  $0d_{3/2}$  and/or  $1s_{1/2}$  protons will have little effect on the 1p energies and thus a different explanation was proposed for the large effect on the 1p splitting. It was suggested that the removal of two protons has a significant effect on the nuclear density in the interior region and that the splitting of the p orbitals is particularly sensitive to the interior density [22].

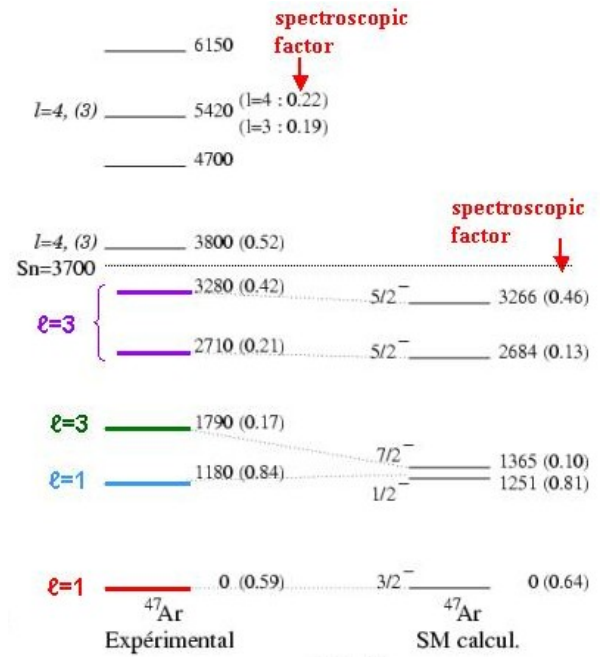
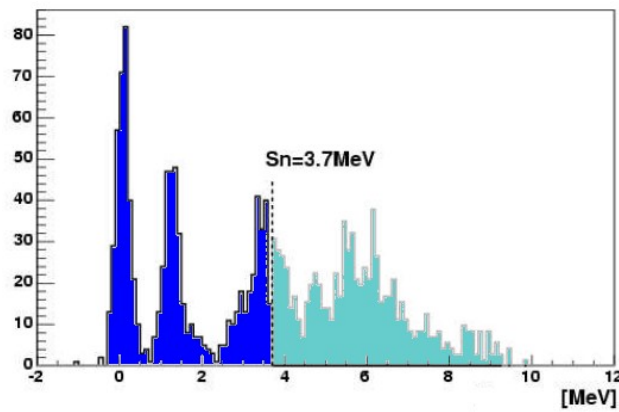


Figure 16: Above, the excitation energy spectrum of  $^{47}\text{Ar}$  calculated from protons produced in the  $^{46}\text{Ar}(d,p)$  reaction in inverse kinematics [21]. Bound and unbound states are tagged by  $^{47}\text{Ar}$  and  $^{46}\text{Ar}$  seen in SPEG, respectively. Right: the energy level scheme deduced for  $^{47}\text{Ar}$  [21], together with the measured spectroscopic factors and shell model calculations.

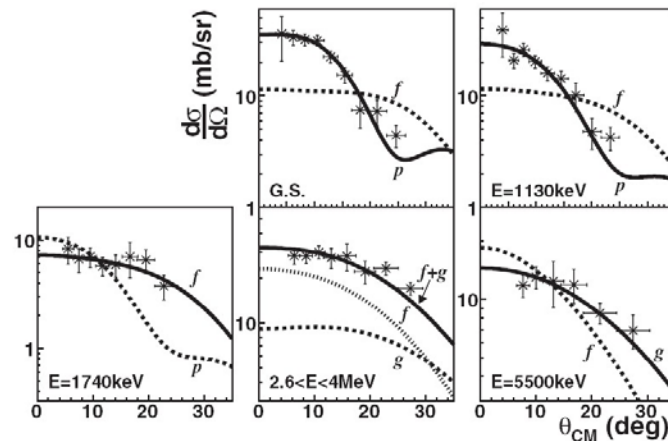


Figure 17: Measured differential cross sections for states in  $^{47}\text{Ar}$  produced by  $(d,p)$ , plotted in the centre of mass frame, together with distorted wave calculations that identify the transferred angular momentum [22].

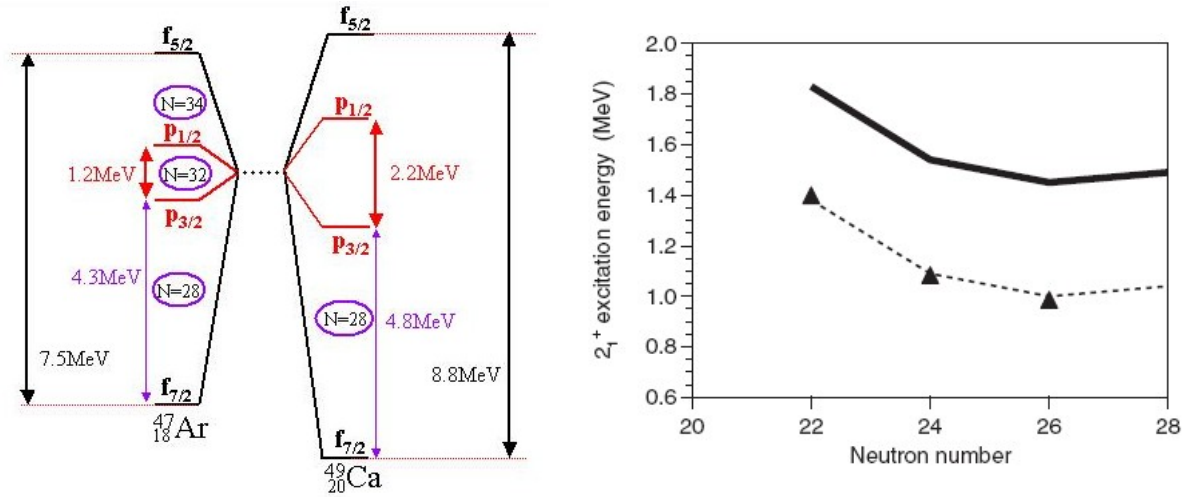


Figure 18: The left panel shows results from the  $^{46}\text{Ar}(d,p)$  experiment, comparing the reduced spin-orbit splitting inferred for  $^{47}\text{Ar}$  with the splitting in  $^{49}\text{Ca}$  [23], which can in part be explained by the removal of two protons from the  $\pi(0d_{3/2}, 1s_{1/2})$  orbitals. The right panel shows, indirectly, the extreme situation predicted when further protons are removed to make Si: the reduced N=28 gap leads to very low energies (dashed line) for the  $2^+$  states in Si isotopes, arising from neutron excitations [24].

## 5. [Planned experiments to extend the study of these effects](#)

Further, approved experiments to extend the work described here will use beams of:  $^8\text{He}$  to improve the results for  $^7\text{He}$  (along with other aims concerning the  $^8\text{He}$  structure),  $^{26}\text{Ne}$  to measure explicitly the spins in  $^{27}\text{Ne}$  and to try and identify the expected low-lying  $7/2^-$  isomeric state,  $^{20}\text{O}$  to track the energy of the  $\nu(0d_{3/2})$  orbital when the  $\pi(0d_{5/2})$  orbital is completely emptied in  $^{21}\text{O}$ , and  $^{34}\text{Si}$  (but, here, having to use a fragmentation beam rather than SPIRAL) to probe the collapse of the N=28 magic number when  $\pi(0d_{3/2})$  is emptied. These experiments are led by Saclay ( $^8\text{He}$ ), the UK TIARA collaboration ( $^{26}\text{Ne}$  and  $^{20}\text{O}$ ) and a GANIL/TIARA/MUST2 collaboration ( $^{34}\text{Si}$ ) respectively. The  $^8\text{He}$  experiment will use MUST and MUST2. The others will use TIARA or a combined TIARA and MUST2 set-up, together with VAMOS and EXOGAM. (Note that additional transfer experiments led by Orsay using MUST2 (+TIARA) with fragmentation beams have been approved).

## 6. [Conclusions and perspectives for new beams at SPIRAL](#)

The work described here has exploited beams of  $^8\text{He}$ ,  $^{24,26}\text{Ne}$  and  $^{46}\text{Ar}$  from SPIRAL, at intensities of  $1.4 \times 10^4$ ,  $1.0 \times 10^5$ ,  $3.0 \times 10^3$  and  $2.0 \times 10^4$  pps. The extensions will further exploit these beams, plus  $^{20}\text{O}$  at an anticipated  $10^4$  pps. Improved intensities, especially for Ne and O would be welcome. The work with Ne and O to probe the regions of the N=16, 20 and 28 magic numbers could be extended to use odd-Z beams to further probe the proton-neutron effective interaction in the shell model. This would involve neutron rich beams of F and Na and possibly (with even Z) Mg. The initiative recently endorsed by the GANIL PAC, to develop intense  $^{11}\text{Li}$  beams for SPIRAL, could be extended to produce Na beams. These are available at ISAC2/TRIUMF at good intensities, but for example the  $^{27}\text{Na}$  beam is subject to contamination from  $^{27}\text{Al}$  at ISAC2

and possibly CIME could give improved purity. Similarly, the  $^{11}\text{Li}$  development could also benefit the alkali element K, perhaps allowing beams up to  $^{47}\text{K}$ . Finally, remembering that a beam of  $^{56}\text{Ni}$  was successfully used for transfer at Argonne [25], it is also perhaps useful to consider producing  $^{56}\text{Ni}$  activity and then preparing it to run in a stand-alone source for CIME. Among the many challenges for  $^{56}\text{Ni}$ , however, is the fact that it decays to  $^{56}\text{Co}$  and then these two nuclides with  $A=56$  are too close in mass to be separated by CIME. Depending on the Co/Ni ratio, a particle-by-particle tagging system could be possible, either before or after the final reaction target. In addition, other types of reaction study could benefit: for example, fusion-evaporation reactions to produce  $N\sim Z$  nuclei near  $^{100}\text{Sn}$  and above may be able to accept a mixed Co/Ni beam.

## 7. [References](#)

- [1] T. Otsuka et al., Phys. Rev. Lett. 95, 232502 (2005)
- [2] J. Dobaczewski et al., Phys. Rev. C53, 2809 (1996)
- [3] H. Grawe et al., Eur. Phys. J. A25, 357 (2005)
- [4] T. Otsuka et al., Phys. Rev. Lett. 97, 162501 (2006)
- [5] A. Poves and A. Zuker, Phys. Rep. 70, 235 (1981)
- [6] Y. Utsuno et al., Phys. Rev. C60, 054315 (1999)
- [7] T. Otsuka et al., Phys. Rev. Lett. 87, 082502 (2001)
- [8] T. Otsuka et al., Prog. Part. and Nucl. Phys. 47, 319 (2001)
- [9] S.D. Pain et al., Phys. Rev. Lett. 96, (2006) 032502
- [10] J.S. Winfield, W.N. Catford and N.A. Orr, Nucl. Inst. Meth. Phys. Res. A396, 147 (1997)
- [11] ADWA Calculations using TWOFNR, W.N. Catford, Private Communication.
- [12] F. Skaza et al., Phys. Rev. C73, 044301 (2006)
- [13] Y. Blumenfeld et al., Nucl. Inst. Meth. Phys. Res. A421, 471 (1999)
- [14] M. Meister et al., Phys. Rev. Lett. 88, 102501 (2002)
- [15] A.H. Wuosmaa et al., Phys. Rev. C72, 061301(R (2005))
- [16] W.N. Catford et al., Eur. Phys. J. A25, 245 (2005)
- [17] B. Fernandez-Dominguez et al, Frontiers in Nucl. Structure: FINUSTAR 2005, S.V. Harissopulos et al., Eds. AIP Conf. Proceedings 831 (2006); W.N. Catford et al., Proc. Carpathian Summer School of Physics 2005, S. Stoica, L. Trache and R.E. Tribble, Eds. (World Scientific, 2006)
- [18] S.W. Padgett et al., Phys. Rev. C72, 064330 (2005)
- [19] A. Obertelli et al., Phys. Lett. B633, 33 (2006)
- [20] J.R. Terry et al., Phys. Lett. B640, 86 (2006)
- [21] L. Gaudefroy, Ph.D. thesis, Orsay (2005).
- [22] L. Gaudefroy et al., Phys. Rev. Lett. 97, 092501 (2006)
- [23] O. Sorlin, private communication
- [24] C.M. Campbell et al., Phys. Rev. Lett. 97, 112501 (2006)
- [25] K.E. Rehm , Phys. Rev. Lett. 80, 676 (1998)



# V. Nuclear shapes and shape coexistence Gamma-ray spectroscopy at SPIRAL

A. Görgen\* for the EXOGAM and AGATA collaborations

\* CEA-SACLAY, DSM/DAPNIA/SPhN, F-91191 Gif-sur-Yvette, France

Report on SPIRAL experiments E344S, E404S, E408S and E493S

Contact: [andreas.goergen@cea.fr](mailto:andreas.goergen@cea.fr)

## 1. Coulomb excitation

Low-energy Coulomb excitation well below the Coulomb barrier is a purely electromagnetic process in which collective states can be excited in multiple steps up to relatively high spins. The electromagnetic matrix elements can be extracted from the measured Coulomb excitation cross section. While the excitation probability is to first order proportional to the square of the transitional matrix elements, *i.e.* to the  $B(E2)$  values, the second-order reorientation effect introduces a dependence on the diagonal matrix elements, so that the cross section becomes sensitive to the static quadrupole moments including their sign. Low-energy Coulomb excitation can thus directly distinguish between prolate and oblate shapes. Such measurements were until recently only possible for stable nuclei. The SPIRAL facility at GANIL provides high-quality radioactive beams at energies near the Coulomb barrier, which are ideally suited for projectile Coulomb excitation. The EXOGAM array of Ge clover detectors is coupled to a highly segmented annular Si detector for the scattered particles in these experiments.

### Shape coexistence in light Krypton isotopes (E344S)

The neutron-deficient krypton isotopes near the  $N=Z$  line are considered to be among the best examples for nuclear shape coexistence. States of prolate and oblate shape are thought to coexist within a narrow energy range of only a few hundred keV. This competition can be understood from the existence of large shell gaps in the single-particle spectrum at proton and neutron numbers 34, 36, and 38, both for prolate and oblate deformation. Experimental evidence for shape coexistence in the light krypton isotopes comes from the observation of low-lying excited  $0^+$  states. Based on their excitation energy, the electric monopole strength of their decay to the ground state, and the distortion of the otherwise regular rotational bands at low spin, a scenario has been proposed in which the ground states of the heavier isotopes  $^{76,78}\text{Kr}$  have a prolate shape, prolate and oblate configurations strongly mix in  $^{74}\text{Kr}$ , and the oblate configuration dominates the ground state of  $^{72}\text{Kr}$  [1]. The experiments of the E344S program aimed at testing this scenario by measuring both transitional and static electromagnetic moments in these nuclei, which represents also a sensitive probe for modern “beyond mean field” theories.

Two experiments to study the radioactive isotopes  $^{76}\text{Kr}$  and  $^{74}\text{Kr}$  were performed in June 2002 and April 2003. In both cases SPIRAL delivered high-quality beams with intensities of  $5 \cdot 10^5$  and  $10^4$  ions per second for  $^{76}\text{Kr}$  and  $^{74}\text{Kr}$ , respectively. Scattered Kr projectiles and recoiling target nuclei were measured in a

highly segmented annular Si detector mounted at forward angles. Deexcitation  $\gamma$ -rays were detected with the EXOGAM spectrometer, which was used in its close configuration with 7 and 11 Ge clover detectors, respectively. Different beam energies and targets (Pb, Ti) were used in order to optimise the sensitivity of the experiment.

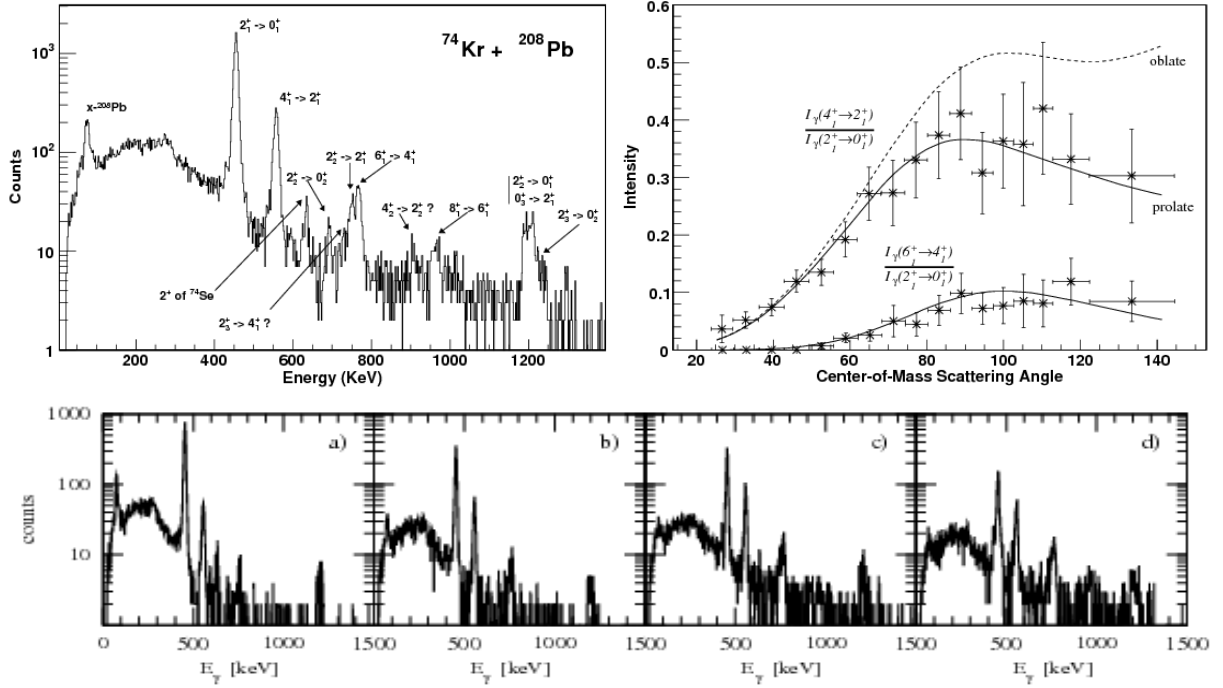


Figure 1: Total  $\gamma$ -ray spectrum after Coulomb excitation of  $^{74}\text{Kr}$  on a  $^{208}\text{Pb}$  target (*top left*). The same spectrum has been divided into different ranges of scattering angles (*bottom*):  $24^\circ < \theta_{\text{cm}} < 54^\circ$  (a),  $54^\circ < \theta_{\text{cm}} < 74^\circ$  (b),  $67^\circ < \theta_{\text{cm}} < 97^\circ$  (c),  $97^\circ < \theta_{\text{cm}} < 145^\circ$  (d). The resulting  $\gamma$ -ray yields for the  $4^+ \rightarrow 2^+$  and  $6^+ \rightarrow 4^+$  transitions, normalized by the  $2^+ \rightarrow 0^+$  transition, as a function of center-of-mass scattering angle (*top right*). The full lines show the intensities calculated from the full set of matrix elements obtained in the GOSIA fit. The dashed line results from inverting the sign of the diagonal matrix elements in the ground-state band from prolate to oblate.

Gamma-ray spectra obtained in the  $^{74}\text{Kr}$  experiment are shown in Fig. 1. The level of statistics reached in the  $^{76}\text{Kr}$  experiment is higher due to the higher beam intensity. The quality of the spectra is comparable to those obtained with stable beams. The beams were pure and only in the case of  $^{74}\text{Kr}$  a small contamination of  $\sim 1\%$  of  $^{74}\text{Se}$  was detected. The excitation probability for several low-lying yrast and non-yrast states in both isotopes was extracted from the  $\gamma$ -ray yields as function of the scattering angle. Both transitional and diagonal matrix elements were determined in a  $\chi^2$  minimization reproducing the observed yields. During the analysis discrepancies with earlier lifetime measurements were found. A new lifetime measurement was performed and confirmed the Coulomb excitation data [2]. The precise transition strengths obtained in this complementary measurement were used as constraints in the Coulomb excitation analysis, improving the sensitivity to the diagonal matrix elements significantly. Positive values are found for the static quadrupole moments of the states in the ground-state band for both  $^{74}\text{Kr}$  and  $^{76}\text{Kr}$ , proving that they have prolate shape. The quadrupole moments of the excited  $2^+$

states are negative, showing their oblate deformation. This result represents the first direct proof for oblate-prolate shape coexistence in the light krypton isotopes. The experiments exploited for the first time the reorientation effect with a radioactive beam. Furthermore, about 15 transitional matrix elements between low-lying states were determined in each isotope, giving information about the mixing of the wave functions.

The analysis of the data is completed and the experiments are the subject of two PhD theses [3,4]. The results have been presented at major conferences in Europe and the US, and a detailed publication is currently being prepared [5]. The experiments have also triggered theoretical work; one detailed comparison between the experimental results and configuration-mixing calculations using the generator coordinate method has already been published [6] and another is in preparation [7].

The experiments have shown that high-precision Coulomb excitation measurements are feasible for collective nuclei with radioactive ion beams of intensities as low as  $10^4$  ions per second. The main advantages of SPIRAL over other RIB facilities such as REX-ISOLDE are the higher beam energy, which allows the use of heavy targets, and the high beam purity, both of which are essential for reorientation measurements.

The next step in this program would be a similar measurement on  $^{72}\text{Kr}$ , which is expected to be one of only very few nuclei with oblate ground-state deformation. The beam intensity for  $^{72}\text{Kr}$  of  $\sim 100$  pps is presently not sufficient for such an experiment. A measurement of  $B(E2)$  values and potentially the quadrupole moment of the first  $2^+$  state would become feasible if the primary  $^{78}\text{Kr}$  beam intensity was increased to the allowed limit of 3 kW by installing the GTS source. Not only SPIRAL experiments with Kr and Ar beams, but also experiments using the SISSI or LISE targets would strongly benefit from the higher primary beam intensity delivered by this source. A full reorientation measurement for  $^{72}\text{Kr}$  would become feasible if  $^{12}\text{C}$  induced fragmentation of Nb or  $\text{ZrO}_2$  targets was used rather than projectile fragmentation.

### **Shell structure and shape coexistence in neutron-rich Ar isotopes (E493S)**

The primary question addressed by this experiment is the possible weakening of the  $N=28$  shell closure in neutron-rich nuclei and, closely connected to that, the development of deformation and shape coexistence in these nuclei. The goals of the first experiment concerning  $^{44}\text{Ar}$  were to measure the transition strength to the first  $2^+$  state with high precision, determine the static quadrupole moment of the  $2^+$  state, identify the  $4^+$  and second  $2^+$  states unambiguously, and measure the matrix elements connecting these states. This multi-step Coulomb excitation experiment at safe energy below the Coulomb barrier is currently only possible at GANIL. The very precise  $B(E2; 0^+ \rightarrow 2^+)$  value resulting from this measurement can be compared to a value obtained at intermediate energy at MSU [8], testing the reliability of intermediate-energy experiments. Together with  $(p,p')$  scattering data from MSU [9], the GANIL experiment will provide a more precise value for the  $M_n/M_p$  ratio of neutron and proton matrix elements. A second part of the program to study the Coulomb excitation of  $^{46}\text{Ar}$  has been presented to the GANIL PAC but was not approved.

The  $^{44}\text{Ar}$  projectiles were Coulomb excited on  $^{208}\text{Pb}$  and  $^{109}\text{Ag}$  targets at two different beam energies. Gamma rays were detected in the EXOGAM array comprising 10 clover detectors (out of 12 that were requested). An improvement over the Coulomb excitation experiments of Kr isotopes was the use of a new silicon detector for the scattered particles with higher segmentation, which resulted in an improved Doppler correction and hence higher resolution of the  $\gamma$ -ray spectra. The silicon detector was equipped with 160 channels of TIARA electronics. Dedicated ASIC electronics for this detector is currently under development at Saclay and will be available in 2008. The CSS1 and CSS2 cyclotrons provided the maximum  $^{48}\text{Ca}$  primary beam intensity of almost 600 W on the SPIRAL target over the entire period of the experiment. The secondary  $^{44}\text{Ar}$  beam had the required intensity of  $\sim 3 \cdot 10^5$  pps and was very stable. A good beam focus and minimization of beam satellites was required in order to limit direct beam impinging on the silicon detector. While this could not be avoided entirely, the machine operators were very efficient in providing a beam of sufficiently high quality. A contamination of the beam with stable  $^{132}\text{Xe}$  was detected during the experiment. This contaminant complicates the data analysis, but will not compromise the main goals.

The experiment was performed in April 2006. Data analysis is currently ongoing at Saclay. Preliminary spectra are shown in Fig. 2. Coulomb excitation on the  $^{208}\text{Pb}$  target populated the first  $2^+$  state in  $^{44}\text{Ar}$  and at least two higher-lying states. With the  $^{109}\text{Ag}$  target both projectile and target nuclei were excited, which can be used to normalize the excitation probability in  $^{44}\text{Ar}$  with the well-known transition strengths of  $^{109}\text{Ag}$ . Having two independent high-statistics measurements will allow extracting a very precise  $B(E2; 0^+ \rightarrow 2^+)$  value. The level of statistics is sufficient to divide the data into several subsets corresponding to different ranges of scattering angles. The static quadrupole moment (including its sign) will be determined from the differential Coulomb excitation cross section. To have data on two different target materials gives additional constraints. Higher-lying states in  $^{44}\text{Ar}$  had been previously observed at GANIL after beta decay of  $^{44}\text{Cl}$  [10], but no firm assignments could be made. At least two of these states are also populated in Coulomb excitation on the  $^{208}\text{Pb}$  target, and their excitation probabilities will allow spin and parity assignments.

Even though the data analysis is still in a preliminary stage, it is anticipated that the main goals of the experiment will be achieved. The static quadrupole moment of the  $2^+$  state will provide information on the prolate or oblate character of the deformation. Experimental matrix elements provide a stringent test for the theoretical description of the development of deformation in the neutron-rich Ar isotopes, for example with configuration mixing calculations using the generator coordinate method based on HFB mean-field states.

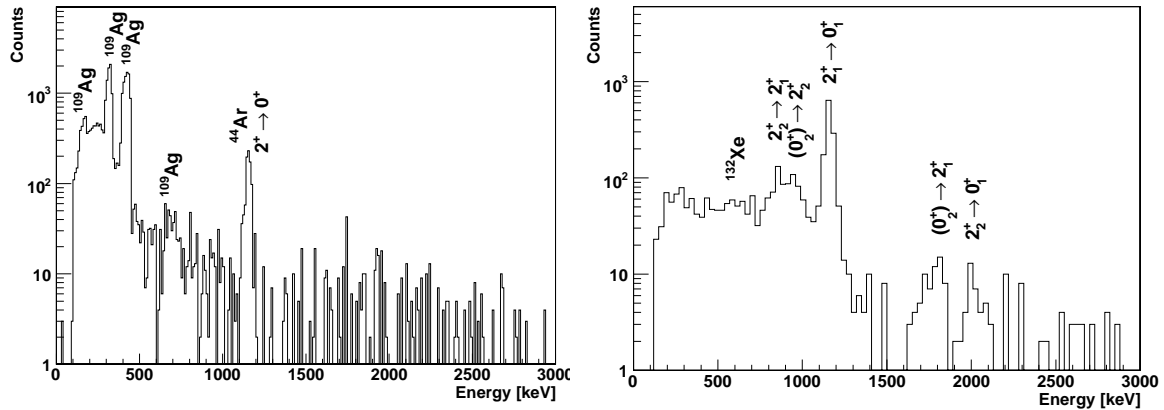


Figure 2. *Left:* Gamma-ray spectrum in coincidence with  $^{44}\text{Ar}$  projectiles scattered on a  $^{109}\text{Ag}$  target, corresponding to scattering angles of  $35^\circ < \theta_{\text{cm}} < 72^\circ$ . The  $2^+ \rightarrow 0^+$  transition is observed together with several transitions in  $^{109}\text{Ag}$ , which can be used for normalization. *Right:* Gamma-ray spectrum in coincidence with recoiling  $^{208}\text{Pb}$  target nuclei, corresponding to scattering angles of  $67^\circ < \theta_{\text{cm}} < 130^\circ$ . In addition to the  $2^+ \rightarrow 0^+$  transition, four transitions from two higher-lying states in  $^{44}\text{Ar}$  are visible. Their spin assignments are preliminary.

Once the data analysis is further advanced and more definitive results can be presented, we plan to propose again the next step in this experimental program: the Coulomb excitation of  $^{46}\text{Ar}$  from SPIRAL. Due to the relatively low collectivity of the neutron-rich Ar isotopes, higher beam intensities are required compared to the Kr experiments. The part on  $^{46}\text{Ar}$  was not approved mainly because the PAC was not convinced of its feasibility with the present beam intensity of  $\sim 10^4$  pps. As is the case for the light Kr beams, the easiest way to improve the intensities of the neutron-rich Ar beams from SPIRAL is the installation of the GTS source, providing higher primary beams of  $^{48}\text{Ca}$ .

## 2. [Fusion-evaporation reactions](#)

Heavy-ion induced fusion-evaporation reactions populate states near the yrast line up to high angular moments. Reactions using stable beams and targets always produce fusion-evaporation residues on the neutron-deficient side of  $\beta$  stability. While such reactions have been exploited extensively over the past decades to study high-spin states in neutron-deficient nuclei in great detail, very little is known about neutron-rich nuclei in general and about high-spin states in neutron-rich nuclei in particular. One of the driving forces for the construction of a RIB facility is the prospect of using neutron-rich radioactive beams re-accelerated to Coulomb barrier energies for fusion-evaporation reactions. Another aspect is the use of neutron-deficient radioactive beams to produce nuclei at or beyond the proton drip line. In some cases the lower intensity of the radioactive beam is compensated by a significant increase in the reaction cross section compared to a reaction with stable beam, in which the same nucleus is produced in a very weak reaction channel.

The main difficulties of using radioactive beams for fusion-evaporation reactions are their low intensity and the high level of background they produce. As a consequence, the  $\gamma$ -ray spectra are usually dominated by the decay of the beam, and novel techniques are required to distinguish the fusion events from the background. With stable beams, for example, the coincidence with the cyclotron RF pulse is usually used to distinguish “prompt” fusion events from random background. This method, however, is not sufficient to select fusion events with a weak radioactive beam because only very few cyclotron cycles contain a beam particle.

## 2.1. Spectroscopy around the drip-line nucleus $^{130}\text{Sm}$ (E404S)

The rare-earth nuclei around  $A \approx 130$  are known to exhibit some of the largest ground-state deformations of the nuclear chart. Mean-field calculations predict quadrupole deformations of  $\beta_2 \approx 0.4$  as protons are added to the  $Z=50$  and neutrons removed from the  $N=82$  shells. The ground-state deformation in these nuclei is similar to the deformation found for the superdeformed second minimum in less neutron-deficient Ce and Nd isotopes. Furthermore, both proton and neutron orbitals with  $\Delta l = 3$  ( $h_{11/2}$  and  $d_{5/2}$ ) are near the Fermi surface, so that low-lying negative-parity states and octupole shapes are expected. The most interesting nuclei are located very close to the proton drip line and are therefore very difficult to reach experimentally. The experiment E404S aimed at populating very neutron-deficient nuclei in this region in fusion-evaporation reactions of a neutron-deficient radioactive  $^{76}\text{Kr}$  beam from SPIRAL on a  $^{58}\text{Ni}$  target at 328 MeV. This experiment represents the first attempt to use a radioactive heavy-ion beam for fusion-evaporation reactions.

A first experiment was performed in June 2002 using an early implementation of EXOGAM comprising six large and two small clover detectors. Charged particles were detected using the DIAMANT array of 56 CsI detectors, which allowed the unambiguous identification of states of relatively high spin in  $^{130}\text{Nd}$  (4p channel),  $^{131}\text{Pm}$  (3p),  $^{127}\text{Pr}$  ( $\alpha$ 3p), and  $^{128}\text{Nd}$  ( $\alpha$ 2p). However, severe accelerator and experimental difficulties were encountered and the experiment was re-scheduled in October 2004. A much improved experimental set-up was available at that time, which included not only 11 full-size clover detectors for EXOGAM, but in particular the VAMOS spectrometer to identify the fusion-evaporation residues. This proved to be crucial in order to distinguish the fusion-evaporation events from the overwhelming background. DIAMANT was again used (in a slightly different configuration) to separate the different charged-particle evaporation channels. The  $^{76}\text{Kr}$  beam with intensity of  $5 \cdot 10^5$  pps was incident on the  $^{58}\text{Ni}$  target of  $1.1 \text{ mg/cm}^2$  thickness. The data from the three complex detection systems EXOGAM, DIAMANT, and VAMOS were time stamped and correlated using the “Centrum” modules. A total of  $6 \cdot 10^8$  events were recorded with either two or more  $\gamma$  rays in coincidence or a signal from the focal plane of VAMOS, which was equipped with two secondary electron detectors (SeD) and an ionisation chamber, measuring the energy loss and time of flight of the recoils and their horizontal and vertical position. Only a fraction of  $10^{-4}$  of the recorded events is associated with the detection of one or more protons. The background radioactivity, however, is completely suppressed for these events.

In addition to the four residual nuclei mentioned above,  $\gamma$  rays could be identified also in  $^{129}\text{Pr}$  (5p channel) and, for the first time, in  $^{130}\text{Pm}$  (3pn). No excited states

were previously known in odd-odd  $^{130}\text{Pm}$ . The known yrast band in  $^{130}\text{Nd}$  has been observed up to spin  $22^+$  together with several states of excited rotational bands. Example spectra are shown in Fig. 3.

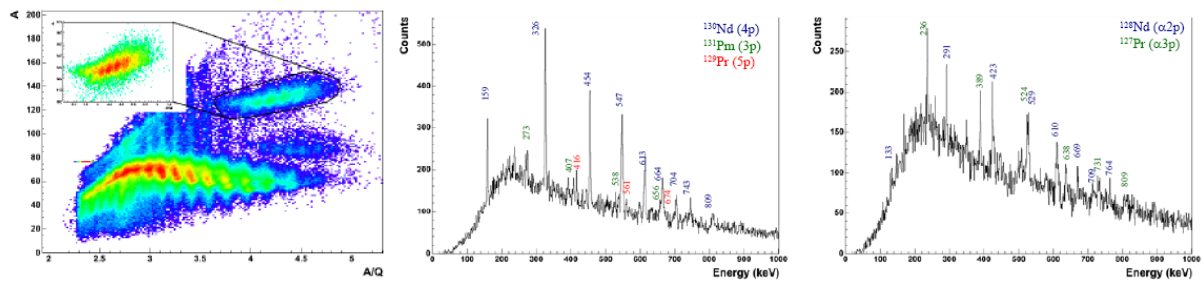


Figure 3: (Left) VAMOS identification matrix. The region corresponding to fusion-evaporation residues is highlighted. (Center) Gamma-ray singles spectra in coincidence with a fusion-evaporation residue detected in VAMOS and three protons detected with DIAMANT. (Right) Gamma-ray singles spectra in coincidence with a fusion-evaporation residue detected in VAMOS and at least one  $\alpha$  particle detected with DIAMANT.

The results have been presented at international conferences [11,12] and are the subject of two PhD theses [13,14]. An article describing the experiment and its results is in preparation. The experiment demonstrated that the set-up comprising EXOGAM, VAMOS, and DIAMANT is well suited to perform fusion-evaporation experiments with radioactive beams and that the massive background from the beam decay can be suppressed by the detection of the fusion-evaporation residues and evaporated charged particles. With a  $^{76}\text{Kr}$  beam, nuclei with unknown excited states can only be reached in reactions involving neutron evaporation, for which the cross sections are predicted in the range between 1 and 10 mb, just at or below the limit of the present experiment. In order to reach these exotic nuclei in strong proton or  $\alpha$  evaporation channels, more neutron-deficient radioactive beams are required. If a  $^{74}\text{Kr}$  beam was available with the same intensity that is reached for  $^{76}\text{Kr}$  today, unknown isotopes such as  $^{127}\text{Pm}$ ,  $^{126}\text{Nd}$ , and  $^{125}\text{Pr}$  could be studied using the reaction  $^{58}\text{Ni}(^{74}\text{Kr},\alpha xp)$ .

## 2.2. Competition between octupole and multi-particle excitations in $^{212}\text{Po}$ and $^{213}\text{At}$ (E408S)

The nuclei with only few valence particles outside the doubly magic  $^{208}\text{Pb}$  core provide great insight into the interplay between vibrational and multi-particle modes of excitation. The objective was to study high-spin states in the nuclides  $^{212}\text{Po}$  and  $^{213}\text{At}$ , using a  $^8\text{He}$  beam on  $^{208}\text{Pb}$  and  $^{209}\text{Bi}$  targets, and thereby to learn about the development of collectivity in these nuclides. The primary experimental focus was to improve the knowledge of the level structure of  $^{212}\text{Po}$ , using the  $^{208}\text{Pb}(^8\text{He},4n)$  reaction at a beam energy of 28 MeV. The neutron-rich location of  $^{212}\text{Po}$  makes experimental access very difficult. Earlier work to study its level structure used an incomplete-fusion reaction with a  $^9\text{Be}$  beam [15], which is the only possibility to reach  $^{212}\text{Po}$  with a stable beam.

The experiment initially formed part of the commissioning of the EXOGAM  $\gamma$ -ray detector array at SPIRAL in 2002 [16]. It was cut short by a SPIRAL target failure. The beam time was re-scheduled in 2004. An average beam intensity of  $2 \cdot 10^5$  pps was achieved over a sustained period of six days, with a peak current of  $8 \cdot 10^5$  pps (at a

primary beam power of 2.8 kW). The  $^8\text{He}$  beam was incident on a  $^{208}\text{Pb}$  target of  $30\text{ mg/cm}^2$  for five days, which was replaced by a  $^{209}\text{Bi}$  target for one day to study  $^{213}\text{At}$ . Four fully shielded EXOGAM clover detectors were used in a very compact geometry with a distance between target and detectors of 68 mm. The full-energy-peak efficiency was measured to be 13.5 % in this configuration. Using a thick target has the advantage that the recoils are stopped and the  $\gamma$  rays are not Doppler broadened, for the price of a higher background from the decay of the beam, which completely dominates the singles spectra. In order to reduce this background, a detector to trigger on the incoming beam particles was installed 2.5 m upstream of the target. This detector, however, caused too much scattering of the beam and was less efficient than expected, so that the technique could not be used in this case.

New spectroscopic results were obtained despite the experimental difficulties. Sample spectra are shown in Fig. 4, and the updated level structure of  $^{212}\text{Po}$  is shown in Fig. 5, based on Ref. [15], with the addition of the 69.4 and 182.8 keV transitions. The relative population of the states up to the  $(12^+)$  state was found to be enhanced compared to the  $^9\text{Be}$ -induced reaction. The full yrast sequence up to the  $\alpha$ -decaying  $18^+$  isomer is now reasonably well established, however, no states above the isomer were observed. Further details are given in Refs. [16,17].

The present work has successfully used a radioactive beam of  $^8\text{He}$  to obtain new spectroscopic information with a fusion-evaporation reaction. This has led to improved knowledge of the level structure of  $^{212}\text{Po}$ . This nuclide remains an interesting case for further study.

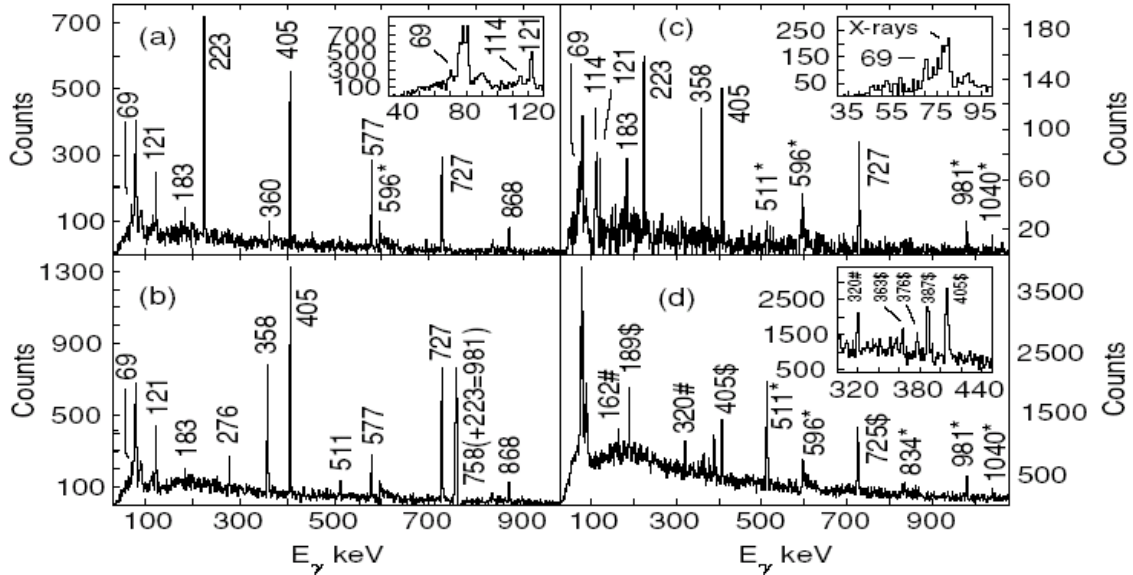


Figure 4: Gamma-gamma coincidence spectra: (a)  $^{212}\text{Po}$  gated by the 358 keV transition; (b)  $^{212}\text{Po}$  with 223 keV gate; (c)  $^{212}\text{Po}$  with 868 keV gate; (d)  $^{213}\text{At}$  (\$) in the total projection of  $\gamma\gamma$  events. This figure is from ref. [17].

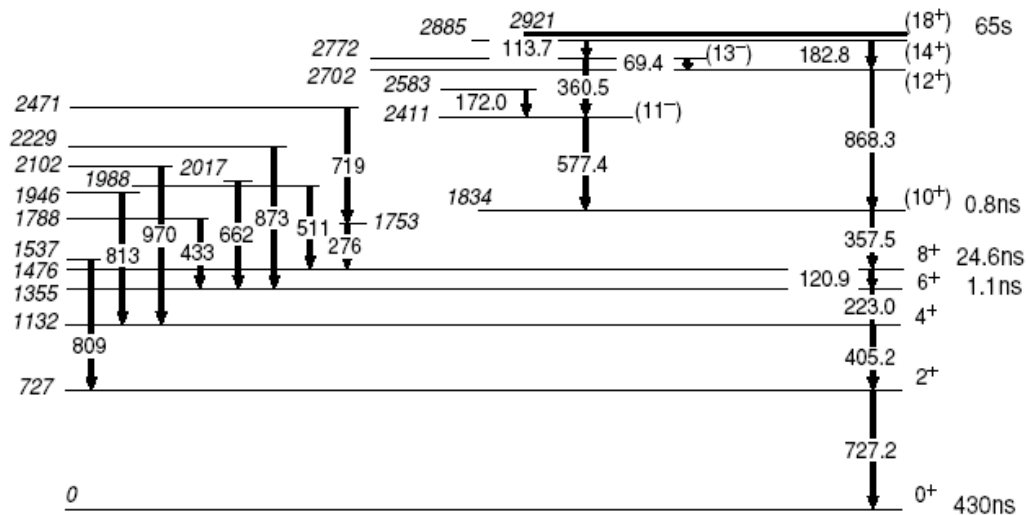


Figure 5: Decay scheme for  $^{212}\text{Po}$ , based on Ref. [15], with new (previously unpublished) placements of the 69.4 and 182.8 keV transitions (see also Fig. 4). This figure is from Ref. [17].

### 3. [Perspectives](#)

#### SPIRAL beam developments

The experimental programs to study nuclear shapes and shape coexistence rely strongly on the use of the Ar and Kr beams delivered by SPIRAL. Higher intensities are required in order to pursue these programs and extend them to nuclei further away from stability. Higher secondary intensities of Kr and Ar beams can be achieved by employing the GTS source, an experimental ECR source jointly developed by Grenoble and GANIL. It is currently available at GANIL as a prototype on a test bench, but not yet installed for operation. As an example, with this source a  $^{78}\text{Kr}$  beam of  $\sim 20 \text{ e}\mu\text{A}$  intensity can be produced at 73-A MeV, thus reaching the allowed 3kW limit for the SPIRAL production target and increasing the radioactive beam intensities by a factor of  $\sim 10$ . The GTS source would also allow using higher charge states and thus producing primary beams at higher energies further improving the experimental conditions at GANIL. Under these conditions a Coulomb excitation measurement of  $^{72}\text{Kr}$  would be possible, and  $^{76,74}\text{Kr}$  beams became available with high intensities suitable to reach unknown nuclei at the proton drip line in fusion-evaporation reactions. A similar increase can be expected for the secondary Ar beams produced by fragmentation of  $^{48}\text{Ca}$ . Experiments using fast fragmentation beams would also benefit from the higher primary beam intensities. The resulting increase of the  $^{72}\text{Kr}$  beam intensity is also interesting for the study of  $np$  pairing in heavy  $N=Z$  nuclei via  $(^3\text{He},p)$  reactions. Even higher intensities for Kr beams can be achieved by using  $^{12}\text{C}$  induced fragmentation of Nb or  $\text{ZrO}_2$  targets, for which an increase by a factor of up to 30 is expected.

In a second stage, new beam species of elements other than noble gases should be developed. This involves the development of new target-ion-sources for SPIRAL. Even though such a development requires a considerable commitment of resources and manpower, we rank it a necessary evolution of the SPIRAL project towards SPIRAL2. New beam species for SPIRAL will not only broaden the physics

program over the next years, but also provide a head start on necessary developments for SPIRAL2. The development of alkaline beams from a surface ionisation source coupled to an  $n^+$  ECR source is currently under discussion. While we welcome and support this initiative, we would also give high priority to the development of metallic beams such as  $^{56}\text{Ni}$  and  $^{60,62}\text{Zn}$ .

## EXOAM phase II

The EXOGAM array was designed to exploit radioactive beams from SPIRAL. The original design consists of 16 large segmented HPGe clover detectors surrounded by a modular Compton suppression shield. The signals from the clover detectors (core and segments) as well as from the Compton suppression shields are presently processed using analogue VXI electronics. Employing a fully digital electronics, capable of higher counting rates and performing pulse-shape analysis on-line could significantly improve the performance of the detector array. Through analysis of the signal rise time and the magnitude of the induced transient signals in adjacent segments, a position resolution well below the size of the individual segments can be achieved, resulting in a much improved Doppler correction. Today the count rate per crystal is limited by the electronics to 10 kHz. Rates of 50 kHz can easily be achieved by a digital system, which should also include the Compton suppression shields. The system should be able to run in a trigger-less and dead-time free mode. Furthermore it is difficult to maintain the existing VXI electronics in the long term. Due to the fragility of the clover detectors it is difficult to maintain the full array at all times. It is therefore important to purchase additional EXOGAM detectors to be able to replace those under repair. The upgraded EXOGAM spectrometer should be fully compatible with the AGATA demonstrator. Especially the count-rate aspect is important in order not to slow down the performance of a coupled AGATA-EXOAM spectrometer. Since AGATA will only be available at GANIL for campaigns, it is important to keep EXOGAM a competitive instrument and the “work horse” for  $\gamma$ -ray spectroscopy at GANIL.

EXOAM remains to be the  $\gamma$ -ray spectrometer of choice for Coulomb excitation experiments, for which the  $\gamma$ -ray multiplicity is moderate. The detectors can be used in their compact configuration, resulting in a high efficiency. Equipped with digital electronics capable of performing pulse-shape analysis, the angular resolution of the spectrometer and hence the energy resolution of the spectra will improve distinctly. The proposed upgrade of EXOGAM ensures that a versatile and competitive spectrometer is available at GANIL also at times when AGATA is not, and offers the perspective of creating an even more powerful spectrometer by coupling EXOGAM and AGATA during a campaign planned in 2009.

## AGATA

The *Advanced Gamma Tracking Array* (AGATA) will comprise 180 highly segmented position-sensitive germanium crystals and uses the novel technique of  $\gamma$ -ray tracking. The main features of AGATA are unprecedented efficiency, angular resolution, and count-rate capability. Depending on the experimental parameters such as  $\gamma$ -ray multiplicity,  $\gamma$ -ray energy, and recoil velocity, the gain in resolving power over conventional  $\gamma$ -ray spectrometers can be up to three orders of magnitude. A sub-array of 15 Ge crystals arranged in five triple-detectors has been funded and is

currently under construction. This so-called *AGATA demonstrator* will be commissioned in 2007 in Legnaro. The demonstrator array is modular and will be subsequently used in campaigns at various European laboratories, while it is continuously growing. The full AGATA array is planned to be completed by 2016. The French AGATA collaboration has submitted a proposal to the AGATA steering committee to host AGATA at GANIL after the Legnaro phase. It is envisioned that AGATA, in its various stages, will be hosted at GANIL every third year for one year.

For the first campaign at GANIL in 2009 it is planned to couple AGATA to the VAMOS spectrometer in G1. At that time, it is anticipated that the demonstrator will be complemented with 3 additional triple Clusters. This setup will therefore consist in 8 triple Clusters. The proposed configuration combines 8 EXOGAM Clovers with this extended demonstrator installed at backward angles. It will be possible to adjust the distance between the target point and the germanium detectors as a function of the experimental conditions, noticeably the gamma-ray multiplicity. In addition, it will be possible to rotate VAMOS when required. Detailed simulations are still undergoing to optimize this coupling. For a coupling with AGATA detectors, it is indispensable that EXOGAM is equipped with a fully digital electronics. It is furthermore essential that the direct beam line from CIME to G1 is completed by 2009 in order to increase the beam time available for AGATA.

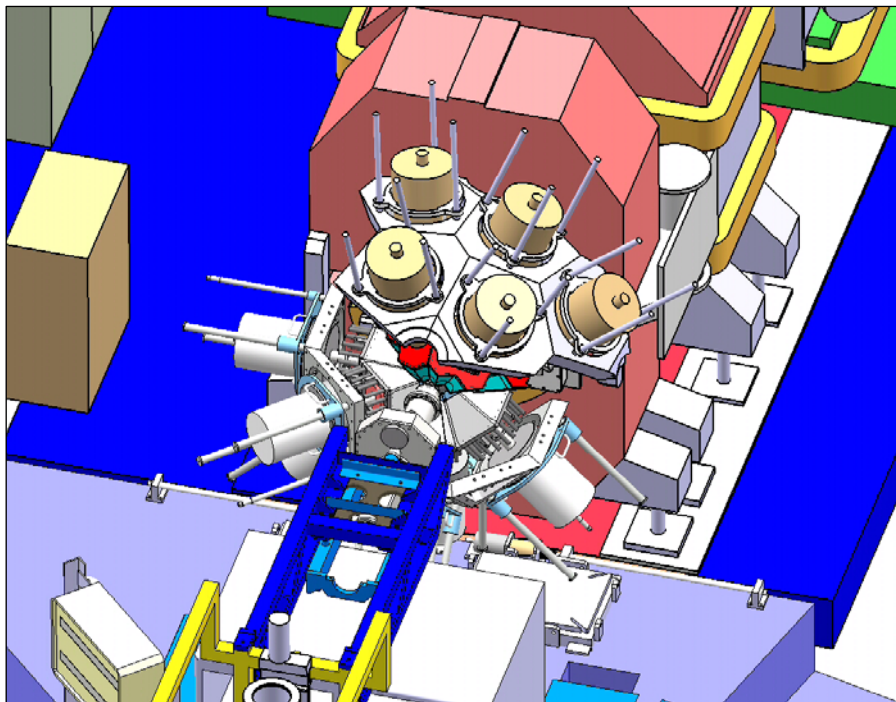


Figure 6: Drawing of the AGATA demonstrator with 8 detectors coupled to the large-acceptance spectrometer VAMOS. Eight AGATA triple clusters are shown in a compact geometry mounted at backward angles together with eight EXOGAM clover detectors. Provided dedicated flanges are mounted, it will be possible to rotate VAMOS with EXOGAM and AGATA detectors up to  $45^\circ$ .

In the following, only the AGATA demonstrator i.e. 5 triple Clusters is considered. The five AGATA modules of the demonstrator alone have a full-energy-peak efficiency between 5 and 8 %, depending on the parameters of the reaction.

Even though the efficiency is smaller than that of the (full) EXOGAM array, the much better energy resolution and peak-to-total ratio result in a superior overall spectrum quality, which can be quantified as the *resolving power* of the instrument. Experiments will also benefit from the higher rate capability of the AGATA demonstrator. The tables 1 and 2 compare the performances of the AGATA demonstrator at a close distance of 10 cm and of the full EXOGAM array. Two realistic examples for Coulomb excitation and fusion-evaporation reactions were chosen. A comparison of the  $\gamma$ -ray spectra following the fusion-evaporation reaction  $^{76}\text{Kr} + ^{58}\text{Ni}$  (E404S) for EXOGAM and the AGATA demonstrator obtained from GEANT4 simulations [18] is shown in Fig. 7. It should be noted that the proposed upgrade of EXOGAM with digital electronics will improve in particular its resolution and count-rate capability, allowing the coupling of AGATA and EXOGAM.

	Ph-efficiency (%)	P/T (%)	FWHM (keV)
EXOGAM	18	45	15
AGATA demonstrator	7.5	65	3

Table 1: Detector performances for the Coulomb excitation of a  $^{46}\text{Ar}$  beam at 160 MeV on a  $^{208}\text{Pb}$  target for a  $\gamma$ -ray energy of 1.3 MeV and low  $\gamma$ -ray multiplicity. The average recoil velocity is  $v/c = 7.5\%$ .

	Ph-efficiency (%)	P/T (%)	FWHM (keV)
EXOGAM	13	31	13
AGATA demonstrator	5	52	2.8

Table 2: Detector performances for the fusion-evaporation reaction of a  $^{72}\text{Kr}$  beam at 280 MeV on a  $^{40}\text{Ca}$  target for a  $\gamma$ -ray energy of 1.3 MeV and a medium  $\gamma$ -ray multiplicity of 15. The inverse kinematics increases the acceptance of the VAMOS spectrometer. The recoil velocity is  $v/c = 5.8\%$ .

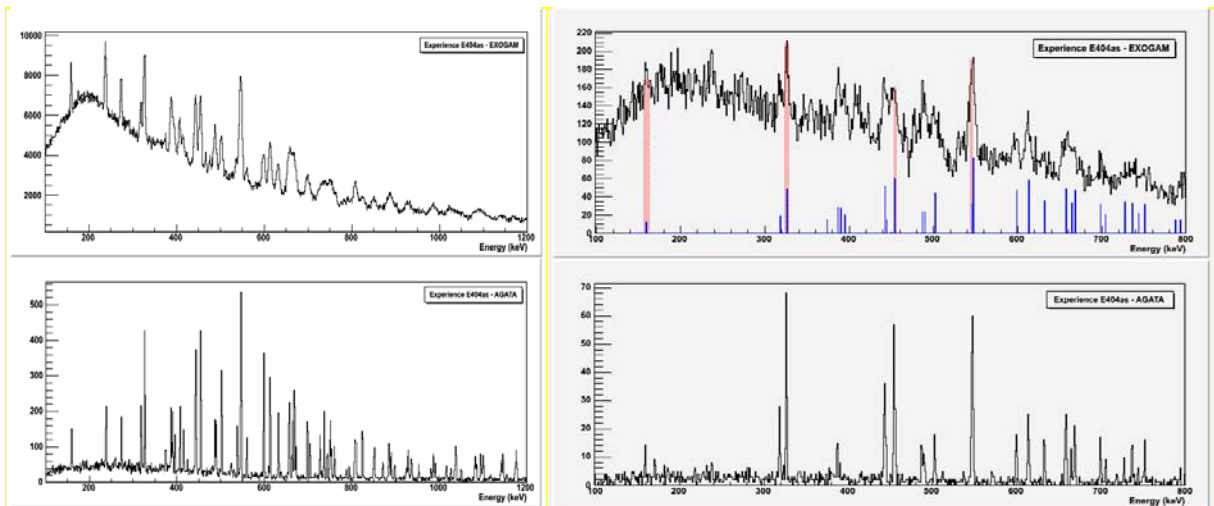


Figure 7: Simulation of the total  $\gamma$ -ray spectrum (*left*) and  $\gamma$ - $\gamma$ -coincidences (*right*) following the reaction  $^{76}\text{Kr} + ^{58}\text{Ni}$  for the EXOGAM spectrometer (*top*) and the AGATA demonstrator (*bottom*). The simulations are based on the experimental yields observed in the E404S experiment. The coincidence spectra show the sum of gates

indicated in red. The conditions to generate the EXOGAM and AGATA spectra are identical [18].

The installation of the AGATA demonstrator at GANIL offers exciting opportunities not only for spectroscopy experiments with SPIRAL beams, but also for experiments with fast fragmentation beams, where a significant gain is expected due to the high granularity of the AGATA detectors. This is illustrated in Fig. 8, which shows the response of the *Château de Cristal*, EXOGAM, and the AGATA demonstrator for the fragmentation of a secondary  $^{37}\text{Ca}$  beam at 61. A MeV to  $^{33}\text{Cl}$ . The simulation [19] is based on experimental results from experiment E450. Even though the efficiency of the AGATA demonstrator is much lower compared to the *Château de Cristal*, the overall spectrum quality is significantly improved. Other areas that will benefit from the performance of AGATA include the spectroscopy of neutron-rich nuclei populated in deep-inelastic reactions and the spectroscopy of heavy elements. In addition to the gain from a higher efficiency, the former will strongly benefit from the improved energy resolution and Doppler correction, whereas the latter takes advantage of the high count-rate capability of AGATA.

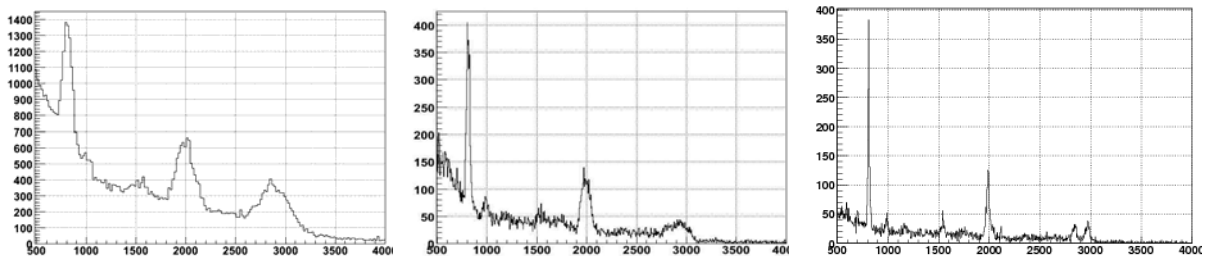


Figure 8: Simulated spectra following the fragmentation of  $^{37}\text{Ca}$  leading to  $^{33}\text{Cl}$  for the *Château de Cristal* (left), EXOGAM (center), and the AGATA demonstrator at a distance of 11.5 cm to the target (right) [19].

A bigger sub-array of AGATA covering about  $2\pi$  of solid angle is expected to be available in 2012. It will be more powerful than any  $\gamma$  spectrometer existing today and preserve its performance even for large  $\gamma$ -ray multiplicities, making it ideally suited to study nuclear shapes at high angular momentum. The first choice for its installation is again in G1 coupled to VAMOS in order to make use of the first beams from SPIRAL2. An interesting alternative would be the use of AGATA detectors at the secondary target point of the  $S^3$  separator-spectrometer, making use of the intense stable beams from LINAG. More details can be found in the Letter of Intent “High-resolution  $\gamma$ -ray spectroscopy at SPIRAL2”.

#### 4. [References](#)

- [1] E. Bouchez et al., Phys. Rev. Lett. 90, 082502 (2003)
- [2] A. Görgen et al., Eur. Phys. J. A26, 153 (2005)
- [3] E. Bouchez, PhD thesis, ULP Strasbourg, November 2003
- [4] E. Clément, PhD thesis, Univ. Paris XI, July 2006
- [5] E. Clément et al., in preparation
- [6] M. Bender, P. Bonche, P.-H. Heenen, Phys. Rev. C74, 024312 (2006)
- [7] J.-P. Delaroche et al., in preparation
- [8] H. Scheit et al., Phys. Rev. Lett. 77, 3967 (1996)

- [9] H. Scheit et al., Phys. Rev. C67, 014604 (2000)
- [10] J. Mrázek et al., Nucl. Phys. A734, E65 (2004)
- [11] B. Rossé et al., AIP Conference Proceedings 831, 541 (2006)
- [12] M. Petri et al., *Phys. Scr.* T125, 214 (2006)
- [13] B. Rossé, PhD Thesis, Université Claude Bernard – Lyon I (2006)
- [14] M. Petri, PhD Thesis, University of Liverpool, in progress
- [15] A.R. Poletti et al., Nucl. Phys. A473, 595 (1987)
- [16] Zs. Podolyak et al., Nucl. Inst. Meth. Phys. Res. A511, 354 (2003)
- [17] A.B. Garnsworthy et al., J. Phys. G: Nucl. Part. Phys. 31, S1851 (2005)
- [18] O. Stézowski, IPN Lyon, private communication
- [19] A. Bürger, Universität Bonn, private communication

## VI. Study of asymmetric nuclear matter at low energy

O. Lopez\* for the INDRA Collaboration

\* Laboratoire de Physique Corpusculaire, IN2P3-CNRS, ISMRA et Université de Caen, F-14050 Caen, France

Report on SPIRAL experiments E475S and E494S

Contact: [lopez@lpccaen.in2p3.fr](mailto:lopez@lpccaen.in2p3.fr)

### 1. Key questions and initial goals

The availability of SPIRAL1 beams allows to begin the study of the properties of asymmetric nuclear systems. These studies are meant to provide unknown information about the spectroscopic properties of nuclei close to the limits of stability. SPIRAL beams will provide tools to explore heavy-ion induced collisions at different impact parameters leading to the production of moderately hot nuclear systems (temperature between 3-5 MeV) under largely unknown conditions in terms of shape (deformation), energy (temperature) and  $N/Z$  asymmetry (isospin). These conditions can be experimentally controlled by carefully choosing the entrance and exit channels. This allows to probe the mechanisms responsible for nuclear excitation, how intrinsic degrees of freedom are converted into collective modes (dissipation), and how relaxation processes towards equilibrium occur within such a small quantum system that is initially out-of-equilibrium. Indeed, the velocities of the reaction products provide natural clocks from which it is possible to determine the equilibration times of various degrees of freedom (e.g.  $N/Z$ , mass, excitation energy) and allow to discuss whether non-equilibrium features or partial equilibration in light and complex fragment emissions are present.

We then propose with some SPIRAL1 beams to study the dynamics and thermodynamics of moderately excited nuclear systems produced in heavy-ion induced reactions, in an exclusive manner, using large solid-angle (if not  $4\pi$ ) arrays, coupled with dedicated apparatus such as spectrometers. Doing this, we hope to provide useful information concerning the isovector part of the nuclear effective interaction, exploring the relevant features of the nuclear equation of state of asymmetric matter. This program can be seen as a step towards SPIRAL2 studies. In the following, we will discuss the issues that can be addressed with SPIRAL1 beams, as well as for the future SPIRAL2 beams.

#### **Limiting temperatures of hot and asymmetric nuclear systems**

Experiments performed with stable beams produce hot nuclear systems, which decay modes have been extensively investigated so far. From the properties of the emitted products, information about excitation energy and temperature have been extracted [19]. Theoretical calculations predict the existence for nuclei of a limiting

temperature called  $T_{lim}$  [2-8]. At low temperatures ( $T < T_{lim}$ ), the nuclear system is described as a heated nuclear drop, which evaporates particles. At high temperatures ( $T > T_{lim}$ ), the thermodynamical conditions make the drop unstable and lead to the break-up of the system. This limiting temperature has been theoretically predicted (see Fig. 1) and experimentally observed [9].

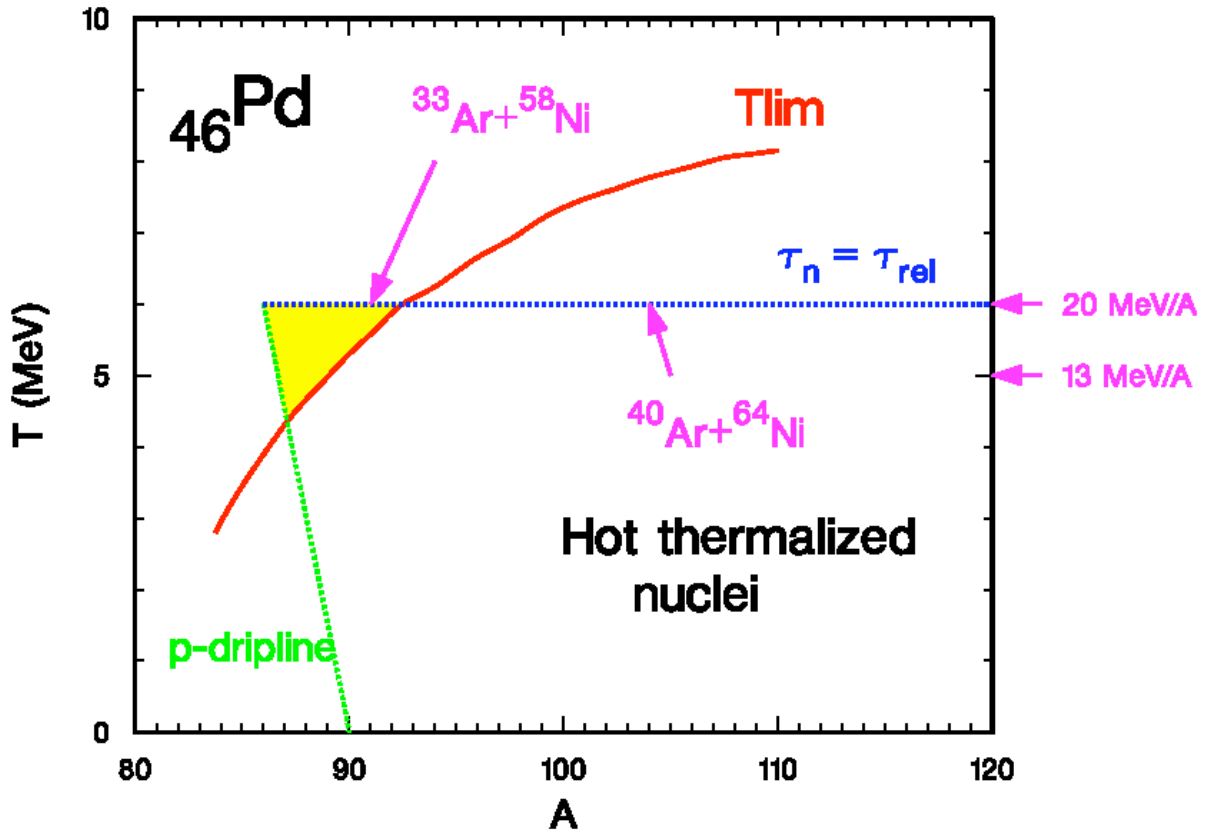


Figure 1: Limiting temperature (red curve) for Pd isotopes as determined in [3]. The horizontal blue curve indicates the temperature where the neutron mean emission time  $\tau_n$  is equal to the energy relaxation time  $\tau_{rel}$  for the system.

From a theoretical point of view, mean-field calculations based on the Skyrme interactions and other parameterisations have predicted a mass-dependent limiting temperature [4, 6, 7], heavier nuclei having a considerably lower limiting temperature than light nuclei. Such features provide important information about the critical temperature  $T_c$  of infinite nuclear matter and for the isoscalar part of the nucleon-nucleon effective interaction.

Experimentally, a systematic study of limiting temperatures has been performed by collecting all the available data on nuclear caloric curves (*i.e.* correlation between the temperature and the excitation energy) [9]. This compilation has shown a decrease of the limiting temperature when increasing the mass of the nuclear system as predicted by theoretical calculations. This observed mass scaling of the limiting temperature has then been associated to an effect of Coulomb instabilities becoming more and more important as the proton fraction increases. These studies were performed with stable beams and therefore quasi-stable nuclear systems with low

$N/Z$  asymmetries. These systems have limiting temperatures comprised between 5 and 9 MeV depending on the mass. However, theoretical expectations are in favour of a decrease of the limiting temperature as one moves away from stability. The authors of Refs. [3, 10] have mapped  $T_{lim}$  as a function of  $N$  and  $Z$ , predicting that very  $N-Z$  asymmetric nuclear systems should present a significant lowering of the limiting temperature. This effect is thought to be induced by the combined effect of Coulomb instabilities and the symmetry energy part of the equation of state; it suggests that it should be possible to study limiting temperatures at low bombarding energy, such as the ones available with SPIRAL1 and SPIRAL2 beams. By producing compound nuclei through fusion reactions with the same mass number  $A$  but different proton over neutron ratios, one can explore the  $N/Z$  dependence of the symmetry energy when going towards the neutron drip line, and the Coulomb instabilities when moving towards the proton drip line. These studies will provide relevant information about the isovector part of the nucleon-nucleon effective interaction and for the symmetry energy. This program can be further extended to systems that are even more asymmetric when SPIRAL2 beams will be available, and also pursued at higher energies with the beams delivered by the third-generation facility EURISOL in the long-term future.

### **$N/Z$ dependence of nuclear level density**

The nuclear level density is a fundamental quantity in Nuclear Physics and plays an essential role in understanding compound nuclear reactions. It is also a basic ingredient for the determination of thermonuclear rates of nuclear species for Astrophysics, with applications both in nucleosynthesis and supernovae dynamics [11, 12]. While the level density around the Fermi surface depends critically on nuclear structure details [13], at higher energy it can be effectively parameterised as a mass, isospin ( $N/Z$ ) and temperature dependent level density parameter  $a(A, N/Z, T)$  [14, 15]. In the high temperature regime ( $T > 2$  MeV), level densities can not be predicted accurately by microscopic calculations due to the finite space of any shell model, and have to be experimentally measured. Indeed, the  $N/Z$  dependence of the level density parameter  $a$  is largely unknown despite some experimental efforts [16, 17] on that point (see Fig. 2).

This program can be accomplished by coincidence measurements of isotopically resolved residues (by using a spectrometer for example) with light particles emitted over the whole solid angle and detected using a  $4\pi$  array. Such measurements will provide stringent constraints on the level density used in statistical models using the Weisskopf or Hauser-Feshbach formalism.

Does the level density parameter suddenly drop near the proton drip line, as extrapolated by some calculations? Answering this question is the aim of experiment E494S, to be run in the spring of 2007, which will couple INDRA and VAMOS.  $^{33-40}\text{Ar}$  beams around 11 A.MeV will bombard  $^{58,60,64}\text{Ni}$  targets in order to form palladium compound nuclei with masses going from 92 - close to the proton drip line - to 104. All de-excitation channels will thus be weighted and compared with the statistical theories, putting strong constraints on the level density parameters.

### Extrapolation of level density parameter starting from stable nuclei

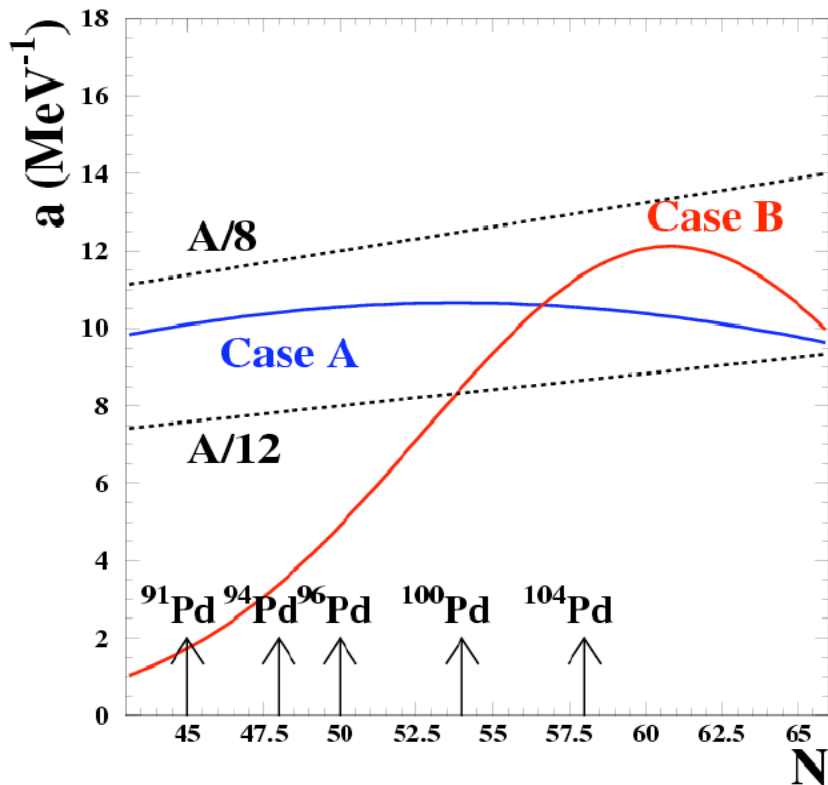


Figure 2: Evolution of the level density parameter,  $a$ , for Pd isotopes as a function of the number of neutrons,  $N$ . The red and blue curves correspond to different parameterisations of  $a$  taken from [14] and [15].

#### E494S: Level density parameter determination for different isotopes

Spokesperson: N. Le Neindre, IPN Orsay, France

Experimentally, we will couple INDRA for light charged particle identification and the VAMOS spectrometer for evaporation residue detection. The detection efficiency is maximized thanks to the  $4\pi$  angular coverage, which allows the use of low intensity beams. Indeed a  $4\pi$  array functions in all cases with no more than some  $10^7$  pps. Complete events (detection of the total charge of the incident system) will be selected, the charge and mass of the residue given by VAMOS and those of all light charged particles and fragments by INDRA. The multiplicity of the undetected neutrons will be obtained by mass difference. The  $4\pi$  angular coverage allows to differentiate more easily fusion reactions from deeply inelastic collisions.

#### Validity of statistical theories for the de-excitation of exotic nuclei

SPIRAL1 as well as SPIRAL2 beams provide a large variety of nuclei at moderate excitation energies. The decay of such systems is well known for stable nuclei and is described by means of statistical models [18, 19, 20]. These models rely on the fundamental assumption of statistical theories: in a microcanonical ensemble, all the final states are equally populated. The corresponding probability is calculated using the level density of the decaying system, depending on excitation

energy and angular momentum. The probabilities at each de-excitation step are assumed to be independent of each other.

For very asymmetric nuclei, one suspects that the particular spectroscopic properties such as quasi-molecular states or halos [21, 22] change dramatically this statement and therefore the decay modes will not be ascribable to standard statistical models such as Weisskopf or Hauser-Feshbach formalisms. Only exclusive measurements and detection of intra-event correlations between emitted products can be used to study such exotic phenomena. A detailed study of the de-excitation of compound nuclei produced with SPIRAL1/SPIRAL2 beams will offer the opportunity of exploring the  $N/Z$  dependence of evaporation of light and complex particles by the means of correlation techniques. This will provide stringent tests for the theories of statistical decay. A first approach to this problem has been addressed in the E475S experiment performed in March 2006.

### **E475S: Isospin dependence in the emission of complex fragments from compound nuclei of $A \approx 115$ and $N \approx Z$**

Spokespersons: J. Gomez del Campo, M. La Commara, J.P. Wieleczko

The experiment, performed in March 2006, ran well and the GANIL facility provided us with the various beams needed with good quality. For example,  $10^5$  pps of  $^{75}\text{Kr}$  were delivered as expected, with a very stable beam during one week of data taking. The INDRA detector ran well. Results obtained on-line are very satisfactory in a sense that clusters such as  $^{12}\text{C}$  have been clearly observed and identified. It is worth noticing that cluster emission has been observed at a bombarding energy well below the standard threshold for such a production process. The data reduction is in progress in order to have a quantitative estimation of the cross section that is the crucial and main aspect of the experiment. The organization and sharing of the various tasks needed to analyse data taken with a complex apparatus as INDRA have been made and a meeting of the collaboration for that experiment is scheduled for next summer.

## **2. Results of the first 5 years**

Experiments have not (yet) been analysed since one of them (E494S) has not been realized so far and the other (E475S) has been done six months ago.

For the E494S experiment, some tests concerning mainly the HARPEE ionisation chamber in the focal plane of VAMOS have been performed in March and September 2006 and will continue in the following months. The mechanical coupling between INDRA and VAMOS has been successfully tested at GANIL. The calibration of the E475S experiment is in progress as already mentioned and results are foreseen in the next years.

## **3. Possible developments**

To cover all the Physics issues mentioned above, experimental results spanning the widest range in terms of mass and isospin for the reaction products have to be collected. SPIRAL1 beams at the highest possible incident energies (**10-15 A.MeV**) can provide interesting outcomes by studying fusion reactions detected in an exclusive way using  $4\pi$  arrays combined with high-resolution apparatus. The needed beam intensities have to be in the range  **$10^6$ - $10^7$  pps**.

One of the objectives of this program is to perform a  $^{72}\text{Kr} + ^{40}\text{Ca}$  reaction since the (statistical?) emission of clusters is expected to strongly increase at the  $N=Z$  line. Moreover, after emission of  $^{12}\text{C}$  from  $^{112}\text{Ba}$  the complementary nucleus is  $^{100}\text{Sn}$ , a key nucleus for spectroscopy studies. Through cluster emission,  $^{100}\text{Sn}$  is expected to be populated in a domain differing from the standard fusion-evaporation process. However, this requires a beam intensity similar to the one we had during the E475S  $^{75}\text{Kr} + ^{40}\text{Ca}$  experiment (i.e. at least  $10^5$  pps).

For systematic studies, we are also interested in studying the de-excitation mechanism of moderately hot exotic nuclei with mass around 50. In this aim, the reactions  $^{18-26}\text{Ne} + ^{24-26}\text{Mg}/^{40-48}\text{Ca}$  at the highest SPIRAL1 energies (10-15 A.MeV) are good candidates.

The INDRA-VAMOS experiment offers for the very first time, to our knowledge, to fully measure and determine both the particles emitted all along the de-excitation chain, and the residue, which follow the production of hot compound nuclei in heavy ion collisions. Moreover, appropriate combination of targets and stable and radioactive beams can form a wide variety of hot isotopes, relevant for studies on level density parameter. According to the results, we can foresee complementary experiments including other Ar isotopes beams such as  $^{33}\text{Ar}$  and  $^{46}\text{Ar}$  or/and different projectile/target combination. Furthermore, for studying limiting temperature effects in those nuclei, a simple beam-energy change is necessary, as it requires the same experimental set-up.

### Technical developments for low energy measurements

To fully exploit the low energy SPIRAL1 and the future SPIRAL2 beams, progresses in the domain of charged particles detection have to be made, taking advantage of our experimental knowledge on that level. This is the aim of the FAZIA project. New experimental apparatus have then to be designed for low energy reaction products, adapted to SPIRAL1/SPIRAL2 beams, together with a good mass resolution, taking advantage of accurate Time-of-Flight measurements and Digital Electronics. In the long-term R&D program called FAZIA (Four- $\pi$  A and Z Identification Array), the capability of doing Pulse Shape Analysis of digitalized current signals for Silicon detectors will be used in order to realize the best possible charge and mass identification. For the moment, tests with single detectors have been performed at the TANDEM Orsay in 2001/2002, GANIL/LISE in 2003, GANIL/CIME in 2006. The results are very encouraging since it is possible to discriminate Carbon, Argon and even Krypton isotopes respectively with  $\Delta A=1,2$  and 4. Eight prototypes of detection cells composed by two Silicon detectors (some of them Double-sided Silicon Strip Detector) followed by a Cesium Iodide scintillator are presently under construction and will be tested during the years 2007-2008 in order to choose among the possible technical solutions. We hope to realize a prototype array in 2012, taking advantage of the advent of SPIRAL2. In a more long-term range, experiments at EURISOL are planned in order to extend our research program at higher incident energies.

## 4. Conclusion

For the first time with SPIRAL1 beams, asymmetric nuclear matter is studied from the point of view of the reaction Dynamics and Thermodynamics. This could

provide unique and possibly unexpected information about the equation of state of nuclear matter, its phase diagram and the nature of the phase transitions. Both experiments (E475S, E494S) should be considered as a test bench using INDRA with low-energy radioactive beams, and at the same time an attempt to combine different apparatus (the VAMOS spectrometer with INDRA). The experimental results will be carefully analysed and will naturally constitute a step towards the study of moderately hot and asymmetric nuclear matter. As an improvement of what has been done or scheduled so far, the following beams at intensities around  $10^6$  pps have to be considered:  $^{72}\text{Kr}$ ,  $^{33}\text{Ar}$ ,  $^{46}\text{Ar}$ . As an extension of the Physics program,  $^{18}\text{Ne}$  and  $^{26}\text{Ne}$  beams are also welcome.

## 5. [References](#)

- [1] E. Suraud et al., Prog. Part. Nucl. Phys. 23, 357 (1989) and Refs. therein
- [2] P. Bonche et al., Nucl. Phys. A427, 278 (1984)
- [3] J. Bresrovany and S. Levitt, Phys. Lett. B217 (1989)
- [4] H.Q. Song et al., Phys. Rev. C44, 2505 (1991)
- [5] H.Q. Song et al., Phys. Rev. C47, 2001 (1993)
- [6] Y. Zhang et al., Phys. Rev. C54, 1137 (1996)
- [7] M. Baldo et al., Phys. Rev. C59, 682 (1999)
- [8] P. Wang et al., Nucl. Phys. A748 (2005)
- [9] J. Natowitz et al., Phys. Rev. C65, 034618 (2002)
- [10] Z. Li et al., Phys. Rev. C 69, 034615 (2004)
- [11] P. Donati et al., Phys. Rev. Lett. 72, 2835 (1974)
- [12] T. Rauscher et al., Phys. Rev. C 56, 1613 (1997)
- [13] W.E. Ormand, Phys. Rev. C 56, R1678 (1997)
- [14] S.I. Al-Quarashi et al., Phys. Rev. C63, 065803 (2001)
- [15] R.J. Charity, Phys. Rev. C67, 044611 (2003)
- [16] W.E. Ormand et al., Phys. Rev. C 40, 1510 (1989)
- [17] M. Lunardon et al., Eur. Phys. J. A 13, 419 (2002)
- [18] W. Weisskopf, Phys. Rev. 52, 295 (1937)
- [19] W. Hauser and H. Feshbach, Phys. Rev. 87, 366 (1952)
- [20] T. Ericson, Adv. Phys. 9, 425 (1960)
- [21] M. Freer, Nucl. Phys. A685, 146c (2001)
- [22] N. Orr et al., Nucl. Phys. A654, 710c (1999)



## VII. Astrophysics applications

F. de Oliveira Santos\*

\* GANIL, CEA/DSM - CNRS/IN2P3, Bvd Henri Becquerel, BP 55027, F-14076 Caen Cedex 5, France

Report on SPIRAL experiments E400S and E442S

Contact: [oliveira@ganil.fr](mailto:oliveira@ganil.fr)

### Abstract:

Two examples of experiments performed at GANIL are presented. These experiments are linked to questions or problems in astrophysics. It is shown how the expected results could help to confirm the models or to solve these problems.

### 1. Introduction

An understanding of most of the critical stellar features, such as time scales, energy production, and nucleosynthesis of the elements, hinges directly on the magnitude of nuclear reactions. Some of these reactions were measured directly at low energy, close to the corresponding energies that prevail in the interior of stars. These direct measurements are not possible for most of the reactions, due to extremely low cross sections. Most of the reactions cross sections were estimated, on the basis of nuclear structure studies and on measured properties. Nowadays, after decades of experimental and theoretical studies, a coherent picture of the Universe can be drawn. This coherent picture and these models remain to be validated. Few problems still remain unsolved. In this paper, two cases are discussed: novae explosions and X-ray bursts.

### 2. Novae explosion

#### **Description of the problem**

Novae explosions are cataclysmic events, which occur in binary stars. They are triggered by a thermonuclear runaway that takes place on the surface of a compact white dwarf star onto which matter is accreted from close companion. Typically, about fifty nova outbursts are expected in the Milky Way per year, becoming the second most frequent type of thermonuclear explosion in the Galaxy after X-ray bursts. Classical novae are expected to recur with periodicities of the order of  $10^4 - 10^5$  years. The amount of mass ejected in novae is  $10^{-4} - 10^{-5}$  solar masses. Although novae scarcely contribute to the Galaxy's overall enrichment in heavy elements, they may inject into the interstellar medium significant amounts of their most abundantly produced species,  $^{13}\text{C}$ ,  $^{15}\text{N}$ ,  $^{17}\text{O}$  and to a minor extent other species such as  $^7\text{Li}$ ,  $^{19}\text{F}$  and  $^{26}\text{Al}$ . Classical novae outbursts on low-mass CO white dwarfs are characterized by a moderate nuclear reaction flow, which does not extend much beyond oxygen. In contrast, novae explosions, which occur with white dwarfs composed of oxygen and neon seed nuclei (ONe)

involve a larger nuclear reaction network, spanning up to the silicon or argon isotopes. This suggests that the observation of large amounts of intermediate-mass nuclei (such as phosphorus, sulphur, chlorine or argon) in a nova explosion reveals the presence of an underlying massive (ONe) white dwarf. In agreement with the elemental observations of the nova ejecta, the theoretical endpoint in novae nucleosynthesis is limited to  $A < 40$ . Models predict that the gamma-ray emission from classical novae is dominated, during the first hours, by positron annihilation resulting from the beta decay of radioactive nuclei. The main contribution comes from the decay of  $^{18}\text{F}$  (half-life of 110 minutes) and hence is directly related to the  $^{18}\text{F}$  formation during the outburst. A good knowledge of the nuclear reaction rates leading to the production and destruction of  $^{18}\text{F}$  is required to calculate the amount of  $^{18}\text{F}$  synthesized in novae and the resulting gamma-ray emission. The reaction rate relevant for the main mode of  $^{18}\text{F}$  destruction (i.e., through  $^{18}\text{F}(p,\alpha)^{15}\text{O}$ ) has been the object of many recent experiments. Despite certain progress, this reaction rate still remains badly known; the rate uncertainty is about a factor 100 in a large range of temperatures. This clearly supports the need of new experimental studies to improve the reliability of the predicted gamma-ray fluxes from novae. The reaction rate uncertainties for the reaction  $^{18}\text{F}(p,\alpha)^{15}\text{O}$  come from the unknown properties of the levels in the compound nucleus  $^{19}\text{Ne}$ , just above the  $^{18}\text{F}+p$  threshold. A comparison between the known levels in the well-studied mirror nucleus  $^{19}\text{F}$  and the levels in  $^{19}\text{Ne}$  shows that many states have not yet been identified in  $^{19}\text{Ne}$ . It is important to determine precisely the energy of the states. For most of the known states in  $^{19}\text{Ne}$ , only tentative assignments have been made so far. It is very important to measure or confirm the assignment of the states. Moreover, most of the level widths are unknown. The largest partial widths are expected for the alpha emission. From the properties of the mirror nucleus we can estimate that the values are in the keV energy range. It is also very important in the calculation of the reaction rate to know precisely the alpha widths of the states. All those defects clearly incite for a new experiment with a very high-energy resolution.

### Experimental method

The method we used (experiment E442S) to investigate the spectroscopy of the  $^{19}\text{Ne}$  nucleus is the resonant elastic scattering at low energy. At low energy it is known that the elastic scattering shows up resonances, which are related to the compound nucleus structure. In this way, to study the spectroscopy of  $^{19}\text{Ne}$  we can measure the reaction  $^{15}\text{O}(\alpha,\alpha)^{15}\text{O}$ . We can use a silicon detector to detect the emitted alpha particles. Since  $^{15}\text{O}$  is a radioactive nucleus, we must measure this elastic reaction in inverse kinematics  $\alpha(^{15}\text{O},\alpha)^{15}\text{O}$  using a thin helium gas target. In fact, the excitation function is measured in one time from the entrance energy to the energy of the outgoing heavy ions, after they have crossed the gas target. The inverse geometry and small specific energy loss of the alpha strikingly reduce the influence of the beam spread and the straggling on the final energy resolution. This method is very well suited for secondary beams since the limited intensity is compensated by the large cross sections (several 100 mbarn/sr). From the shape of the resonances one can obtain the angular momentum of the reaction, and finally deduce the spin assignment of the states. The

predicted excitation function is shown in Fig. 1. The energy broadening of the alpha particles is minimal at zero degree. At zero degree, with a very narrow angle aperture of  $1^\circ$  ( $\sim 1$  msr), using a high energy resolution silicon surface barrier detector, and a thin helium gas target ( $100 \mu\text{g}/\text{cm}^2$ ), we can achieve a resolution better than 4 keV in centre of mass frame, a real improvement in the spectroscopy of this nucleus.

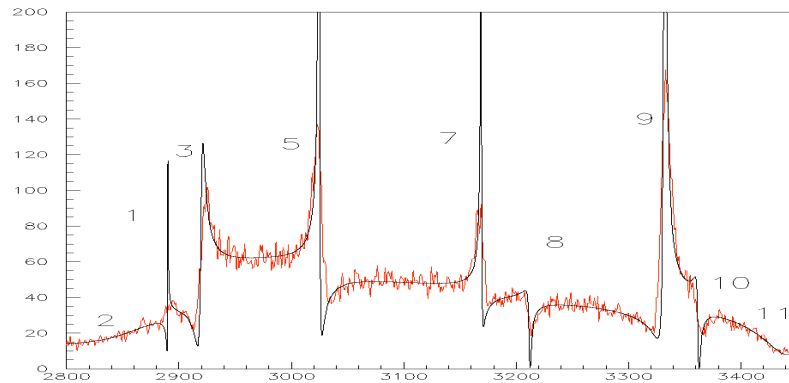


Figure 1: Number of counts (per keV) versus energy in centre of mass frame. This figure is a simulation using predicted levels (labelled). The line corresponds to an R-Matrix analysis.

## Results

### $p(^{14}\text{N},p)^{14}\text{N}$

We performed several measurements to calibrate our silicon detector and to validate the analysis procedure.

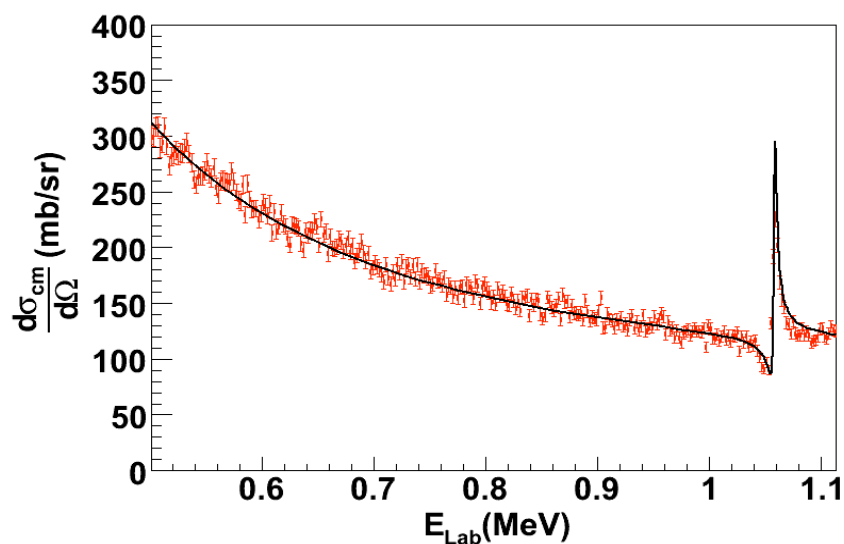


Figure 2: Excitation function for the  $p(^{14}\text{N},p)^{14}\text{N}$  reaction. An excellent energy resolution was obtained since a narrow resonance is observed at  $\sim 1.1$  MeV in  $^{15}\text{O}$  with a width of  $\sim 3.6$  keV.

The  $p(^{14}\text{N},p)^{14}\text{N}$  reaction is one of the reactions we used for the calibration, using a thick solid polypropylene target. The results obtained for this reaction

are shown in Fig. 2. We achieved a very nice resolution of few keV. The R-matrix analysis (continuous line) is in perfect agreement with the known data.

### $p(^{15}\text{O},p)^{15}\text{O}$

We have found new and interesting results for the unbound compound nucleus  $^{16}\text{F}$ . The ground and two excited states are clearly visible in Fig. 3. Using an R-Matrix analysis, the properties of these states were determined with a high precision.

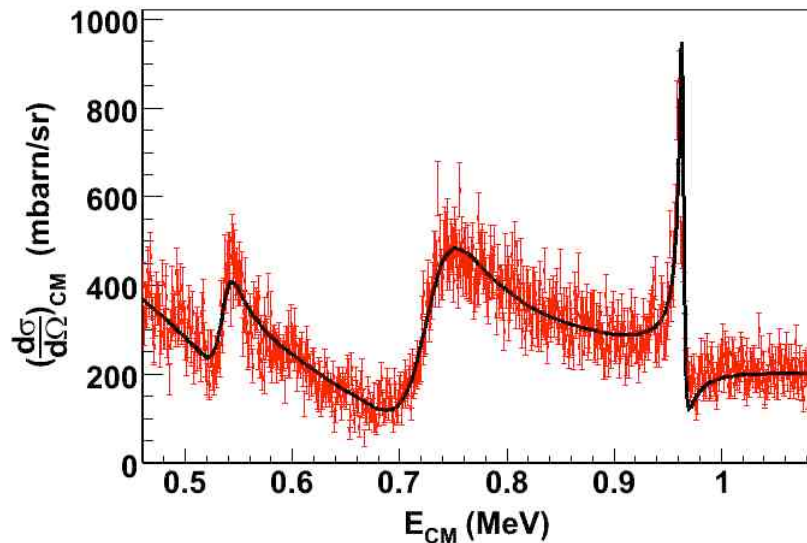


Figure 3: Excitation function for the  $p(^{15}\text{O},p)^{15}\text{O}$  reaction. Peaks correspond to states in  $^{16}\text{F}$ , the height, width, position and shape of which can be used to determine the lifetime, energy and spin of the states.

### $^4\text{He}(^{15}\text{O},\alpha)^{15}\text{O}$

Unfortunately, the gas target encountered several problems. The thickness of the entrance and exit windows of the gas target continuously changed due to the degradation by the beam interaction, and probably the scattering of the incident beam on the edges of the windows. It prevented us to achieve the expected energy resolution.

### Conclusions

This experiment has proved that resonant elastic scattering measurements can achieve very high-energy resolution (better than 4 keV) and can determine the main properties of the states (energy, spin and parity, width). The  $^{18}\text{F}(p,\alpha)^{15}\text{O}$  reaction still remains badly known and requires further investigations. A thin gas target that can sustain high beam intensities is needed. Results obtained in the E442S experiment for the  $^{16}\text{F}$  nucleus were used in the X-ray bursts reaction rates (see next section).

### 3. X-ray bursts

#### Description of the problem

X-ray bursts are cataclysmic events, which occur in binary systems. In these astronomical events, accretion takes place from an extended companion star onto the surface of a neutron star (type I X-ray bursts). The accreted matter is compressed until it reaches sufficiently high-pressure conditions to trigger a thermonuclear runaway. In these explosive events, the stable elements are mainly transformed into drip-line nuclei by successive rapid proton captures. For example,  $^{16}\text{O}$  nuclei are transformed by rapid proton captures into  $^{18}\text{Ne}$  via  $^{16}\text{O}(p,\gamma)^{17}\text{F}(p,\gamma)^{18}\text{Ne}$ . Then, the pathway for new proton captures is hindered by the presence of proton-unbound nuclei. In the previous example, the  $^{18}\text{Ne}$  nucleus captures a proton to produce the  $^{19}\text{Na}$  nucleus, which is unbound for proton emission and which decays instantly into  $^{18}\text{Ne} + p$ . The reaction flux and the energy generation are then limited by the relatively slow  $\beta^+$  decay of  $^{18}\text{Ne}$ , which is a waiting point nucleus. The sudden and intense release of energy observed in X-ray bursts requires to circumvent the limited energy generation by breakout reactions. The  $^{15}\text{O}(\alpha,\gamma)^{19}\text{Ne}$  reaction is considered to be one of the key reactions in this context. It makes the transition into the nucleosynthetic rp process (rapid proton capture). Several alternative reactions are also studied. Goerres *et al* proposed the double proton capture reaction to bridge the unbound nuclei. In the previous example, this corresponds to the reaction  $^{18}\text{Ne}(2p,\gamma)^{20}\text{Mg}$ . This two-proton capture process was calculated to be significant for extreme densities (larger than  $10^{11} \text{ g/cm}^3$ ), but this conclusion was based on the predicted properties for  $^{19}\text{Na}$  using shell model calculations. The objective of the E400S experiment was to confirm or to correct this conclusion by measuring the properties of the  $^{19}\text{Na}$  nucleus. One of the objectives of the E442S experiment was to measure the properties of the unbound nucleus  $^{16}\text{F}$ .

#### Experimental method

We used the method described in the E442S experiment, which is the measurement of the resonant elastic scattering of a radioactive  $^{18}\text{Ne}$  beam onto a proton target. A solid cryogenic hydrogen target was used; it was thick enough (1 mm) to stop the beam inside the target. This solid hydrogen cryogenic target was used for two important reasons. First, the use of compound targets (e.g.  $(\text{CH}_2)_n$ ) introduces atoms (e.g. carbon) in which nuclear reactions can occur and pollute the measurement. Second, the use of a pure hydrogen target maximizes the counting rate because the higher stoichiometric ratio leads to the highest effective target thickness. The main requirements imposed for solid hydrogen targets usable under vacuum with a particle beam are: thickness about 1 mm (in the future, probably thinner), very thin windows, and uniform thickness and density. A special cryogenic system has been designed for the present experiment. It is composed of a  $\text{H}_2$  target cell and a He cell on either side of the target. During the hydrogen target production phase, equivalent He pressure is maintained on either side of the target windows up to the complete formation of the solid  $\text{H}_2$  target. Once the target is formed, the helium gas is evacuated. After the scattering, the ejected

protons were measured by using a silicon detector placed at zero degree to achieve the best energy resolution.

Similarly, the investigation of the  $^{16}\text{F}$  properties was performed by the study of the resonant elastic scattering reaction  $\text{H}(^{15}\text{O},\text{p})^{15}\text{O}$  using a beam of  $^{15}\text{O}$  produced by the Spiral facility onto a thick polypropylene target.

## Results

In the case of the radioactive  $^{18}\text{Ne}$  beam, the results are shown in Fig. 4. It represents a measurement that last for 38 hours.

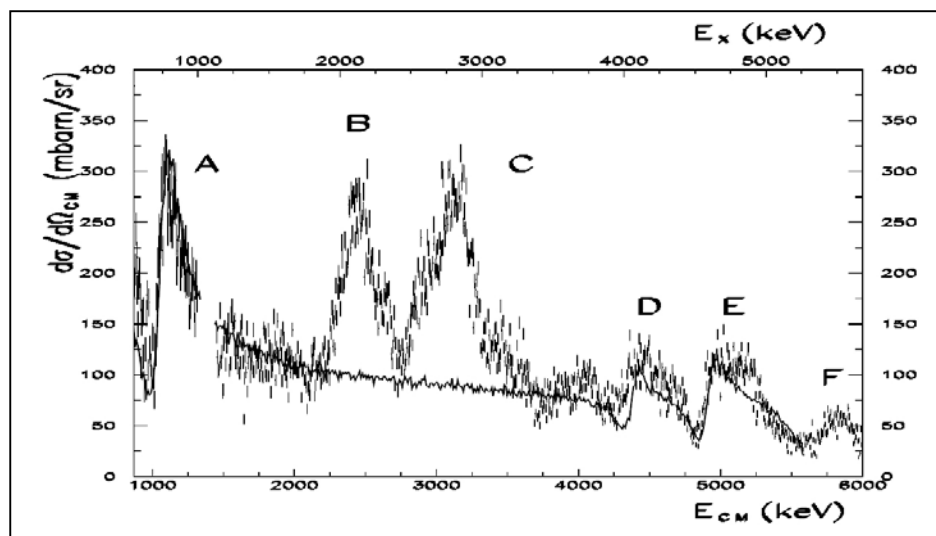


Figure 4: Excitation function of the  $\text{H}(^{18}\text{Ne},\text{p})^{18}\text{Ne}$  reaction. Peaks labelled A, D, E, and F correspond to discrete states in  $^{19}\text{Na}$ . Peaks labelled B and C correspond to inelastic scattering followed by two-proton emission.

An R-Matrix analysis of the spectrum allowed us to extract the main properties of 6 states in  $^{19}\text{Na}$ . The excitation function corresponding to the  $^{16}\text{F}$  measurement is shown in Fig. 3. The analysis was also performed by using an R-Matrix calculation. In this nucleus, the ground and 2 excited states were measured precisely.

In the case of  $^{19}\text{Na}$ , the newly obtained results do not change the conclusions drawn about the double proton capture reaction. This reaction works only at extreme densities. This holds true for  $^{16}\text{F}$ . We have calculated another alternative reaction, the  $^{15}\text{O}(\text{p},\beta^+)^{16}\text{O}$  reaction, which may bypass the  $^{15}\text{O}$  waiting point. This reaction was found to compete with the double proton capture at high temperatures. For temperatures lower than 100 millions degrees, this reaction is more intense than the double proton capture but not faster than the  $^{15}\text{O}$  beta decay. We have also proposed the sequential reaction process  $^{15}\text{O}(\text{p},\gamma)(\beta^+)^{16}\text{O}$  as a new pathway to bypass the  $^{15}\text{O}$  waiting point (see Fig. 5). This exotic reaction is found to have a surprisingly high cross section, approximately  $10^{10}$  times larger than the  $^{15}\text{O}(\text{p},\beta^+)^{16}\text{O}$  reaction. The large  $(\text{p},\gamma)(\beta^+)$  cross section can be understood to arise from the more efficient feeding of the low energy wing of the ground state resonance by the

gamma decay. The implications of this new reaction in X-ray bursts remain to be studied.

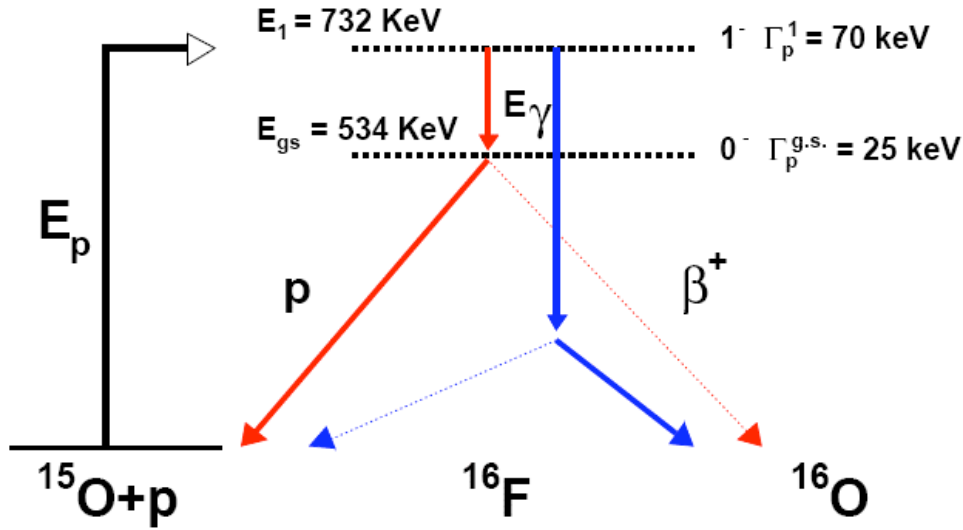


Figure 5: Schematic representation of the  $^{15}\text{O}(p,\gamma)(\beta^+)^{16}\text{O}$  reaction (see text). Two cases are represented. In red,  $\gamma$ -transitions populate the  $^{16}\text{F}$  g.s. at the resonance energy. In that case,  $^{16}\text{F}$  mainly decays by proton emission. In blue, high-energy  $\gamma$ -transitions populate the low energy wing of the g.s. resonance. In that case,  $\beta^+$ -decay dominates.

#### 4. [Conclusions](#)

Several resonant elastic scattering reactions were measured at GANIL using stable and radioactive beams from the Spiral facility. Astrophysics calculations were performed using the measured properties of unbound states. In X-ray burst, neither the double proton capture nor the  $(p,\beta^+)$  reaction seem to be interesting alternatives reactions. A new alternative process  $(p,\gamma)(\beta^+)$  was proposed and applied to the case of  $^{15}\text{O}$ , with the reaction  $^{15}\text{O}(p,\gamma)(\beta^+)^{16}\text{O}$ . This new process could be efficient in X-ray bursts conditions. In the future, we would like to perform and develop other experiments of this kind, since the resonant elastic scattering method can achieve high-energy resolution and high cross sections. It is of high interest to demonstrate or reject the  $(p,\gamma)(\beta^+)$  process, and this can be done by measuring gamma transitions in unbound nuclei for example. For this purpose, the development of beams of neutron-deficient light nuclei is required. One of our main objectives is to measure the reaction  $^{15}\text{O}(p,\gamma)(\beta^+)^{16}\text{O}$  using a  $^{15}\text{O}$  beam with the largest available intensity ( $I > 10^8$  pps).

#### 5. [References](#)

- J. Goerres et al., Phys. Rev. C51, 392 (1995).  
 F. de Oliveira et al., Eur. Phys. J. A24, 237 (2005).

Eprint: nucl-ex/0603020

Ph D. Iulian Stefan 19th December 2006

F. de Oliveira Santos et al., Tours Symposium On Nuclear Physics IV: Tours  
2000, AIP Conference Proceedings, p561

## VIII. Experiments at the low energy beam lines of SPIRAL

B. Blank\*

\* CEN Bordeaux-Gradignan, IN2P3-CNRS, Université de Bordeaux I, F-33170 Gradignan, France

Report on SPIRAL experiments E342aS and E476aS and on the SIRa experiment E512

Contact: [blank@cenbg.in2p3.fr](mailto:blank@cenbg.in2p3.fr)

### Introduction

Up to now, two experiments have been performed at the low-energy beam line LIRAT of SPIRAL: The beta-neutrino correlation experiment of the LPC Caen / GANIL (E476aS) and the study of proton and multi-proton emission from  $^{31,32,33}\text{Ar}$  by a collaboration from Bordeaux, Madrid, Aarhus, Alger, and GSI (E342aS). The former experiment is permanently installed at the LIRAT beam line, which is necessary due to its large and complicated instrumentation. The second experiment was performed at the SPIRAL identification station, which was partly dismantled for the purpose of the experiment. Both experiments will be described in the following and future perspectives will be presented.

In 2007, the SIRa test bench dedicated to the development of SPIRAL beams has been adapted to perform the first laser spectroscopy experiment ever run at GANIL in nuclear physics (E512). The results of this “première” are presented.

#### 1. Beta-delayed one- and two-proton emission from $^{31,32,33}\text{Ar}$

Beta delayed multi-particle emission becomes increasingly important when approaching the drip lines as the  $Q_\beta$  values increase and the particle emission separation energy decreases. In particular, much attention has been paid on the proton rich side to  $\beta$ -delayed 2-proton emission ( $\beta 2p$ ), since one expects to access direct information about the two-proton correlation inside the nucleus.

After the first observation of  $\beta$ -delayed 2-proton emission of  $^{22}\text{Al}$  in 1983, eight more  $\beta 2p$  emitters have been identified:  $^{23}\text{Si}$ ,  $^{26}\text{P}$ ,  $^{27}\text{S}$ ,  $^{31}\text{Ar}$ ,  $^{35}\text{Ca}$ ,  $^{39}\text{Ti}$ ,  $^{43}\text{Cr}$  and  $^{50}\text{Ni}$ .

In the LIRAT experiment, correlated two-proton (2p) emission was searched for in the decay of  $^{31}\text{Ar}$ . This 2p emission may exhibit an angular and energy correlation being indicative of an  $S=0$  state ( $^2\text{He}$ ) for the two protons emitted. After experiments at ISOLDE where 2p emission was studied to a level of about 0.2% of the decay branching ratio and no angular correlation has been found, the aim of the present experiment was to study 2p emission and to search for 3p emission to a branching ratio level of about 0.01%, which seemed to be possible due to the expected four times higher production rates from the SPIRAL source (about 10-15  $^{31}\text{Ar}$  per second) and a much higher efficiency of the detection set-up. Especially,  $l = 0$  2p transitions from the isobaric analogue state in  $^{31}\text{Cl}$ , but also from Gamow-Teller fed states are very promising candidates for a correlated 2p emission which, if observed, should help us to better understand pairing correlations in nuclei. Due to limited statistics, these transitions could not be studied in a detailed way at ISOLDE.

## 1.1. Production

The  $^{31}\text{Ar}^{3+}$  was produced in the fragmentation of a  $^{36}\text{Ar}$  primary beam at 95 A.MeV. The final energy of the  $^{31}\text{Ar}^{3+}$  beam was 30 keV (no CIME post acceleration), so it could be easily stopped in a thin foil that would not affect the energy of the emitted particles. The rate of implanted  $^{31}\text{Ar}^{3+}$  was on average only 0.6/sec and a total of only about  $10^5$   $^{31}\text{Ar}^{3+}$  could be implanted into the detection set-up during the experiment, which is 10 times less than for the last ISOLDE experiment. For  $^{32}\text{Ar}$ , we obtained a production rate of about 3 pps for a primary beam intensity of 7-8  $\mu\text{A}$ . For  $^{33}\text{Ar}$ , the rate was about 7000 pps.

Another important point about the production of  $^{31}\text{Ar}^{3+}$  at LIRAT was that  $^{31}\text{Ar}$  was contaminated by  $^{33}\text{Ar}$  at a rate of about 10/sec. This nucleus decays by  $\beta\text{p}$  and  $\beta\gamma$  to  $^{32}\text{S}$  and  $^{33}\text{Cl}$ . Many of the proton peaks from the  $^{33}\text{Ar}$  decay contaminate therefore the  $^{31}\text{Ar}$  proton decay spectrum. The  $^{33}\text{Ar}$  activity could have been significantly suppressed by an on-off cycling of the LIRAT beam, however, this was first of all not implemented for the experiment and in addition, this would have still reduced the overall counting statistics.

## 1.2. Detection set-up

The detection set-up (Fig. 1) was installed at the identification station, IBE, of SPIRAL. The nuclei were implanted into a  $0.9\ \mu\text{m}$  thin aluminised Mylar foil placed in the middle of the 'Silicon Cube'.

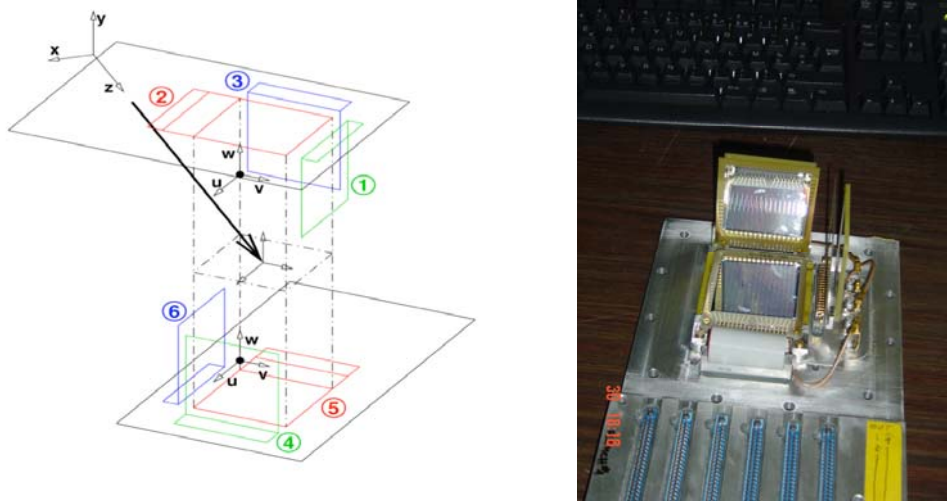


Figure 1: The silicon cube is a set-up consisting of six double-sided silicon strip detectors backed by a large-area silicon detector in very close geometry. A beam catcher or an activity transport tape can intercept the beam in the centre of the cube.

The Silicon Cube is composed of six  $48 \times 48\ \text{mm}^2$  double-sided silicon strip detectors (DSSSD) placed in a cube-like geometry, each DSSSD being backed by a  $50 \times 50\ \text{mm}^2$  square silicon detector at 4 mm distance used as a veto detector for  $\beta$  particles. The DSSSDs give a granularity of 1536 pixels. The cube was designed to have a distance between the implantation point (the centre of the cube) and each of

the strip detectors of 36.3 mm leading to a geometrical 1p efficiency of 55% of  $4\pi$  and to a 2p efficiency of 30% of  $(4\pi)^2$ . A typical resolution of the DSSSDs was 35-50 keV.

However, during the experiment, one of the DSSSDs and the veto detectors did not work properly and were therefore not used in the analysis. In addition, one DSSSD was placed further away from the collection point. This lowered the 1p efficiency to 42% and the 2p efficiency to 18%. The last ISOLDE experiment had a 1p efficiency of 25% of  $4\pi$  and a granularity of 271 pixels.

Figure 2 shows the multiplicity-one spectrum obtained for the setting on  $^{31}\text{Ar}$  and  $^{33}\text{Ar}$ . This spectrum clearly evidences the strong contamination of  $^{31}\text{Ar}$  by  $^{33}\text{Ar}$ . In addition, to  $^{31}\text{Ar}$  and  $^{33}\text{Ar}$ ,  $^{32}\text{Ar}$  was also studied. In this case, a contamination from  $^{34}\text{Ar}$  was observed. However, as  $^{34}\text{Ar}$  does not emit protons, this contamination was less troublesome.

The analysis of the experimental data is far from being finished. Therefore, only a few spectra for 2p emission from  $^{31}\text{Ar}$  will be shown and the possible outcome of the analysis will be described.

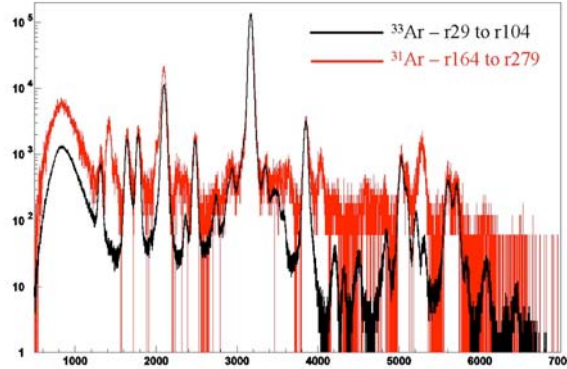


Figure 2: Multiplicity 1p spectra for  $^{31}\text{Ar}$  and  $^{33}\text{Ar}$  (full statistics): in black  $^{33}\text{Ar}$  during the setting on  $^{33}\text{Ar}^{3+}$  and in red (scaled as to have the same height for the 3171.7 keV peak from  $^{33}\text{Ar}$ ),  $^{31}\text{Ar} + ^{33}\text{Ar}$  during the setting on  $^{31}\text{Ar}^{3+}$ .

### 1.3. $\beta$ -p emission from $^{31}\text{Ar}$ , $^{32}\text{Ar}$ and $^{33}\text{Ar}$

All nuclei studied in the present work decay by  $\beta$ -p and  $\beta\gamma$  emission. For  $^{32,33}\text{Ar}$ , these are the only possible decay modes. As the proton-emission spectrum of both nuclei is reasonably well known, both nuclei were first of all studied for energy calibration purposes. However, it was also hoped to significantly improve the knowledge about the decay characteristics of both nuclei. In addition, it is tried to establish the spins of the proton emitting levels by a proton -  $\beta$ -particle angular correlation analysis. As the  $\beta$ -p spectrum from  $^{31}\text{Ar}$  is heavily contaminated, this spectrum cannot be analysed.

### 1.4. $\beta$ -2p emission from $^{31}\text{Ar}$

The energy available for the 2p emission,  $Q_{2p}$ , can be calculated as follows:

$$Q_{2p} = E_{p1} + E_{p2} + \frac{m_p}{M_{D2}} (E_{p1} + E_{p2} + 2\sqrt{E_{p1}E_{p2}} \cos\theta_{2p})$$

where  $E_{p1}$  and  $E_{p2}$  are the individual energies of the detected protons for multiplicity 2,  $m_p$  is the proton mass,  $M_{D2}$  is the mass of the 2p daughter and  $\theta_{2p}$  is the angle between the two protons.

From previous ISOLDE experiments, it is known that the IAS in  $^{31}\text{Cl}$  decays via 2p emission to the ground state and to two excited states in  $^{29}\text{P}$ . These three transitions can be identified in the right-hand side of Fig. 3 by the three arrows at 5.7, 6.3 and 7.6 MeV. The most pronounced and the best-isolated peak is the 7.6 MeV (207 events in the peak).

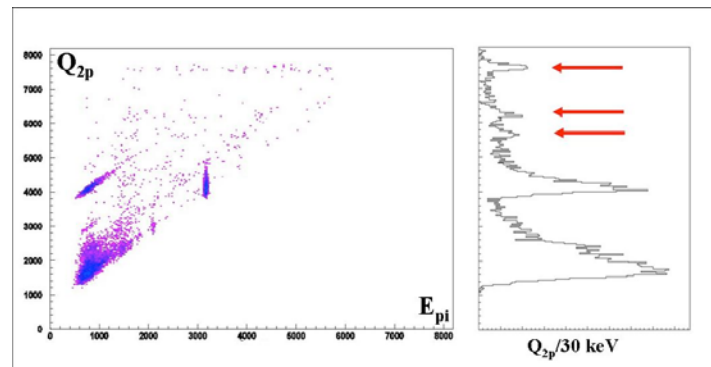


Figure 3: Multiplicity 2 events for  $^{31}\text{Ar}$ . On the left-hand side, a scatter plot of  $Q_{2p}$  against the energy  $E_{pi}$  of individual protons is shown. Each event is represented by two points on the same horizontal line. The right-hand side is the projection of this spectrum onto the  $Q_{2p}$  axis.

The two-proton events are plotted again in Fig. 4, where, on the left-hand side, the energy of one proton is plotted against the energy of the other proton. The regions of the two-proton events from the IAS are indicated by the frames.

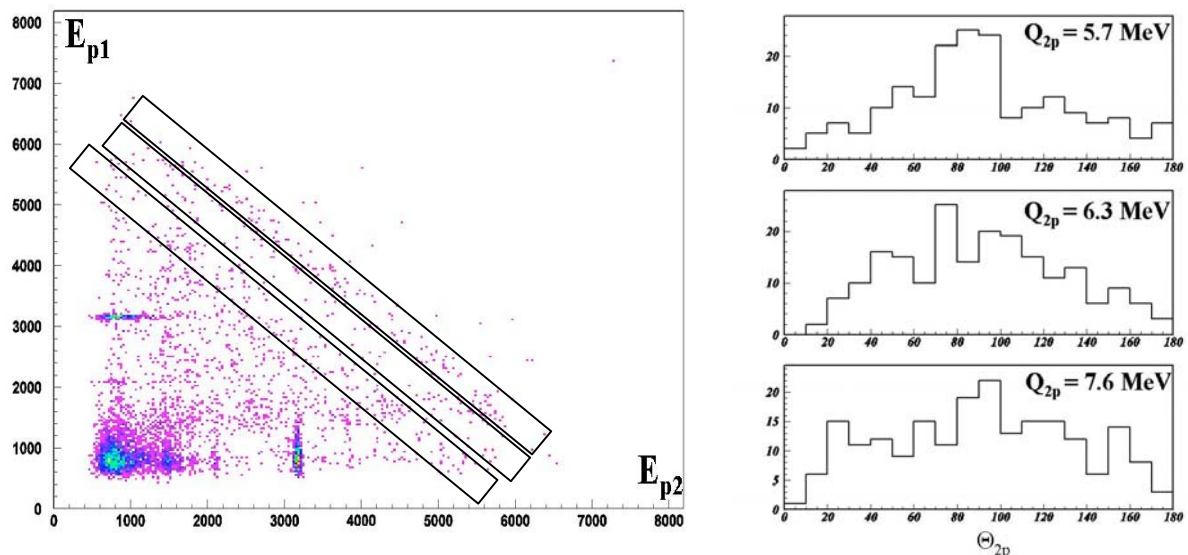


Figure 4: Multiplicity 2 events from  $^{31}\text{Ar}$ . On the left side, a scatter plot of  $E_{p1}$  against  $E_{p2}$ . On the right side, the angle between the 2 protons for the 3 peaks marked by a red flash in Fig. 3 (the 2p decay of the IAS)

These events are plotted on the right-hand side as a function of their relative angle. Although the analysis is not finished, it will be probably rather difficult with the present statistics to use cuts to e.g. take only events with similar energies for the two protons to search for a forward angular correlation between the two protons, which might be expected for a  ${}^2\text{He}$  type decay pattern. Without cuts, the distributions are dominated by the energetically allowed sequential decay via intermediate levels in  ${}^{30}\text{S}$ . In this case, an isotropic distribution is expected.

## 1.5. Summary and outlook

Unfortunately and unexpectedly, the production rate especially for  ${}^{31}\text{Ar}$  was about a factor of 20 lower than predicted before the experiment. It is likely that the prediction of the  ${}^{31}\text{Ar}$  rate was based on a  ${}^{33}\text{Ar}$  contaminated spectrum. This is possible, as some of the prominent  ${}^{31}\text{Ar}$  one-proton peaks are very close to one-proton peaks of  ${}^{33}\text{Ar}$  and can therefore not be distinguished from each other, if both nuclei are present at the same time. It is interesting to note that the contaminant rate of  ${}^{33}\text{Ar}$  in the  ${}^{31}\text{Ar}$  rate was about 10 pps, close to the predicted  ${}^{31}\text{Ar}$  rate.

The reason for this contamination is not clear. Under normal conditions,  ${}^{31}\text{Ar}$  and  ${}^{33}\text{Ar}$  as well as  ${}^{32}\text{Ar}$  and  ${}^{34}\text{Ar}$  have magnetic rigidities sufficiently different in order not to be selected at the same time, in particular with the mass selection slits closed to let pass only one mass. Possible explanations evoked during the experiment are that less exotic contaminants, which are produced more frequently by several orders of magnitude, arrive at the detection set-up as a neutral gas. However, this seems to be rather unlikely due to the flight path of several tens of meters. Another explanation was that these contaminants pass behind the slits, again rather unlikely. To understand this problem, additional tests on the LIRAT beam line are needed.

Despite the significantly higher detection efficiency as compared to the last ISOLDE experiment, the collected statistics, in particular for  ${}^{31}\text{Ar}$  is much lower. Therefore, it is not expected to improve the results from the ISOLDE runs, where the decay of  ${}^{31}\text{Ar}$  was studied several times over the last two decades. It is possible, that the correlation of  $\beta$ -particles and protons will allow for a determination of some of the spins of the proton emitting levels.

To achieve the initial goals of the experiment, the production rate for  ${}^{31}\text{Ar}$  has to be increased by a factor 10-50 (see the report of J.-C. Thomas for this Scientific Council). The detection set-up has been improved in the mean time to overcome some shortcomings from the previous version. In particular, the calibration of the different detectors, which necessitates the dismantling of some of the detectors, is greatly eased by an independent mounting of all detectors. In addition, the beam entrance slit was increase and the insertion of the catcher foil was modified in order to allow also for the insertion of the radioactive sources for calibration. Therefore, the silicon cube is right now ready for a new experiment.

## 2. [Beta-recoil correlation from the decay of \${}^6\text{He}\$ with the LPCTrap](#)

In the standard electroweak model, nuclear  $\beta$  decay is described in terms of vector (V) and axial-vector (A) couplings. Lorentz invariance allows other couplings such as scalar (S), pseudo-scalar (P) or tensor (T) to be present in the interaction,

but these are forbidden by the standard model (SM). The observation of such exotic couplings would provide signatures of new physics, which are actively searched for both, at the high-energy frontier with colliders and at low energies, like in nuclear  $\beta$  decay.

For allowed transitions, the decay rate computed from the general Hamiltonian for angular correlation measurements has the following form:

$$W(E, \theta) = W_0(E) \left( 1 + b \frac{m}{E} + a \frac{v}{c} \cos \theta \right)$$

where  $W_0(E)$  corresponds to Fermi's expression of the  $\beta$  decay rate,  $m$ ,  $v$  and  $E$  are respectively the mass, the velocity and the energy of the  $\beta$  particle, and  $\theta$  is the angle between the directions of emission of the electron and the neutrino. The parameters  $b$  and  $a$  are respectively the Fierz interference term and the  $\beta$ - $\nu$  angular correlation parameter. They depend on  $C_i$  and  $C_i'$ , the relative amplitudes of the different currents, through rather complicated expressions. These can be simplified for pure Fermi (F) or Gamow-Teller (GT) transitions, where they become sensitive only to  $C_S$  and  $C_V$  (F) or  $C_T$  and  $C_A$  (GT). Measurements of the correlation between the emitted particles in a pure  $\beta$  decay enable one to infer the angular correlation parameter and thus to test the SM values ( $a_F = 1$ ,  $a_{GT} = -1/3$ ). The measurements performed so far are consistent with the SM, within a precision of 0.5% and 1% for  $a_F$  and  $a_{GT}$ , respectively. The LPCTrap experiment is an attempt to improve the precision on  $a_{GT}$ , which has not been addressed since 1963.

## 2.1. The LPCTrap set-up

The SPIRAL ECR source delivers a  ${}^6\text{He}^+$  beam at 10-34 keV with an emittance of about  $80 \pi$  mm.mrad. The confinement in a trap of such a beam requires slowing down, cooling and bunching the ions. The general layout of the LPCTrap set-up is presented in Fig. 5.

The reduction of the beam emittance is achieved by means of the buffer gas cooling technique associated with the use of a Radio-Frequency Quadrupole (RFQ). A critical point of this project was to demonstrate the feasibility of cooling light ions with this technique. This was achieved in an experiment performed at GANIL. Stable  ${}^4\text{He}^+$  ions, produced by an ECR source at 10 keV, were cooled and bunched using  $\text{H}_2$  as a buffer gas. An efficiency of 10 % was obtained for a bunching period shorter than 1 ms. The efficiency decreases when the bunching period is increased due to the ion lifetime in the buncher. For  ${}^6\text{He}$ , an optimal duty cycle of about 100 ms can be estimated, and in this case the RFQ transmission is about 2%.

The radioactive ions are then confined in a Paul trap. The operating principle of this device enables one to install detectors very close to the trap, which can have a very simple and transparent structure, as the "ring" trap presented in Fig. 5. The ion cloud in the trap is monitored by a micro-channel plate detector (MCP) located along the beam direction, downstream from the trap (see Fig. 5). The time-of-flight (TOF) between the extraction signal from the buncher and the MCP ion signal is continuously measured. A trapping efficiency of 20 % has been achieved. The lifetime of the ions in the trap has been measured to be typically 250 ms.

The trap is located at the centre of the chamber, and the electron and ion detectors are arranged in a back-to-back geometry. The relative position of the detectors is fixed by the characteristics of a pure GT transition, for which the  $\beta$  particle and the recoil ion are preferentially emitted back-to-back for a tensor interaction. The  $\beta$  particle telescope has a time resolution of 200 ps, an energy resolution of 10 % for 1 MeV electrons, and a spatial resolution of 1 mm. The absolute efficiency of the recoil detector MCP reaches about 52 % above 2.5 keV and is constant within 1 % in a 5 keV energy window. It has a time resolution of the order of 200 ps and a position resolution of 110 (26)  $\mu\text{m}$ . The two detectors are located at 10 cm from the trap center. The total efficiency of the detection set-up reaches 0.28 %, taking into account the anisotropy of the event distribution in the  ${}^6\text{He}$  decay and the absolute efficiency of the MCP.

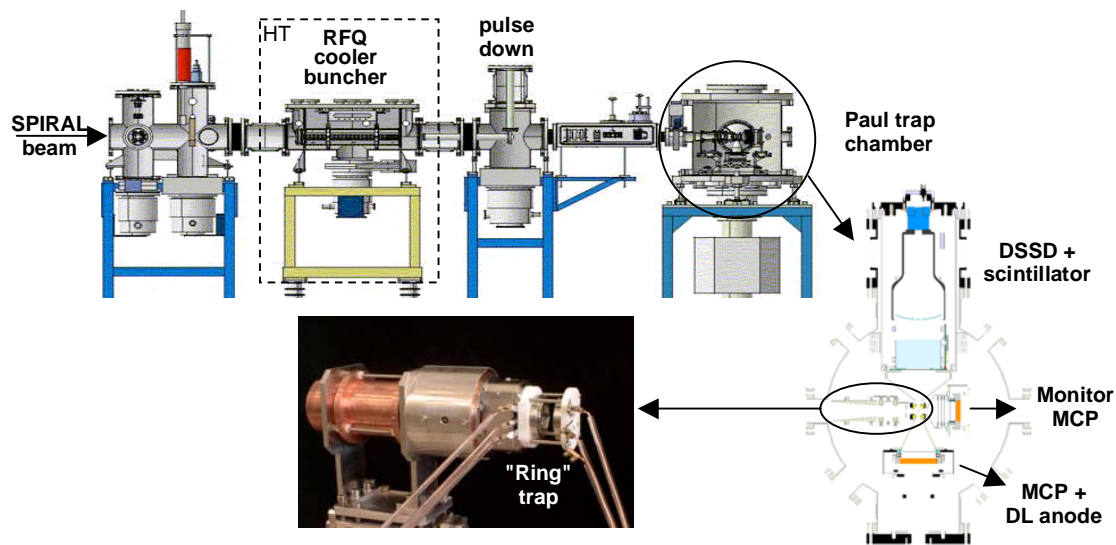


Figure 5: Layout of the LPCTrap set-up installed at LIRAT, with schemes of the Paul trap chamber and the "ring" trap.

The detection set-up gives access to three observables of the kinematics: the  $\beta$  energy, the recoil energy and the  $\beta$ -recoil angle. The combination of these parameters should enable one to reject false coincidences and to control systematic effects.

## 2.2. Results

After a proof of principle measurement in 2005, the first data-taking run took place in July 2006. The low energy beam line was tuned with a special setting to separate the  ${}^{12}\text{C}^{2+}$  contaminants. Under these conditions, the largest  ${}^6\text{He}^+$  beam intensity measured at the entrance of the RFQ was  $1.2 \times 10^8$  ions/s. Although the extraction voltage from the ECS was set to 10 kV, the measured intensity is consistent with expected values when including a loss factor of about 2 due to the special tune of the beam line to realize the mass separation. The measured intensity reflects an improvement by a factor of 4 in the low-energy beam extraction and transmission relative to the commissioning run in July 2005.

The overall efficiency measured during the run was about  $10^{-4}$  including the cooling, bunching, and trapping of the  ${}^6\text{He}^+$  ions. This is significantly lower than efficiencies achieved during off-line tests with  ${}^4\text{He}^+$  ions. Part of the reduction is known to be caused by the first pulse-down electrode, which was found few days before the run to operate with degraded transmission and could not be fixed in time.

During this beam time, up to  $10^5$  coincidences were recorded. Figures 6a and 6c show examples of experimental spectra obtained on line. The two-dimensional spectrum presents the distribution of the  $\beta$  kinetic energy versus the TOF of the recoil ions. The second spectrum is a projection on the TOF axis.

Figures 7 and 6d show the same quantities simulated with  $a = -1/3$ . The simulation is performed for a point-like source located in the middle of the trap and with cuts in the kinematics corresponding to the detector geometry. The trap RF field is not taken into account. The comparison shows the quality of the data: The signal over noise ratio is excellent and the behaviour of the data follows the pattern of the 'standard' simulation. A statistical precision of about 2 % should be reached with the present statistics. These first data should also allow for a study of some of the systematic effects due to e.g. the response function of the detectors. The effects of the trap RF field and the ion cloud temperature on the recoil motion will also be investigated with the set of parameters recorded for each event.

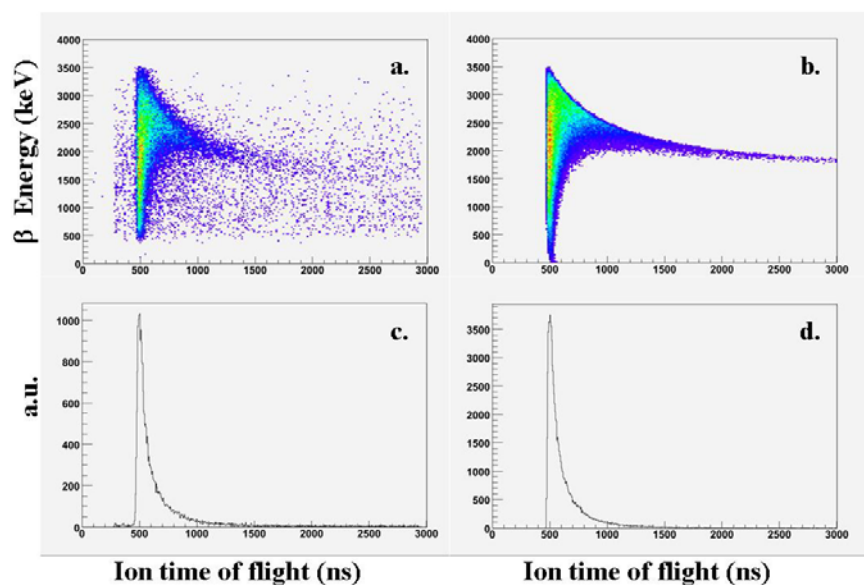


Figure 6: Figure a (b) shows the energy distribution versus the recoil ion TOF from experimental data (simulation data). Figures c (experiment) and d (simulation) are the corresponding TOF distributions for the coincidence events. The experimental spectra content about one fourth of the total statistics.

### 2.3. Improvements and future experiments

Further efforts are needed to increase the collected statistics by a factor of 20, reaching thereby a relative precision level of 0.5 %. Such a factor should be within reach after a study in more detail of the following points:

- i) The operation with a higher extraction voltage from the ion source and hence with a larger beam energy. Tests have been performed both, with stable

- beams before the 2006 run and with  ${}^6\text{He}^+$  at the end of the 2006 run but further tests with stable beams are needed to draw clear conclusions.
- ii) The low energy beam optics used to separate the  ${}^6\text{He}^+$  and  ${}^{12}\text{C}^{2+}$  beams. The  ${}^6\text{He}^+$  transmission from the source to the RFQ could still be improved by a factor 1.4. The effect on the efficiency of the set-up due to  ${}^{12}\text{C}^{2+}$  contaminant needs to be optimised.
  - iii) The control of the injection optics into the RFQ by the addition of a position sensitive detector for the monitoring of the  ${}^6\text{He}$  beam spot distribution. Small drifts in the injection parameters strongly affect the efficiency of the RFQ. The absence of adapted beam diagnostics at the entrance of the RFQ renders the reaction inefficient.
  - iv) The configuration of the first pulse-down electrode and its operation under nominal performance. This should improve the overall efficiency by a factor of 10.
  - v) The stabilization of the system to run continuously under the best conditions. System instabilities during the 2006 run resulted in an average coincidence rate, which was a factor of 2 lower than the rate measured under the best conditions. Such variations could be due to temperature drifts or related with magnetic remnance effects in a dipole magnet but the actual source could not be identified.

For 2007, a new beam time with a high-intensity  ${}^6\text{He}^+$  is planned at LIRAT, which should allow for the accumulation of a data sample corresponding to a relative statistical precision of 0.5 % on  $a_{\text{GT}}$ .

### **3. Laser spectroscopic determination of the ${}^8\text{He}$ nuclear charge radius**

The understanding of the nuclear structure of neutron-rich light nuclei such as  ${}^6\text{He}$  and  ${}^8\text{He}$  represents a challenge for modern theories aiming at reproducing the basic properties of the atomic nucleus from bare nucleon-nucleon interactions. In particular, neutron correlations in these so-called “halo nuclei” are still under investigation. Up-to-date laser spectroscopy techniques allowing the determination of nuclear charge radii along an isotopic chain can be used to address this question. Following pioneering work initiated at Argonne, USA and leading to the measurement of the nuclear charge radius of  ${}^6\text{He}$  relative to  ${}^4\text{He}$ , the same set-up was installed at the SIRa test bench to determine the nuclear charge radii of  ${}^6\text{He}$  and  ${}^8\text{He}$ .

#### **3.1. Experimental technique**

The difference in charge radius between several isotopes can be derived from the measurement of atomic isotope shifts combined with precise atomic theory calculations. The isotopic shift is extracted from the small frequency variations of the hyperfine structure of the trapped atoms, probed by means of a tuneable laser light.  ${}^6\text{He}$  and  ${}^8\text{He}$  were produced at SIRa in the fragmentation of a 75 A.MeV  ${}^{13}\text{C}$  beam in a graphite target. Atoms were ionized in a  $1^+$  charge state in an ECR source similar to the one in use at SPIRAL, extracted, mass separated and neutralized in a hot graphite foil (Fig. 7). Released as atoms, the helium isotopes were excited into a meta-stable state by means of a RF discharge. They were further laser cooled and trapped inside a MOT trap where their hyperfine structure was probed.

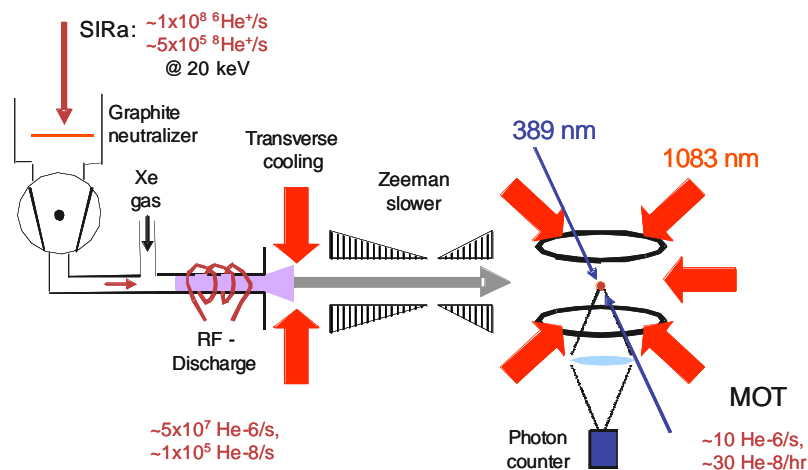


Figure 7: Experimental set-up installed at the SIRa test bench to measure the nuclear charge radii of  ${}^6\text{He}$  and  ${}^8\text{He}$  relative to  ${}^4\text{He}$ .

### 3.2. Results

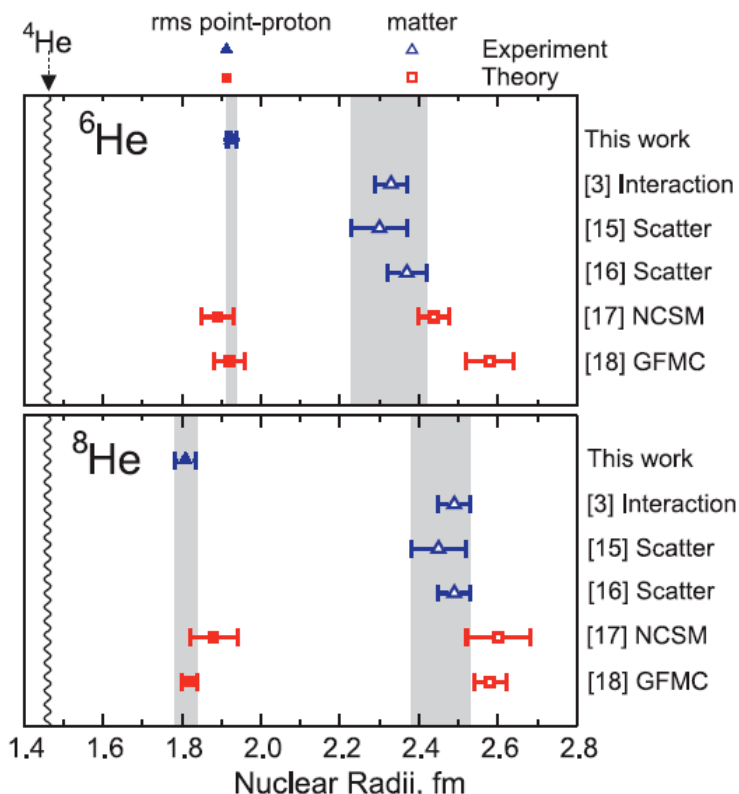


Figure 8: Comparison of rms point-proton radii (closed symbols) and matter radii (open symbols) for  ${}^6\text{He}$  and  ${}^8\text{He}$  between experiment (triangles) and theory (squares), relative to  ${}^4\text{He}$ .

Figure 8 shows a comparison of the root-mean-square (rms) charge radii of  ${}^6\text{He}$  (2.068(11)) and  ${}^8\text{He}$  (1.929(26) fm) relative to  ${}^4\text{He}$  (1.676(6) fm). Results are in agreement with *ab initio* calculations based on the no-core shell model (NCSM) and Green's Function Monte Carlo (GFMC) approaches, thus confirming the reduction of the nuclear charge radius of  ${}^8\text{He}$  as compared to  ${}^6\text{He}$ . Together with the measured

matter radii, the obtained results allow to describe  ${}^6\text{He}$  as a  $\alpha$ -like core plus two correlated neutrons, while for  ${}^8\text{He}$ , the four additional neutrons present a more spherical spatial distribution.

### 3.3. Outlook

This first laser spectroscopy experiment has shown that such techniques are well suited for the low-energy ISOL beams produced at SPIRAL. The trapping of neutral atoms may be considered in the future as a complementary tool to study exotic nuclei, depending on their production yields.

## 4. Summary and outlook

Due to the rather limited space available at the SPIRAL low-energy beam line and the rather limited list of available beams, only two different experiments were performed up to now. In addition, the conditions for the argon experiment were far from optimum in terms of space, availability of the beam line, and selectivity of the beam line and purity of the ISOL beam as well as of radioactive beam intensity.

The argon experiment will not reach its goal of search for proton-proton correlations in  $\beta$ -2p decay and of improving significantly the ISOLDE results. To reach this goal, the  ${}^{31}\text{Ar}$  beam intensity and its purity has to be improved significantly.

The LPCTrap experiment will most likely reach in the near future the design goal of a precision of 0.5 % on the  $a_{GT}$  parameter, which describes the mixture of axial-vector and tensor currents in the weak interaction. In the future, other nuclei could be studied.

The laser spectroscopy experiment paved the way for future studies of trapped atoms at SPIRAL.

It is believed that, with an extension of the beam line into the room ahead of the LPCTrap, the installation of several beam lines in this room, and an increase of the number of available and authorised beams, the low-energy beams from SPIRAL could yield high-level scientific results and be an ideal training ground for the future DESIR facility at SPIRAL2.

## 5. References

- H. Fynbo et al., Phys. Rev. C59, 2275 (1999)
- H. Fynbo et al., Nucl. Phys. A677, 38 (2000)
- J. Thaysen et al., Phys. Lett. B467, 194 (1999)
  
- G. Ban et al., Nucl. Inst. Meth. Phys. Res. A 518, 712 (2004)
- G. Darius et al., Rev. Sci. Inst. 75, 4804 (2004)
- D. Rodríguez et al., Nucl. Inst. Meth. Phys. Res. A 565, 876 (2006)
- G. Ban et al., Nucl. Phys. A 752, 67c (2005)
- E. Liénard et al., Nucl. Inst. Meth. Phys. Res. A 551, 375 (2005)
  
- L.-B. Wang et al., Phys. Rev. Lett. 93, 142501 (2004)

P. Mueller et al., Phys. Rev. Lett. 99, 252501 (2007)

## IX. SPIRAL1 – Possible development strategies

J.-C. Thomas\*

\* GANIL, CEA/DSM - CNRS/IN2P3, Bvd Henri Becquerel, BP 55027, F-14076 Caen Cedex 5, France

Contact: [thomasjc@ganil.fr](mailto:thomasjc@ganil.fr)

### 1. SPIRAL beam developments

Possible strategies for the development of SPIRAL beams were presented at the last GANIL Colloquium (May-June 2006). They follow the BUG recommendations presented to the GANIL Scientific Committee in December 2004 (see Appendix I) and discussions between the GANIL Physics Group and the GANIL Ion Production Group. These propositions are of 2 types:

- Development of new targets and improvement of GANIL beams (section 1.1)
- Implementation of new radioactive ion sources (section 1.2)

Alternative solutions are considered in section 1.3.

#### 1.1. Development of new targets and improvement of GANIL beams

The SPIRAL production cave is designed to accept as much as 6 kW of beam power, but the intensity of stable beams is limited in the GANIL facility to  $2 \cdot 10^{13}$  pps for safety considerations. Nowadays, two types of carbon target are in use at SPIRAL: the first one is specifically dedicated to the production of He ions and can sustain up to 3 kW of beam power. The second one is used to produce O, F, Ne, Ar and Kr ions and is designed to sustain 1.5 kW of beam power at maximum.

Table 1 gives a list of the radioactive beams (RIBs) available at SPIRAL and the characteristics of the stable beams that are used for their production. As shown in the table, the intensity limitation of  $2 \cdot 10^{13}$  pps is almost reached only for the production of He ions. For all other elements, different actions can be taken to increase the intensity of available beams. They are listed in sections 1.1.1. to 1.1.4.

RIBs	Stable beam	Beam Power (kW)	Energy (A.MeV)	Intensity (pps)
<sup>6,8</sup> He	<sup>13</sup> C <sup>6+</sup>	2.5	75	$1.6 \cdot 10^{13}$
<sup>15</sup> O	<sup>16</sup> O <sup>8+</sup>	1.4	95	$5.8 \cdot 10^{12}$
<sup>19,20,21,22</sup> O, <sup>23,24,25,26,27</sup> Ne	<sup>36</sup> S <sup>16+</sup>	1.4	77.5	$3.1 \cdot 10^{12}$
<sup>18</sup> F, <sup>17,18,19</sup> Ne	<sup>20</sup> Ne <sup>10+</sup>	1.4	95	$4.6 \cdot 10^{12}$
<sup>31,32,33,34,35</sup> Ar	<sup>36</sup> Ar <sup>18+</sup>	1.4	95	$2.6 \cdot 10^{12}$
<sup>44, 46</sup> Ar	<sup>48</sup> Ca <sup>20+</sup>	0.6	60	$1.3 \cdot 10^{12}$
<sup>72,73,74,75,76,77</sup> Kr	<sup>78</sup> Kr <sup>34+</sup>	1.2	70	$1.4 \cdot 10^{12}$

Table 1: Characteristics of the stable beams used for the production of the RIBs delivered by the SPIRAL facility to the GANIL experimental areas. Isotopes for which the BUG has recommended increased intensities are quoted in red.

New SPIRAL beams could be produced using appropriate targets, either by means of the target-fragmentation technique or via the formation of molecules. These possible developments are discussed in sections 1.1.4 and 1.1.5, respectively.

### 1.1.1. Development of high-power carbon targets

The design of 3 to 6 kW carbon targets can be studied. Two main issues have to be considered: the first one is related to radiation damages that could shorten the lifetime of the SPIRAL ion source. The second one deals with the beam-power dissipation inside the target. In addition, to improve the intensity of specific RIBs, the design of the targets must also take into account the range of the atoms of interest, in order to optimise their production yield and their release by the target. Such dedicated developments would take 12 man.months per given target. They are supported by the BUG recommendations for an intensity increase of the following RIBs:  $^{15}\text{O}$ ,  $^{18}\text{F}$ ,  $^{24}\text{Ne}$ ,  $^{33,34,44,46}\text{Ar}$ ,  $^{72}\text{Kr}$  and  $^{74}\text{Kr}$  (see table 1).

### 1.1.2. Increase of primary beam intensities

The development of high-power carbon targets only makes sense if the intensity of the stable beams delivered by the GANIL facility can be simultaneously increased. Table 2 presents the high-energy beam power achievable at GANIL and expectations associated with the upgrade of the currently used stable ion sources.

Stable beams	Available beam power	Expected performances	Comments
$^{16}\text{O}$	4.5 kW	-	safety limitation
$^{20}\text{Ne}$	6 kW	-	safety limitation
$^{36}\text{S}$	3.2 kW	4.1 kW	source limitation
$^{36}\text{Ar}$	3 kW	-	accelerator limitation
$^{48}\text{Ca}$	0.8 kW	1.2 kW	source limitation
$^{78}\text{Kr}$	1.3 kW	1.9 kW	source limitation

Table 2: Current and expected power of the stable beams delivered by the GANIL facility to produce radioactive beams at SPIRAL.

According to tables 1 and 2, 3 kW high-energy beams are already available at GANIL for the production of radioactive isotopes lighter than  $^{35}\text{Ar}$ . However, as illustrated by the example of  $^{36}\text{Ar}$ , the beam power of which is limited by the acceleration process and not by the stable ion-source performances, the main issue is related to the stability of the high-energy and high-power beams delivered to SPIRAL. In other words, the development of 6 kW carbon targets will only be relevant if combined with an upgrade of the GANIL accelerators and beam lines. The development of 3 kW targets should therefore be considered as a first objective, allowing for a gain of a factor of 2 and stable running conditions for the production of O, F, Ne and neutron-deficient Ar isotopes at SPIRAL.

The production yield of neutron-rich Ar and of Kr isotopes is limited by the performances of the stable ion sources, the efficiency of which drops when highly-charged  $^{48}\text{Ca}$  and  $^{78}\text{Kr}$  ions have to be produced. Small power gains of the order of 30 % are expected in these two cases, from an upgrade of the existing stable ion sources. Such developments would require from 1 to 3 man.months of manpower. The existing stable ion sources could be replaced by a stable ion source providing higher yields of highly-charged ions. A prototype of such a source is available at

GANIL and could be further developed. The so-called GTS device would provide a gain in intensity of a factor of 2 for all the stable beams presented in table 2. The realization of the GTS project requires 3.2 man.years of manpower, disregarding the human resources needed to modify the test and production installations.

In the specific case of  $^{24}\text{Ne}$ , the intensity increase of which is requested by the BUG committee, the use of  $^{26}\text{Mg}$  as a stable beam instead of  $^{36}\text{S}$  would enhance the SPIRAL production yield by a factor of 2. Recently, a high intensity  $^{24}\text{Mg}^{5+}$  beam has been extracted from the stable ion source of GANIL. Further developments would allow the use of a 3kW  $^{26}\text{Mg}$  beam at 76 A.MeV, resulting in an overall gain of a factor of 5 for the production of  $^{24}\text{Ne}$  at SPIRAL. Such a stable beam development would require 2 man.months. The intensity of  $^{23}\text{Ne}$  and  $^{21,22}\text{O}$  SPIRAL beams would also be increased by almost a factor of 5 and 4, respectively.

### 1.1.3. Target developments for short-lived isotopes

The intensity of short-lived isotopes is limited by the diffusion time of the fragments stopped inside the target, and by the time they need to effuse towards the ionisation volume of the ECR source. Figure 1 shows the target-ion source (TIS) efficiency for neutron-deficient Ar isotopes. Results are compared to a semi-empirical modelization of the total efficiency, deduced from time dependent parameterisations of the diffusion and effusion processes. While the total efficiency of the TIS ensemble gets close to 100 % for the production of stable or long-lived noble gases, it decreases to about 10 % for noble gases with lifetimes of the order of 100 ms.

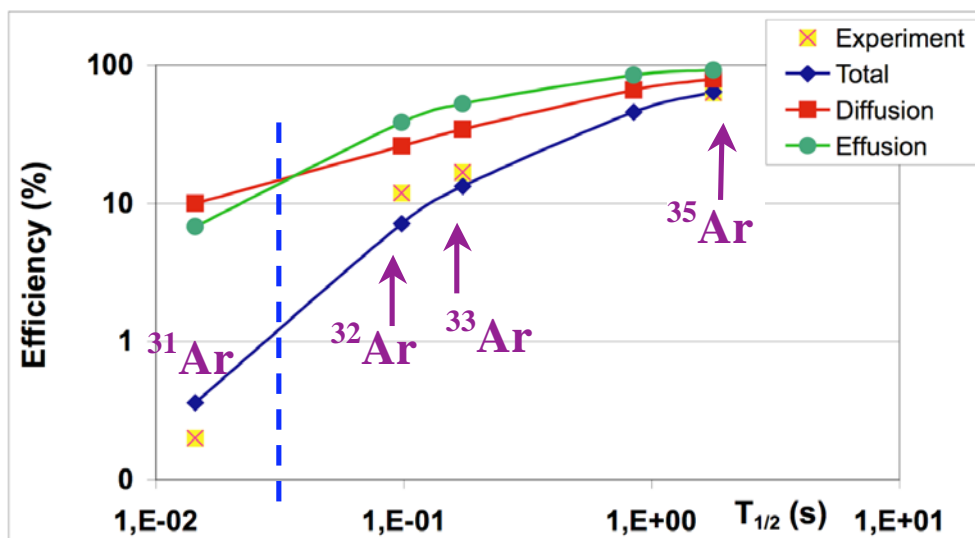


Figure 1: Efficiency of the SPIRAL target-ion source for neutron-deficient Ar isotopes. Experimental results are compared to semi-empirical modelizations of the diffusion and effusion processes.

Two regimes can be distinguished depending on the lifetime of the isotopes of interest: above a few tens of ms, the effusion process limits the efficiency. Below, the diffusion process becomes the main limitation.

The effusion speed of the fragments released by the target is limited by the conductance between the target and ionisation chambers and by the large volume of the target chamber. The latter can be reduced bringing the target closer to the

transfer tube of the target-ion source. In addition, the conductance can presumably be increased by a factor of 10 by modifying the geometry of the target-ion source. The associated shortening of the effusion time would give rise to higher production yields for short-lived isotopes. As illustrated in Fig. 2, such modifications could lead to production yields 10 times higher for  $T_{1/2} \sim 10$  ms radioactive isotopes such as  $^{31}\text{Ar}$ , the intensity increase of which is recommended by GANIL users.

In parallel, specific targets dedicated to the production of short-lived isotopes can be developed in order to accelerate the diffusion process: provided that the fragments of interest have a longer range in the target than the primary beam, that is to say if the  $Z$  value of the fragment is much lower than the one of the projectile, a target consisting in two separated layers can be implemented: the first part where the beam fragmentation takes place would be made of carbon. The second one where fragments are stopped could be built in a material such as aerogel ensuring a faster release.

A modified target-ion source providing a faster effusion process has to be built and tested. For such a task, 9 man.months are required. Dedicated target developments would take 6 man.months per given target. In case such targets could not be housed in the existing target chamber, further manpower would be needed to implement the newly designed TIS inside the SPIRAL production cave. Safety issues would also need to be considered.

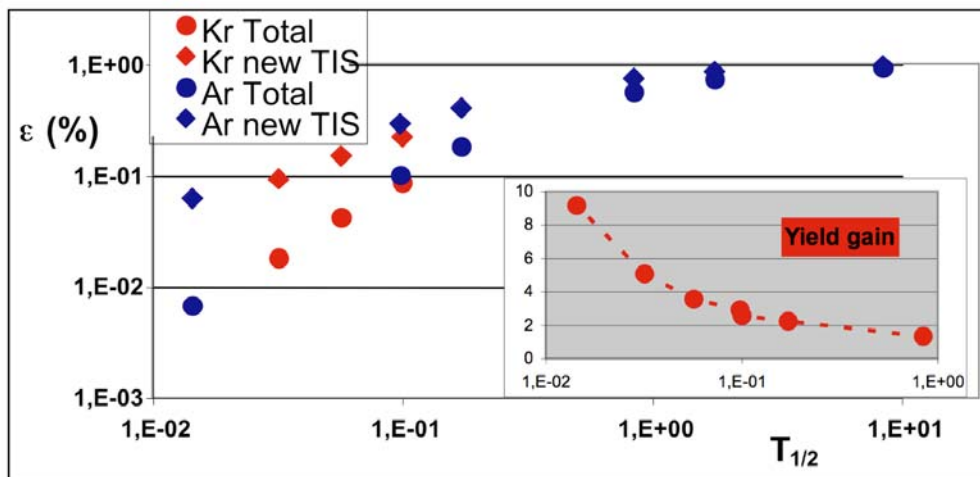


Figure 2: Expected gain for the production of short-lived noble gases using a new target-ion source (TIS) device with a better conductance and a smaller target-chamber volume.

#### 1.1.4. The target-fragmentation technique

A preliminary study by M.-G. Saint-Laurent shows that the production yield of neutron-deficient Kr isotopes could be increased significantly using the heavy-ion induced target-fragmentation technique instead of the projectile fragmentation. Nb and  $\text{ZrO}_2$  targets are foreseen. Table 3 presents the expected in-target production gain using a 3.6 kW  $^{12}\text{C}^{6+}$  primary beam (corresponding to the safety limit of  $2 \cdot 10^{13}$  pps) to induce the fragmentation of a Nb target as compared to the conventional technique consisting in the fragmentation of a 1.2 kW  $^{78}\text{Kr}$  beam in a C target.

A gain of a factor of 8 to 10 is within reach for  $^{72}\text{Kr}$  and  $^{74}\text{Kr}$ , for which increased yields are recommended by the BUG committee. In contrast with the beam-

fragmentation technique, the target-fragmentation method can be used to produce neutron-deficient as well as neutron-rich nuclei, depending on the beam and target combination. As an illustration, Fig. 3 compares the production cross-section of Kr isotopes obtained using the SIGMASIRA code for a 95 A.MeV  $^{12}\text{C}$  primary beam impinging on natural Nb and Zr targets. Similar cross sections in the  $\mu\text{barn}$  range are expected for  $^{92}\text{Kr}$  and  $^{72}\text{Kr}$ , thus opening new physics opportunities on the neutron-rich side of the nuclide chart.

$^A\text{Kr}$	Beam fragmentation (C target) 1.2 kW $^{78}\text{Kr}$ @ 70 A.MeV	Nb target fragmentation 3.6 kW $^{12}\text{C}$ beam @ 95 A.MeV	Expected gain
72	$9.0 \cdot 10^4$	$7.4 \cdot 10^5$	8
73	$1.3 \cdot 10^6$	$1.4 \cdot 10^7$	11
74	$1.4 \cdot 10^7$	$1.4 \cdot 10^8$	10
75	$1.1 \cdot 10^8$	$8.6 \cdot 10^8$	8
76	$6.9 \cdot 10^8$	$3.0 \cdot 10^9$	4
77	$2.9 \cdot 10^9$	$6.1 \cdot 10^9$	2

Table 3: Expected gain for the production of neutron-deficient Kr isotopes at SPIRAL (in pps) using the target fragmentation technique as compared to the fragmentation of a  $^{78}\text{Kr}$  beam in a conventional C target. Production yields are given in the target.

The design of high power Nb or  $\text{ZrO}_2$  targets represents an important research and development program for which 48 man.months of manpower would be required.

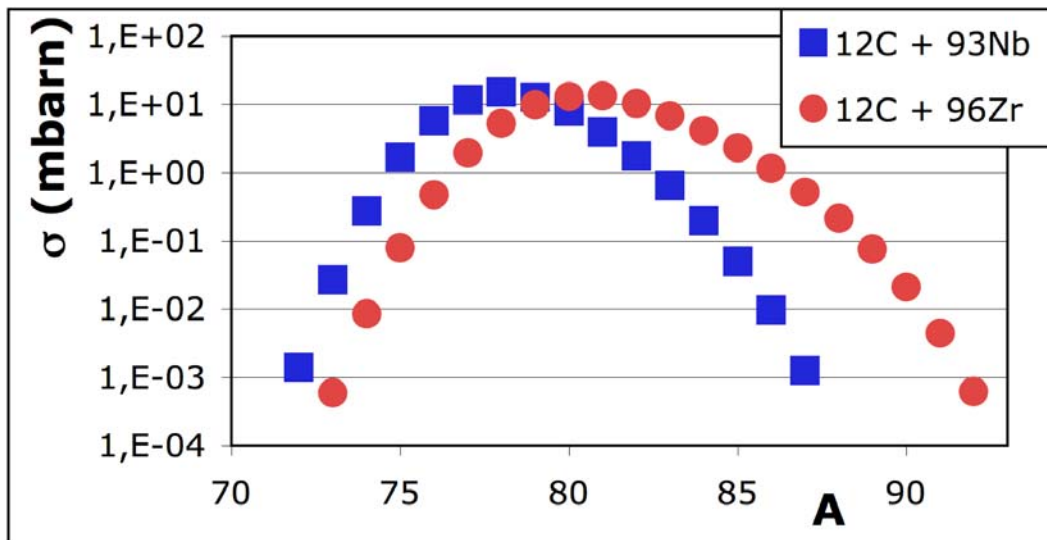


Figure 3: Kr production cross-sections obtained in the  $^{12}\text{C}$  induced fragmentation of Nb and Zr targets at 95 A.MeV. They were obtained using the SIGMASIRA code.

The coupling of Nb or  $\text{ZrO}_2$  targets with different ionisation sources such as the one described in section II.2 may be investigated to provide new exotic beams at the SPIRAL facility. However, several issues have to be considered:

- Nb targets are currently used in other facilities like TRIUMF and ISOLDE, but the power dissipation inside the target would be 10 times higher at SPIRAL because

high-energy heavy ions are used instead of high-energy protons. Target developments are therefore needed before the target-fragmentation technique can be implemented at SPIRAL.

- The fragmentation of a Nb ( $ZrO_2$ ) target will also lead to the production of long-lived isotopes (e.g.  $^{85}Kr$  with  $T_{1/2} = 10.8$  y), which may limit the primary-beam intensity.

- At present, only carbon targets can be used at SPIRAL. The implementation of new targets must be approved by the safety authorities and has to be compatible with the radiation sustainability of the ion source.

#### 1.1.5. New SPIRAL beams from molecular compounds

The production of radioactive nuclei from the formation of molecules inside the fragmentation target has been investigated at SPIRAL and at the SIRa test bench within the TARGISOL collaboration. Using conventional C targets, radioactive  $^{14,15,19-22}O$  and  $^{13}N$  beams were produced at these two facilities in the fragmentation of  $^{16}O$  and  $^{36}S$ . The fragments combined with C atoms from the target to form CO and CN molecules that were transported to the ionisation volume and broken in the plasma generated by the ECR source.

In recent works, several oxide fibre targets ( $HfO_2$ ,  $Al_2O_3$ ,  $ZrO_2$ ) have also been tested at the SIRa test bench to produce singly-charged C radioactive ions. C atoms produced in the fragmentation of a  $^{22}Ne$  primary beam were released from the targets as oxide molecules, and ionised in an  $1^+$  ECR source. Yields higher than  $10^3$  atoms/s were obtained at SIRa for  $^{10,11,15}C$ , with about 10 pA of primary beam intensity. A gain of about 100 may therefore be expected at SPIRAL provided that a dedicated target providing similar release conditions can be built. Even more neutron-rich C beams would then be available at the SPIRAL facility.

In line with these studies, the use of active gases with which condensable elements could form molecules could be investigated to produce new beams at SPIRAL. However, further tests would be needed to define the best target (gas) - beam combinations and to characterize the molecular formation and dissociation processes. Such studies would require from 12 to 24 man.months per given element, depending on whether or not the technique has already been tested elsewhere.

### 1.2. Implementation of new radioactive ion sources at SPIRAL

The aim of the SPIRAL facility is to deliver post-accelerated RIBs of noble gas elements. The target-ion source system was therefore designed to produce directly multi-charged ions in rather good purity conditions. The choice of an ECR source was motivated by its high efficiency for the ionisation of noble gases. Its selectivity is provided by a cold transfer tube between the target chamber and the ionisation volume. The direct coupling of dedicated  $1^+$  ion sources to the present  $n^+$  ion source is possible but difficult owing to the compactness of the source. In addition, the position of the target with respect to the  $n^+$  ion source is constrained by the sensitivity of the magnet to neutrons. A solution would consist in coupling the dedicated  $1^+$  ion sources to a distant and "universal" charge breeder. It would allow for the production of new beams at SPIRAL and experiments at very low energy would benefit from the availability of more intense  $1^+$  RIBs. The implementations of a  $1^+$  ECR source and of a surface ionisation source are discussed in the following sections 1.2.1 and 1.2.2.

### 1.2.1. Implementation of a 1<sup>+</sup> ECR source

Experiments have been performed at the SIRa test bench using a 1<sup>+</sup> ECR source (MiniMono) directly coupled to the target chamber. The ionisation of the released fragments in only one charge state (1<sup>+</sup>) led to production yields for <sup>72,73</sup>Kr 10 times higher than the one obtained in the same beam conditions at SPIRAL, where the charge state distribution ranges up to 11<sup>+</sup>.

The absence of a cold transfer tube between the target chamber and the ionisation volumes and the short distance between them allowed the direct production of reactive elements such as Br and Se, unavailable at SPIRAL. Such a compact geometry is also expected to accelerate the effusion of short-lived isotopes, thus increasing their intensities.

The direct coupling of a 1<sup>+</sup> ECR source to a target chamber favours also the effusion of molecular compounds associating fragments and target or gaseous atoms. The production of several condensable elements such as As, Cl, S, P, Al and Mg was indeed observed, originating from the combination of these elements with residual H atoms. During these tests, the production of reactive elements as compound molecules with O or other gases has not been investigated. Furthermore, the target design was not optimised with respect to the range of the fragments of interest.

The implementation of such a target-ion source at SPIRAL could be appropriate for the production of condensable elements such as P and S, as recommended by the BUG committee. However, further studies are necessary in order to understand the molecular formation and dissociation processes, and to optimise the efficiency of the assembly. The development of a 1<sup>+</sup> ECR source would require at least 24 man.months of manpower.

The coupling of such a 1<sup>+</sup> target-ion source with a multi-charged ion source such as the one installed at SPIRAL would require some modifications of the production cave and of the ECR handling system. Additional manpower would therefore be required to implement such a new TIS in the SPIRAL production cave.

### 1.2.2. Implementation of a surface ionisation source

The development of a 1<sup>+</sup> surface ionisation source dedicated to the production of alkali elements is undergoing (MonoNake project) and is supported by the BUG recommendations. In recent tests using a carbon ioniser, neutron-rich Al isotopes have been observed in the fragmentation of <sup>48</sup>Ca, at the same time as Li, Na and K elements. It demonstrates that the current development could be adapted for the production of different elements, depending on their ionising potential and on the ionising material. As an illustration, Fig. 4 shows the probability of contact ionisation at 1500 K for different elements as a function of the ionising power of the contact surface.

An ionisation power close to 6 eV can be obtained with materials such as Pt and Ir, allowing for the production of a large variety of RIBs. The selectivity of the surface ionisation source depends on the choice of the ionising material, but also on the beam and target combination. Depending on the range of the isotopes of interest, specific designs of the production target should be considered. The availability of singly-charged <sup>22</sup>Al ion beams is recommended by the BUG committee and the production of neutron-deficient Al ions with the surface ionisation source could be further investigated.

The coupling of the surface ionisation source with a charge breeder similar to the SPIRAL ECRIS could be performed. However, the production cave and the ECR handling system could have to be adapted to face new requirements. Such a target-ion source ensemble may be less selective than the one operated at SPIRAL. In such a case, technical solutions to trap impurities would have to be investigated.

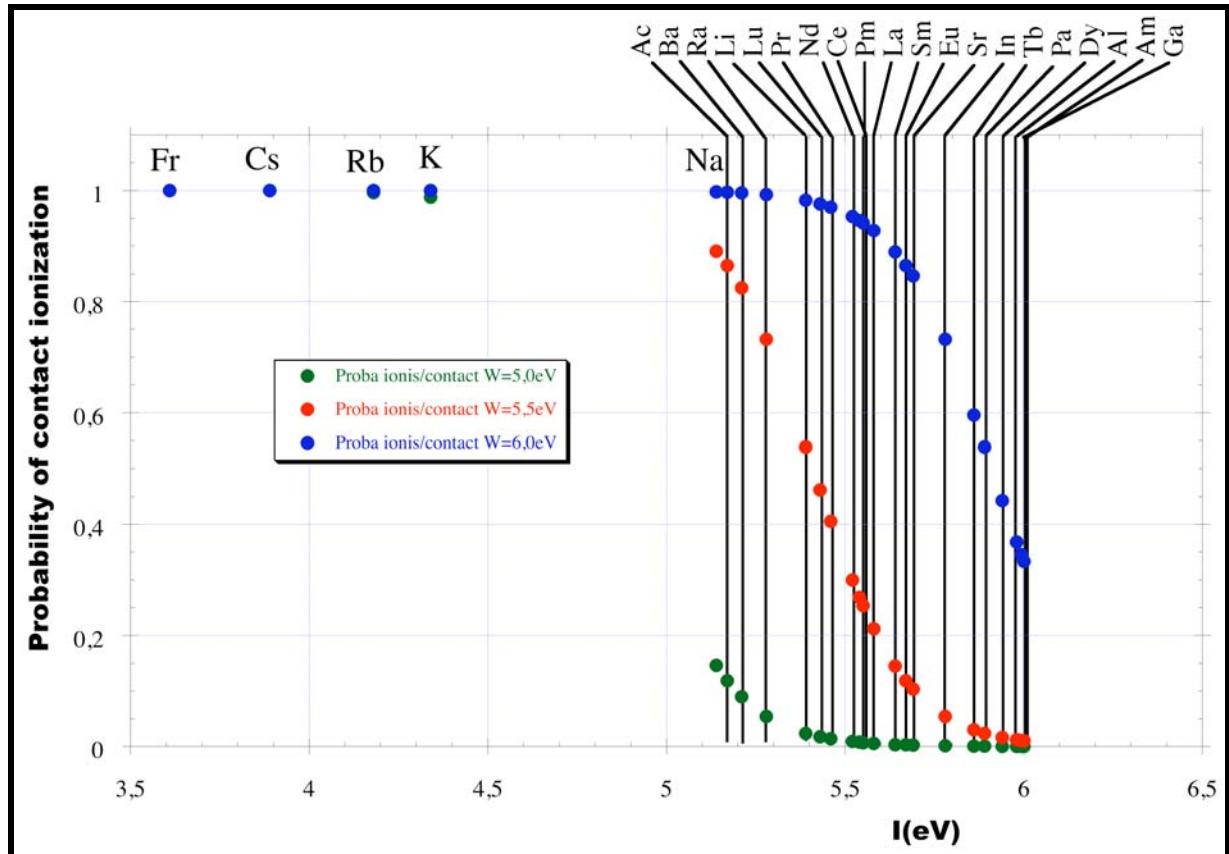


Figure 4: Probability of contact ionisation at 1500 K for several chemical elements and for three different values of contact-ionisation power ( $W$ ).

### 1.3. Alternative solutions

#### 1.3.1. Implementation of a radiation-resistant target-ion source

If the radiation sustainability of the existing SPIRAL ECR source appears to be an important limitation with respect to the use of higher primary-beam intensities, the development of a new generation of radiation-resistant target-ionisation source may be investigated. A  $1^+$  ECR source using coils instead of permanent magnets has already been successfully tested off-line (MonoBob). The design of a radiation-resistant multi-charged ECRIS based on the same technology could be studied. It should also take into account the possibility to put the fragmentation target as close as possible to the ionisation source. It would indeed increase the overall efficiency for the production of short-lived nuclei as well as condensable elements.

Such a development would require several years and modifications of the TIS handling system might have to be considered.

#### 1.3.2. Implementation of a solenoid for the extraction of SPIRAL beams

Two Einzel lenses located at the exit of the target-ion source are tuned to extract the radioactive beams from the source and to inject them in the low-energy beam line of SPIRAL. The optical quality of the extracted beams is crucial to ensure a good transmission of the selected ions through the first analysing dipole. As reported in the ASPI working group report (DIR/P/ASPI/01-A), the fine-tuning of the second Einzel lens is delicate and hardly reproducible from one experiment to another. Furthermore, the production yields extrapolated from tests performed on the SIRa test bench are sometimes higher than the one measured at SPIRAL. Since the extraction of radioactive beams is performed at SIRa by means of an Einzel lens and a solenoid, the use of such a solenoid instead of a second Einzel lens may allow improving the extraction of SPIRAL beams. A better stability and an intensity gain of a factor of 2 are expected for the more delicate radioactive beams injected into CIME. The implementation of such a solenoid would require at least 6 months of work, during which SPIRAL could not be used.

### 1.3.3. Implementation of a 60 kV high-voltage platform

SPIRAL beams are extracted from the source at a maximum voltage of 32 kV. The implementation of a 60 kV high-voltage platform would improve the transport efficiency in the low-energy beam line and in the CIME cyclotron by reducing space charge effects. The increased magnetic rigidity would also improve the transport efficiency of  $1^+$  radioactive beams, thus increasing the intensity of the beams available at the LIRAT facility. A preliminary study would be necessary to investigate all the modifications that would have to be considered. Such a development would take several years.

### 1.3.4. Production of new beams by means of fusion evaporation

The production of neutron-deficient ions by means of fusion-evaporation reactions can be investigated. The present target would be replaced by a thin foil followed by a heated graphite catcher allowing the release of the fusion-evaporation products. As a feasibility test, the ... reaction could be tested. The implementation of this technique at SPIRAL would require specific safety authorisations.

### 1.3.5. Production of $^{44}\text{Ti}$ and $^{56}\text{Ni}$ post-accelerated beams

$^{44}\text{Ti}$  and  $^{56}\text{Ni}$  beams can be produced at SPIRAL in the fragmentation of  $^{50}\text{Cr}$  and  $^{58}\text{Ni}$  for which 0.8 and 8.5  $\mu\text{A}$  are available today at 82 and 75 A.MeV, respectively. The production yields in a thick carbon target would be about  $2.7 \cdot 10^7$  pps for  $^{44}\text{Ti}$  and  $1.2 \cdot 10^8$  pps for  $^{56}\text{Ni}$ .

Since both Ti and Ni are relatively long-lived refractory elements, their extraction from a thick target could be performed by means of off-line chemistry techniques, which is not possible at GANIL nowadays. The prepared samples would be further conditioned by appropriate means before they are used in dedicated ionisation sources. The shorter-lived  $^{56}\text{Ni}$  isotope decays to  $^{56}\text{Co}$ , which will be ionised at the same time unless the target-ion source device is selective enough. Due to their small relative atomic-mass difference (about  $4.1 \cdot 10^{-5}$ ),  $^{56}\text{Ni}$  and  $^{56}\text{Co}$  would not be separated by the CIME cyclotron. Stripping the ions after post-acceleration could

allow selecting the radioactive beam of interest. The contamination of the beam transport lines and of the post-accelerator by  $^{56}\text{Co}$  may be an important issue.

The extraction of Ti and Ni atoms from the source as molecular compounds could also be investigated. Dedicated oxide targets would have to be designed and tested to evaluate the overall efficiency of such a production technique.

## 1.4. Conclusion

Several strategies for the improvement of SPIRAL beams have been considered, either to increase the intensity of existing RIBs or to produce new radioactive beams at SPIRAL.

The development of 3 kW targets would translate into a gain of 2 for the production of Ar and Kr isotopes, provided that the existing stable ion sources of the GANIL facility are upgraded, or replaced by a new generation of stable ion source such as GTS. The latter would be well suited for the production of heavy ions, even of metallic nature. The possibility to use high-intensity stable beams heavier than  $^{78}\text{Kr}$  to produce new beams at SPIRAL could therefore be considered. However, the power dissipation of such heavy-ion stable beams in the SPIRAL targets would be a major issue.

Improving the conductance of the SPIRAL target-ion source would further enhance the production of short-lived nuclei. A gain of a factor of 10 can presumably be reached for  $T_{1/2} \sim 10$  ms isotopes. In case fragments of interest have a larger range than the projectile, specific target developments could accelerate the diffusion process, thus increasing the RIBs intensities.

For Kr radioactive beams, the implementation of the target-fragmentation technique would lead to higher intensities, and would give the possibility to produce neutron-rich isotopes unavailable today. However, the development of high power Nb or Zr target should be studied and safety considerations may introduce intensity limitations.

New beams of condensable elements could also be produced via the formation of molecular compounds associating fragments with atoms originating from the target or from injected gases. Further studies are required to understand the formation and dissociation processes. To optimise the effusion of the produced molecules, the technique could be implemented using a compact  $1^+$  target-ion source, possibly coupled to the existing SPIRAL ECRIS if post-accelerated beams are considered.

The current development of a surface ionisation source and its further coupling to the SPIRAL ECR source would provide a large variety of new beams, starting from alkali isotopes. The ensemble called NanoNake is being tested and could be implemented at SPIRAL by 2010.

With respect to the BUG recommendations, the intensity increase of existing beams ( $^{15}\text{O}$ ,  $^{24}\text{Ne}$ ,  $^{18}\text{F}$ ,  $^{33,34,44,46}\text{Ar}$  and  $^{72,74}\text{Kr}$ ) can be obtained via the development of dedicated high-power targets and using high-intensity primary beams. For  $^{72,74}\text{Kr}$  beams, the target-fragmentation technique looks more promising in terms of expected yields. Technical solutions are also foreseen to increase significantly the production of short-lived isotopes such as  $^{31}\text{Ar}$ .

Some of the new beams requested by the GANIL users such as  $^{11}\text{Li}$  and, presumably,  $^{22}\text{Al}$  can be produced by the implementation of a surface ionisation source. However, in the case of  $^{11}\text{Li}$ , specific target developments adapted to its long range and short lifetime should be performed in order to achieve reasonable yields.

In addition, its rather high second and third ionisation potentials will limit dramatically the intensity of the post-accelerated beams.

For condensable elements such as  $^{26}\text{P}$  and  $^{27}\text{S}$ , a compact  $1^+$  ECR source can be considered as the most relevant technical solution. For other requested beams, namely  $^{44}\text{Ti}$  and  $^{56}\text{Ni}$ , alternative solutions involving hot chemistry or the formation of molecular compounds and the development of dedicated ionisation sources could be studied.

Although a radiation-resistant target-ion source would be more difficult to design, it may be well suited for the production of short-lived isotopes and/or reactive elements at high primary beam intensities.

Estimates of the manpower required to perform the proposed developments are summarized in table 4. They concern only the Ion Production Group and they do not take into account the human resources needed to perform mechanical studies and realizations, building modifications nor on-line tests.

<b>Suggested development</b>	<b>Manpower request</b>
High-power C targets	12 man.months / target
Higher stable beam intensity or GTS	1 to 3 man.months / beam or 3.2 man.years
Fast effusion TIS and/or Fast release C target*	9 man.months and/or 6 man.months / target
Target fragmentation technique*	48 man.months
Molecular compounds*	from 12 to 24 man.months / element
$1^+$ ECR**	24 man.months
Surface ionisation source**	24 man.months
Radiation-resistant TIS**	3 to 4 man.years

Table 4: Estimates of the manpower required for the suggested SPIRAL beam developments. Tasks labelled with a symbol may (\*) or will (\*\*) need modifications of the SPIRAL production cave and of the target-ion source (TIS) handling system. The manpower needed to perform such adaptations as well as on-line tests is not considered.

The proposed tasks require the hiring of experienced technicians and/or engineers. For important developments, the contribution of PhD students should be considered. Estimates do not take into account the manpower needed to prepare and to perform experiments at the SIRa test bench and to modify the SPIRAL production cave and TIS handling system when necessary. With the increasing number of TIS, the time needed to test and to implement them will grow significantly. Additional manpower should consequently be considered.

Possible time schedules associated with different objectives are proposed in Appendix II and III. They cannot be run in parallel unless the required manpower is available.

Finally, two issues have to be considered before defining a strategy for the development of SPIRAL beams:

- If more intense primary beams are considered, the lifetime of the existing ionisation sources could be shortened. The design of a new target-ion source system

sustaining higher radiation levels can be regarded as an alternative, although its development would take a longer time.

- Some of the proposed developments will need radiobiological impact studies and/or new safety authorizations. If important modifications of the SPIRAL production cave are necessary, the available beam time may decrease significantly.

## 2. [The LIRAT 2 project](#)

Although the SPIRAL facility provides mainly radioactive beams in the 1.7 to 25 A.MeV range, mass-separated radioactive ions are also available at very low energy. The implementation of a low-energy facility at SPIRAL as been proposed to the GANIL Scientific Committee in 1998, and was supported by a nuclear physicist community gathered in a workshop held at Bordeaux in 1999. The so-called LIRAT project as been recommended by the GANIL Scientific Committee in 2000, on the basis of a first technical report (DIR/P/LIRAT 01-A-APS). A short version of the initial project was finally built and is in operation since 2005. The LIRAT2 project consists in the extension of the existing LIRAT facility, as planned at the beginning. It can be considered as a possible development strategy for SPIRAL and is supported by the following arguments:

- Strong physics cases motivate the building of such a low-energy beam facility, which would enhance the attractivity and the visibility of SPIRAL.
- The LIRAT2 project would allow preparing the implementation of the DESIR facility at SPIRAL2 and developing synergies with other low-energy beam facilities worldwide.

The physics motivations for the building of LIRAT2 are listed below in section B.I. Both scientific and technical objectives are described. The LIRAT2 implantation scheme and associated technical requirements are presented in section B.II. A preliminary cost estimate, a construction time schedule and an evaluation of the required manpower are given in section B.III.

### 2.1. [Physics motivations](#)

#### 2.1.1. [Search for exotic currents in the weak interaction](#)

The LPCTrap device installed at the LIRAT facility has proved in the last two years that high-intensity radioactive beams of light ions can be trapped and studied in rather clean conditions, allowing the search for a scalar (tensor) contribution to Fermi (Gamow-Teller)  $\beta$  transitions. Such evidences for physics beyond the Standard Model are currently sought at LIRAT in the angular distribution of the  $\beta^-$  and anti-neutrino particles emitted by trapped  ${}^6\text{He}^{1+}$  ions. The high production yield available, the relatively long lifetime and the high  $Q_\beta$  value of this pure Gamow-Teller  $\beta$ -decaying nucleus will allow controlling all the systematic effects that usually weaken the precision of such kind of measurements. Further studies of Gamow-Teller and Fermi  $\beta$ -decaying nuclei such as  ${}^8\text{He}$  and  ${}^{19}\text{Ne}$ , which are abundantly produced at SPIRAL, could be studied at LIRAT2 in the future.

#### 2.1.2. [0<sup>+</sup> → 0<sup>+</sup> super-allowed Fermi transitions](#)

The precise measurement of the  $Ft$  values associated with  $0^+ \rightarrow 0^+$  super-allowed Fermi transitions allows so far for a confirmation of the vector-current conservation hypothesis assumed by the Standard Model. However, the level of precision that can be reached is crucial in order to constrain the computation of the vector coupling constant  $G'_v$ , from which the unitarity of the quark-mixing matrix can be probed, and physics beyond the Standard Model searched for. The precision on the  $Ft$  values is still limited for  $^{18}\text{Ne}$  and  $^{34}\text{Ar}$  by the accuracy of their lifetime and  $\beta$ -branching ratio measurements. The production yields provided by SPIRAL for these two isotopes are large enough to perform such kind of measurements at LIRAT2 with a relative precision of 0.1 % or below.

If metallic radioactive beams are produced in the future at SPIRAL, precise  $\beta$ -branching ratio measurements could also be performed in the decay of  $^{26}\text{Si}$  and  $^{38}\text{Ca}$ .

### 2.1.3. $\beta$ -decay studies

$\beta$ -decay spectroscopy is a powerful tool to obtain information about the decay properties and the nuclear structure of radioactive nuclei. The precise measurement of the  $\beta$ -decay strength provides also valuable information about the strong interaction within the atomic nucleus through the determination of the matrix elements of the  $\beta$  transitions.

Few nuclei exhibit complex decay patterns involving the beta-delayed emission of several particles. Such rare decay modes offer the possibility to study the nucleon-nucleon interaction or cluster structures inside the atomic nucleus through angular and energetic correlations measurements. The production of these exotic nuclei at very low energy opens unique opportunities to perform such kind of studies with a high precision level. Low-energy beams can indeed be easily stopped inside multi-detector systems providing high detection efficiency and more precise emission-angle measurements as compared to set-ups installed at the focal point of fragmentation facilities.

A signature for a correlation between the 2 protons emitted in the  $\beta$  decay of  $^{31}\text{Ar}$  has already been sought for at LIRAT and could be repeated at LIRAT2. A factor of 10 in the production yield of this short-lived nucleus is missing at the moment. It could be obtained by developing a dedicated target-ion source at SPIRAL, with improved diffusion and effusion efficiencies. Other  $\beta$ -delayed 2p emitters such as  $^{22}\text{Al}$ ,  $^{26}\text{P}$  or  $^{27}\text{S}$  could also be considered. The implementation at SPIRAL of a surface ionisation source to produce Al beams or of a  $1^+$  ECR source devoted to the production of condensable elements such as P and S could provide the opportunity to study the decay properties of these nuclei.

Another short-lived isotope of interest is  $^{13}\text{O}$ . This  $\beta$ -delayed proton emitter is decaying to high-energy excited states in  $^{13}\text{N}$  that are expected to be of molecular nature. This feature could manifest itself in large  $\beta$ -asymmetry values for the associated  $\beta$ -decay branches with respect to the mirror  $\beta$ -transitions in the decay of  $^{13}\text{B}$  to excited states in  $^{13}\text{C}$ . High-energy excited states of  $^{13}\text{N}$  are also expected to be unbound versus the emission of  $p-3\alpha$  and  $n-3\alpha$  clusters, thus allowing one to probe the correlations between the three  $\alpha$  particles inside the emitting nuclei. These correlation studies could possibly be performed at LIRAT2 with a similar target-ion source development as the one suggested above for  $^{31}\text{Ar}$ .

## 2.2. Research and development in synergy with other low-energy beam facilities

Anticipating the implementation of several low-energy beam facilities such as DESIR at SPIRAL2, DESPEC and NCAP at FAIR/NuSTAR and SLOWRI at RIKEN, a dedicated beam-line could be devoted at LIRAT2 to test beam-preparation and beam-handling instruments as well as detection systems adapted to the specific properties of the radioactive beams that will be produced in these facilities.

### 2.2.1. Detection tools

Fast tape transport systems and compact and segmented particle detection arrays will be required in the future to study very exotic isotopes with short lifetimes and complex decay modes. A universal charged-particle detection set-up will be built in the next four years within a collaboration involving several institutes, and funded by the ANR French agency. The VS3 set-up is presented in Fig. 5. It should provide a significant gain in detection efficiency and cleaner charged-particle energy spectra.

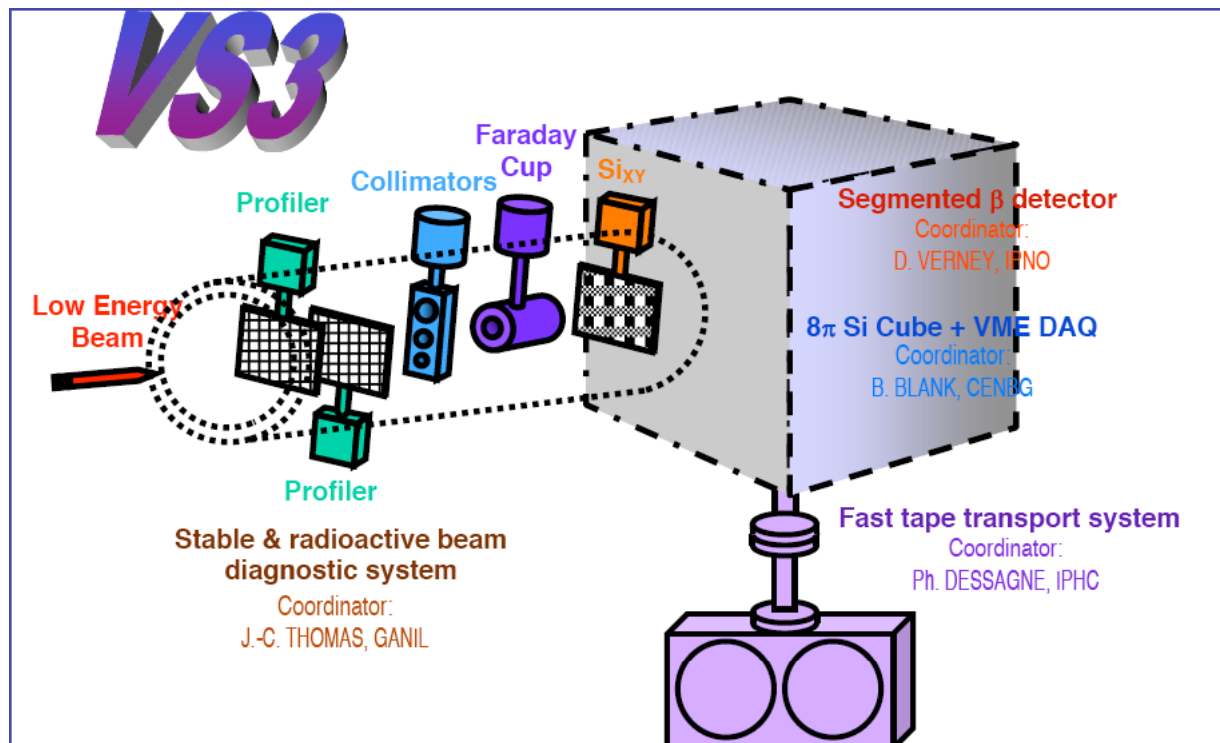


Figure 5: Schematic drawing of the VS3 universal set-up devoted to charged-particle decay studies of short-lived nuclei produced at low counting rates and very low energy.

Such a set-up could be installed at the LIRAT2 facility and further upgraded to include gamma and neutron detection arrays.

## 2.2.2. Beam preparation and beam handling instruments

Part of the VS3 set-up presented above consists in a beam-diagnostic section. A research and development program is planned to design low-energy beam diagnostic tools providing intensity and position measurements for low-intensity stable as well as radioactive beams. Some of these developments are also required for the identification and the transport of SPIRAL2 beams.

Within the DESIR project, radio frequency quadrupoles will be used to condition the radioactive beams before they are injected in a high-resolution separator or in the experimental lines. Penning and Paul traps are also foreseen, for purification or decay study purposes. All these equipments could be developed and tested at LIRAT2 on a dedicated beam line.

## 2.3 LIRAT2 implantation scheme

At the beginning of the LIRAT project, several implantation schemes have been proposed for an extended low-energy beam facility at SPIRAL. Figure 6 shows a possible layout of LIRAT2, adapted from an earlier technical study (DIR/P/LIRAT 04-A).

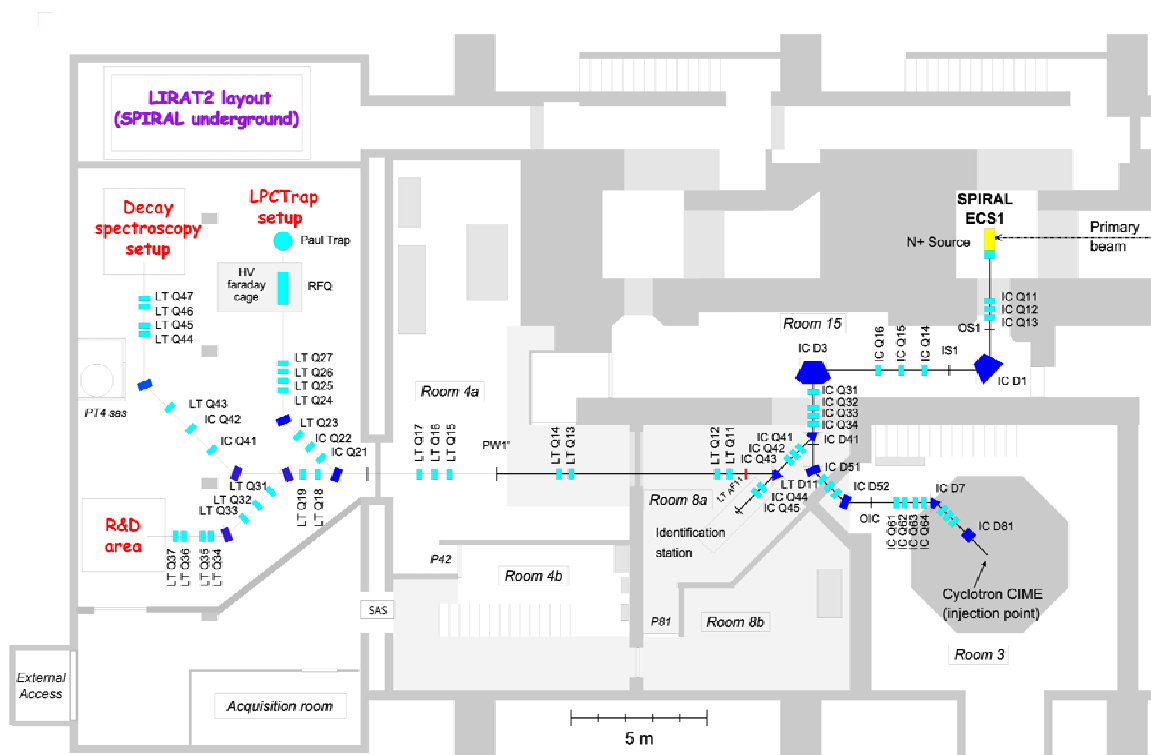


Figure 6: Suggested implantation scheme of the LIRAT2 facility.

The beam optics specifications are the same as the one of the present LIRAT facility. Namely, SPIRAL beams up to the mass  $A=89$  would be transported in a  $1^+$  charged state with 100 % transmission efficiency for an emittance of  $80 \pi \cdot \text{mm} \cdot \text{mrad}$ .

Three beam lines are proposed that would allow performing the scientific research program and the technical developments mentioned in section B.I. An external access by means of an elevator is required in order to bring in the underground of the SPIRAL building the different equipments to be installed in the experimental and acquisition rooms.

The proposed layout is compatible with the future connection of the SPIRAL2 n<sup>+</sup> low-energy beam line to the CIME cyclotron and with the building of the DESIR experimental hall presumably located on the left side of the picture.

## 2.4 Time schedule, cost estimate and manpower requirement

The LIRAT facility was built in about 3 years. One more year was necessary to perform the commissioning of the installation with stable beams and to obtain safety authorisations to run a first experiment with radioactive ions. For the LIRAT2 facility, 6 months would be necessary to study the required building modifications. The beam transport lines are already fully characterized and 30 months would be needed to build up the complete installation.

The LIRAT2 facility is a prolongation of the existing LIRAT installation, with the same characteristics in terms of beam optics. Therefore, radiobiological hazards are the same as those already evaluated within the LIRAT project. At present, radiation protection allows the LIRAT users to work in a supervised area, with a dose rate lower than 7.5 μSv/h. They were built in order to accept maximum beam intensities of  $2.8 \cdot 10^9$  pps of <sup>19</sup>Ne<sup>1+</sup> and  $1.2 \cdot 10^9$  pps of <sup>35</sup>Ar<sup>1+</sup>. With similar radiation protections, only <sup>15</sup>O<sup>1+</sup> would have to be limited in intensity among all the beams that SPIRAL could deliver to the LIRAT2 facility. Thus, safety authorisations to run the new installation should not be too difficult to obtain and the safety report could be sent at the very beginning of the building phase. Table 5 presents a preliminary time schedule for the building of LIRAT2 at SPIRAL. Radioactive beams should be available 40 months after the beginning of the project.

Year 1		Year 2		Year 3		Year 4	
Building modifications study	Beam line implementation and building modifications				Commissioning with radioactive beams	First experiment with radioactive beams	
Beam line components purchase	Safety authorization request		radiation protection and secured accesses				

**Table 5:** Proposed time schedule for the implementation of the LIRAT2 facility at GANIL.

The global cost of the existing LIRAT facility was about 380 k€, including 350k€ for the implementation of about 11 meters of beam lines and 30 k€ for building modifications. The cost of the LIRAT2 project can be roughly estimated by applying a scaling factor proportional to the ratio of the beam-line lengths between the two installations. Table B.2 presents different cost estimates associated with three different options: the three beam lines displayed in Fig. 6 are quoted a, b and c, and are respectively associated with the LPCTrap set-up (11.8 m long), the experimental area devoted to decay-spectroscopy studies (17.5 m) and with the R&D area for low-energy beam preparation tools and particle detection instruments (12.9 m). The three options considered are the building of the a and b lines, a and c and a, b and c. Taking into account the overlap between the three beam lines, the total beam-line

length for the three options is 24 m for a+b, 19.4 m for a+c and 29.6 m for a+b+c. The cost estimates for building modifications were arbitrarily fixed to 200 k€. It corresponds to about 3 times the building cost expenses of LIRAT. A rough estimate for the building of the LIRAT2 facility ranges from 820 and 1140 k€, depending on the considered option.

The manpower required for the building of the LIRAT facility was estimated to be about 76 man.months. Applying a scaling factor derived from a comparison of the costs of the LIRAT and LIRAT2 facilities, the manpower needed for the implementation of the latter is expected to be about 190 to 230 man.months depending on the considered option. For the complete installation including three beam lines to be built within three years, the manpower requirement is thus expected to be about 6.3 man.years.

<b>LIRAT2 options</b>	<b>Beams lines (k€)</b>	<b>Building modifications (k€)</b>	<b>Overall estimated cost (k€)</b>
a+b	764	200	964
a+c	617	200	817
<b>a+b+c</b>	942	200	<b>1142</b>

**Table 7: Rough estimates of the cost of the LIRAT2 facility for the three options considered.**

## **2.5 Conclusion**

The implementation of an extended low-energy beam line at SPIRAL would improve the scientific impact of the SPIRAL facility. The LIRAT2 project is supported by a large physicist community, as illustrated by the DESIR letter of intent proposing such a low-energy radioactive beam facility at SPIRAL2.

Several physics cases could be addressed at LIRAT2, provided that all SPIRAL beams will be available and that specific developments of existing or new target-ion source ensembles are performed at SPIRAL in the near future.

LIRAT2 would finally offer the possibility of develop and to test low-energy beam preparation and beam handling instruments as well as particle detection devices that will be used in the next generation of low-energy radioactive beam facilities.

## Appendix I

### BUG recommendations for the improvement of SPIRAL I beams and suggested developments (ASPI report DIR/P/ASPI/01-A)

Isotope	I (pps)	Energy (MeV/u)	Primary beam	Present Intensity (pps)	Suggested developments
$^{11}\text{Li}$			$^{18}\text{O}$		New ECS
$^{15}\text{O}$	$10^8$		$^{16}\text{O}$	$9 \cdot 10^7$ at IBE	3 kW target $4 \cdot 10^7$ possible
Al, Si					To be studied
$^{18}\text{F}$	$> 10^7$		$^{20}\text{Ne}$	$2 \cdot 10^5$ at 300W	6 kW target $2 \cdot 10^6$ pps possible
$^{24}\text{Ne}$	$> 10^7$	5	$^{26}\text{Mg}$	$2 \cdot 10^5$ pps with $^{36}\text{S}$	3 kW target $^{26}\text{Mg}$ primary beam
$^{26}\text{P} (1+)$		low	$^{36}\text{Ar}$		New ECS
$^{27}\text{S} (1+)$		low	$^{36}\text{Ar}$		New ECS
$^{33}\text{Ar}$	$> 10^6$		$^{36}\text{Ar}$	$3 \cdot 10^3$	3 kW target
$^{34}\text{Ar}$	$> 10^7$		$^{36}\text{Ar}$	$7 \cdot 10^5$ expected	
$^{42}\text{Ar}$	$> 10^7$	5	$^{48}\text{Ca}$	$10^7$ expected	Dedicated target
$^{44}\text{Ar}$	$> 10^7$	5	$^{48}\text{Ca}$	$2 \cdot 10^5$ pps	
$^{44}\text{Ti}$	$> 10^6$				To be studied
$^{56}\text{Ni}$	$> 10^6$				To be studied
$^{72}\text{Kr}$	$> 10^4$	5	$^{78}\text{Kr}$	$2 \cdot 10^2$ pps at IBE	Dedicated target + $^{78}\text{Kr}$ increased intensity or target-fragmentation technique

## B. Experiments



A. Bey, B. Blank, G. Cachel, C. Dossat, J. Giovinazzo, I. Matea<sup>1</sup>  
 F. de Oliveira, J.-C. Thomas<sup>2</sup>  
 M. Alcorta, M.J.G. Borge, R. Domínguez-Reyes, M. Madurga, A. Perea, O. Tengblad<sup>3</sup>  
 H.O.U. Fynbo, H. Knudsen<sup>4</sup>  
 N. Adimi<sup>5</sup>  
 K. Sümmerer<sup>6</sup>

- 1) CEN Bordeaux-Gradignan, IN2P3-CNRS, Université de Bordeaux I, F-33170 Gradignan, France
- 2) GANIL, CEA/DSM - CNRS/IN2P3, BP 55027, F-14076 Caen Cedex 5, France
- 3) Instituto de Estructura de la Materia, CSIC, E-28006 Madrid, Spain
- 4) Department of Physics and Astronomy, University of Aarhus, 8000 Aarhus C, Denmark
- 5) Faculté de Physique, USTHB, B.P. 32, El Alia, 16111 Bab Ezzouar, Alger, Algeria
- 6) Gesellschaft für Schwerionenforschung mbH, D-64291 Darmstadt, Germany

Contact person: [blank@cenbg.in2p3.fr](mailto:blank@cenbg.in2p3.fr)

## 1. Key question and initial goals

Measurement of proton-proton correlation in  $\beta$ -2p emission of  $^{31}\text{Ar}$  and study of  $\beta$ -p emission of  $^{31,32,33}\text{Ar}$ ; improve results obtained a few years ago at ISOLDE.

## 2. Experiment set-up

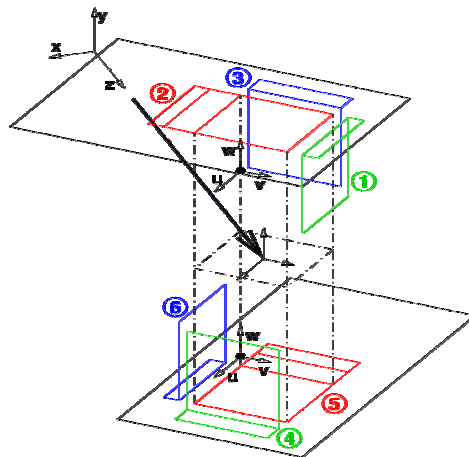


Figure 1: “Silicon cube” consisting of 6 DSSSDs backed by large-area silicon detectors to veto  $\beta$  particles and a beam catcher in the centre; 5 DSSSDs worked fine, the veto detectors had rather large noise level.

### **3. Results and achievements**

The analysis is still ongoing at Bordeaux, Madrid, and Alger. Due to production rates much lower than expected, especially the statistics for  $^{31}\text{Ar}$  in about an order of magnitude lower than at ISOLDE despite the increased detection efficiency. No improvement expected for  $^{31}\text{Ar}$ , maybe for  $^{32,33}\text{Ar}$ .

### **4. Conclusion and prospective**

$^{31}\text{Ar}$  was contaminated with  $^{33}\text{Ar}$  (factor of 20 more) and  $^{32}\text{Ar}$  with  $^{34}\text{Ar}$ . The reason is not known. Therefore, the one-proton spectra for  $^{31}\text{Ar}$  are almost not useable. To improve, the production rate and the purity have to be increased.

### **5. References**

- [1] H. Fynbo et al., Phys. Rev. C59, 2275 (1999)
- [2] H. Fynbo et al., Nucl. Phys. A677, 38 (2000)
- [3] J. Thaysen et al., Phys. Lett. B467, 194 (1999)

## E344aS

# Shape coexistence near the N=Z line investigated by low-energy Coulomb excitation of secondary reaction products” and “Shape coexistence near the N=Z line and collective properties of Kr isotopes investigated by low-energy Coulomb excitation of radioactive ion beams

E. Clément, E. Bouchez, A. Chatillon, A. Görgen, A. Hürstel, W. Korten, Y. Le Coz, Ch. Theisen, J.N. Wilson, M. Zielińska<sup>1</sup>  
T. Czosnyka, J. Iwanicki, P. Napiorkowski<sup>2</sup>  
C. Andreoiu, P.A. Butler, R.-D. Herzberg, D.G. Jenkins, G.D. Jones<sup>3</sup>  
F. Becker, J. Gerl<sup>4</sup>  
J.M. Casandjian, G. de France<sup>5</sup>  
W.N. Catford, C.N. Timis<sup>6</sup>  
G. Sletten<sup>7</sup>

- 1) CEA Saclay, DSM/DAPNIA/SPhN, F-91191 Gif-sur-Yvette, France
- 2) Heavy Ion Laboratory, Warsaw University, Pl 02-097 Warsaw, Poland
- 3) Department of Physics, University of Liverpool, Liverpool L69 7ZE, United Kingdom
- 4) Gesellschaft für Schwerionenforschung mbH, D-64291 Darmstadt, Germany
- 5) GANIL, CEA/DSM - CNRS/IN2P3, BP 55027, F-14076 Caen Cedex 5, France
- 6) Department of Physics, University of Surrey, Surrey GU2 7XH, United Kingdom
- 7) The Niels Bohr Institute, Tandem Accelerator Laboratory, DK-4000 Roskilde, Denmark

Contact person: [andreas.goergen@cea.fr](mailto:andreas.goergen@cea.fr)

## 1. Key question and initial goals

The experiments E344S and E344aS aimed at a more detailed understanding of the shape coexistence phenomenon in neutron-deficient Kr isotopes, as testified by the observation of low-lying shape isomeric  $0^+$  states. In particular, the “collectivity” of the excited states, i.e. their E2 transition strength, and their static quadrupole moments should be determined. These experiments require radioactive ion beams at an energy close to the Coulomb barrier, e.g. around 4.5 MeV for a lead target, which are today only available at SPIRAL.

## 2. Experiment set-up

Two experiments to study the radioactive isotopes  $^{76}\text{Kr}$  and  $^{74}\text{Kr}$  in low-energy Coulomb excitation were performed in June 2002 and April 2003. In both cases excellent beams from the SPIRAL facility were available with intensities very close to expected values, e.g.  $5 \cdot 10^5$  and  $10^4$  ions/s for  $^{76}\text{Kr}$  and  $^{74}\text{Kr}$ , respectively. Inelastically scattered Kr ions and recoiling target nuclei were measured in an annular Si detector

mounted at forward angles, which allowed that the non-interacting beam left the scattering chamber. De-excitation  $\gamma$ -rays were detected with the EXOGAM spectrometer, which was used in its close configuration with 7 and 11 Ge clover detectors, respectively. Different beam energies and targets (Pb, Ti) were used in order to optimise the sensitivity of the experiment.

### **3. Results and achievements**

The  $\gamma$ -ray spectra obtained in the two experiments are shown in Fig. 1. The quality of the spectra is comparable to those obtained with stable beams. Even in the  $^{74}\text{Kr}$  case only a very small contamination ( $\sim 2\%$ ) from the isotone  $^{74}\text{Se}$  was observed. From the experimental data the excitation probability for several low-lying states in  $^{74,76}\text{Kr}$  was obtained as function of the scattering angle. The analysis of the data is terminated and the results are published in two PhD thesis [1,2]. A large number of E2 strengths between low-lying states were obtained and compared with theoretical calculations. In addition it was possible to extract static quadrupole moments using the reorientation technique for the first time from a radioactive beam experiment [3].

### **4. Conclusion and prospective**

The experiments have shown that high-precision Coulomb excitation measurements are feasible with radioactive ion beams with intensities as low as  $10^4$  ions/s provided that a high-efficiency set-up for a coincidence measurement of  $\gamma$ -rays and particles is available and that the beam purity is sufficiently good ( $> 95\%$ ). They have also shown that beam energies of around 5 A.MeV are advantageous since heavy targets can be used which in turn provide larger Coulomb excitation cross sections and a higher sensitivity to the reorientation effect.

Key nuclei for similar experiments are the N=Z nuclei  $^{72}\text{Kr}$  and  $^{68}\text{Se}$ , which are among the few cases in the nuclear chart where a strong oblate deformation of the ground state is expected. Unfortunately the intensity of the  $^{72}\text{Kr}$  beam at SPIRAL is too low ( $< 100$  ions/s) for a continuation experiment and Se is not an element that can be produced with the current SPIRAL ECR source. The  $^{72}\text{Kr}$  experiment would be feasible if the primary  $^{78}\text{Kr}$  beam reached the allowed maximum intensity of 3 kW in the SPIRAL production target.

### **5. References**

- [1] E. Bouchez, PhD thesis, ULP Strasbourg, November 2003
- [2] E. Clément, PhD thesis, Univ. Paris-Sud, 2006
- [3] E. Clément, et al., Phys. Rev. C 75, 054313 (2007)

## E350aS Isobaric analogue states of $^7\text{He}$ and $^9\text{He}$

C.E. Demonchy, J.M. Casandjian, L. Giot, G. de France, M. Lewitowicz, W. Mittig, F. de Oliveira, S. Pita, P. Roussel-Chomaz, H.Savajols<sup>1</sup>

G. Ter-Akopian, A. Fomichev, A. Rodin, S. Sidurtchuk, S. Stepansov, R. Wolski<sup>2</sup>

N. Alamanos, F. Auger, V. Lapoux, E. Pollacco, L. Nalpas<sup>3</sup>

1) GANIL, CEA/DSM - CNRS/IN2P3, BP 55027, F-14076 Caen Cedex 5, France

2) Russian Flerov Laboratory of Nuclear Reactions, JINR, Dubna, RU-141980 Russia

3) CEA Saclay, DSM/DAPNIA/SPhN, F-91191 Gif-sur-Yvette, France

Contact person: [mittig@msu.edu](mailto:mittig@msu.edu)

### 1. Key question and initial goals

We propose to study the Isobaric Analog States (IAS) of the neutron-rich unstable nuclei  $^7\text{He}$  and  $^9\text{He}$  using the elastic resonance scattering  $^6\text{He}+p$  and  $^8\text{He}+p$  in inverse kinematics. Measurement of the positions, the quantum number,  $J^\pi$ , and the spectroscopic factors of the IAS in these nuclei will give us detailed information on the structure of these extremely neutron-rich nuclei. A new versatile active target-detector will be used.

### 2. Experiment set-up

This experiment used the active target Maya, mainly in the G3 experimental area of the GANIL facility.

### 3. Results and achievements

Reactions induced on protons at low incident energy (3.5-3.9 A.MeV) were measured with  $^8\text{He}$  and  $^6\text{He}$  beams accelerated by SPIRAL at GANIL. The particles were detected in the active target MAYA, filled with  $\text{C}_4\text{H}_{10}$  gas. The beam was stopped in the detector, so energies from incident beam energy down to detector threshold were covered. Proton elastic scattering, one neutron pick-up (p,d) and (p,t) reactions were observed.

In the (p,d) reaction very high cross sections of the order of 1 barn were observed, that could be reproduced using a direct reaction formalism. *This is the first time that this strong increase of transfer reaction cross sections at very low energy predicted for loosely bound systems was observed.*

Spectroscopic factors are in agreement with a simple shell model configuration. No evidence for a low lying excited state in  $^7\text{He}$  was found. Some of the results are published in references [1-4].

In Fig. 1, we show an angular distribution of the  $^8\text{He}(p,d)^7\text{He}$  reaction at an incident energy of 3 A.MeV. Figure 2 shows the angle integrated cross-sections, compared to theory with  $C^2S = 4$ . As can be seen, at low energy the cross-section reaches very high values, of the order of one barn. The origin of this very high cross-section is the good momentum matching at this low energy of the loosely bound neutron in the initial and final state.

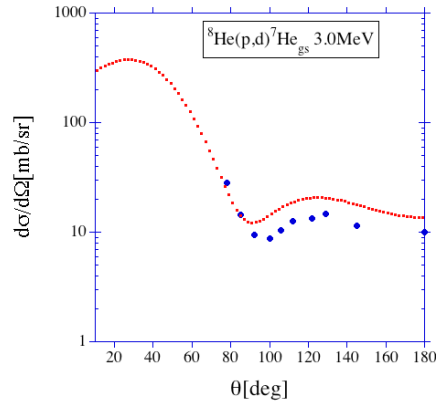


Figure 1: Experimental angular distributions compared to DWBA calculations with  $C^2S=4$ .

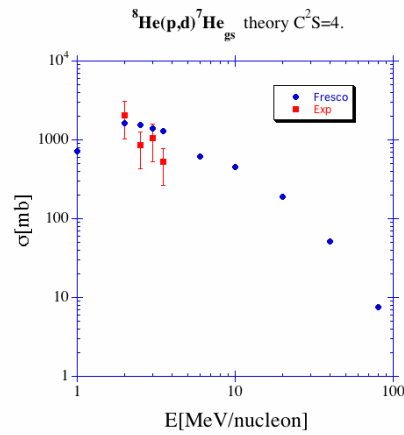


Figure 2: Experimental and theoretical cross-sections for the  $^8\text{He}(p,d)^7\text{He}$  reaction.

Figures 3 and 4 show the scatter plots of the range of the heavy reaction partner and the energy deposited in Si detectors, conditioned by the identification of protons and deuterons respectively. Due to the fact that the beam was stopped in the detector, it was possible to extract an excitation function for these reactions with energies between the incident beam energy and essentially zero energy. The region of highest particle energy and shortest range corresponds to reactions at the entry of the detector, i.e. reactions with the highest energy.

The extraction of information on excited states in  $^7\text{He}$  from experimental spectra must take into account the fact that the widths are large, and the width and the population cross-section are energy dependent. We treated the energy dependence of the decay width in two ways with very similar results. One was the energy dependence as given by R-matrix formalism, the other was the calculation of single particle resonance width by the code Fresco.

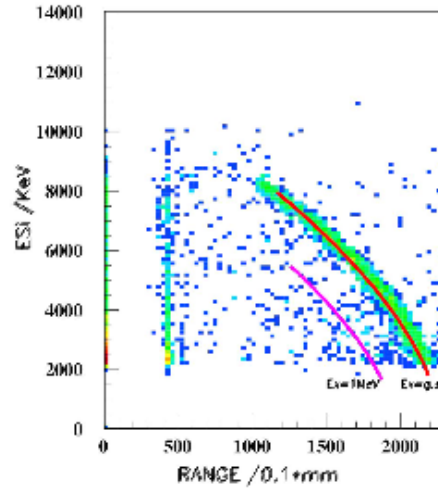


Figure 3: Scatter plot for particles leaving the gas volume, conditioned by the identification of protons, of the energy deposited in one of the Si-detectors, as a function of the range of the heavy reaction partner measured inside the gas. The two lines represent kinematical calculations for elastic scattering of  $^8\text{He}$  on protons, and an (hypothetical) excited state at 1 MeV above the ground state. An experimental excitation energy resolution of 160 keV (FWHM) can be deduced.

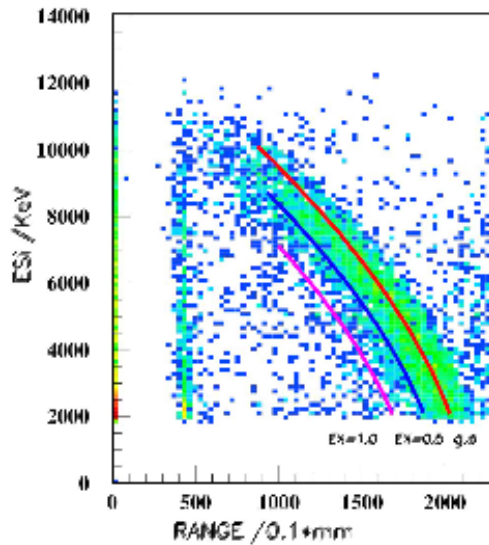


Figure 4: Scatter plot for particles leaving the gas volume, conditioned by the identification of deuterons, of the energy deposited in one of the Si-detectors, as a function of the range of the heavy reaction partner measured inside the gas. The three lines represent kinematical calculations for the (p,d) leading to the unbound ground state of  $^7\text{He}$  and to excited states at 0.5 and 1 MeV above the ground state. As can be seen by comparison with Fig. 3 the width of the distribution is essentially due to the finite width of the states in  $^7\text{He}$ .

The experimental energy resolution being much better than the observed structure, it was not necessary to take it into account in the simulation. The individual contributions for these three resonances are shown, with arbitrary normalization, in

Fig. 5. The final fit is shown as solid line. In this fit the contribution relative to the ground state for the state at  $E_r = 1$  MeV was  $(-0.015 \pm 0.082)$ . This means no contribution of such a state is seen, and the upper limit is far below the contribution of Meitner et al., 2002.

A different way to study the  ${}^7\text{He}$  is via the isobaric analogue resonance in the  ${}^6\text{He}(p,n){}^6\text{Li}$  reaction. The efficiency of the MAYA detector is illustrated by the fact that this result was obtained in some hours of parasitic beam. The result is shown in Fig. 6.

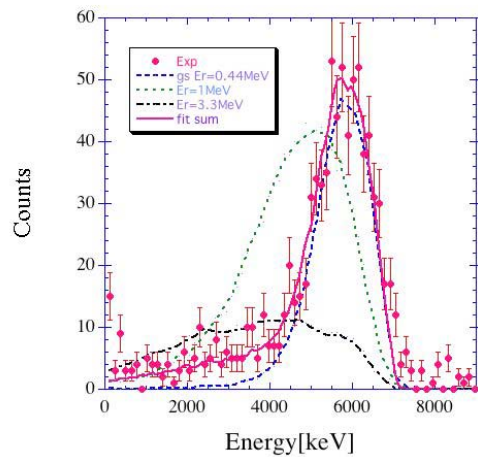


Figure 5: Projected deuteron energy spectrum for the (p,d) reaction. The experimental count rate/energy bite is compared to a Monte-Carlo simulation of this spectrum, including the effect of the energy dependant decay width, recoil broadening, energy dependence of the population cross-section. The individual contributions, with arbitrary normalisations, are shown for the ground state, a hypothetical state at 1 MeV separation energy, and a state at 3.3 MeV separation energy. The fitted sum of these contributions is shown, too. See text for details.

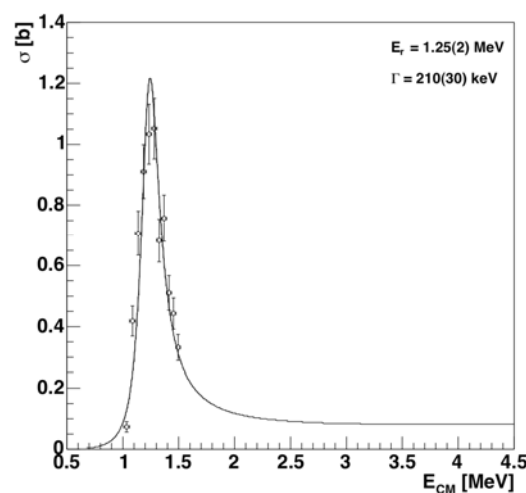


Figure 6: Isobaric analogue resonance in the system  ${}^6\text{He}(p,n){}^6\text{Li}$  as obtained by the MAYA detector (L. Gaudefroy, preliminary).

Final spectroscopic factors are resumed in the table.1 They were extracted by comparing experimental cross sections to Fresco calculations for the transfer reactions, and for the resonances to single particle resonance widths. A very coherent result is obtained, that shows that  ${}^7\text{He}$  can be considered to a good degree as a core coupled to a neutron, with the exception of the result of Wuosma et al., that gives a quite low spectroscopic factor.

**Table 1**

- From IAS  ${}^6\text{He}(p,n)$   $S=0.69\pm 0.10(\text{th})\pm 0.13(\text{exp})$   
 $\Gamma=270\text{keV}$ , from Tilev, V.Rogachev et al, present work+analysis
- From width of gs  ${}^7\text{He}$   $S=0.95\pm 0.1(\text{th})\pm 0.1$   
ENS-compilation+analysis
- From (d,p)  $S=0.37\pm 0.07$   
A.H.Wuosmaa et al.
- Theory(A.H.Wuosma et al)  $S=0.53-0.59$
- For  ${}^8\text{He}(p,d)$  at  $11.5\text{MeV/n}$   $C^2S=4.4\pm 0.4$   
F.Skaza et al.
- For  ${}^8\text{He}(p,d)$  at  $3-4\text{MeV/n}$   $C^2S=3.6\pm 0.4$   
C.E.Demonchy et al, W. Mittig et al.

Table 1: Spectroscopic factors for  ${}^7\text{He}$ .

#### 4. Conclusion and prospective

See the report of D. Beaumel to the SC on this subject.

As was seen, high cross-sections for transfer and resonant reactions are observed in the energy domain of Spiral2. A unique possibility for studying drip-line nuclei exists therefore and IAS are particularly promising. Intensities needed with the Maya detector are of the order of 1000 particles/s. With reasonable extraction efficiencies, most of the neutron rich Be, B, C, N, O, F and Ne isotopes should give such intensities. Be and B being very difficult, C, N, and O would provide for us very interesting isotopic chains to study single particle and collective properties (see the LOI to the SAC of Spiral2 on the ACTAR device by P. Roussel-Chomaz et al.)

#### 5. References

- [1] W. Mittig, Nucl. Phys. A722, 10c (2003)
- [2] W. Mittig et al., NENS2003 conference proceedings
- [3] W. Mittig, Eur. Phys. J. A25 supplement 1, 263 (2005)
- [4] C.E. Demonchy et al., J. Phys. G31, S1831 (2005)
- Y. Mizoi et al., Nucl. Inst. Meth. Phys. Res. A431, 112 (1999)
- C.-E. Demonchy, thesis, University of Caen, France, 2003
- M. Caamano et al., to be published in Journal of Physics
- M. Caamano, thesis, University of Santiago de Compostela, Spain, 2006
- P. Roussel-Chomaz et al., Nucl. Phys A693, 495 (2001)



F. de Oliveira Santos, F. Becker, G. de France, F. Dembinski, C.E. Demonchy, P. Dolégiéviez, G. Georgiev, L. Giot, M. Lewitowicz, I. Matea, W. Mittig, P. Roussel-Chomaz, M.G. Saint Laurent, H. Savajols, M. Stanoiu, C. Stodel, D. Verney, A.C.C. Villari<sup>1</sup>  
 J.M. Daugas, M.J. Lopez Jimenez<sup>2</sup>  
 F. Sarazin<sup>3</sup>  
 M. Sawicka<sup>4</sup>  
 I. Stefan<sup>5</sup>  
 P. Himpe, G. Neyens, N. Smirnova<sup>6</sup>  
 N.L. Achouri, J.C. Angélique, S. Grévy, E. Liénard, N. Orr<sup>7</sup>  
 C. Angulo<sup>8</sup>  
 M. Bellegui, C. Donzaud, D. Guillemaud Mueller, F. Pougheon, O. Sorlin<sup>9</sup>  
 D. Baiborodin, Z. Dlouhy, G. Thiamova<sup>10</sup>  
 E. Berthoumieux, V. Lapoux<sup>11</sup>  
 C. Borcea, F. Negoita<sup>12</sup>  
 B. Blank<sup>13</sup>,  
 A. Cassimi<sup>14</sup>  
 L. Axelsson, K. Markenroth<sup>15</sup>

- 1) GANIL, CEA/DSM - CNRS/IN2P3, BP 55027, F-14076 Caen Cedex 5, France
- 2) CEA/DIF/DPTA/PN, BP 12, F-91680 Bruyères le Châtel, France
- 3) TRIUMF, 4004 Westbrook Mall, Vancouver, British Columbia, V6T 2A3, Canada
- 4) Institute of Experimental Physics, University of Warsaw, PL-00-681 Warsaw, Hoza 69, Poland
- 5) Institute of Atomic Physics, P.O. Box MG6, Bucharest-Margurele, Romania
- 6) Instituut voor Kern- en Stralingsfysica, University of Leuven, B-3001 Leuven, Belgium
- 7) Laboratoire de Physique Corpusculaire, IN2P3-CNRS, ISMRA et Université de Caen, F-14050 Caen, France
- 8) Centre de Recherches du Cyclotron, UCL, B-1348 Louvain-la-Neuve, Belgium
- 9) IPN Orsay, IN2P3-CNRS, Université Paris-Sud, F-91406 Orsay, France
- 10) Nuclear Physics Institute ASCR, CZ-25068 Rez, Czech Republic
- 11) CEA Saclay, DSM/DAPNIA/SPhN, F-91191 Gif-sur-Yvette, France
- 12) Institute of Atomic Physics, P.O. Box MG6, Bucharest-Margurele, Romania
- 13) CEN Bordeaux-Gradignan, IN2P3-CNRS, Université de Bordeaux I, F-33170 Gradignan, France
- 14) CIRIL, Rue Claude Bloch, BP 5133, F-14070 Caen, France
- 15) Experimentell fysik, Chalmers Tekniska Högskola och Göteborgs Universitet, S-412 96 Göteborg, Sweden

Contact person: [oliveira@ganil.fr](mailto:oliveira@ganil.fr)

## 1. Key question and initial goals

The aim of our experiment was to measure the widths, spectroscopic factors, spin and the energies of the low-lying states in  $^{19}\text{Na}$ . The ground state of  $^{19}\text{Na}$  is proton unbound by  $Q = -0.320$  MeV. This nucleus contains 8 neutrons ( $^{19}\text{Na} = ^{16}\text{O} + 3p$ ). Very little was known about this nucleus, no spin assignment, only the energy of the ground and first excited states were known. Several theoretical aspects can be investigated with the study of this nucleus:

Unbound nuclei are fascinating objects, exhibiting antagonistic properties: a very short lifetime, sometimes shorter than the time for a nucleon to pass through the nucleus, and a very well arranged structure with well defined states.

Coulomb effect. In the hypothesis of the charge independence of nuclear forces, the level schemes of mirror nuclei should be identical. Sometimes, large energy shift between mirror pairs are observed. This shift is principally a direct Coulomb energy correction. Our measurement of  $^{19}\text{Na}$  and the comparison to the well known  $^{19}\text{O}$  (the mirror nucleus) is a compelling investigation.

Isospin symmetry. Studying proton-rich nuclei is the way to test the isospin symmetry. An Isospin-dependence may be evidenced in  $^{19}\text{Na}$  by the comparison of the energies and spectroscopic factors of the states.

Borromean system. The nucleus  $^{20}\text{Mg}$  is borromean, since  $^{20}\text{Mg} = ^{18}\text{Ne} + 2p$ . Studying the intermediate nucleus  $^{19}\text{Na}$  is a step forwards a better understanding of  $^{20}\text{Mg}$ .

Two-proton emission. The emission of two correlated protons, a kind of “ $^2\text{He}$ ” emission, is a specific phenomenon that is opened for the low-lying states in exotic proton-rich nuclei.

Astrophysics. Unbound nuclei are also involved in astrophysics studies. The  $^{19}\text{Na}$  nucleus is involved in the reaction  $^{18}\text{Ne}(2p,\gamma)^{20}\text{Mg}$  reaction, an exotic reaction that may be at work in explosive sites.

## 2. Experiment set-up

The properties of  $^{19}\text{Na}$  were investigated by resonant elastic scattering. In our case, we sent a radioactive  $^{18}\text{Ne}$  beam on a 1 mm-thick cryogenic hydrogen target developed at GANIL. Inside the target, the heavy ions are slowed down by energy loss. If their energy, at some point along their path, corresponds to a resonance of the compound nucleus ( $^{19}\text{Na}$ ), the probability for a scattering reaction  $\text{H}(^{18}\text{Ne},p)^{18}\text{Ne}$  increases dramatically (resonant effect). After a scattering event, the recoil proton is ejected in the forward laboratory direction, and is subsequently detected by an array of silicon detectors. In order to cover a larger energy interval, a thick Si detector was used. The inverse geometry and small specific energy loss of the protons strikingly reduce the influence of the beam spread on the final resolution. The thick target makes it possible to obtain a continuous excitation function over a wide energy range without changing the beam energy. The method is very well suited for secondary beams since the limited intensity is compensated by the large cross sections ( $> 100$  mb/sr). From the shape of the resonance one can obtain the spin assignment.

## 3. Results and achievements

The measurement of the resonant elastic scattering reaction  $\text{H}(^{18}\text{Ne},p)^{18}\text{Ne}$  allowed the extraction of the properties of 3 states in  $^{19}\text{Na}$ , as shown in Fig. 1. The properties of the states were analysed and found to be in good agreement with models and with the mirror nucleus. The first peak corresponds to the third excited state, and the comparison with the mirror nucleus shows one of the largest energy shifts. We found that it is due to Coulomb effect. The two peaks 2 and 3 could not be analysed by the R-Matrix model; these don't correspond to resonant elastic scattering. Since we used a silicon strip detector, it was possible to demonstrate that

those events arise from two-proton events, which are two-proton emissions induced by resonance states, see Fig. 2.

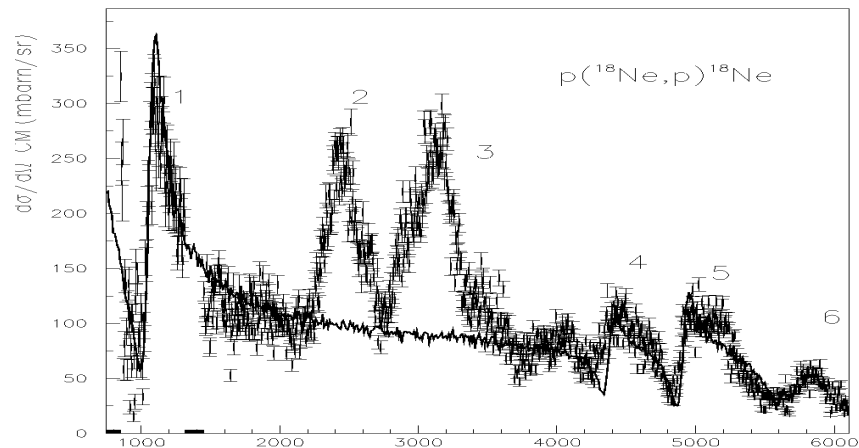


Figure 1: Excitation function measured for the elastic scattering reaction  $H(^{18}\text{Ne},p)^{18}\text{Ne}$ . Peaks 1, 4, 5, 6 correspond to states in  $^{19}\text{Na}$ . The line corresponds to one R-Matrix analysis. The peaks 2 and 3 could not be analysed.

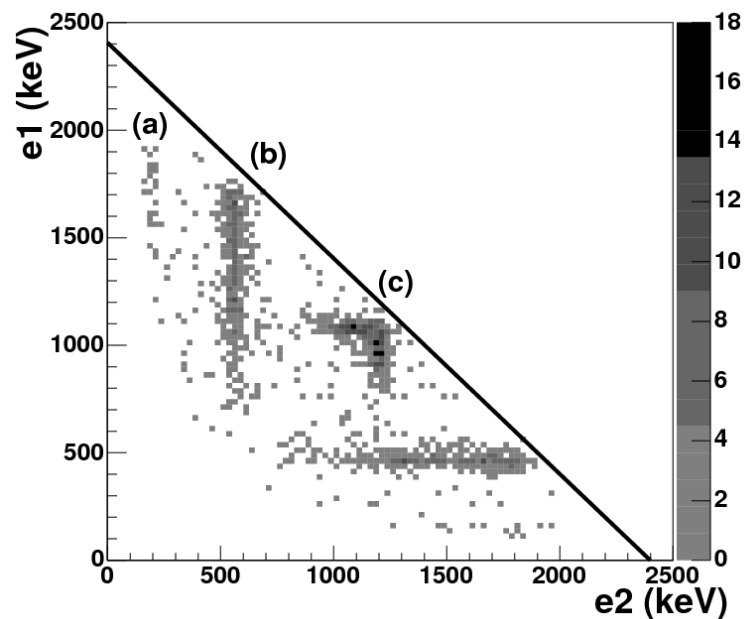


Figure 2: The events observed in the peaks 2 and 3 of Fig. 1 correspond to two proton events. Here, the centre of mass energy of one proton is shown as a function of the energy of the second proton.

One of the two-proton transitions was very discussed since, in that case, the protons exhibit exactly the same energy (events c in Fig. 2), and this is what is expected in case of  $^2\text{He}$  emission. The summary of the results and conclusions are shown in Fig. 3.

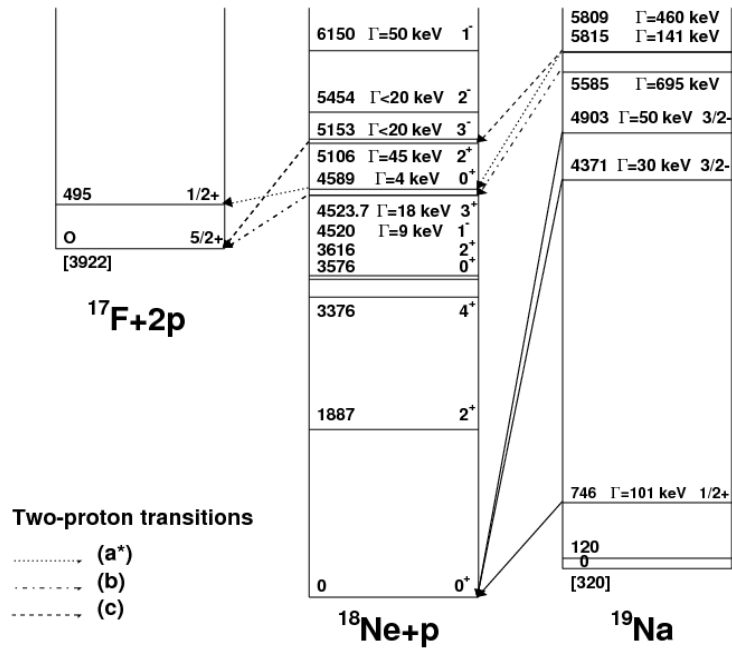


Figure 3: Summary of the results obtained in our experiment. We measured resonant elastic scattering on 3 states in  $^{19}\text{Na}$ , and 3 two-proton emissions induced via resonance reaction.

#### 4. Conclusion and prospective

In conclusion, the properties of 3 new states in  $^{19}\text{Na}$  were measured. These are in agreement with models and with the known properties of the mirror nucleus. Surprisingly, quite intense two-proton emissions were also observed. These were analysed and found to correspond to 3 sequential transitions from  $^{19}\text{Na}$  to  $^{17}\text{F}$ . One of the two-proton transitions was very discussed in terms of  $^2\text{He}$  emission. There are several axes in prospective:

- Astrophysical consequences
- Use inelastic scattering reaction in inverse kinematics as a new method to investigate the incident ion spectroscopy (see E521S experiment).
- Improve energy resolution and try to measure the ground and the first excited state
- Search for  $^2\text{He}$  emission signature in other nuclei

#### 5. References

Eur. Phys. J. A24, 237-247 (2005) and references therein.  
 C. Angulo et al., Phys. Rev. C67, 014308 (2003)  
 F. de Oliveira Santos et al., PROTON-EMITTING NUCLEI: Second International Symposium; PROCON 2003 - AIP Conference Proceedings, p681  
 F. de Oliveira Santos et al., Tours Symposium On Nuclear Physics IV: Tours 2000, AIP Conference Proceedings, p561  
 F. de Oliveira Santos et al., AIP Conference Proceedings (FINUSTAR, 2005) 831, (2006)

# E401S Study of ${}^9\text{He}$ via the $d({}^8\text{He},p){}^9\text{He}$ reaction

E. Tryggvæst, S. Fortier, D. Beaumel, E. Becheva, Y. Blumenfeld, S. Gales, L. Gaudefroy, F. Hammache, V. Lima, E. Rich, J.-A. Scarpaci, O. Sorlin<sup>1</sup>

A. Drouart, A. Gillibert, N. Keeley, V. Lapoux, L. Nalpas, A. Obertelli, E.C. Pollaco, F. Skaza<sup>2</sup>

K.W. Kemper<sup>3</sup>

U. Datta Pramanik<sup>4</sup>

A. Navin<sup>5</sup>

D. Patiris<sup>6</sup>

1) IPN Orsay, IN2P3-CNRS, Université Paris-Sud, F-91406 Orsay, France

2) CEA Saclay, DSM/DAPNIA/SPhN, F-91191 Gif-sur-Yvette, France

3) Department of Physics, Florida State University, Tallahassee, Florida 32306, USA

4) Saha Institute of Nuclear Physics, 1/AF, Bidhannagar, Kolkata 700064, India

5) Nuclear Physics Division, Bhabha Atomic Research Centre, Mumbai 400085, India

6) Department of Physics, University of Ioannina, 45110 Ioannina, Greece

Contact person: [fortier@ipno.in2p3.fr](mailto:fortier@ipno.in2p3.fr)

## 1. Key question and initial goals

The  $d({}^8\text{He},p){}^9\text{He}$  experiment was part of our research program using one-nucleon transfer reactions in order to determine the shell structure of very light neutron-rich nuclei. The  $(d,p)$  transfer reaction is the key experiment to investigate distribution of single-particle neutron strengths, allowing to search for a possible  $p_{1/2}$ - $s_{1/2}$  shell inversion in the next  $N=7$  nucleus  ${}^9\text{He}$ , as previously observed in  ${}^{11}\text{Be}$  and  ${}^{10}\text{Li}$  [1-2]. This very neutron-rich unstable nucleus was previously studied using double-charge exchange experiments [3-4] on  ${}^9\text{Be}$ , proposing a narrow resonant state at 1.3 MeV above neutron threshold as  ${}^9\text{He}$  ground state. On the other hand, results of  ${}^{11}\text{Be}$  fragmentation [5] at MSU were found to be consistent with the existence of a  $s_{1/2}$  ground state at 0.1 MeV above threshold.

**International competition:** Same  $(d,p)$  reaction studied in November 2005 at Dubna at 25 A.MeV. High statistics, but with poor resolution due to gas target and without proton angular distribution data. Angular correlations of decay  ${}^8\text{He}$  show interference effects between overlapping  $s_{1/2}$  ground state and  $p_{1/2}$  first excited resonant state [6].

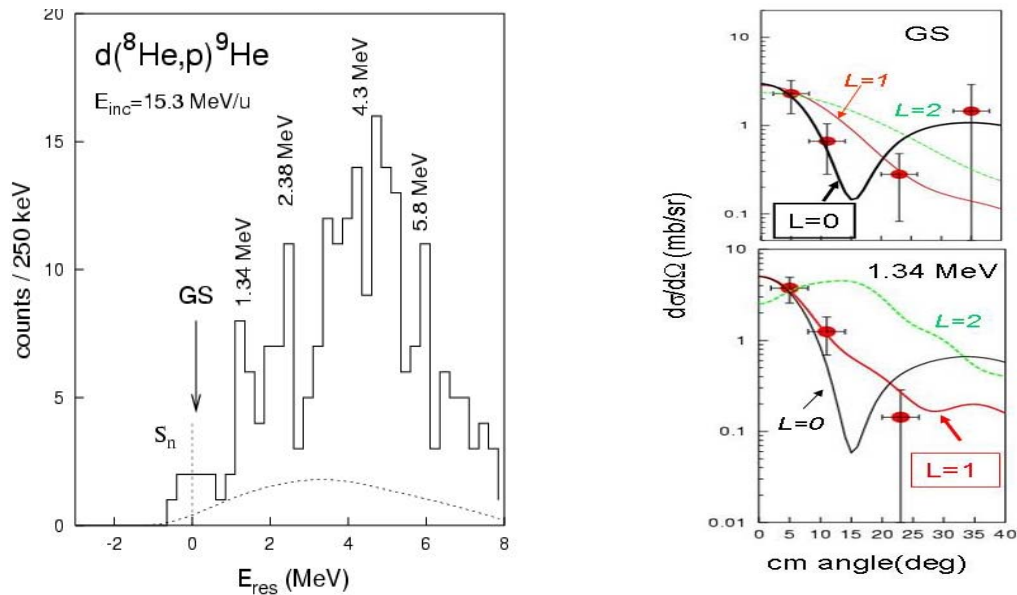
## 2. Experiment set-up

The reaction was studied at  $E = 15.3$  A.MeV using a thin  $\text{CD}_2$  target. Energies of resonant states in  ${}^9\text{He}$  were obtained by measuring kinetic energies and emission angles of the protons detected at backward angles by the MUST charged particle array. Background could be suppressed by gating on  ${}^8\text{He}$  (from  ${}^9\text{He}$  decay) stopped in a plastic telescope. Unfortunately beam intensity was quite low during this experiment (mean value 3500/s), so that achieved statistics was about 3-4 times weaker than expected. Preliminary results concerning only half of this available statistics (due to lack of target homogeneity) were presented in 2004 at the Giens meeting [7]. Since that time, some additional singles data on the  ${}^8\text{He}(d,p){}^9\text{He}$

reaction could be obtained using one prototype of the next generation detector MUST2 placed at backward angles during another experiment, which aimed at the study of the “tetra-neutron”. Moreover E401S data were reanalysed, using a better extrapolation of energy calibration at low proton energies and correcting for possible non-homogeneity of the target thickness. This new procedure insures the use of the full data set and a significant improvement of the c.m. energy resolution (0.5 MeV).

### 3. Results and achievements

The left hand side of the figure shows the missing mass spectrum of  ${}^9\text{He}$ , whereas the right part shows the angular distribution gated on the g.s. (top) and on the first excited state (bottom) at 1.34 MeV. Results are compared to DWBA calculations. Present data clearly establish that the  ${}^9\text{He}$  ground state is located just above neutron threshold ( $E=0.1$  MeV) and has  $J^\pi = 1/2^+$ , in agreement with the results of ref. [5]. A better fit of the angular distribution is obtained for  $L = 0$ . A fragmentation of the  $p_{1/2}$  and  $d_{5/2}$  strengths in  ${}^9\text{He}$  is also evidenced by the data.



### 4. Conclusion and prospective

Important data about  ${}^9\text{He}$  (evidence for a  $s_{1/2}$  ground state close to the neutron emission threshold, fragmentation of p and d strengths) could be obtained from E401S in spite of unexpectedly low statistics due to the small intensity of  ${}^8\text{He}$  beam obtained during the run. A paper will soon be submitted for publication. However a new experiment with a more intense  ${}^8\text{He}$  beam, a thinner  $\text{CD}_2$  target and using the MUST2 detector array has been carried out to get additional data with better energy resolution and statistics.

### 5. References

- [1] S. Fortier et al., Phys. Lett. B461, 22 (1999); J.S. Winfield et al., Nucl. Phys. A683, 48 (2001)
- [2] S. Pita, Thèse Université Paris VI, France, 2000; S. Pita et al., to be published
- [3] K.K. Seth et al., Phys. Rev. Lett. 58, 19 (1987)

- [4] H.G. Bohlen et al., Z. Phys. A330, 227 (1988); H.G. Bohlen et al., Prog. Part. Nucl. Phys 42, 17 (1999)
- [5] L. Chen et al., to be published in Phys. Lett. B505, 21 (2001)
- [6] M.S. Golovkov et al., results presented at RNB7 and EXON06
- [7] E. Tryggestad et al., talk at Journées GANIL, Giens, 2004



# Direct and compound reactions induced by E403S unstable helium beams near the Coulomb barrier

A. Navin, A. Chatterjee, S. Kailas, K. Mahata, K. Ramachandran, A. Shrivastava, V. Tripathi<sup>1</sup>  
Y. Blumenfeld, E. Tryggestad<sup>2</sup>  
Y. V. Nanal, R. G. Pillay<sup>3</sup>  
J. M. Casandjian, G. de France, M. Rejmund, C. Simenel<sup>4</sup>  
R. Raabe, E. C. Pollacco, J. L. Sida<sup>5</sup>  
D. Bazin<sup>6</sup>  
M. Dasgupta<sup>7</sup>  
R. C. Lemmon<sup>8</sup>

- 1) Nuclear Physics Division, Bhabha Atomic Research Centre, Mumbai 400085, India
- 2) IPN Orsay, IN2P3-CNRS, Université Paris-Sud, F-91406 Orsay, France
- 3) Department of Nuclear and Atomic Physics, Tata Institute of Fundamental Research, Mumbai 400005, India
- 4) GANIL, CEA/DSM - CNRS/IN2P3, BP 55027, F-14076 Caen Cedex 5, France
- 5) CEA Saclay, DSM/DAPNIA/SPhN, F-91191 Gif-sur-Yvette, France
- 6) NSCL, Michigan State University, East Lansing, Michigan 48824, USA
- 7) Department of Nuclear Physics, Australian National University, Canberra, Australian Capital Territory 0200, Australia
- 8) CRLC, Daresbury Laboratory, Daresbury, Warrington, WA4 4AD, United Kingdom

Contact person: [navin@ganil.fr](mailto:navin@ganil.fr)

## 1. Key question and initial goals

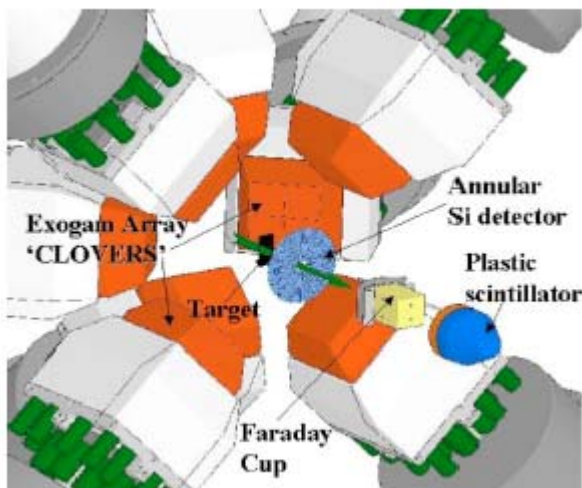
Fusion studies with radioactive ion beams are currently investigating the conflicting results/predictions of the influence of weak binding of the projectile. The origin of this is in the fundamentally different treatment of the role of the break-up channel, arising from the low binding of the neutron-rich isotopes. One approach treated the elastic and break-up channels incoherently (as a loss of flux) whereas in the other, the role of break-up was treated in coupled channels formalism as an inelastic excitation in the continuum, implying a coherent superposition of the elastic and break-up channels.

The weak binding of these projectiles leads to a significant cross section for both elastic break-up, transfer reactions and/or break-up followed by capture of a part of it by the target (incomplete fusion, massive transfer or stripping/stripping). Therefore, before interpreting results of fusion cross section measurements with weakly bound projectiles, it is of paramount importance to ensure that the quoted fusion cross section does not contain contributions from other mechanisms.

In the present work the goal is to obtain a more complete understanding of low energy reactions induced by the neutron-rich Borromean nuclei  ${}^6,8\text{He}$ , on both medium mass  ${}^{63,65}\text{Cu}$  and heavy  ${}^{188,190,192}\text{Os}$  targets, by relying on a model independent comparison with  ${}^4\text{He}$  induced reactions. In the case of the  ${}^6\text{He}$  beam inclusive prompt  $\gamma$ -ray measurements have been performed in order to obtain residue cross sections (fusion and neutron transfer), and for the first time in a radioactive beam experiment, coincident measurements between  $\gamma$  rays and light charged particles have been attempted to address the separation of fusion and neutron transfer mechanisms. In the case of  ${}^8\text{He}$ , the weak beam intensity and the presence

of large background from  $^8\text{He}$   $\beta$ -decay precluded a successful singles measurement; however, coincidences between the charged particles and characteristic  $\gamma$  rays could be observed. Additionally, elastic scattering angular distributions were measured and analysed for both projectiles to obtain the reaction cross-section. In the case of the very tightly bound  $^4\text{He}$  projectiles, direct processes are expected to be weak in the energy range studied, and only  $\gamma$ -ray singles were measured to obtain the complete fusion cross sections. A similar measurement for  $^6\text{He} + ^{64}\text{Zn}$  system, have been performed at Louvain-la-Neuve.

## 2. [Experiment set-up](#)



The experiment used the very early stage of the EXOGAM array coupled with an annular strip detector. A Current amplifier to measure  $10^7$  p/sec was used to measure the current for  $^6\text{He}$ . 6 Ut were lost as there was a problem with some safety aspects of the source. So rather than waste the beam time the setup was modified to use was made to use the primary beam of  $^{12}\text{C}$  at 144 MeV.

## 3. [Results and achievements](#)

Reactions induced by radioactive  $^{6,8}\text{He}$  beams from the SPIRAL facility were studied on  $^{63,65}\text{Cu}$  and  $^{188,190,192}\text{Os}$  targets and compared to reactions with the stable  $^4\text{He}$  projectiles from the Mumbai Pelletron. Partial residue cross sections for fusion and neutron transfer obtained from the measured intensities of characteristic in-beam  $\gamma$ -rays for the  $^6\text{He} + ^{63,65}\text{Cu}$  systems are presented. Coincidence measurements of heavy reaction products, identified by their characteristic  $\gamma$ -rays, with projectile like charged particles, provide direct evidence for a large transfer cross section with Borromean nuclei  $^6\text{He}$  at 19.5 and 30 MeV and  $^8\text{He}$  at 27 MeV. Reaction cross sections were also obtained from measured elastic angular distributions for  $^{6,8}\text{He} + \text{Cu}$  systems. Cross sections for fusion and direct reactions with  $^{4,6}\text{He}$  beams on heavier targets of  $^{188,192}\text{Os}$  at 30 MeV are also presented. The present work underlines the need to distinguish between various reaction mechanisms leading to the same products before drawing conclusions about the effect of weak binding on the fusion process. The feasibility of extracting small cross sections from inclusive in-beam  $\gamma$ -ray measurements for reaction studies near the Coulomb barrier with low intensity isotope separation on-line beams is highlighted.

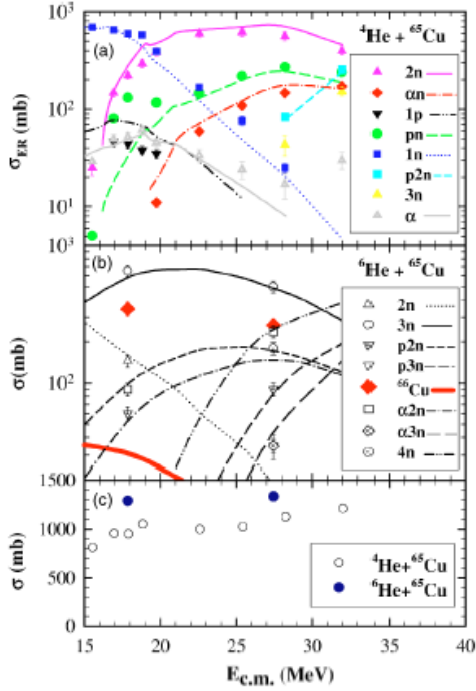


FIG. (a) Measured partial residue cross sections indicated by different symbols for  ${}^4\text{He}+{}^{65}\text{Cu}$  system as a function of the center of mass energy. The lines are obtained using the statistical model code CASCADE (see text). (b) Same as in (a) for the  ${}^6\text{He}+{}^{65}\text{Cu}$  system. (c) Total residue cross section for  ${}^4\text{He}+{}^{65}\text{Cu}$  (open symbols) and  ${}^6\text{He}+{}^{65}\text{Cu}$  (filled symbols). Only statistical errors are shown.

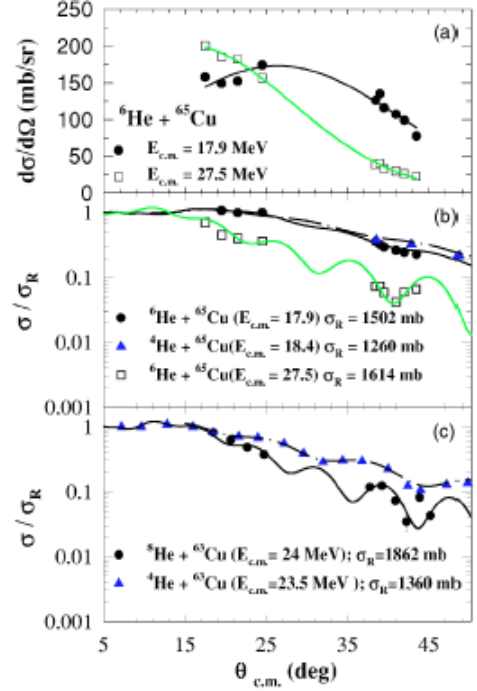


FIG. (a)  $\alpha$ -particle angular distributions in coincidence with the 185.9 keV  $\gamma$  transition in  ${}^{66}\text{Cu}$  for  ${}^6\text{He}+{}^{65}\text{Cu}$ . The lines are Gaussian fits to the data. (b) Elastic angular distributions for  ${}^6\text{He}+{}^{65}\text{Cu}$  and for  ${}^4\text{He}+{}^{65}\text{Cu}$  (Ref. [42]). The lines are calculations using ECIS97. (c) Same as in (b) for  ${}^8\text{He}+{}^{63}\text{Cu}$  and  ${}^4\text{He}+{}^{63}\text{Cu}$  (Ref. [43]). Only statistical errors are indicated.

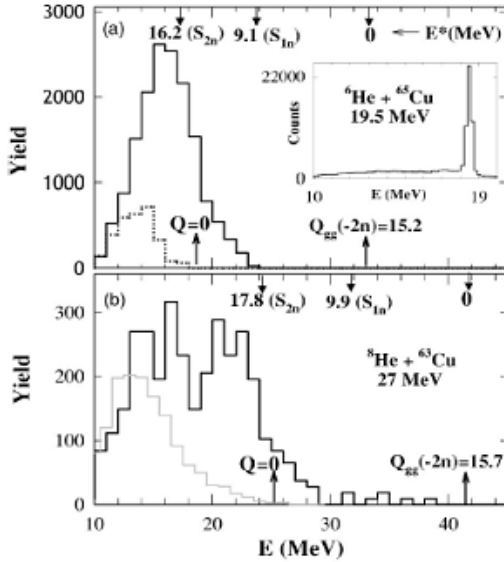


FIG. Charged particles measured in the annular Si detector. (a) In coincidence with the 185.9 keV  $\gamma$  transition in  ${}^{66}\text{Cu}$  (full line) and 1115.5 keV in  ${}^{65}\text{Cu}$  (dotted line) for  ${}^6\text{He}+{}^{65}\text{Cu}$  at 19.5 MeV at  $\theta_{lab}=35^\circ$ . The yields have been corrected for efficiency and branching of the gating transition. Inset shows the corresponding inclusive spectrum. (b)  ${}^8\text{He}+{}^{63}\text{Cu}$  at 27 MeV gated by the 159.1 keV transition in  ${}^{64}\text{Cu}$  at  $\theta_{lab}=37^\circ$ . The gray curve is a calculated  $\alpha$  evaporation spectrum using a statistical model. The ground state  $Q$  values ( $Q_{gg}$ ) and the neutron separation energies ( $S_n$ ) in the residual nucleus in a two-neutron stripping reaction are indicated.

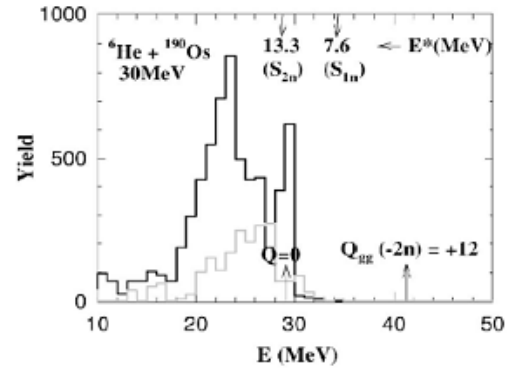


FIG. Charged particles measured in the annular Si detector in coincidence with the 186.7 keV  $\gamma$  transition in  ${}^{190}\text{Os}$  (full line) and the 175.7 keV transition in  ${}^{191}\text{Os}$  (gray line) for  ${}^6\text{He}+{}^{190}\text{Os}$  reaction at 30 MeV at  $\theta_{lab}=37^\circ$ . The yields have been corrected for efficiency and branching of the gating transition. The ground state  $Q$  values ( $Q_{gg}$ ) and the neutron separation energies ( $S_n$ ) in the residual nucleus in a two-neutron stripping reaction are indicated.

#### **4. Conclusion and prospective**

In summary, we have presented results for fusion, transfer, stripping, and elastic scattering of  $^{4,6,8}\text{He}$  on (medium mass) Cu and (heavy) Os targets near the Coulomb barrier. The feasibility of measuring small cross sections using *inclusive* in-beam  $\gamma$ -ray measurements with low intensity ISOL beams in conjunction with highly efficient arrays has been demonstrated. Large neutron transfer cross-sections were obtained through direct measurements, and were found to be larger than those for stripping. The importance of identifying and delineating the mechanisms of residue formation for understanding fusion with RIBs has been clearly illustrated. Kinematically complete experiments including the measurement of neutrons are now necessary to distinguish between compound and direct reactions and also between one- and two-neutron transfer processes, in order to advance toward a more complete picture of low energy reaction dynamics with neutron-rich projectiles.

#### **5. References**

- A. Navin et al., Phys. Rev. C70, 044601 (2004)
- A. Di Pietro et al., Phys. Rev. C69, 044613 (2004)

A. Navin, S. Bhattacharya, A. Chatterjee<sup>2</sup>, G. de France, A. Lemanson, M. Rejmund, I. Stefan<sup>1</sup>

A. Shrivastava, R. Ramachandran<sup>2</sup>,

V. Nanal, R.G. Pillay<sup>3</sup>

J. Nyberg<sup>4</sup>

Y. Blumenfeld, J.-A. Scarpaci, D. Beaumel<sup>5</sup>

R. Raabe<sup>6</sup>

R.C. Lemmon<sup>7</sup>

D. Bazin<sup>8</sup>

C. Simenel<sup>9</sup>

M. Labiche, C. Timis<sup>10</sup>

1) GANIL, CEA/DSM - CNRS/IN2P3, BP 55027, F-14076 Caen Cedex 5, France

2) Nuclear Physics Division, Bhabha Atomic Research Centre, Mumbai 400085, India

3) Department of Nuclear and Atomic Physics, Tata Institute of Fundamental Research, Mumbai 400005, India

4) Department of Radiation Sciences, Uppsala University, Uppsala, Sweden

5) IPN Orsay, IN2P3-CNRS, Université Paris-Sud, F-91406 Orsay, France

6) Instituut voor Kern- en Stralingsfysica, University of Leuven, B-3001 Leuven, Belgium

7) CRLC, Daresbury Laboratory, Daresbury, Warrington, WA4 4AD, United Kingdom

8) NSCL, Michigan State University, East Lansing, Michigan 48824, USA

9) CEA Saclay, DSM/DAPNIA/SPhN, F-91191 Gif-sur-Yvette, France

10) Department of Physics, University of Surrey, Surrey GU2 7XH, United Kingdom

Contact person: [navin@ganil.fr](mailto:navin@ganil.fr)

## 1. Key question and initial goals

In the present proposal the main issue is - understanding of the dynamical processes involving the quantum tunnelling of dilute nucleonic systems from the study of fusion and other direct reactions around the Coulomb barrier. This is obtained by studying the interconnectivity, which is manifested very strongly at energies near the Coulomb barrier between the intrinsic structure of the colliding nuclei and the fusion process. This proposal focuses on the effect of Borromean structure on the reaction mechanism. It deals with complete measurement of elastic, transfer and fusion for these nuclei on an intermediate mass target at energies near the Coulomb barrier. For such systems the identification of complete fusion (events arising from the amalgamation of projectile + target) and separation between 1n and 2n transfer and break-up reactions require exclusive measurements. In this experiment the goal was two fold:

- a) From the angular distribution for 1n and 2n transfer reactions get the spatial correlations between two valence neutrons in <sup>6</sup>He and get the significance of coupling of these reactions on other reaction processes
- b) To make the first measurement of fusion cross-section with the double borromean system <sup>8</sup>He at energies near the barrier.

### ***International competition***

- a) Total cross sections for 1n and 2n transfer have been measured at the University of Notre Dame on a Bi target from the measurement of neutron in coincidence with alpha particles showed a dominance of the 2n channel.

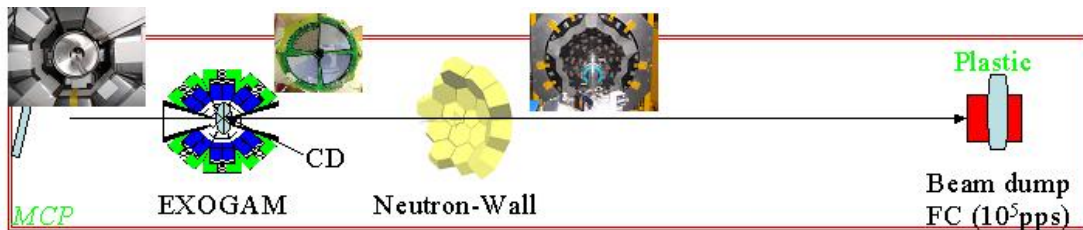
Angular distributions for  ${}^6\text{He}(p,d/t)$  are measured at Louvain-la-Neuve.

The present proposal used **triple** coincidence between particle, gamma and neutrons for the de-convolution of 1n and 2n transfer angular distributions, as the residual nuclei are the same after both reactions. The neutron measurement was required since the ejectile ( ${}^5\text{He}$ ) in case of 1n transfer is unstable and the 2n transfer is followed by evaporation of neutron. This measurement is thus insensitive to the large break-up component.

- b) For the second part there is no competition as presently there is no other low energy  ${}^8\text{He}$  facility.

## 2. Experiment set-up

The set-up used the EXOGAM gamma array, a  $\Delta E$ -E Si CD and the neutron wall. The EXOGAM was optimised to minimize dead time and room background and was used with full Compton shields for the first time. The Neutron wall was set-up and tested. Both the intensity ( ${}^6\text{He}$ ,  $4.5 \cdot 10^7$  pps;  ${}^8\text{He}$ ,  $1.1 \cdot 10^5$  pps) and beam spot size (**3.5mm FWHM**) delivered in this experiment are unparalleled so far.



## 3. Results and achievements

The data is an advanced stage of analysis.

These are the first successful triple coincidence experiments at energies near the Coulomb barrier with radioactive ion beams. This was the first use of the neutron wall for measurement of absolute energies. The measurements of absolute cross sections with the  ${}^8\text{He}$  beam are one of the most sensitive measurements using the in beam gamma decay. The experience gained with this experiment is serving as a benchmark for experiments to be done with SPIRAL2 in terms of the radioactivity of the beam. Preliminary analysis of the data have been presented at FUSION06 and NN06 conferences

## 4. Conclusion and prospective

The angular distribution measurement of 1n and 2n transfer and break-up will provide useful information on coupling to the continuum and its influence on fusion and elastic scattering. The correct treatment of continuum in coupled channels calculation is of current theoretical interest and present experiment will provide a useful input for the theoretical models.

Based on the success of the present experiment with the  ${}^8\text{He}$  beam, we are attempting to measure lower cross sections at energies lower than the Coulomb barrier.

## 5. References

- R. Raabe et al., Nature 431, 823 (2004)  
D. Hinde and M. Dasgupta, Nature 431, 748 (2004)  
A. Di Pietro et al., Phys. Rev. C69, 044613 (2004)  
A. Navin et al., Phys. Rev. C70, 044601 (2004)  
Yu.E. Penionzhkevich, Phys. Rev. Lett. 96, 162701 (2006)  
L.F. Canto et al., Phys. Rep. 424, 1 (2006)



# E404aS Identification of gamma rays in nuclei around the dripline nucleus $^{130}\text{Sm}$ : probing the maximally deformed light rare-earth region

P.J. Nolan, A.J. Boston, R.J. Cooper, M.R. Dimmock, S. Gros, B.M. McGuirk, E.S. Paul, M. Petri, H.C. Scraggs, G. Turk<sup>1</sup>  
N. Redon, D. Guinet, Ph. Laitesse, M. Meyer, B. Rossé, Ch. Schmitt, O. Stézowski<sup>2</sup>  
G. De France, S. Bhattachasya, G. Mukherjee, F. Rejmund, M. Rejmund, H. Savajols<sup>3</sup>  
J.N. Scheurer<sup>3</sup>  
A. Astier<sup>4</sup>  
I. Deloncle, A. Prévost<sup>5</sup>  
B.M. Nyakó, J. Gál, J. Molnár, J. Timár, L. Zolnai<sup>6</sup>  
K. Juhász<sup>7</sup>  
V.F.E. Pucknell<sup>8</sup>  
R. Wadsworth, P. Joshi<sup>9</sup>  
G. La Rana, R. Moro, M. Trotta, E. Vardaci<sup>10</sup>  
G. Ball, G. Hackman<sup>11</sup>

- 1) Oliver Lodge Laboratory, University of Liverpool, Liverpool L69 7ZE, United Kingdom
- 2) IPN Lyon, IN2P3-CNRS, Université C. Bernard Lyon-1, F-69622 Villeurbanne, France
- 3) GANIL, CEA/DSM - CNRS/IN2P3, BP 55027, F-14076 Caen Cedex 5, France
- 4) CEN Bordeaux-Gradignan, IN2P3-CNRS, Université de Bordeaux I, F-33170 Gradignan, France
- 5) CSNSM Orsay, IN2P3-CNRS, Université Paris-Sud, F-91405 Orsay, France
- 6) Institute of Nuclear research of the Hungarian Academy of Sciences, H-4001 Debrecen, Hungary
- 7) Institute of Mathematics and Informatics, University of Debrecen, H-4001 Debrecen, Hungary
- 8) CCLRC Daresbury Laboratory, Daresbury, Warrington WA4 4AD, United Kingdom
- 9) Department of Physics, University of York, Heslington, York YO10 5DD, United Kingdom
- 10) INFN and Dipartimento di Scienze Fisiche, Mostra d'Oltremare, Pad 20, 80125 Napoli, Italy
- 11) TRIUMF, 4004 Westbrook Mall, Vancouver, British Columbia, V6T 2A3, Canada

Contact person: [Nolan@liverpool.ac.uk](mailto:Nolan@liverpool.ac.uk)

## 1. Key question and initial goals

Mapping and understanding major regions of deformation away from closed shells is an important aspect of nuclear structure physics. Adding protons above  $Z = 50$  while removing neutrons from  $N = 82$  produces a major region of deformation. By fusing a  $^{76}\text{Kr}$  radioactive beam with a  $^{58}\text{Ni}$  target, it was proposed that it may be possible to identify, for the first time, excited states in extremely neutron-deficient nuclei around the  $T_z = 3$  nucleus  $^{130}\text{Sm}$ . This nucleus is predicted to be the lightest proton-bound samarium isotope, i.e. it lies at the proton dripline. Nuclei close to  $^{130}\text{Sm}$  are predicted to possess large prolate quadrupole deformation ( $\beta_2 \approx 0.4$ ) in their ground states, comparable to that of the high-spin superdeformed band in  $^{132}\text{Ce}$ , which has a 3:2 nuclear axis ratio.

Deformation trends may be followed by simply examining the energies of the lowest one or two transitions of rotational bands in these nuclei. For even-even nuclei the energy of the  $2^+ \rightarrow 0^+$  transition is inversely proportional to the nuclear moment of inertia and hence deformation, e.g. the Grodzins formula. The nucleus  $^{130}\text{Sm}$  is a particularly useful case to assess the present experimental arrangement since its  $2^+$

energy of  $\approx 121$  keV has already been inferred from the fine structure in the ground-state proton decay of  $^{131}\text{Eu}$  [1], although no  $\gamma$ -ray decay has yet been seen in  $^{130}\text{Sm}$ .

## 2. Experiment set-up

The SPIRAL facility delivered a  $^{76}\text{Kr}$  radioactive ion beam (RIB) of energy 4.34 A.MeV and with an average intensity of  $5 \times 10^5$  particles per second. The RIB impinged on a target consisting of  $1.1 \text{ mg.cm}^{-2}$  of  $^{58}\text{Ni}$  on a thin carbon foil. The present reaction represents one of the first ever fusion-evaporation reactions that has been performed using RIBs. The experimental arrangement consisted of the EXOGAM [2]  $\gamma$ -ray detectors (11 segmented clover HPGe detectors) coupled together for the first time with both the DIAMANT [3] charged-particle array (47 CsI(Tl) scintillation crystals) and the wide angular and momentum acceptance VAMOS [4] spectrometer (QQDWF dispersive mode). The trigger condition required an EXOGAM  $\gamma$ - $\gamma$  event (including any coincident DIAMANT signals) or a VAMOS event. A total of  $1.3 \times 10^9$  such events were recorded.

## 3. Results and achievements

Only a very small fraction of the recorded events (0.04 %) correspond to real fusion-evaporation reactions, since the RIB induced a high background in the  $\gamma$ -ray spectra ( $^{76}\text{Kr}$  decays to  $^{77}\text{r}$  with a half-life of 14.8 h, which then decays to stable  $^{76}\text{Se}$  with a half-life of 16.2 h).

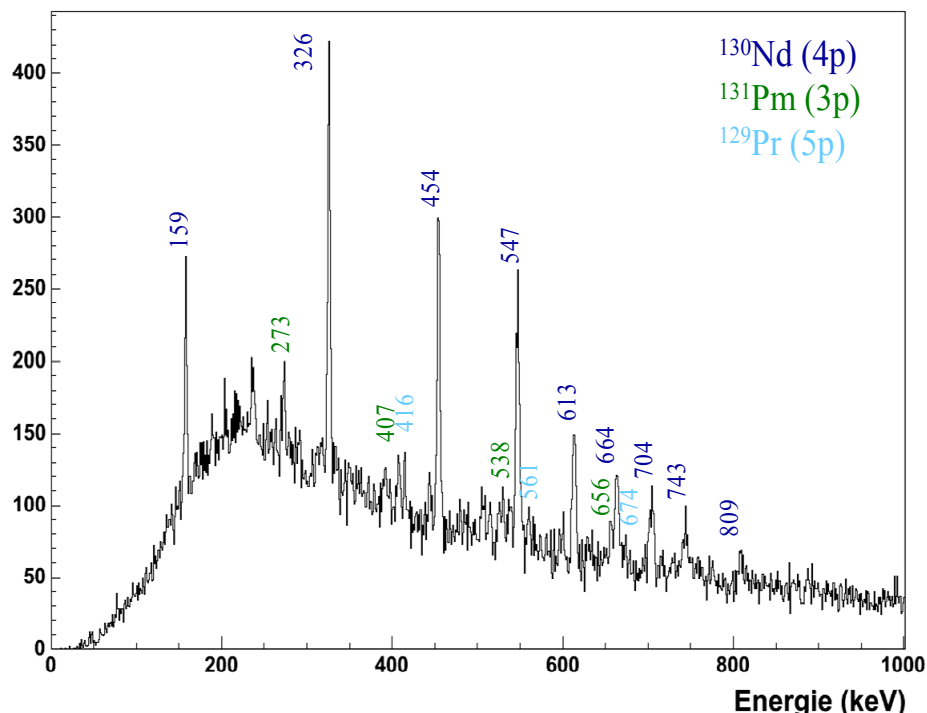


Figure 1: Doppler-corrected  $\gamma$ -ray spectrum gated by charged particles identified with DIAMANT. The spectrum is gated on at least three protons.

However, by gating on DIAMANT it was possible to pick out  $\gamma$ -rays in prompt coincidence with evaporated charged particles, i.e.  $\gamma$ -rays emanating from fusion-evaporation reactions. Such  $\gamma$ -rays from the pure charged-particle reaction channels,

with predicted cross sections in the range 10-100 mb, are shown in Figs. 1 and 2, respectively. These Doppler-corrected ( $v = 0.054$  c) spectra show transitions assigned to  $^{130}\text{Nd}$  (4p),  $^{131}\text{Pm}$  (3p),  $^{129}\text{Pr}$  (5p),  $^{128}\text{Nd}$  ( $\alpha 2p$ ), and  $^{127}\text{Pr}$  ( $\alpha 3p$ ). In these two spectra, all the radioactivity lines, which represent more than 99.9 % of the events collected in the experiment, have been completely removed due to the coincidence required between the three detection systems (EXOAM, DIAMANT and VAMOS).

The yrast bands of five known nuclei have been observed:  $^{130}\text{Nd}$  (up to  $22^+$ ),  $^{131}\text{Pm}$  (up to  $27/2^-$ ),  $^{129}\text{Pr}$  (up to  $27/2^-$ ) by gating on at least three evaporated protons detected in DIAMANT (Fig. 1), and  $^{128}\text{Nd}$  (up to  $16^+$ ) and  $^{127}\text{Pr}$  (up to  $35/2^-$ ) by gating on at least one evaporated  $\alpha$ -particle (Fig. 2). For the most strongly populated isotope,  $^{130}\text{Nd}$ , some levels in excited sidebands have also been observed.

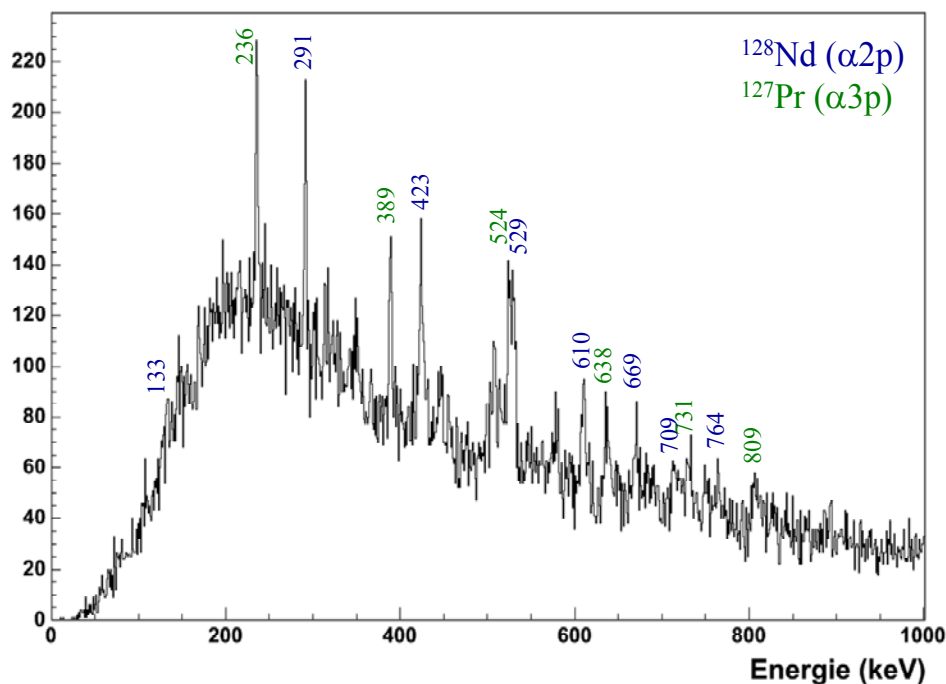


Figure 2: Doppler-corrected  $\gamma$ -ray spectrum gated by charged particles identified with DIAMANT. The spectrum is gated on at least one  $\alpha$ -particle.

#### 4. Conclusion and prospective

With the present  $^{76}\text{Kr}$  radioactive beam ( $5 \times 10^5$  particles per second), new nuclei (with unknown excited states) can only be reached via fusion-evaporation reactions involving neutron emission. Nuclei produced by single-neutron evaporation (e.g. 2pn, 3pn, 4pn,  $\alpha 2pn$ ) are predicted with cross sections in the range 1-10 mb, which is just at or below the limit of the present experiment. Furthermore, two-neutron evaporation (e.g. 2p2n leading to  $^{130}\text{Sm}$ ) is yet an order of magnitude lower ( $< 1$  mb) necessitating the use of intense radioactive beams. Alternatively, more neutron-deficient radioactive beams, such as  $^{72}\text{Kr}$ , could be used to populate the nuclei of interest directly via pure charged-particle evaporation. Beams of such exotic radioactive species are however currently much too weak for viable studies.

## 5. References

- [1] A. Sonzogni et al., Phys. Rev. Lett. 83, 1116 (1999)
- [2] F. Azaiez, Nucl. Phys. A 654, 1003c (1999)
- [3] J. Gál et al., Nucl. Inst. Meth. Phys. Res. A516, 502 (2004)
- [4] H. Savajols, Nucl. Inst. Meth. Phys. Res. B204, 146 (2003)

# Structure of the exotic ${}^8\text{He}$ nucleus via the E405S elastic and inelastic scattering on proton target

F. Skaza<sup>2</sup>, V. Lapoux, N. Keeley, N. Alamanos, F. Auger, A. Drouart, A. Gillibert, L. Nalpas<sup>7</sup>, A. Pakou, E.C. Pollacco, R. Raabe, J.L. Sida<sup>1</sup>

D. Beaumel, E. Becheva, Y. Blumenfeld, F. Delaunay, J.-A. Scarpaci<sup>2</sup>

L. Giot, P. Roussel-Chomaz<sup>3</sup>

K.W. Kemper<sup>4</sup>

S. Stepantsov, R. Wolski<sup>6,5</sup>

1) CEA Saclay, DSM/DAPNIA/SPhN, F-91191 Gif-sur-Yvette, France

2) IPN Orsay, IN2P3-CNRS, Université Paris-Sud, F-91406 Orsay, France

3) GANIL, CEA/DSM - CNRS/IN2P3, BP 55027, F-14076 Caen Cedex 5, France

4) Department of Physics, Florida State University, Tallahassee, Florida 32306, USA

5) Russian Flerov Laboratory of Nuclear Reactions, JINR, Dubna, RU-141980 Russia

6) H. Niewodniczański Institute of Nuclear Physics, 152 31-342 Cracow, Poland

7) Department of Physics, University of Ioannina, 45110 Ioannina, Greece

Contact person: [vlapoux@cea.fr](mailto:vlapoux@cea.fr)

## 1. Key question and initial goals

In order to test the validity of the nuclear models and to improve their predictive power, the properties of the exotic nuclei are experimentally investigated using radioactive ion beams. In this scope and to clarify the nuclear correlations producing the weakly bound structures close or at to the drip line, we have studied the structure and the spectroscopy of the  ${}^{6,8}\text{He}$  exotic nuclei using  $(p,p')$  scattering. The goals were to obtain the low-lying resonant states and to measure the  $(p,p')$  angular distributions, allowing to test the validity of microscopic few-body calculations and to deduce the features of the nuclear interaction inside a nucleus with very low nuclear-matter density. The weakly bound isotope  ${}^6\text{He}$  was investigated by the MUST collaboration using a fragmented GANIL beam. The inelastic  $(p,p')$  cross sections to the  $2^+$  state were shown to be in favour of a halo configuration in  ${}^6\text{He}$  [1]. Following this program, our aim was to explore the properties of the expected four-neutron skin structure of the  ${}^8\text{He}$  nucleus. We carried out the E405S experiment in Nov. 2001, the  ${}^8\text{He}(p,p')$  measurement was done using the first  ${}^8\text{He}$  beam accelerated by SPIRAL. All previous data prior to E405S were not conclusive about the resonant states above the known first  $2^+$  excited state obtained at Riken [2]. The inelastic  ${}^8\text{He}(p,p')$  scattering to the first  $2^+$  state was measured at 73 A.MeV [2] but there was not enough statistics to provide information on the  ${}^8\text{He}$  structure and on other resonant states. In the E405S, we combined two assets: an optimal particle detection set-up and the low-energy SPIRAL beam of  ${}^8\text{He}$ , the intensity of which was large enough to provide new information.

## 2. Experiment set-up

We perform the experiments in inverse kinematics. The beam of interest impinges on a target containing the light probe (p, d, or t) and the light recoil is

identified in a position-sensitive particle detector in coincidence with the heavy ejectile detected in a plastic scintillator or in a spectrometer. We use the dedicated tools to study direct reactions induced by radioactive beams: the beam tracking detectors CATS [3], built by the DAPNIA, and the Si-strip telescope array MUST [4], realized in collaboration with IPN-Orsay and DAM/SPN. For E405S, the direct reactions of  $^8\text{He}$  on a proton-rich target of polypropylene foil were measured at the incident energy of 15.7 A.MeV.

The emitted light charged particles, proton, deuteron or triton were detected by the wall of 8 MUST modules, in coincidence with the heavy ejectile detected at forward angles in a plastic scintillator. Mean intensity during the experiment (25UT) was 5000/s, we reached the nominal value of  $10^4$  /s only in the last 3 UT.

With the CATS and MUST devices we obtained an angular resolution of  $0.4^\circ$  in the lab. frame and an energy resolution ranging from 600 keV to 1.2 MeV in the excitation spectrum measured from proton scattering with the thin ( $1.48 \text{ mg/cm}^2$ ) to measure the angles below  $40^\circ_{\text{c.m}}$ ) and thick ( $8.25 \text{ mg/cm}^2$ ) target.

### 3. Results and achievements

The analysis of the  $^8\text{He}+p$  data was the subject of F. Skaza's PhD thesis [5], done at SPhN. Elastic, inelastic and transfer reaction cross-sections were extracted from the data and compared to theoretical calculations yielding accurate results on the structure of the  $^8\text{He}$  [6,7]. The  $^8\text{He}(p,d)$  cross sections were found as large as the elastic ones in the angular range from  $30$  to  $60^\circ_{\text{c.m}}$ , showing strong coupled-channel (CC) effects [6]. Therefore, the data were analysed using the coupled-reaction-channel (CRC) method. The entrance channel potential was calculated with the microscopic complex JLM [8] nucleon-nucleus potential, using the no-core shell model (NCSM)  $^8\text{He}$  g.s. densities [9]. Including explicitly the coupling to the (p,d) reaction channel, the elastic scattering is well reproduced [6]. From the coupled-channels Born approximation (CCBA) analysis [7] the spectroscopic factor for neutron pick-up to the  $^7\text{He}_{\text{gs}}$  was  $C^2S = 4.4 \pm 1.3$ ; through the improved continuum discretized CC analysis the best fit gave  $C^2S = 3.3$  [6]. Moreover, strong coupling effects from the pick-up reaction (p,d) to the elastic scattering  $^8\text{He}(p,p)$  were observed. A CC analysis using microscopic potentials and explicit coupling to the (p,d) channel has demonstrated its ability to reproduce both elastic and (p,d) data (Fig. 1).

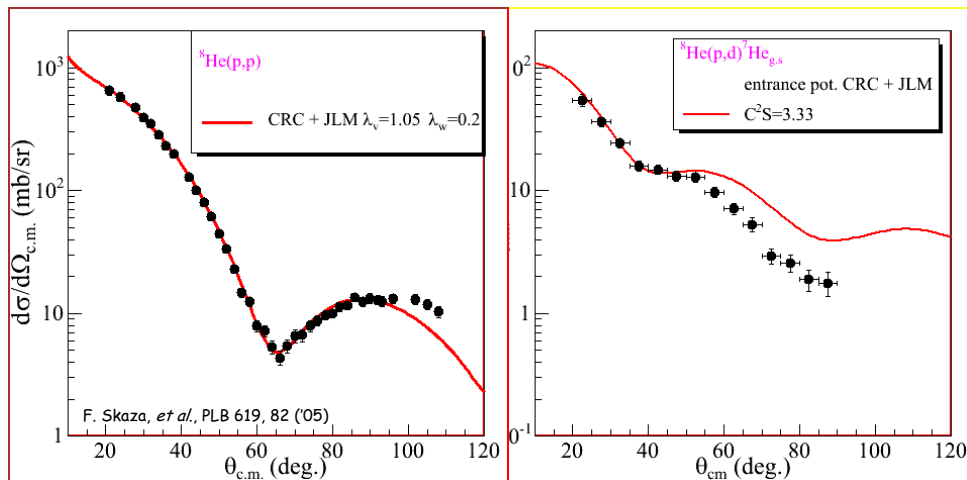


Figure 1:  $^8\text{He}(p,p)$  elastic and  $^8\text{He}(p,d)^7\text{He}$  transfer reaction at 15.7 A.MeV.

Including also the (p,t) channel in the coupled reaction scheme, with the (p,p) and (p,d), the whole set of reactions were reproduced [10].

### Resonant states in ${}^7,8\text{He}$

The  ${}^7\text{He}$  [7] and  ${}^8\text{He}$  [11] excitation energy spectra were extracted by the missing mass method from the  ${}^8\text{He}(p,d)$  and  $(p,p')$  reactions, respectively. We found the ground state (g.s.) at 0.36 MeV above the  ${}^6\text{He} + n$  threshold, with a width of  $0.17 \pm 0.05$  MeV, and a broad resonance at  $2.9 \pm 0.1$  MeV ( $\Gamma = 2.1(8)$  MeV), which is consistent with the values obtained in the first measurement of the  ${}^8\text{He}(p,d)$  reaction at Riken [12]. Another excited resonant state at  $E^* = 0.9 \pm 0.5$  MeV (1.3 MeV above threshold) with a width  $\Gamma = 1.0(9)$  MeV was indicated, and found consistent with the results of GSI [13]. This low-lying state is predicted in most studies to be a  $1/2^-$  but expected at higher energies. Even if it could not be extracted with enough statistics in the present work, this state was not excluded by our data, and it is in contrast with the conclusions from [14] based on the observation of the IAS of  ${}^7\text{He}$  in  ${}^7\text{Li}$ . The existence of this state at low energy is a controversial topic both on experimental and theoretical point of views [15].

From the  $(p,p')$  analysis, the characteristics of the first two resonant excited states of  ${}^8\text{He}$  were extracted: the first  $2^+$  is obtained at  $3.62 \pm 0.14$  MeV (width  $0.3 \pm 0.2$  MeV), consistent with the values given in [2] and a second state was found at  $5.4 \pm 0.5$  MeV (width  $0.3 \pm 0.5$  MeV) [11]. The values for the first  $2^+$  state are consistent with the previous data obtained by  $(p,p')$  [2], by multi-nucleon transfer [16,17] or break-up [18] reactions, and in contrast with the data in [19].

The resonances predicted by various theories, like the ab-initio calculations [20] or the ab-initio NCSM [9] overestimate our results. In models including the particle continuum effects, like the continuum shell model [21], the predictions for the 2 resonant states are consistent with our data.

## 4. [Conclusion and prospective](#)

The results obtained in the case of  ${}^8\text{He}$  are important for future structure studies: they demonstrate the need for a complete data set of direct reactions in order to understand the coupled-channel effects between elastic, inelastic and transfer reactions. This is a necessary step to be able to investigate the structure of weakly bound nuclei. The same features can be expected throughout the nuclear chart, and particularly for neutron-rich nuclei with low particle threshold and continuum states close to the ground state.

The measured resonances for  ${}^7,8\text{He}$  can be used as benchmarks for the most recent structure models developed for the light nuclei. They are found to be better described in the theories including explicitly the continuum-coupling effects.

The search for the low-lying resonant states of  ${}^6\text{He}$  via the  ${}^8\text{He}(p,t)$  reaction at 15.7 A.MeV will be the goal of the E525S experiment, to be done at GANIL in March-April 2007. To improve efficiency, angular coverage and resolution, the new Si-strip telescope array MUST2 has been developed recently in a DAPNIA-IN2P3-GANIL collaboration. We will benefit from the large angular coverage of 5 MUST2 detectors which will be used to detect the He ejectiles at forward angles, in coincidence with the light particles (p,d,t).

For the next step, we plan to study the evolution of neutron excitations in neutron-rich Ne, Ar, Se and Kr isotopes, and also inspect the behaviour of the neutrons in the vicinity of the expected neutron shell gaps, by measuring the cross sections of (p,p'), (p,d), and (d,p) reactions with beams produced by the SPIRAL facility. The experimental program will require beams of  $^{27-28}\text{Ne}$ ,  $^{46-48}\text{Ar}$ , and  $^{84-86}\text{Se}$ ,  $^{88-92}\text{Kr}$ . For a complete spectroscopy, it would be desirable to couple VAMOS and EXOGAM to MUST2. Information on unbound states is only given by the additional proton detection. However, such a measurement can only be performed with a thin target, and beam intensities of at least few  $10^4$  pps are required.

## 5. [References](#)

- [1] A. Lagoyannis et al., Phys. Lett. B518, 27 (2001)
- [2] A.A. Korshennikov et al., Phys. Lett. B316, 38 (1993)
- [3] S. Ottini et al., NIM A431, 476 (1999)
- [4] The MUST collaboration, NIM A421, 471 (1999)
- [5] F. Skaza, PhD Thesis University of Paris-Sud, Orsay, DAPNIA-04-13-T, (2004)
- [6] F. Skaza et al., Phys. Lett. B619, 82 (2005)
- [7] F. Skaza et al., Phys. Rev. C 73, 044301 (2006)
- [8] J.-P. Jeukenne, A. Lejeune, and C. Mahaux, Phys. Rev. C16, 80 (1977)
- [9] P. Navrátil and W.E. Ormand, Phys. Rev. Lett. 88, 152502 (2002); P. Navrátil, private communication
- [10] N. Keeley et al., Phys. Lett. B646, 222 (2007)
- [11] F. Skaza et al., Proceedings of the 2<sup>nd</sup> International Conference "Collective Motion in Nuclei under Extreme Conditions" COMEX2, Sankt Goar, Germany June 2006. Nucl. Phys A788, 260 (2007)
- [12] A. A. Korshennikov et al., Phys. Rev. Lett. 82, 3581 (1999)
- [13] M. Meister et al., Phys. Rev. Lett. 88, 102501 (2002)
- [14] G.V. Rogachev et al., Phys. Rev. Lett. 92, 232502 (2004); P. Boutachkov et al., Phys. Rev. Lett. 95, 132502 (2005)
- [15] D. Halderson, Phys. Rev. C 70, 041603(R) (2004)
- [16] H.G. Bohlen et al., Prog. Part. Nucl. Phys. 42, 17 (1999)
- [17] W. von Oertzen, Nucl. Phys. A588, 129c (1995)
- [18] T. Nilsson et al., Nucl. Phys. A583, 795 (1995)
- [19] K. Markenroth et al., Nucl. Phys. A679, 462 (2001)
- [20] S. C. Pieper, R. B. Wiringa, and J. Carlson, Phys. Rev. C70, 054325 (2004)
- [21] A. Volya and V. Zelevinsky, Phys. Rev. Lett. 94, 052501 (2005)

# E406S Study of extremely neutron-rich light nuclei with a new technique

M. Caamaño<sup>2</sup>, D. Cortina-Gil<sup>1</sup>

C. E. Demonchy, B. Jurado, W. Mittig, F. Rejmund, M. Rejmund, P. Roussel-Chomaz, H. Savajols<sup>2</sup>

M. Chartier, B. Fernandez, M. B. Gomez Hornillos<sup>3</sup>

A. Gillibert, A. Obertelli<sup>4</sup>

O. Kiselev<sup>5,6</sup>

R. Lemmon<sup>7</sup>

R. Wolski<sup>8</sup>

1) Dept. of Particle Physics, Universidade de Santiago de Compostela, E-15782 Santiago de Compostela, Spain

2) GANIL, CEA/DSM - CNRS/IN2P3, BP 55027, F-14076 Caen Cedex 5, France

3) Oliver Lodge Laboratory, University of Liverpool, Liverpool L69 7ZE, United Kingdom

4) CEA Saclay, DSM/DAPNIA/SPhN, F-91191 Gif-sur-Yvette, France

5) Institut für Kernchemie, Universität Mainz, D-55128 Mainz, Germany

6) St. Petersburg Nuclear Physics Institute, 188350 Gatchina, Russia

7) CCLRC Daresbury Laboratory, Daresbury, Warrington WA4 4AD, United Kingdom

8) H. Niewodniczański Institute of Nuclear Physics, 152 31-342 Cracow, Poland

Contact person: [savajols@ganil.fr](mailto:savajols@ganil.fr)

## 1. Key question and initial goals

A major goal in nuclear physics is to understand how nuclear stability and structure arise from the underlying interaction between individual nucleons. Systematic measurements of exotic nuclei not found in nature are a valuable tool to test the present models, which are mainly based on properties of stable nuclear matter, and check the validity of their predictions extended to exotic nuclei. Recent developments in the production of radioactive beams, as ISOL and In-Flight techniques, bring new opportunities to study these nuclei. The study of resonances beyond the drip lines, the limits in number of neutrons and protons able to form a bound system, is relatively accessible for neutron-rich light nuclei, such as hydrogen and helium, where the limit is reached with the addition of only a few neutrons to the stable isotopes.

From the theoretical point of view, the case of light nuclei is particularly interesting because the low number of nucleons involved allows various descriptions which can be compared with experimental results and extract valuable conclusions. Calculations in “ab-initio” approaches [1,2], which are based on realistic nucleon-nucleon interaction, showed that three-body interactions are important and necessary to be included in the descriptions. In other approaches, the loosely bound character of these nuclei was the base for a core coupled to individual nucleons [3], or cluster structures [4,5]. Coupling to continuum becomes also important [6] and hyperspherical functions methods resulted to be successful in this region [7,8].

The experimental search in the hydrogen isotopic for isotopes heavier than tritium started more than 30 years ago [9]. However, the map of the super-heavy hydrogen isotopes is presently far from being complete. Whereas experiments have reported the existence of  $^4\text{H}$ ,  $^5\text{H}$  and  $^6\text{H}$  as resonances [10–14], their fundamental properties are not unambiguously determined. In this situation, the searching for a new component of the isotopic chain aims to complete important systematics, such as the evolution of the binding energy with the number of neutrons. Moreover, the confirmation of the existence of  $^7\text{H}$  would reveal the nuclear system with the most

extreme neutron to proton ratio presently reached, with  $N/Z = 7$ , and the last member of the hydrogen isotopic chain.

Recent results from some of these approaches have predicted the existence of the  ${}^7\text{H}$  resonance with a resonance energy above the  $3\text{H}+4\text{n}$  mass varying from around 1 MeV in a Hyperspherical Basis approach [7] up to 7 MeV in an Antisymmetrized Molecular Dynamics calculation [1]. In parallel, experimental studies performed by Korshennikov et al. [15] show a sharp increase in the  $p({}^8\text{He},pp)$  channel close to the  $3\text{H}+4\text{n}$  disintegration threshold, interpreted as a first tentative evidence of the existence of  ${}^7\text{H}$  as a low lying resonance. Our work is a major step in this direction and represents a clear experimental proof of the existence of  ${}^7\text{H}$  as a nuclear system along its characterisation as a resonance.

## 2. Experiment set-up

The experiment was performed at GANIL (France) using the SPIRAL facility based on the Isotope Separation On Line (ISOL) technique [16] of beam production. A secondary beam of  ${}^8\text{He}$  at 15.4 A MeV, with an intensity of  $10^4$  pps, was produced using a primary  ${}^{13}\text{C}$  beam on a thick  ${}^{12}\text{C}$  target. The  ${}^7\text{H}$  system was then studied via the  ${}^{12}\text{C}({}^8\text{He}, {}^7\text{H} \rightarrow {}^3\text{H} + 4\text{n}){}^{13}\text{N}$  transfer reaction.

The experimental set-up used in the present experiment detected the charged particles involved in the reaction using the active-target MAYA [17], which is specially well suited for detecting reaction products in a very low energy kinematic domain. This detector is a Time-Charge Projection Chamber where the detection gas plays also the role of reaction target. The beam particles and the reaction products ionise the gas along their paths. The electrons released in the ionisation process drift toward the amplification area where they are accelerated around a plane of amplification wires after traversing a Frisch grid. The accelerated electrons ionise again the surrounding gas inducing a mirror charge in the pads of a segmented cathode placed below the wires.

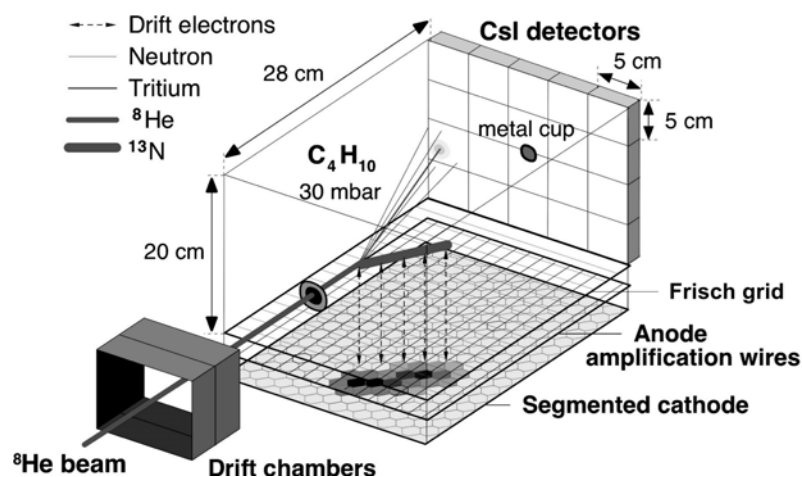


Figure 1: Experimental set-up.

Measurements of the drift time and the charge induced on the segmented cathode enable a complete 3-dimensional tracking of those reaction products that lose enough energy to be detected. A segmented wall of twenty cesium-iodide (CsI) crystals placed at forward angles detects those particles that do not stop inside the

gas volume. The detection of a charged particle in any CsI detector was used for triggering the acquisition during the experiment. Two drift chambers located before MAYA are used as beam monitors. The non-reacting projectiles are stopped in a small metal cup at the end of MAYA. Figure 1 shows a schematic view of the experimental set-up.

### 3. Results and achievements

In a typical event where  ${}^7\text{H}$  is produced, a  ${}^8\text{He}$  projectile enters in the detector and transfers one proton to the nucleus of a  ${}^{12}\text{C}$  atom of the gas,  $\text{C}_4\text{H}_{10}$  at 30 mbar, which corresponds to a target thickness of  $3.2 \cdot 10^{19} \text{ }^{12}\text{C}/\text{cm}^2$ . The scattered  ${}^7\text{H}$  decays immediately into  ${}^3\text{H}$  with relatively high energy and four neutrons. The first step in the selection of the  ${}^{12}\text{C}({}^8\text{He}, {}^7\text{H} \rightarrow {}^3\text{H} + 4n){}^{13}\text{N}$  channel consists in the coincident identification of the charged reaction products, tritium and nitrogen. The triton is stopped in the segmented CsI wall and identified via the relation between the total energy and the fast component of the CsI signal output, which is sensitive to the mass and charge of the particle [18] (see Fig. 2). The nitrogen recoil, with a total energy between 3 and 15 MeV, corresponding to ranges between 40 and 160 mm, is stopped inside the detector. The range and angle are measured using the charge image projected on the segmented cathode, with typical uncertainties of  $\pm 2$  mm and  $\pm 5$  deg respectively. The identification of the recoil is done by means of the relation between the measured range and the deposited charge, which is a function of the total energy when the recoil is completely stopped inside the gas. The nitrogen total energy is then calculated from the measured range using the available code SRIM [19]. Figure 2 shows the selection of nitrogen among other recoil species by means of their different range over charge ratios. The largest peak corresponds to carbon isotopes mainly coming from elastic reactions. Higher range over charge ratios are populated with isotopes with lower charges, such as boron isotopes produced in  ${}^{12}\text{C}({}^8\text{He}, {}^x\text{Li}){}^{20-x}\text{B}$  reactions. The right peak is populated with charges greater than carbon. In the present case the largest recoil charge detected in coincidence with any particle in the CsI wall corresponds to Nitrogen isotopes. The inner grey histogram shows in Fig. 2 the distribution conditioned to the identification of a triton in the CsI wall. Counts corresponding to carbon isotopes still remain after the condition, possibly due to helium contamination in the triton identification and three-body reaction channels. However the good separation in the carbon and nitrogen identification after the triton coincidence allows avoiding contributions from these channels. The different 1p-xn transfer reaction channels producing  ${}^3\text{H}$  and a nitrogen recoil are separated afterwards by their different kinematics. Contributions from other reaction channels, such as fusion-evaporation, are eliminated with the coincident detection of a single recoil, identified as nitrogen, and a single scattered particle in the CsI wall, identified as a triton with relatively high energy.

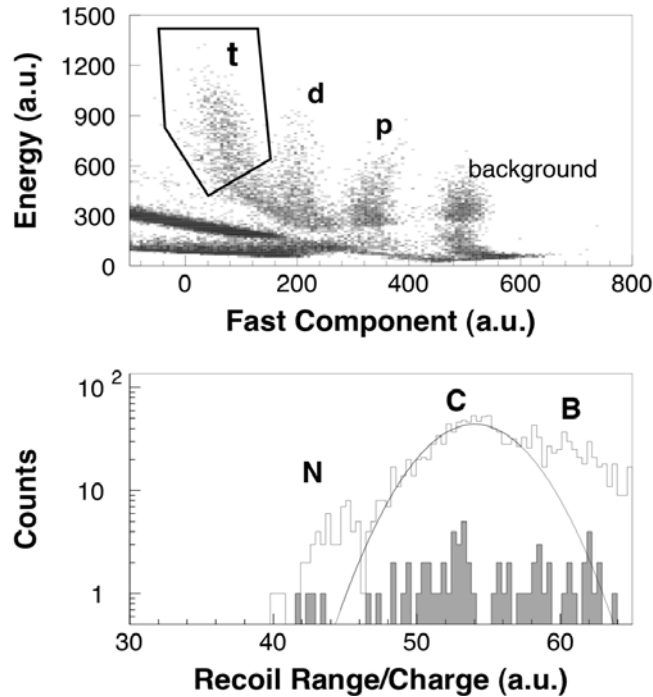


Figure 2: Triton and nitrogen identification.

The  $^{12}\text{C}(^8\text{He}, ^7\text{H})^{13}\text{N}$  one-proton transfer is a binary reaction with two particles in the final state. Conservation of energy and momentum allows reconstructing the reaction kinematics from the information of only one of the reaction products. In the present work, the reconstruction is done with the nitrogen recoil angles and energies measured with the 3-dimensional tracking of MAYA. The kinematic information can be reduced to the excitation energy of the  $^7\text{H}$  system applying a missing mass calculation. The excitation energy is then defined as the difference between the calculated mass of the  $^7\text{H}$  system with respect to the reference  $^3\text{H}+4\text{n}$  sub-system mass.

The identification of the  $^7\text{H}$  events is done after the identification of the events corresponding to other reaction channels with  $^3\text{H}$  and nitrogen as products, such as  $^6\text{H}$  and  $^5\text{H}$ . Upper panel in Fig. 3 shows the excitation energy distribution corresponding to  $^5\text{H}$  production. This is calculated assuming that the detected nitrogen is  $^{15}\text{N}$  and the sub-system mass is  $^3\text{H}+2\text{n}$ . Those events marked as a grey histogram lie on a region defined by the width of the  $^5\text{H}$  resonance and centred in its energy, according to previous experiments [12,13], and they are associated to the  $^5\text{H}$  channel. Middle panel shows the excitation energy distribution corresponding to  $^6\text{H}$  production. The calculation was done assuming the detected nitrogen as  $^{14}\text{N}$  and a  $^3\text{H}+3\text{n}$  subsystem mass. The events in the peak marked as a grey histogram are different from those associated with  $^5\text{H}$  and lie on the region also defined by the  $^6\text{H}$  resonance width and energy observed in previous experiments [14]. These events correspond to the  $^6\text{H}$  channel. Finally, the lower panel shows the excitation energy distribution assuming the detected nitrogen as  $^{13}\text{N}$  and the sub-system mass as  $^3\text{H}+4\text{n}$ . The events lying on the peak marked in grey around the  $^3\text{H}+4\text{n}$  disintegration threshold are different from those previously associated to  $^5\text{H}$  and  $^6\text{H}$  channels. In addition, other reactions produced in the present experimental set-up, such as fusion-evaporation, are estimated to populate the kinematic region of the  $^7\text{H}$  with less than one count after the  $^3\text{H}$ +nitrogen selection. Estimations on the six-body  $^{13}\text{N}+^3\text{H}+4\text{n}$

phase-space of the  ${}^7\text{H}$  channel, and phase space associated with  ${}^6\text{H}$  and  ${}^5\text{H}$  channels result in a background contribution, which begins to be appreciable around -10 MeV below the  ${}^3\text{H}+4n$  threshold. Under these considerations those events located in the marked region are identified as  ${}^7\text{H}$  production reactions, resulting in seven events among the total data. The peaked distribution is a signature of a well-defined state and represents a background free confirmation of the production of the  ${}^7\text{H}$  resonance.

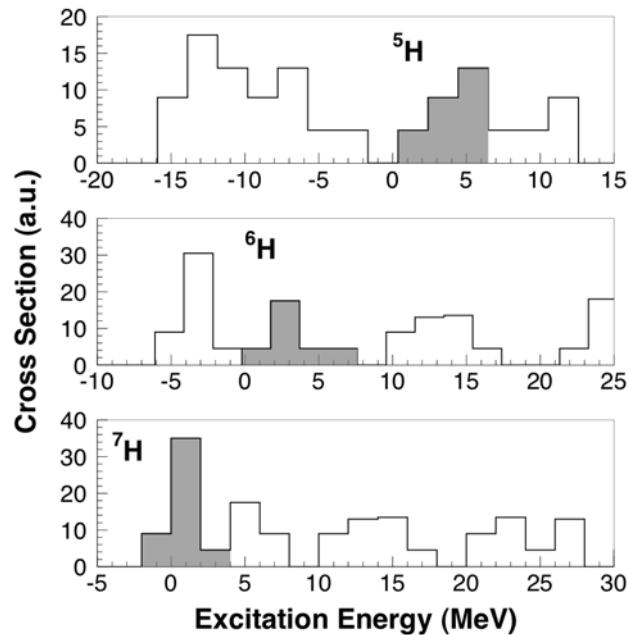


Figure 3: Identification of  ${}^5\text{H}$ ,  ${}^6\text{H}$  and  ${}^7\text{H}$  reaction channels.

The low lying character of the resonance allows to detect some events very close to the  ${}^3\text{H}+4n$  decay threshold, which then may appear at negative energies due to the uncertainty in the excitation energy reconstruction. The cross section of the  ${}^7\text{H}$  production was determined as the number of detected  ${}^7\text{H}$  events normalized to the number of incident projectiles and target nuclei. This calculation is corrected by the efficiency of the detection system. A mean differential cross section of  $d\sigma/d\Omega = 40.1 +58.0 -30.6 \mu\text{b}/\text{sr}$ , was obtained within the angular coverage of MAYA, calculated as  $9.7 - 48.2 \text{ deg}$  in the centre of mass frame.

The peak in excitation energy corresponding to the production of  ${}^7\text{H}$  (Fig. 4) is described in this work with a modified Breit-Wigner distribution [20], where the production cross-section depends on the excitation energy through the resonance energy and width. The formula includes a modification factor of the width, proportional to the square of the energy, to take into account energy dependence of the system barrier.

The Breit-Wigner function is fitted to the experimental values of the excitation energy using a multiparametric Maximum Likelihood procedure, which is especially suited to low statistics samples.

The total likelihood is calculated in an event-by-event basis, multiplying the individual contributions. Each event contributes to the total Likelihood as a Gaussian function centred in the measured excitation energy and with a variance equal to its calculated uncertainty, convoluted and normalized with the Breit-Wigner distribution.

The energy and width of the resonance are scanned until the maximum Likelihood is found. The uncertainty associated to each event is mainly dominated by the tracking reconstruction process, resulting in an average value of 2.5 MeV. The contribution of the estimated uncertainty is reflected in the error bars associated to the resonance width calculated by the Likelihood procedure.

The fitted parameters result in a width of  $0.09 +0.94 -0.06$  MeV, and a resonance energy of  $0.57 +0.42 -0.21$  MeV above the threshold of the  ${}^3\text{H}+4\text{n}$  sub-system. In Fig. 4 with the fitted Breit-Wigner distribution is displayed over the excitation energy distribution of the  ${}^7\text{H}$  detected events.

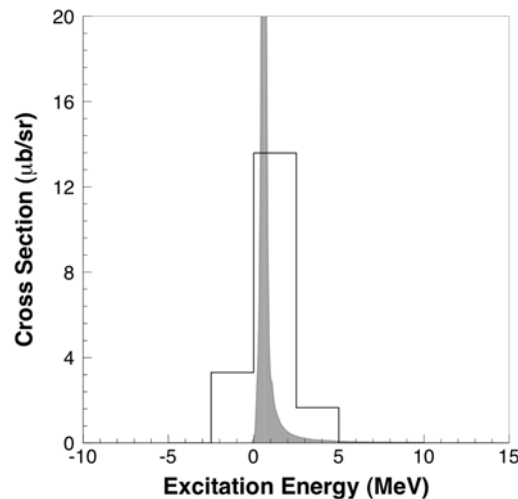


Figure 4: Experimental and calculated  ${}^7\text{H}$  resonance peak.

#### 4. [Conclusion and prospective](#)

The previous experimental observation of Korshennikov et al. [15], where a sharp increase of the cross section appeared close to the  ${}^3\text{H}+4\text{n}$  threshold, is in qualitative agreement with the resonance energy evaluated in this work. Regarding theoretical descriptions, calculations based on a Hyperspherical Functions Method applied on a shell model basis are closest to the present work [7,8], even though the predicted resonance energies range between 1 MeV [7] and 3 MeV [8]. In any case, it is difficult to conclude that this is the appropriate description due to the lack of predictions for  ${}^7\text{H}$  from other approaches. Estimations of the width of the resonance were also done in a work of Golovkov et al. [21] resulting in a theoretical width around three orders of magnitude lower than the present work. The resonance width is related to the decay rate and it contains information about the decay mechanism. The resulting narrow width extracted in this work may be a hint of a fast and unique four-neutron decay [15,22]. Future studies of the  ${}^7\text{H}$  nuclear state structure may result in more information about a possible 4-neutron cluster, also interesting for the current discussion about the existence of tetra-neutron ( $4\text{n}$ ) state [23,24].

The present results constitute a major step forward in the existence of the most exotic nuclear systems ever found, showing that nuclear matter with  $N/Z$  up to 6 can still exist, and they provide essential input for developing theoretical descriptions and improving in general our understanding of nuclear matter.

## 5. References

- [1] S. Aoyama and N. Itagaki, Nucl. Phys. A738, 362 (2004)
- [2] P. Navrátil, J. Vary, and B. Barrett, Phys. Rev. Lett. 84, 5728 (2000)
- [3] G. Blanchon, A. Bonaccorso, and N. Vinh Mau, Nucl. Phys. A739, 259 (2004)
- [4] P. Descouvemont and A. Kharbach, Phys. Rev. C63, 027001 (2001)
- [5] K. Arai, Phys. Rev. C68, 034303 (2003)
- [6] A. Volya and V. Zelevinsky, Phys. Rev. Lett. 94, 052501 (2005)
- [7] N.K. Timofeyuk, Phys. Rev. C65, 064306 (2002)
- [8] N.K. Timofeyuk, Phys. Rev. C69, 034336 (2004)
- [9] E. Argan et al., Phys. Rev. Lett. 9, 405 (1962)
- [10] A.V. Belozyorov et al., Nucl. Phys. A460, 352 (1986)
- [11] S.I. Sidorchuk et al., Phys. Lett. B594, 54 (2004)
- [12] M. Meister et al., Phys. Rev. Lett. 91, 162504 (2003)
- [13] A.A. Korsheninnikov, M. S. Golovkov, and I. Tanihata, Phys. Rev. Lett. 87, 092501 (2001)
- [14] D. Aleksandrov et al., Sov. J. Nucl. Phys. 39, 323 (1984)
- [15] A.A. Korsheninnikov et al., Phys. Rev. Lett. 90, 082501 (2003)
- [16] A.C.C. Villari et al., Nucl. Phys. A588, 267c (1995)
- [17] W. Mittig et al., Nucl. Phys. A722, 10c (2003)
- [18] G.F. Knoll, Radiation Detection and Measurement (J. Wiley and sons, Inc., 1989)
- [19] J.F. Ziegler (2005), <http://www.srim.org>
- [20] G. Breit and E. Wigner, Phys. Rev. 49, 519 (1936)
- [21] M.S. Golovkov, Phys. Lett. B588, 163 (2004)
- [22] A. A. Korsheninnikov, Nucl. Phys. A751, 501c (2005)
- [23] F.M. Marquès et al., Phys. Rev. C65, 044006 (2002)
- [24] S.C. Pieper, Phys. Rev. Lett. 90, 252501 (2003)



## E408S

# Competition between octupole and multi-particle excitations in $^{212}\text{Po}$ and $^{213}\text{At}$

P.M. Walker, Zs. Podolyak, A.B. Garnsworthy, N.J. Thompson, S.J. Williams, H. Mach, G. de France, G. Sletten, F. Azaiez, K. Andgren, A.M. Bruce, A.P. Byrne, W.N. Catford, J.M. Casandjian, B. Cederwall, D.M. Cullen, Z. Dombradi, G.D. Dracoulis, L.M. Fraile, S. Franchoo, H. Fynbo, M. Gorska, G.A. Jones, B. McGuirk, Y. Kopatch, G.J. Lane, S. Mandal, L. Milechina, J. Molnar, C. O'Leary, E.S. Paul, W. Plociennik, V. Pucknell, P. Raddon, N. Redon, B. Rosse, R.J. Senior, E. Ruchowska, M. Stanoiu, O. Tengblad, C. Wheldon and R. Wood

Surrey, GANIL, Uppsala, Copenhagen, Orsay, Stockholm, Manchester, Debrecen, ANU, Madrid, CERN, Aarhus, GSI, York, Swierk, Daresbury, Lyon, Brighton, Liverpool

Contact person: [walker@surrey.ac.uk](mailto:walker@surrey.ac.uk)

### 1. Key question and initial goals

The objective was to study the high-spin excited states of the nuclides  $^{212}\text{Po}$  and  $^{213}\text{At}$ , using a  $^8\text{He}$  beam on  $^{208}\text{Pb}$  and  $^{209}\text{Bi}$  targets, and thereby to learn about the development of collectivity in nuclides with a few neutrons and protons outside the  $^{208}\text{Pb}$  doubly magic core. The primary experimental focus was to improve the knowledge of the level structure on  $^{212}\text{Po}$ , using the  $^{208}\text{Pb}(^8\text{He},4n)$  reaction. This builds on the earlier work of Poletti et al. [1], who used an incomplete-fusion reaction with a  $^9\text{Be}$  beam. The neutron-rich location of  $^{212}\text{Po}$  makes experimental access very difficult.

### 2. Experiment set-up

The experiment initially formed part of the commissioning of the new EXOGAM gamma-ray detector array at SPIRAL [2]. It was cut short by a SPIRAL target failure. The second scheduled beam time yielded new spectroscopic results for  $^{212}\text{Po}$  [3]. However, the results were less extensive than hoped for. This was due to a failure to implement the  $^8\text{He}$  beam detector.

### 3. Results and achievements

Much was learnt about running a radioactive-beam, fusion-evaporation experiment. Sample spectra are shown in Fig. 1, and the updated level structure of  $^{212}\text{Po}$  is shown in Fig. 2, based on ref. [1], with the addition of the 69.4 and 182.8 keV transitions. The full yrast sequence up to the  $18^+$  isomer is now reasonably well established, but we have not been able to find higher levels. Further details are given in refs [2,3].

### 4. Conclusion and prospective



## 5. References

- [1] A.R. Poletti et al., Nucl. Phys. A473, 595 (1987)
- [2] Zs. Podolyak et al., Nucl. Inst. Meth. Phys. Res. A511, 354 (2003)
- [3] A.B. Garnsworthy et al., J. Phys. G31, S1851 (2005)



# Deep Inelastic collisions induced by neutron rich beams from SPIRAL and in beam gamma spectroscopy using EXOGAM

F. Azaiez<sup>1</sup>  
G. Benzoni<sup>2</sup>

1) IPN Orsay, IN2P3-CNRS, Université Paris-Sud, F-91406 Orsay, France

2) Università degli Studi e INFN sezione di Milano, Via Celoria 16, I-20133 Milano, Italy

Contact person: [azaiez@ipno.in2p3.fr](mailto:azaiez@ipno.in2p3.fr)

## 1. Key question and initial goals

Study of the deep inelastic reaction mechanism employing radioactive beams. For this purpose a beam of  $^{24}\text{Ne}$  has been selected and shoot over a  $^{208}\text{Pb}$  target. Reaction products were detected and selected in the VAMOS spectrometer in coincidence with prompt gamma radiation measured in the EXOGAM array.

The availability at SPIRAL of the ensemble VAMOS-EXOGAM is unique in the world for the study of multi nucleon transfer reactions with radioactive beams. This reaction mechanism is thought to be a possibility at SPIRAL2 of populating more exotic nuclei for the study of their structure.

## 2. Experiment set-up

VAMOS spectrometer coupled to the EXOGAM array. VAMOS consisted of standard detectors: 2 position sensitive drift chambers, the ionisation chamber and the Si wall consisting of 21 silicon detectors. The SeD detector, even if installed and working was found to be only 20% efficient for light ions. 11 EXOGAM detectors were used in this experiment, two of which not equipped with anti-Compton shields.

No major problem was found during the beam time and in the data analysis.

## 3. Results and achievements

7 days of  $^{24}\text{Ne}$  (190 MeV) at an average intensity of  $2 \cdot 10^5$  pps allowed to collect  $\sim 10^3$  ion-gamma coincidences, mainly due to Ne ions close to the beam ( $^{23-25}\text{Ne}$ ). The population of F and O isotopes has been confirmed by the corresponding gamma spectra. Selectivity in the population of states of different nature (single particle vs. collective) has been observed and is under further investigation. Precise cross section determination is also under analysis.

## 4. Conclusion and prospective

It appeared that in order to get absolute cross-sections and to firmly establish the selectivity of single particle states of such reactions, a measurement of the response function of VAMOS (both angular acceptance and momentum acceptance) should be measured. The collaboration is therefore hoping to get some beam time (with stable beams) in order to achieve this important measurement.

## 5. [References](#)

Proceedings of the "International conference on Reaction Mechanisms and Nuclear Structure at the Coulomb barrier - FUSION06"; AIP853, 49 (2006)  
In print in EPJ, Proceeding of the "7<sup>th</sup> international conference on Radioactive Nuclear Beams - RNB7"



The excitation energy spectrum in the 4n system deduced from the  ${}^6\text{Li}$  energy and angle is represented on Fig. 1. This spectrum is gated by the detection of at least one neutron in plastic detectors placed in the forward direction. Counts observed below the  $\alpha+4n$  threshold can be accounted for the background originated from  ${}^{12}\text{C}$  in the  $\text{CD}_2$  target. Namely, no bound tetra-neutrons are observed in the limits of the statistics. Above the  $\alpha+4n$  threshold, a smooth increase of the cross-section is observed. The data cannot be satisfactorily reproduced by a pure 5-body phase-space calculation, which represents a clear evidence of correlations between the 4 neutrons in the exit channel. These correlations have been investigated using simple simulations of 2n-2n interaction in the final-state. More sophisticated analysis is to be done in the near future.

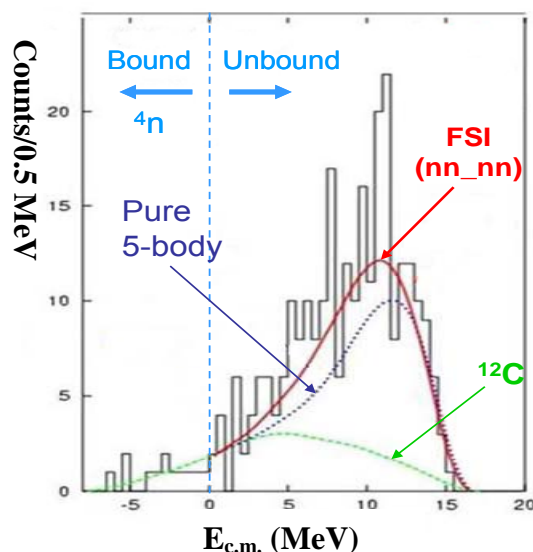


Figure 1: Excitation energy spectrum in the 4n system reconstructed from the  ${}^6\text{Li}$  particles and gated by the plastic detectors. The blue dotted line and the red line represent respectively a pure 5-body phase-space spectrum and a simulation including 2n-2n correlations. The  ${}^{12}\text{C}$  contribution has been added to obtain both curves.

On the theory side, state-of-the-art quantum Monte-Carlo calculations lead to the conclusion that a bound tetra-neutron would not be compatible with our present knowledge on nuclear forces [2]. These calculations however cannot yet make reliable predictions concerning the unbound case. Recently, Faddeev method calculations could be achieved by Lazauskas and Carbonell [3] in which no resonant state was found.

#### 4. Conclusion and prospective

In conclusion, both experiment and theory seem to agree at the present time that bound four-neutron clusters do not exist. The situation is less clear concerning resonances, such state being more difficult to observe especially in the case where it would be broad.

Concerning the 4-neutron system, two-protons pickup on  ${}^6\text{He}$  nucleus can be envisaged using the intense  ${}^6\text{He}$  beam of SPIRAL. A test experiment aiming to establish the experimental method to measure this exotic reaction with a cryogenic

helium target is already scheduled. The same reaction could be used to study the 6-neutron system with the  $^8\text{He}$  beam provided that the intensity would be 1 or 2 orders of magnitudes as it is presently.

Similarly, an intense  $^8\text{He}$  (and also  $^{11}\text{Li}$ ) beam could be used to search for  $^6\text{n}$  and  $^8\text{n}$  with the MAYA active target as was recently proposed by Roussel-Chomaz and Villari in a letter of intend submitted to the GANIL PAC.

## 5. [References](#)

- [1] F.M. Marques et al., Phys. Rev. C65, 044006 (2002)
- [2] S. Pieper, Phys. Rev. Lett. 90, 252501 (2003)
- [3] R. Lazauskas and J. Carbonnel, Phys. Rev. C72, 034003 (2005)



# E442S Very High Resolution Spectroscopy of $^{19}\text{Ne}$ for Application to Astrophysics

I. Stefan<sup>2</sup>, F. de Oliveira Santos, M.G. Pellegriti, M. Fadil, S. Grévy, M. Lenhardt, M. Lewitowicz, L. Perrot, M.G. Saint Laurent, I. Ray, O. Sorlin, C. Stodel, J.C. Thomas<sup>1</sup>  
G. Dumitru, A. Buta, R. Borcea, F. Negoita, D. Pantelica<sup>2</sup>  
J.C. Angélique, M. Angélique<sup>3</sup>  
E. Berthoumieux<sup>4</sup>  
A. Coc, J. Kiener, A. Lefebvre-Schuhl, V. Tatischeff<sup>5</sup>  
J.M. Daugas, O. Roig<sup>6</sup>  
T. Davinson<sup>7</sup>  
M. Stanoiu<sup>8</sup>

- 1) GANIL, CEA/DSM - CNRS/IN2P3, BP 55027, F-14076 Caen Cedex 5, France
- 2) Institute of Atomic Physics, P.O. Box MG6, Bucharest-Margurele, Romania
- 3) Laboratoire de Physique Corpusculaire, IN2P3-CNRS, ISMRA et Université de Caen, F-14050 Caen, France
- 4) CEA Saclay, DSM/DAPNIA/SPhN, F-91191 Gif-sur-Yvette, France
- 5) CSNSM, CNRS-IN2P3, Université Paris-Sud, F-91405 Orsay, France
- 6) CEA/DIF/DPTA/PN, BP 12, F-91680 Bruyères le Châtel, France
- 7) Department of Physics and Astronomy University of Edinburgh, Edinburgh EH9 3JZ, United Kingdom
- 8) IPN Orsay, IN2P3-CNRS, Université Paris-Sud, F-91406 Orsay, France

Contact person: [oliveira@ganil.fr](mailto:oliveira@ganil.fr)

## 1. Key question and initial goals

Astrophysical motivations. Gamma-ray emission from classical novae is dominated, during the first hours, by positron annihilation resulting from the beta decay of radioactive nuclei. The main contribution comes from the decay of  $^{18}\text{F}$  (half-life of 110 minutes) and hence is directly related to  $^{18}\text{F}$  formation during the outburst. A good knowledge of the nuclear reaction rates of production and destruction of  $^{18}\text{F}$  is required to calculate the amount of  $^{18}\text{F}$  synthesized in novae and the resulting gamma-ray emission. The rate relevant for the main mode of  $^{18}\text{F}$  destruction (i.e., through  $^{18}\text{F}(\text{p},\alpha)^{15}\text{O}$ ) has been the object of many recent experiments. Despite certain progress, this reaction rate still remains badly known; the rate uncertainty is about a factor 100 in a large range of temperature. This clearly supports the need of new experimental studies to improve the reliability of the predicted gamma-ray fluxes from novae.

Very high-energy resolution. Achieving very high-energy resolution (better than 4 keV) with charged particles is an experimental challenge, and this challenge is stronger when dealing with radioactive beams.

Gas target. In our experiment, we had to develop a thin helium gas cell that can sustain intense radioactive beams and the experimental constraints (energy resolution).

## 2. Experiment set-up

The method we used to investigate the spectroscopy of the  $^{19}\text{Ne}$  nucleus is the resonant elastic scattering. At low energies, it is known that the elastic scattering shows up anomalies (resonances), which are related to the structure of the compound nucleus. In this way, the spectroscopy of  $^{19}\text{Ne}$  can be achieved by the measurement of the  $^{15}\text{O}(\alpha,\alpha)^{15}\text{O}$  reaction. We can use a silicon detector to detect the emitted alpha. Since  $^{15}\text{O}$  is radioactive, we have to measure this elastic reaction in inverse kinematics  $\alpha(^{15}\text{O},\alpha)^{15}\text{O}$  using a thin helium gas target. In fact, the excitation function is measured in one time, from the entrance energy down to the outgoing energy of the heavy ions after they have crossed the gas target. The inverse geometry and small specific energy loss of the alpha strikingly reduce the influence of the beam spread and straggling on the final resolution. This method is very well suited for secondary beams since the limited intensity is compensated by the large cross sections (several 100 mbarn/sr). From the shape of the resonances, one can obtain the angular momentum of the reaction, and finally deduce the spin assignment of the states. Another advantage in that case is that the first excited state in  $^{15}\text{O}$  is at very high energy, at 5183 keV, which means inelastic scattering contributions are forbidden. In fact, all inelastic processes producing alpha particles are totally forbidden. The energy broadening of the alpha is minimum at zero degree. At zero degree, with a very narrow angle aperture of  $1^\circ$  ( $\sim 1$  msr), using a high-energy resolution silicon surface barrier detector, with a very thin helium gas target ( $100 \mu\text{g}/\text{cm}^2$ ), we can achieve a resolution better than 4 keV in centre of mass frame, a real improvement in the spectroscopy of this nucleus.

### 3. [Results and achievements](#)

#### $\alpha(^{15}\text{O},\alpha)^{15}\text{O}$

The analysis of this reaction is still going on (the experiment was scheduled in April 2005). Unfortunately, the gas target suffered several problems, mainly a continuous change of the windows thickness due to the degradation by the beam interaction. This main problem prevented us to achieve the expected energy resolution.

#### $p(^{14}\text{N},p)^{14}\text{N}$

We performed several measurements to calibrate our silicon detector and to validate the analysis. The  $p(^{14}\text{N},p)^{14}\text{N}$  reaction was one of the reactions we used for the calibration. The results obtained for this reaction are shown in Fig. 1. We achieved a very nice resolution (better than 4 keV in CM) since we used a solid target. The R-matrix analysis (continuous line) is in perfect agreement with the data.

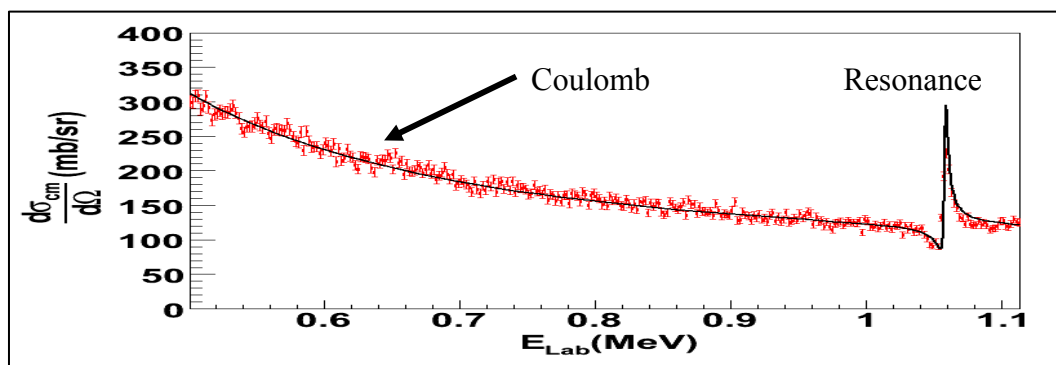


Figure 1: Excitation function for the  $p(^{14}\text{N},p)^{14}\text{N}$  reaction. A very nice resolution was obtained since a narrow resonance in  $^{15}\text{O}$  is observed at  $\sim 1.1$  MeV with a width of  $\sim 3.6$  keV.



This reaction is one of the reactions we wanted to use for the calibration, but we found new and interesting results for the unbound compound nucleus  $^{16}\text{F}$ . See Fig. 2.

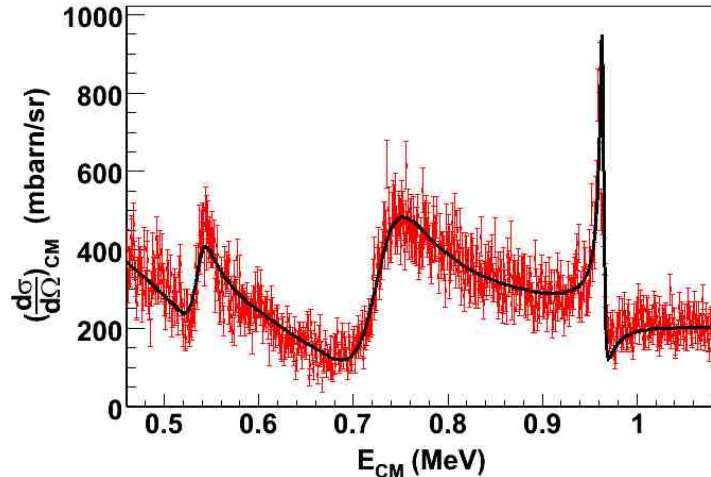


Figure 2: Excitation function for the  $p(^{15}\text{O},p)^{15}\text{O}$  reaction. Peaks correspond to states in  $^{16}\text{F}$ .

#### New reaction pathway to bypass the $^{15}\text{O}$ waiting point

We have proposed a new and very exotic process involving unbound nuclei. Using the new results obtained for  $^{16}\text{F}$ , we applied the new ideas to this case. We have proposed a new reaction pathway to bypass the  $^{15}\text{O}$  waiting point in astrophysics. It is the sequential reaction process  $^{15}\text{O}(p,\gamma)(\beta^+)^{16}\text{O}$ . This exotic reaction is found to have a surprisingly high cross section, approximately  $10^{10}$  times higher than the  $^{15}\text{O}(p,\beta^+)^{16}\text{O}$ . The large cross section can be understood to arise from the more efficient feeding of the low energy wing of the ground state resonance by the gamma decay, see Fig. 3.

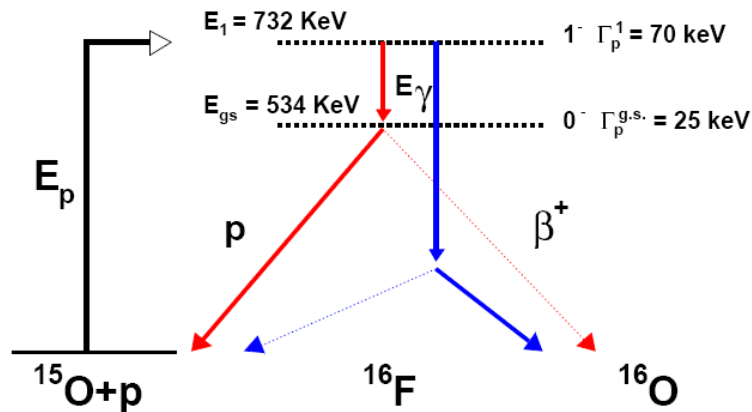


Figure 3: The new proposed reaction pathway. Red and blue lines correspond to two different gamma transitions from the first excited state to the ground state resonance of  $^{16}\text{F}$ .

#### **4. Conclusion and prospective**

In conclusion, it was not possible to achieve a high-energy resolution measurement of the resonant elastic scattering reaction  $^4\text{He}(^{15}\text{O},\alpha)^{15}\text{O}$ . This was mainly due to the fact that the thin helium gas target was not homogeneous. We measured the properties of the low-lying states in  $^{16}\text{F}$  with  $\text{H}(^{15}\text{O},\text{p})^{15}\text{O}$ , using a solid target. We applied the new results into a new reaction pathway  $^{15}\text{O}(\text{p},\gamma)(\beta^+)^{16}\text{O}$ . This reaction is very promising.

There are a lot of subjects in prospective:

- To achieve the best energy resolution (better than 100 eV?) with our method
- To develop a homogeneous helium gas target that can sustain intense beams
- To develop the (p,gamma)(beta) reaction ideas and related ideas: non exponential decay, quasi-bound unbound nucleus, test of the Heisenberg relationship etc...

#### **5. References**

Tours Symposium on Nuclear Physics VI, Tours 2006, AIP Conference Proceedings 891, to be published  
I. Stefan, PhD thesis, Univ. Caen/Basse-Normandie, 2006, GANIL T 06 02

# E443S Study of N = 16 and the sd-fp shell gap far from stability

A. Obertelli, N. Alamanos, M. Alvarez, F. Auger, R. Dayras, A. Drouart, A. Gillibert, N. Keeley, V. Lapoux, L. Nalpas, X. Mougeot, E. C. Pollacco, F. Skaza<sup>1</sup>  
G. de France, B. Jurado, W. Mittig, F. Rejmund, M. Rejmund, P. Roussel-Chomaz, H. Savajols<sup>2</sup>  
A. Pakou, N. Patronis<sup>3</sup>

1) CEA Saclay, DSM/DAPNIA/SPhN, F-91191 Gif-sur-Yvette, France

2) GANIL, CEA/DSM - CNRS/IN2P3, BP 55027, F-14076 Caen Cedex 5, France

3) Department of Physics, University of Ioannina, 45110 Ioannina, Greece

Contact person: [aobertel@cea.fr](mailto:aobertel@cea.fr)

## 1. Key question and initial goals

The evolution of shell effects with neutron excess is one of the most currently discussed topics. N = 16 has been proposed recently to be a new magic number far from stability, both from experimental and theoretical considerations. New calculations suggest an enhancement with isospin of the gap between the  $s_{1/2}$  and  $d_{3/2}$  subshells of the sd neutron shell. The attractive interaction between protons in the  $d_{5/2}$  and neutrons in the  $d_{3/2}$  subshells seems to play an important role. Then, removing protons from  $^{30}\text{Si}$  to  $^{24}\text{O}$  would make the neutron  $d_{3/2}$  subshell less bound.

More information may be obtained with the N = 17 isotones, since the study of the single particle excitations is well suited to determine the spacing between the  $d_{3/2}$  subshell and the fp shell. As a consequence of the possible shell closure at N = 16, we expect a reduction in the excitation energy of the negative parity states for N = 17 nuclei. The lowest excitation energies of the negative parity states for the most bound N = 17 isotones ( $^{35}\text{Ar}$ ,  $^{33}\text{S}$  and  $^{31}\text{Si}$ ) are high, around 3.5 MeV, reflecting the N = 20 major shell gap for stable nuclei. There is a sudden drop for  $^{29}\text{Mg}$  down to 1.5 MeV. The next N = 17 isotone is  $^{27}\text{Ne}$  for which little information are available [1]. The new  $^{26}\text{Ne}$  beam delivered by the SPIRAL facility has been used to study the single particle states in  $^{27}\text{Ne}$  with the one neutron transfer reaction  $^{26}\text{Ne}(d,p)^{27}\text{Ne}$  [2].

At the same time,  $^{27}\text{Ne}$  was also studied in RIKEN and MSU with the one neutron knockout from a  $^{28}\text{Ne}$  beam at much higher incident energy [3,4].

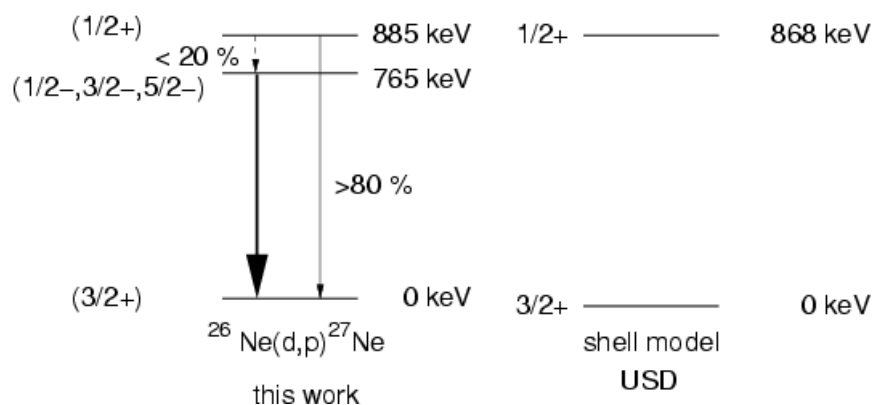
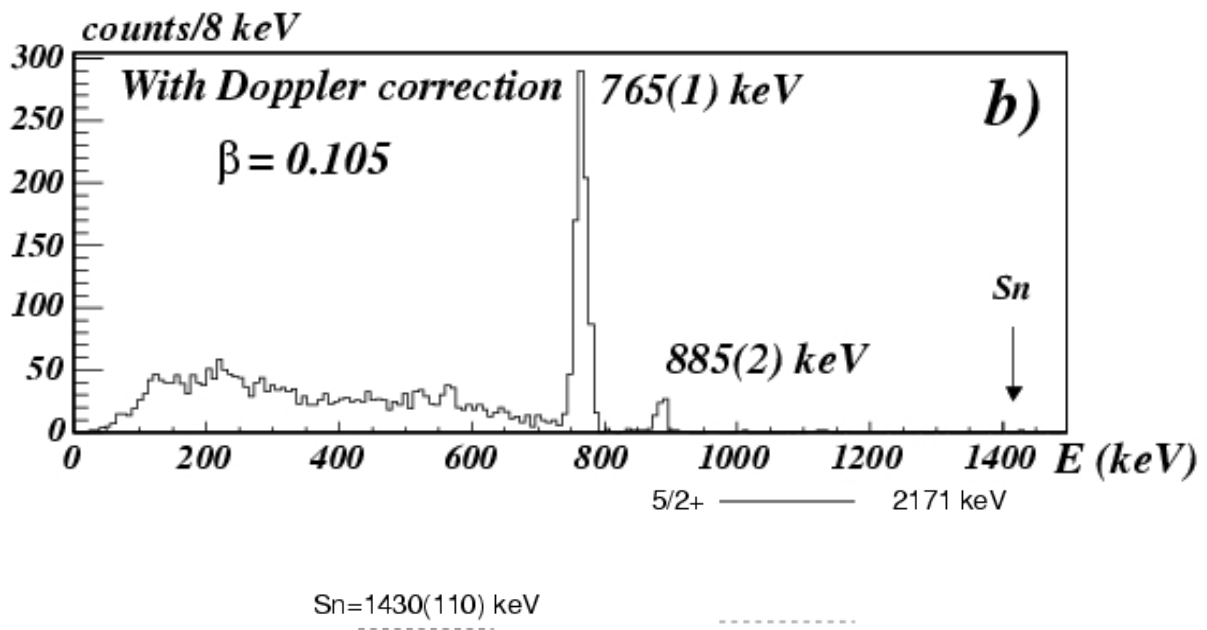
## 2. Experiment set-up

$^{26}\text{Ne}(d,p)^{27}\text{Ne}$  has been studied in inverse kinematics at 9.7 A.MeV. Due to the low intensity of the new  $^{26}\text{Ne}$  SPIRAL beam, we used a 1 mm thick cryogenic solid deuterium target, developed at GANIL. We measured coincidences between the ejectile  $^{27}\text{Ne}$  in the magnetic spectrometer VAMOS and the photons emitted in flight, detected with the EXOGAM set-up around the target.

## 3. Results and achievements

After selection of  $^{27}\text{Ne}$  and the off line Doppler correction, we obtained the following  $\gamma$  spectrum with two transitions at 765 and 885 keV. Due to the low 1n

emission threshold in  $^{27}\text{Ne}$  (1.4 MeV), the two transitions were associated to two bound states decaying directly to the ground state. USD shell model calculations predict only one positive-parity bound state below  $S_{1n}$ , a  $1/2^+$  state at 868 keV, which suggests that one of the observed states may be a negative parity state. Combining all the experimental information (cross-section, selection rules and constraints on the life time and transferred angular momentum) from the  $1n$  transfer and  $1n$  knockout experiments, we can propose a  $(1/2^-, 3/2^-)$  assignment for the 765 keV state. Recent shell model calculations including the  $fp$  subshells with a reduced  $sd$ - $fp$  shell gap predict  $7/2^-$  and  $3/2^-$  states at very low excitation energy [4], the latter being consistent with the transition we observed at 765 keV. The non-observation of the  $7/2^-$  state may be due to the slow M2 decay to the ground state.



#### 4. Conclusion and perspectives

Two bound states were observed at low excitation energy, one of them is consistent with a negative parity state in  $^{27}\text{Ne}$ . This may be understood as a reduction of the  $sd$ - $fp$  shell gap, possibly due to either a reduction of the spherical

shell gap or a deformation effect, or even both effects. The tensor interaction recently proposed in [5] could explain such an effect. The spherical sd-fp shell gap may be more directly investigated in a  $^{24}\text{O}(d,p)^{25}\text{O}$  experiment, however an increase of the  $^{24}\text{O}$  beam intensity is crucial for that goal.

## 5. [References](#)

- [1] M. Stanoiu et al., Phys. Rev. C69, 034312 (2004)
- [2] A. Obertelli et al., Phys. Lett. B633, 33 (2006)
- [3] Zs. Dombradi et al., Phys. Rev. Lett. 96, 182501 (2006)
- [4] J. R. Terry et al., Phys. Lett. B640, 86 (2006)
- [5] T. Otsuka et al., Phys. Rev. Lett. 95, 232502 (2005)



## E445S

# Transfer Study of $^{23}\text{F}$ in Inverse Kinematics

R.C. Lemmon, V.P.E. Pucknell, D.D. Warner<sup>1</sup>  
M. Chartier, B. Fernandez-Dominguez<sup>2</sup>  
T.D. Baldwin, W.N. Catford, W. Gelletly, S.D. Pain, C. Timis<sup>3</sup>  
M. Labiche, N. Amzal, M. Burns, R. Chapman, X. Liang, K. Spohr<sup>4</sup>  
N. Ashwood, N. Curtis, M. Freer<sup>5</sup>  
L. Caballero, B. Rubio<sup>6</sup>  
G. de France, M. Rejmund, H. Savajols<sup>7</sup>  
N.A. Orr<sup>8</sup>  
O. Sorlin<sup>9</sup>  
C. Thiesen<sup>10</sup>  
and The TIARA Collaboration

- 1) CCLRC Daresbury Laboratory, Daresbury, Warrington WA4 4AD, United Kingdom
- 2) Department of Physics, University of Liverpool, Liverpool L69 7ZE, United Kingdom
- 3) Department of Physics, University of Surrey, Surrey GU2 7XH, United Kingdom
- 4) The Institute of Physical Research, University of Paisley, Paisley PA1 2BE, United Kingdom
- 5) School of Physics and Astronomy, University of Birmingham B15 2TT, United Kingdom
- 6) IFIC, CSIC-Universidad de Valencia, E-46071 Valencia, Spain
- 7) GANIL, CEA/DSM - CNRS/IN2P3, BP 55027, F-14076 Caen Cedex 5, France
- 8) Laboratoire de Physique Corpusculaire, IN2P3-CNRS, ISMRA et Université de Caen, F-14050 Caen, France
- 9) IPN Orsay, IN2P3-CNRS, Université Paris-Sud, F-91406 Orsay, France
- 10) CEA Saclay, DSM/DAPNIA/SPhN, F-91191 Gif-sur-Yvette, France

Contact person: [R.C.Lemmon@dl.ac.uk](mailto:R.C.Lemmon@dl.ac.uk)

## 1. Key question and initial goals

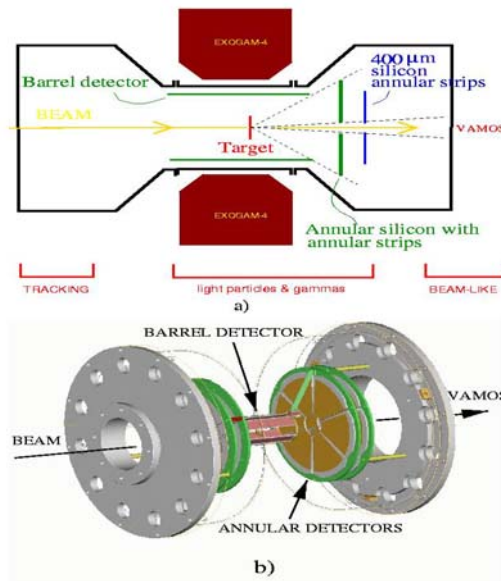
It was proposed to carry out a prototypical nucleon transfer study of  $^{23}\text{F}$  using the neutron rich beam  $^{24}\text{Ne}$ , available from the SPIRAL 1 facility. The experiment was designed to study all single-nucleon transfer reactions to/from the  $^{24}\text{Ne}$  projectile using a deuterium target. These included the  $^{24}\text{Ne}(d,p)^{25}\text{Ne}$ ,  $^{24}\text{Ne}(d,^3\text{He})^{23}\text{F}$  and  $^{24}\text{Ne}(d,t)^{23}\text{Ne}$  reactions to examine the structure of  $^{25}\text{Ne}$ ,  $^{23}\text{F}$  and  $^{23}\text{Ne}$  respectively. For example, the N=16 shell closure could be examined in  $^{25}\text{Ne}$ , the “tentative”  $1/2^-$  state in  $^{23}\text{F}$  could be populated directly by proton removal from  $^{24}\text{Ne}$  to observe its gamma-decay (500 keV) to the “missing”  $1/2^+$  state and information about the ground state of  $^{24}\text{Ne}$  could be obtained by determining its parentage in terms of  $^{23}\text{Ne}$  plus a neutron.

All of these topics address the general question of the evolution of shell structure in neutron-rich nuclei and specifically the appearance of the new shell closure at N=16. This topic is of great current interest in the international nuclear physics community and actively investigated at many laboratories worldwide.

## 2. Experiment set-up

An isotopically pure  $^{24}\text{Ne}$  beam at 10 A.MeV with an intensity of  $10^5$  pps was delivered by the SPIRAL facility. It was focused onto a self-supporting  $\text{CD}_2$  target of 1

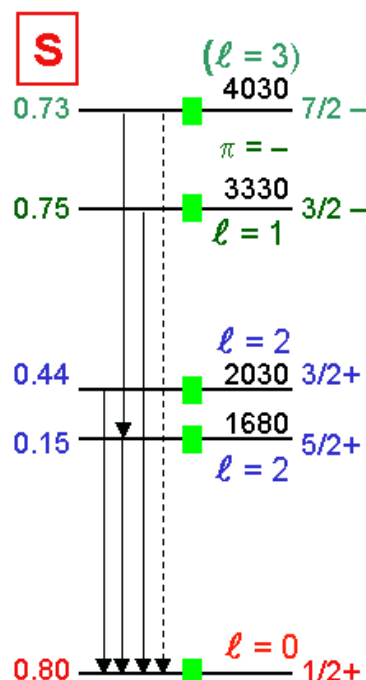
mg/cm<sup>2</sup>. The experimental set-up is shown schematically below. The principal detectors are the TIARA silicon strip array, the EXOGAM Ge array and the VAMOS magnetic spectrometer. The annular and barrel detectors of TIARA are designed to record the light (<sup>3</sup>He and t) ejectiles from transfer reactions induced on the (CD<sub>2</sub>)<sub>n</sub>



target and cover laboratory angles from 5.6° to 143°. The EXOGAM array is used in its “cube” configuration to form a compact 90° ring around the target. This is used to detect  $\gamma$ -rays emitted from the excited states populated in the transfer reaction and so ‘tag’ these states. The heavy ejectiles are detected and identified by A and Z in the VAMOS spectrometer. Fortunately, whilst there was a failure of the EXOGAM electronics and DAQ, we were able to compensate with our own electronics although this meant the loss of Ge segmentation data.

### 3. [Results and achievements](#)

The majority of our results relate to our study of the  $^{24}\text{Ne}(d,p)^{25}\text{Ne}$  reaction. The level scheme determined in the reaction for  $^{25}\text{Ne}$  is shown below, together with spectroscopic factors extracted from measured proton angular distributions. The



transfer of a neutron onto  $^{24}\text{Ne}$  to make the ground state of  $^{25}\text{Ne}$  populates the  $1s_{1/2}$  neutron orbital. The relative energy of the next orbital ( $0d_{3/2}$ , lying just above  $N=16$ ) is well measured by the energy of the  $3/2^+$  single-particle excited state. The energy of the lower,  $0d_{5/2}$  orbital can also be measured, through weak population of the  $5/2^+$  state, and the gap at  $N=20$  between the  $0d_{3/2}$  and the  $0f_{7/2}/1p_{3/2}$  orbitals is measured directly through the transfer to the  $fp$  shell. We have been able to identify the  $3/2^+$  state in  $^{25}\text{Ne}$  for the first time [5], revealing a large gap at  $N=16$ , and we also identified the negative parity  $fp$  levels for the first time and hence the closing of the energy gap at  $N=20$ . This shows the dramatic evolution from  $N=20$  being magic, to  $N=16$  instead, and cannot be explained by normal USD shell model calculations. Our gamma-ray data were crucial, to resolve and identify the states. These data in fact represent the first demonstration of the excellent capabilities of the fully operational coupling of VAMOS and EXOGAM with TIARA. The results from the  $^{24}\text{Ne}(d,t)^{23}\text{Ne}$  reaction are being finalized. Unfortunately there were insufficient statistics to analyse the  $^{24}\text{Ne}(d,^3\text{He})^{23}\text{F}$  reaction.

#### 4. [Conclusion and prospective](#)

Further results will come from our  $^{24}\text{Ne}$  experiment, for  $^{24}\text{Ne}(d,t)^{23}\text{Ne}$ . To follow up the  $^{25}\text{Ne}$ , we have proposals approved at SPIRAL to study  $^{26}\text{Ne}(d,p)^{27}\text{Ne}$  and  $^{20}\text{O}(d,p)^{21}\text{O}$  which will further clarify the  $N=20/16$  migration. TIARA will also be operated together with MUST2 on a series of approved transfer experiments at GANIL. In the longer term, TIARA itself with its high efficiency for particles and gamma rays will be an excellent tool for studying heavier nuclei and we plan to pursue this with heavier beams at SPIRAL and, in due course, with fission fragment beams from SPIRAL2, keeping to our physics goal of studying the migration of magic numbers and the changing shell structure for exotic nuclei.

#### 5. [References](#)

- [1] W.N. Catford et al., CAARI 2002, AIP Conference Proceedings 680, p. 329
- [2] W.N. Catford et al., Tours Symposium V, AIP Conference Proceedings 704, p. 185
- [3] M. Labiche et al., NUSTAR 05 Proceedings, J. Phys. G31, S1691 (2005)
- [4] M. Labiche et al., Nucl. Inst. Meth. Phys. Res. A, in preparation
- [5] W.N. Catford et al., Eur. Phys. J., A25, 245 (2005)
- [6] W.N. Catford et al., NUSTAR 05 Proceedings, J. Phys. G31, S1655 (2005)
- [7] W.N. Catford et al., Proc. 2005 Carpathian Summer School, World Scientific, in press
- [8] B. Fernandez et al., FINUSTAR 2005, AIP Conference Proceedings, in press
- [9] W.N. Catford et al., Letter in preparation



# E456S Study of the N=28 shell closure via the $^{46}\text{Ar}(d,p)^{47}\text{Ar}$ reaction

L. Gaudefroy<sup>1</sup>, O. Sorlin<sup>1,2</sup>, D. Beaumel<sup>1</sup>, Y. Blumenfeld<sup>1</sup>, Z. Dombrádi<sup>3</sup>, S. Fortier<sup>1</sup>, S. Franchoo<sup>1</sup>, M. Gélín<sup>2</sup>, J. Gibelin<sup>1</sup>, S. Grévy<sup>2</sup>, F. Hammache<sup>1</sup>, F. Ibrahim<sup>1</sup>, K.W. Kemper<sup>4</sup>, K.-L. Kratz<sup>5</sup>, S.M.Lukyanov<sup>6</sup>, C. Monrozeau<sup>1</sup>, L. Nalpas<sup>7</sup>, F. Nowacki<sup>8</sup>, A.N. Ostrowski<sup>5</sup>, T. Otsuka<sup>9</sup>, Yu.-E. Penionzhkevich<sup>10</sup>, J. Piekarewicz<sup>4</sup>, E.C. Pollacco<sup>7</sup>, P. Roussel-Chomaz<sup>2</sup>, E. Rich<sup>1</sup>, J.A. Scarpaci<sup>1</sup>, M.G. St. Laurent<sup>2</sup>, T. Rauscher<sup>10</sup>, D.Sohler<sup>3</sup>, M. Stanoiu<sup>11</sup>, T. Suzuki<sup>9</sup>, E. Tryggestad<sup>1</sup>, and D.Verney<sup>1</sup>.

- 1) IPN Orsay, IN2P3-CNRS, Université Paris-Sud, F-91406 Orsay, France
- 2) GANIL, CEA/DSM - CNRS/IN2P3, BP 55027, F-14076 Caen Cedex 5, France
- 3) Institute of Nuclear Research of the Hungarian Academy of Sciences, H-4026 Debrecen, Hungary
- 4) Department of Physics, Florida State University, Tallahassee, Florida 32306, USA
- 5) Institut für Kernchemie, Universität Mainz, D-55128 Mainz, Germany
- 6) Russian Flerov Laboratory of Nuclear Reactions, JINR, Dubna, RU-141980, Russia
- 7) CEA Saclay, DSM/DAPNIA/SPhN, F-91191 Gif-sur-Yvette, France
- 8) IReS, IN2P3-CNRS, Université Louis Pasteur, BP 28, F-67037 Strasbourg Cedex, France
- 9) Department of Physics, University of Tokyo, Hongo, Bunkyo-ku, Tokyo, 113-0033 Japan
- 10) Departement für Physik und Astronomie, Universität Basel, Switzerland
- 11) GSI, D-64291, Darmstadt, Germany

Contact person: [sorlin@ganil.fr](mailto:sorlin@ganil.fr)

## 1. Key question and initial goals

The study of the evolution of shell closures far from stability is one of the main goals of the research in nuclear physics. This evolution is intimately entwined with that of nuclear forces, such as the tensor and spin-orbit ones. The N=28 shell closure is the first arising from the action of the spin-orbit interaction. Therefore any modification of the N=28 shell gap could be linked to that of the spin-orbit interaction and vice versa. In addition the study of the neutron-rich N=28 isotopes enables to probe the action of the proton-neutron tensor forces in atomic nuclei, as the suitable valence orbital are present. This force plays a significant role in the evolution of the magicity towards the  $^{42}\text{Si}$  nucleus and potentially in many other regions of the chart of nuclides where such forces are encountered.

## 2. Experiment set-up

A mean to study the role of such forces is to determine the evolution of the neutron single particle energies  $f_{7/2}$ ,  $p_{3/2}$ ,  $p_{1/2}$  and  $f_{5/2}$  when protons are removed from the sd shells, i.e. south to  $^{48}\text{Ca}$ . We have carried out the  $^{46}\text{Ar}(d,p)^{47}\text{Ar}$  transfer reaction using a pure  $^{46}\text{Ar}$  radioactive beam of 10.2 (1) A.MeV delivered by the SPIRAL facility at a mean intensity of  $2 \cdot 10^4$  pps. The position of the beam (which had an angular dispersion smaller than 2 mrad) on the target was measured using a position-sensitive Multi Wire Proportional Chamber (MWPC) [1] placed 11 cm downstream from a 0.38(6) mg/cm<sup>2</sup> thick CD<sub>2</sub> target in which the reaction took place. The energy and angle of the reaction protons were measured with the MUST [2] detector array comprising eight highly segmented double-sided Si detectors covering polar angles ranging from 110 to 170 degrees with respect to the beam direction. The

transfer-like products  $^{47}\text{Ar}$  ( $^{46}\text{Ar}$ ) were selected and identified by the SPEG [3] spectrometer in the case of a neutron pick-up to bound (unbound) states in  $^{47}\text{Ar}$ .

### 3. Results and achievements

Energies of the neutron  $p_{3/2}$ ,  $p_{1/2}$  and  $f_{5/2}$  states in  $^{47}\text{Ar}$  were obtained from the energy and angle of the protons by applying proper kinematical formula. The corresponding spectroscopic factors and angular momenta were obtained from the comparison of the proton angular distribution gated on individual states and DWBA calculations. The excitation energy spectrum and some fitted proton angular distributions are presented in Fig. 1. As soon as one departs from a doubly magic nucleus the single particle strength of the states become fragmented as they couple to excitations of the core nucleus.

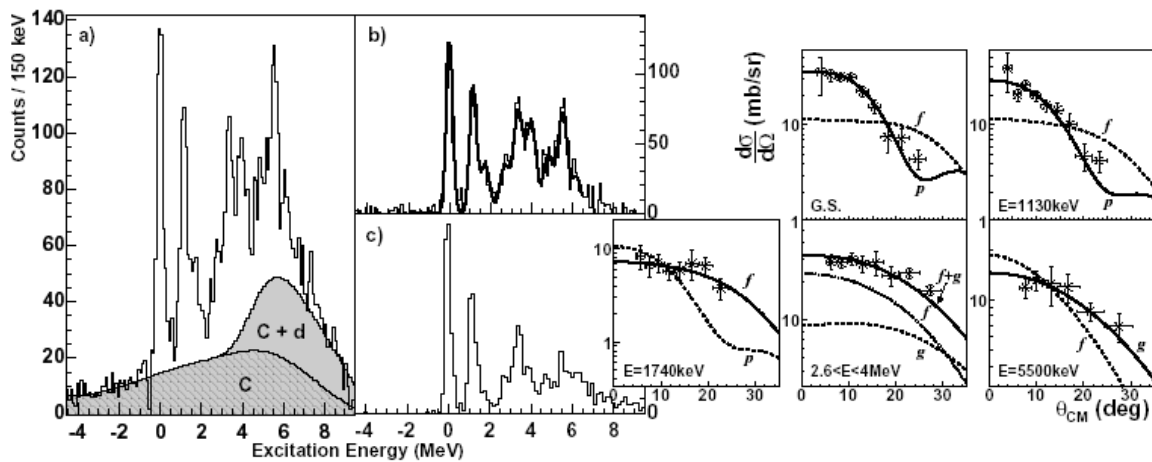


Figure 1: a) Inclusive excitation energy spectrum of the  $^{47}\text{Ar}$  nucleus obtained with the  $^{46}\text{Ar}(d,p)^{47}\text{Ar}$  transfer reaction. The contributions marked with (C) and (d) correspond to reactions induced with the C nuclei and to the deuteron break-up reaction channel, respectively. b) and c) background-subtracted inclusive and exclusive spectra (with requiring the detection of transfer-like nuclei in SPEG), respectively.

Right: Experimental proton angular distributions of several states in  $^{47}\text{Ar}$ . The curves correspond to DWBA calculations assuming transfer to p, f and g states. The two top ones better correspond to transfer to p states, the bottom ones to f and g states.

After having unfolded the proper nuclear correlations, the evolution of the single particle energies between  $^{49}\text{Ca}$  and  $^{47}\text{Ar}$  have been obtained. It was used to determine the evolution of the N=28 shell closure, of the spin-orbit (SO) splittings between the p states and between the f states. It was deduced [4,5] :

- i) a reduction of the N=28 gap by 330(80) keV
- ii) a SO weakening for the neutron p states by about 15%
- iii) the SO weakening for the neutron f states by about 8%.

These changes were ascribed to specific proton-neutron interactions between protons in sd shells and neutrons in fp shells, while 2 protons are removed between Ca and Ar isotones. The role of the tensor and the two-body LS interactions have been pointed out in Ref.[4,5].

#### **4. Conclusion and prospective**

The evolution of neutron single particle energies have been determined between the N=28 Ca and Ar isotopes by means of (d,p) transfer reaction using a radioactive beam of  $^{46}\text{Ar}$ . A reduction of the N=28 gap and a global compression of the p and f orbits are found. As these features arise from the removal of only two protons from  $^{48}\text{Ca}$ , a drastic structural change is expected while moving to  $^{42}\text{Si}$  after the removal of 6 protons. This compression of neutron single particle states favours quadrupole E2 excitations between the neutron f and p states, explaining partly why  $^{42}\text{Si}$  is deformed [6]. A future experimental program will address the reason of the SO reduction for the neutron p states. It happens when protons are removed from the s orbit, i.e. when creating a depletion at the centre of the nucleus [7]. If confirmed this would probe the central density dependence of the SO interaction, which could not have been made so far, 50 years after the discovery of this interaction.

#### **5. References**

- [1] S. Ottini-Hustache Nucl. Instr. Meth. A 431, 476 (1999)
- [2] Y. Blumenfeld et al., Nucl. Instr. Meth. A 421, 471 (1999)
- [3] L. Bianchi et al., Nucl. Instr. Meth. A 276, 509 (1989)
- [4] L. Gaudefroy et al., Phys. Rev. Lett. 97, 092501 (2006)
- [5] L. Gaudefroy et al., Phys. Rev. Lett. 99, 099202 (2007)
- [6] B. Bastin et al., Phys. Rev. Lett. 99, 022503 (2007)
- [7] B.G.Todd-Rutel, J. Piekarewicz, and P.D. Cottle, Phys. Rev. C 69, 021301(R) (2004)



## E473S

## Study of ${}^9\text{He}$ via the $d({}^8\text{He},p){}^9\text{He}$ reaction

T. Al Kalanee<sup>1,2</sup>, J. Gibelin<sup>1</sup>, P. Roussel-Chomaz<sup>1</sup>, Y. Blumenfeld<sup>3</sup>, C. Force<sup>1</sup>, L. Gaodefroy<sup>1</sup>, A. Gillibert<sup>4</sup>, J. Guillot<sup>3</sup>, H. Iwasaki<sup>3</sup>, S. Krupko<sup>5</sup>, V. Lapoux<sup>4</sup>, W. Mittig<sup>1</sup>, X. Mougeot<sup>4</sup>, L. Nalpas<sup>4</sup>, E.C. Pollaco<sup>4</sup>, K. Rusek<sup>6</sup>, T. Roger<sup>1</sup>, H. Savajols<sup>1</sup>, N. de Sereville<sup>3</sup>, S. Sidorchuk<sup>5</sup>, D. Suzuki<sup>3</sup>, I. Strojek<sup>6</sup>

- 1) GANIL, CEA/DSM - CNRS/IN2P3, BP 55027, F-14076 Caen Cedex 5, France
- 2) Laboratoire de Physique Corpusculaire, IN2P3-CNRS, ISMRA, Université de Caen, F-14050 Caen, France
- 3) IPN Orsay, IN2P3-CNRS, Université Paris-Sud, F-91406 Orsay, France
- 4) CEA Saclay, DSM/DAPNIA/SPhN, F-91191 Gif-sur-Yvette, France
- 5) Russian Flerov Laboratory of Nuclear Reactions, JINR, Dubna, RU-141980 Russia
- 6) Warsaw University, Poland

Contact person: [patricia.chomaz@ganil.fr](mailto:patricia.chomaz@ganil.fr)

### 1. Key question and initial goals

E473s was initially approved to study  ${}^5\text{H}$  via  ${}^8\text{He}(p,\alpha){}^5\text{H}$  reaction in inverse kinematics at low energy. However considering the difficulties encountered in the comparison of the different results obtained on  ${}^9\text{He}$ , in the months before the scheduling of E473s, we asked for the authorization to change the goal of the experiment. This request was accepted and we therefore studied the  ${}^8\text{He}(d,p){}^9\text{He}$  reaction. Indeed the situation on this light neutron rich nucleus is very confuse on the experimental point of view. Since the very first experiments claiming for a ground state slightly above 1 MeV above the  ${}^8\text{He}+n$  threshold [1,2], several conflicting results have been obtained. In the knock out results of Chen et al. [3], the ground state was identified as a virtual state around the threshold with a  $L=0$  multipolarity. Our colleagues from IPN Orsay have analysed the results of the  ${}^8\text{He}(d,p){}^9\text{He}$  reaction studied in E401S (S. Fortier et al.). Although the statistics is rather low, several states could be identified. Within the INTAS collaboration we performed with our colleagues from Dubna another experiment studying the same reaction  ${}^8\text{He}(d,p){}^9\text{He}$  [4]. The spectra present a very high statistics and two broad bumps, very different from the narrow peaks obtained in E401S. We also measured some years ago in a test experiment for MAYA, the resonant elastic scattering of  ${}^8\text{He}$  on proton, which gives access to isomeric states of  ${}^9\text{He}$ . In that last case, the results are consistent with a ground state of  ${}^9\text{He}$  at 1.3 MeV, in agreement with the results of [1,2] but in contradiction with the more recent results mentioned previously [5].

This explains why we wanted to measure once again the same reaction  ${}^8\text{He}(d,p){}^9\text{He}$ , with a much higher statistics than what could be achieved in E401S due to several beam problems, and with a good energy resolution.

**International competition:** see above

### 2. Experiment set-up

We used the MUST2 array. E473S was part of the first campaign of this array, on the SPEG beam line, scheduled at the end 2006-beginning 2007. Figure 1 presents the experimental set-up installed in the SPEG reaction chamber. Four MUST2 telescopes were mounted at backward angles (on the right of the picture) to detect the recoil protons from (d,p) reactions. One telescope was placed at  $\approx 70^\circ$  to detect deuterons from elastic scattering. Finally a sixth telescope was mounted at  $0^\circ$ , in

order to identify the projectile residues ( ${}^{4,6,8}\text{He}$ ). A small plastic scintillator ( $2 \times 2 \text{ cm}^2$ ) was placed in front of this telescope in order to intercept the beam.

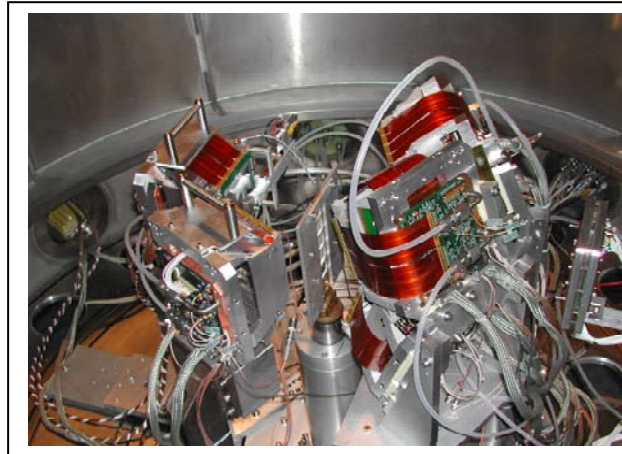


Figure 1: experimental set-up including the MUST2 array of telescopes.

### 3. [Results and achievements](#)

Figure 2 presents the results obtained for the calibration reaction measured during the same experiment:  ${}^{16}\text{O}(d,p){}^{17}\text{O}$ . The left part presents the correlation between the proton energy and angle (in the laboratory frame), where clear kinematical lines corresponding to the population of different levels in  ${}^{17}\text{O}$  can be recognized. The right part presents the excitation energy spectrum reconstructed for  ${}^{17}\text{O}$ . These spectra allow to verify that the trajectories are well reconstructed, for both the incoming particles with the CATS beam tracking detectors, and for the recoil particles after transfer reactions.

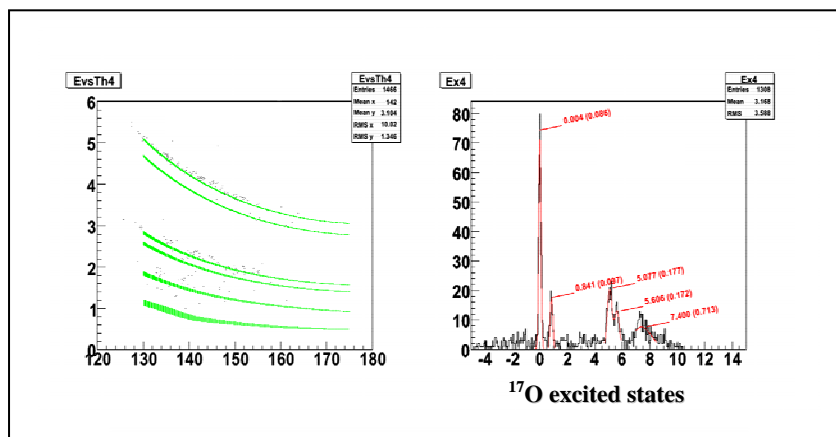


Figure 2: excitation energy spectrum of  ${}^{17}\text{O}$  (left) derived from the proton spectrum (right).

### 4. [Conclusion and prospective](#)

The previous spectra show the excellent performances of the MUST2 array. The resolution obtained in the centre of mass of  ${}^{17}\text{O}$  is of the order of 100 keV. The angular distributions obtained for the different states are in perfect agreement with the calculations, and show that the position reconstruction and the efficiency calculations are also well under control.

After the calibration procedure, test of reconstruction hypotheses, and of the analysis code performed with the test run with  $^{16}\text{O}$ , the data on  $^8\text{He}$  are presently under analysis. The analysis is in this case more difficult due to the very important background due to  $\beta$  decay random coincidences. Indeed with the compact geometry of the experiment, the radioactive beam was stopped very close to the MUST2 telescopes placed at backward angles. Therefore more stringent conditions have to be defined in order to obtain clean spectra and identify the states populated in  $^9\text{He}$ . We hope to obtain the first results in the next few weeks.

## 5. [References](#)

- [1] K. Seth et al., Phys. Rev. Lett. 58 (1987) 1930
- [2] H.G. Bohlen et al., Prog. Part. and Nucl. Phys. 42 (1999) 17
- [3] L. Chen et al., Phys. Lett. B 505 (2001) 21
- [4] M. Golovkov et al, Phys. Rev. C76 (2007) 021605 R
- [5] W. Mittig et al, EPJ A 25 (2005) 263



# E475S Isospin dependence in the emission of complex fragments from compound nuclei of mass=115 and N~Z

J. Gomez del Campo<sup>1</sup>  
M. La Commara<sup>2</sup>  
J.-P. Wieleczko<sup>3</sup>

1) Oak Ridge National Laboratory, P.O. Box 2008, Oak Ridge, TN 37831, USA  
2) Università degli Studi e INFN sezione di Milano, Via Celoria 16, I-20133 Milano, Italy  
3) GANIL, CEA/DSM - CNRS/IN2P3, BP 55027, F-14076 Caen Cedex 5, France

Contact person: [wieleczko@ganil.fr](mailto:wieleczko@ganil.fr)

## 1. Key questions and initial goals

New radioactive ion beam facilities allow to create excited nuclei in unexplored regions of the nuclear landscape. The disintegration phenomena of nuclei at the limit of the nuclear chart are unknown. With the use of proton-rich radioactive beams delivered by the SPIRAL1 facility at GANIL, compound nuclei can be formed close to the proton-drip line. For these nuclei the possible decay modes should be explored, particularly since the neutron decay becomes strongly inhibited. The initial goal of the experiment was to measure the possible enhancement of the complex fragment production, mainly  $^{12}\text{C}$ . To fulfil our goal, we have proposed to measure the deexcitation products emitted in the reaction  $^{75}\text{Kr} + ^{40}\text{Ca}$  at 5.5 A.MeV using the SPIRAL1 facility and measuring the charged fragment with the  $4\pi$  array INDRA. Reactions using  $^{78}\text{Kr}$  and  $^{82}\text{Kr}$  beams have been performed to provide a reference point for less exotic compound nuclei.

## 2. Results of the first 5 years

The experiment has been performed during March 2006. The experiment was successful and the GANIL facility provided us with the various beams needed with good quality. For example,  $10^5$ pps of  $^{75}\text{Kr}$  were delivered as expected with a very stable beam during one week of taking data. The INDRA detector ran well. Results obtained on-line are very satisfactory in a sense that clusters such as  $^{12}\text{C}$  have been clearly observed and identified. It is worth noticing that clusters have been observed at a bombarding energy well below the standard threshold for such a production process. The data reduction is in progress in order to have a quantitative estimation of the cross section that is the crucial and main aspect of the experiment. The organization and sharing of the various tasks needed to analyse data taken with a complex apparatus as INDRA have been made and a meeting of the collaboration for that experiment is scheduled for the next summer.

## 3. Possible developments

The ultimate objective of the program is to perform  $^{72}\text{Kr} + ^{40}\text{Ca}$  reaction since the emission of clusters is expected to strongly increase at the  $N=Z$  line. Moreover, after emission of  $^{12}\text{C}$  from  $^{112}\text{Ba}$  the complementary nucleus is  $^{100}\text{Sn}$ , a key nucleus for spectroscopy studies. Through cluster emission we expect to populate  $^{100}\text{Sn}$  in a domain differing from the standard fusion evaporation process. However, this requires a beam intensity similar that the one we had during the  $^{75}\text{Kr} + ^{40}\text{Ca}$  experiment.

#### 4. Conclusion

We have measured the disintegration products coming from compound nuclei formed with the reaction  $^{75}\text{Kr} + ^{40}\text{Ca}$  at 5.5 A.MeV. Charged products have been measured with the INDRA detector.  $^{12}\text{C}$  clusters have been observed. Further analyses are underway in order to measure the cross section of the cluster emission.

# E476aS Measurement of the $\beta$ - $\nu$ angular correlation coefficient in the $\beta$ decay of ${}^6\text{He}$

G. Ban, D. Durand, F. Duval, X. Fléchar, M. Labalme, E. Liénard, F. Mauger, A. Méry, O. Naviliat-Cuncic<sup>1</sup>, D. Rodríguez<sup>2</sup>, J.-C. Thomas<sup>3</sup>

1) Laboratoire de Physique Corpusculaire, IN2P3-CNRS, ISMRA, Université de Caen, F-14050 Caen, France

2) Departamento de Física Aplicada, Universidad de Huelva, Campus de El Carmen – E-21071 Huelva, Spain

3) GANIL, CEA/DSM - CNRS/IN2P3, BP 55027, F-14076 Caen Cedex 5, France

Contact person: [naviliat@lpccaen.in2p3.fr](mailto:naviliat@lpccaen.in2p3.fr)

## 1. Key question and initial goals

**Abstract.** This experiment aims to measure the  $\beta$ - $\nu$  angular correlation parameter,  $a$ , in the  $\beta$  decay of  ${}^6\text{He}$  with a relative precision below 1%, to search for the presence of tensor type contributions in the weak interaction. The experiment uses the low-energy beams from LIRAT and a novel ion-trapping set-up.

**Introduction.** In the standard electroweak model, nuclear  $\beta$  decay is described in terms of vector (V) and axial-vector (A) couplings. Lorentz invariance allows other couplings to be present in the interaction, such as scalar (S), pseudo-scalar (P) or tensor (T), but the standard model forbids them. The observation of such exotic couplings would provide signatures of new physics, which are actively searched for both, at the high-energy frontier near colliders [1] and at low energies, like in nuclear  $\beta$  decay [2].

**Phenomenology of allowed beta-decay.** The most general description of  $\beta$  decay, without restrictions with respect to space and time symmetries, involves five Lorentz invariant interactions [3] whose amplitudes are driven by 10 complex couplings,  $C_i$  and  $C'_i$ , where  $i = S, P, V, A, T$ . In the standard model the couplings are real,  $C_V = -C'_V = 1$ ,  $C_A = -C'_A$ , and all others vanish.

Ignoring the  $\beta$  particle spin observables, the decay rate from unpolarized nuclei leads, in the allowed approximation, to [3]:

$$W(E) = W_0(E) \left( 1 + b \frac{m}{E} + a \frac{\mathbf{p} \cdot \mathbf{p}_\nu}{EE_\nu} \right) \quad (1)$$

where  $m$ ,  $E$  and  $\mathbf{p}$  are respectively the mass, the total energy and the momentum of the  $\beta$  particle,  $E_\nu$  and  $\mathbf{p}_\nu$  are respectively the energy and the momentum of the neutrino, and  $W_0(E)$  is a function of the  $\beta$  energy which takes into account the decay phase space as well as the static coulomb correction due to the interaction of the  $\beta$  particle with the field of the daughter nucleus.

The dynamics of the weak interaction is contained in the Fierz interference term,  $b$ , and in the angular correlation coefficient,  $a$ . The expression of  $a$  as a function of the couplings  $C_i$  is of the form:

$$a \approx a_0(1 - \alpha) \quad (2)$$

where  $a_0$  is the value of the angular correlation coefficient predicted by the standard model and  $\alpha$  contains contributions of possible exotic interactions. According to the type of the  $\beta$  decay transition one has:

$$\begin{array}{ll} \text{Fermi transitions: } a_0 = 1 & \alpha = (|C_S|^2 + |C'_S|^2)/|C_V|^2 \\ \text{Gamow-Teller transitions: } a_0 = -1/3 & \alpha = (|C_T|^2 + |C'_T|^2)/|C_A|^2 \end{array}$$

It is to note that the Fierz interference term cancels under the assumption of right-handed exotic couplings but not so the angular correlation coefficient due to its quadratic dependence on the couplings.

Present constraints on exotic couplings. The tightest constraints on scalar couplings have been obtained from measurements of  $a$  in the pure Fermi transitions of  $^{32}\text{Ar}$  and  $^{38\text{m}}\text{K}$  [4,5]. In  $^{32}\text{Ar}$ , the daughter nucleus following beta-decay is proton unstable and  $a$  was deduced from the kinematic broadening of the proton energy peak [4]. The measurement with  $^{38\text{m}}\text{K}$  was performed by recording beta-ion coincidences from decays of atoms confined in a Magneto-Optical-Trap [5]. Both experiments have similar precisions and lead, at the 95% C.L. to:

$$|C_S/C_V| < 0.08. \quad (3)$$

For pure Gamow-Teller transitions the most precise measurement was performed more than 40 years ago [6] in the decay of  $^6\text{He}$ , with a relative precision of 1%. The results from this experiment have been re-analysed [7] to account for radiative corrections and leads, at the 95% C.L., to the following limit on a tensor coupling:

$$|C_T/C_A| < 0.11. \quad (4)$$

In absolute terms, because  $C_A/C_V \approx 1.27$  in neutron decay [2], the constraints on tensor couplings are presently a factor of about 2 worse than those on scalar couplings.

New search for tensor couplings. In order to improve the limit on the tensor contributions, or find a deviation from the standard model prediction, we proposed a new experiment based on an innovative ion trapping technique for which the proof of principle has been demonstrated [8]. Singly charged  $^6\text{He}^+$  ions are confined in a transparent Paul trap where they decay. The  $\beta$  particles and the recoil ions resulting from the decay are recorded in coincidence and the angular correlation coefficient is deduced from the analysis of the time of flight distribution of the recoil ions relative to the  $\beta$ .

The  $\beta$ -decay of  $^6\text{He}$  presents a number of advantages for such a measurement: *i)* it is a pure Gamow-Teller transition with a 100% branching to the  $^6\text{Li}$  ground state.

- ii) the half-life, ( $T_{1/2} = 808$  ms), is sufficiently long for the manipulation of the low-energy ion beams.
- iii) the  $Q_{\beta}$  value and the small mass result in a “large” kinetic energy of the recoil,  $T_{\max} = 1.4$  keV, on comparison with other decays.
- iv) the  ${}^6\text{He}$  production rate at SPIRAL is high.

The goal of the project is to reach a relative precision of at least 0.5 % on  $a$ , what represents an improvement by a factor of 2 with respect to the previous most precise experiment [6]. The aim of the first phase of the experiment was to reach a relative precision of 1%. The possibility to go beyond the 0.5 % level will be assessed after a detailed study of all sources of systematic effects as well as the available and possible means to control and correct them.

## 2. Experiment set-up

The experimental set-up is installed at the low energy exit (LIRAT) of the SPIRAL facility.  ${}^6\text{He}^+$  ions, extracted from the ECR source at an energy of about 10 keV, are transported to the experiment after a crude mass separation ( $\Delta M/M \approx 1/250$ ). They are then cooled and bunched by means of the buffer gas technique with a Radio Frequency Quadrupole (RFQ) filled with  $\text{H}_2$  gas. The RFQ operates on a high voltage platform set at a voltage 100 V lower than the extraction voltage from the ECR source. More details about the operation of the RFQ can be found elsewhere [9].

Paul trap and detectors. Cold bunches extracted from the RFQ are injected into the Paul trap (see Fig. 1). The transfer of ions from the RFQ, at high voltage, to the trap chamber at ground, is achieved with two pulse-down electrodes, located between the RFQ and the trap, which reduce the ion energy for an efficient trapping. The trap is made of a set of coaxial rings providing an open access for injection and extraction of ions and for the detection of the decay products. Ions are confined in the Paul trap by a RF field (120 V peak-to-peak, and  $\nu = 1.14$  MHz). The RF voltage is applied to the inner rings of the trap. The  $\beta$  particles from in trap decays are detected by a telescope constituted by a double-sided position sensitive silicon strip detector (SSD) followed by a thick plastic scintillator. The recoil ions are counted by a position sensitive micro-channel plate ( $\mu\text{CP}$ ). A second  $\mu\text{CP}$ , located downstream, serves to monitor the trapped ions and measures continuously the ions remaining in the trap at the end of the cycle. The arrangement of the  $\beta$  telescope and ion detector, in a back-to-back geometry, is the most sensitive to search for tensor couplings in Gamow-Teller decays.

Measuring sequence. Ion bunches from the RFQ are continuously injected/extracted into/from the Paul trap, with a repetition rate of 100 ms. The repetition rate is adjustable depending of the effective storage time of ions in the trap. After injection, the RF voltage is permanently applied to the rings of the Paul trap. The production of a signal by the plastic scintillator generates the trigger of an event, which in most cases is a  $\beta$  particle in singles. Following a trigger the SSD is read out and a start signal is generated for the time measurement, waiting for a signal from the  $\mu\text{CP}$  over a 8  $\mu\text{s}$  range. During the flight, the motion of the ion from the trap is somewhat affected by the RF field. The phase of the RF signal is then registered at the trigger time, to study off-line the effect of the RF field on the measured time of

flight. The time after injection of the ions in the trap is also registered to study effects related with ion cloud phase space evolution in the trap.

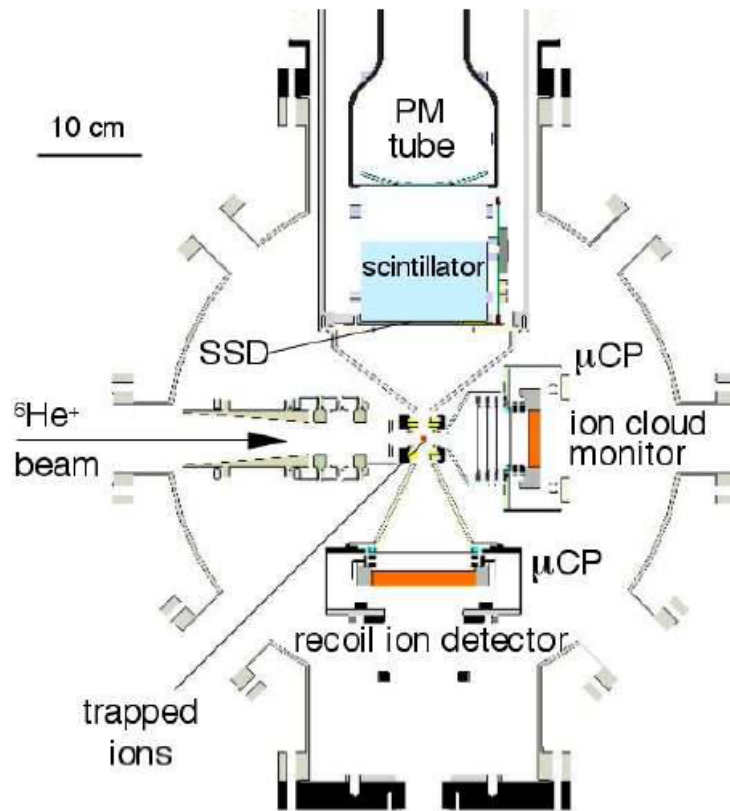


Figure 1: Top view of the experimental set-up.

### 3. [Results and achievements](#)

Our first data-taking run took place in July 2006. The low energy beam line was tuned with a special setting to separate the  ${}^{12}\text{C}^{2+}$  contaminants. Under such conditions, the largest  ${}^6\text{He}^+$  beam intensity measured at the entrance of the RFQ was  $1.2 \times 10^8$  ions/s. Although the extraction voltage from the ECS was set to 10 kV, the measured intensity is consistent with expected values when including a factor of about 2 less due to the special tune of the beam line to realize the mass separation. The measured intensity reflects an improvement by a factor 4 in the low energy beam extraction and transmission relative to the commissioning run in July 2005. It was an achievement of the GANIL machine crew, following a series of tests with stable beams before the run. In addition, the tune resulted in a reduction of the  ${}^{12}\text{C}$  intensity to a level that does not affect the operation of the RFQ. The total current measured at the entrance of the RFQ varied between 0.3 and 15 nA without any impact of the efficiency of the apparatus.

The overall efficiency measured during the run was about  $10^{-4}$  including the cooling, bunching, and trapping of the  ${}^6\text{He}^+$  ions. This is significantly lower than efficiencies achieved during off-line tests [10] with  ${}^4\text{He}^+$  ions. Part of the reduction is known to be caused by the first pulse-down electrode, which was found few days before the run to operate with degraded transmission and could not be fixed in time.

Figure 2 shows the time of flight spectra obtained in 2005 (a) and in 2006 (b). The improvement anticipated in the previous proposal [8] is clear. The gain in real

coincidences integrated over the full run is about 2000. The available data corresponds to a relative precision on  $a$  of 1.4 %.

The quality and the amount of data accumulated in 2006 enabled us to initiate a detailed study of instrumental systematic effects. The analysis is in progress. Among the most critical effects we can list:

- i)* the interaction of the RF field with the recoiling ions during flight. This would affect both, the time of flight of the ion and the measured position of the ion on the  $\mu$ CP.
- ii)* the finite extension of the source, that is the size of the ion cloud inside the trap. This is directly related to the temperature of the ions in the trap, which affects the initial position and velocity of the recoiling ions.
- iii)* the relative beta telescope efficiency and its effective response function as a function of the  $\beta$  particle energy. In particular the backscattering of beta particles on the 300  $\mu$ m thick SSD and on the plastic scintillator affects the shape of the beta spectrum.

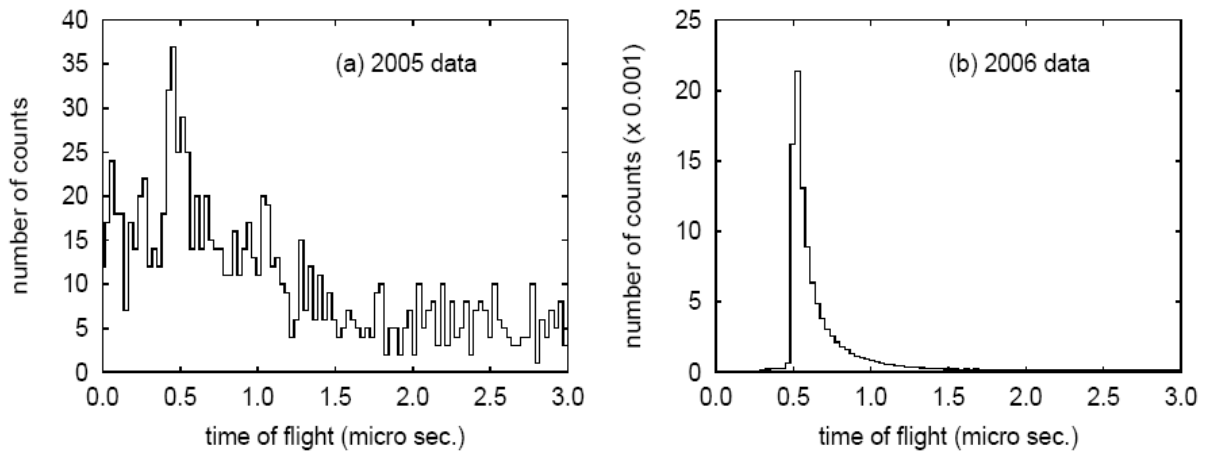


Figure 2: a) time of flight spectrum measured in 2005; (b) same spectrum measured in 2006

Monte-Carlo simulations, performed using GEANT-4, are being carried out to study these and other effects. The impact of the RF field has been studied by comparing the shape of the time of flight distributions measured at different RF phases. The effect is visible and is consistent with simulations [11]. The global effect of the ion cloud phase space has been studied by comparing the time of flight distributions measured during two time windows after the injection of ions in the trap. If the ions are further thermalized while stored in the trap, the effect of the ions cloud size should be smaller for decays occurring late during the trapping interval. This effect has a smaller impact on the time of flight distribution than the RF field and the observations are again consistent with simulations. The control of this effect by the Monte-Carlo simulations requires the determination of the actual ion cloud temperature. This can possibly be obtained by requiring the stored events to be constrained by kinematics [11]. Such a constrain is independent of the dynamics and does not require a very precise determination of the beta telescope response function.

#### **4. Conclusion and prospective**

Further efforts are needed to improve any aspect, which would enable us to increase the collected statistics by a factor of 20, reaching thereby the relative precision level of 0.5 %. We are confident that such a factor is within reach and intend to study in more detail the following points:

- i)* the operation with a higher extraction voltage from the ion source and hence with a larger beam energy. Tests have been performed both, with stable beams before the 2006 run and with  ${}^6\text{He}^+$  at the end of the run but further tests with stable beams are needed to draw clear conclusions.
- ii)* the low energy beam optics used to separate the  ${}^6\text{He}^+$  and  ${}^{12}\text{C}^{2+}$  beams. The  ${}^6\text{He}^+$  transmission from the source to the RFQ could still be improved by a factor 1.4. The effect on the efficiency of the set-up due to  ${}^{12}\text{C}^{2+}$  contaminant needs to be optimised.
- iii)* the control of the injection optics into the RFQ by the addition of a position sensitive detector for the monitoring of the  ${}^6\text{He}$  beam spot distribution. Small drifts in the injection parameters strongly affect the efficiency of the RFQ. The absence of adapted beam diagnostics at the entrance of the RFQ renders the reaction inefficient.
- iv)* the configuration of the first pulse-down electrode and its operation under nominal performance. This should improve the overall efficiency by a factor 10.
- v)* the stabilization of the system to run continuously under the best conditions. System instabilities during the 2006 run resulted in an average coincidence rate, which was a factor of 2 lower than the rate measured under the best conditions. Such variations could be due to temperature drifts or related with magnetic remnance effects in a dipole magnet but the actual source could not be identified.

A new beam time request has been submitted to the PAC and will be discussed in November 2006.

## 5. [References](#)

- [1] See e.g. P. Langacker, J. Phys. G29, 35 (2003)
- [2] N. Severijns, M. Beck and O. Naviliat-Cuncic, Rev. Mod. Phys. 78, 991 (2006)
- [3] J.D. Jackson, S.B. Treiman, and H.W. Wyld JR, Nucl. Phys. 4, 206 (1957)
- [4] E.G. Adelberger et al., Phys. Rev. Lett. 83 (1999) 1299; (E) Phys. Rev. Lett. 83, 3101 (1999)
- [5] A. Gorelov et al., Phys. Rev. Lett. 94, 142501 (2005)
- [6] C.H. Johnson et al., Phys. Rev. 132, 1149 (1963)
- [7] F. Gluck, Nucl. Phys. A628, 493 (1998)
- [8] G. Ban et al., Addendum for an experiment at GANIL, November 2005.
- [9] G. Ban et al., Nucl. Inst. Meth. Phys. Res. A518, 712 (2004)
- [10] D. Rodríguez et al., Nucl. Inst. Meth. Phys. Res. A565, 876 (2006)
- [11] D. Rodríguez et al., contribution to Int. Conf. on Trapped Charged Particles and Fundamental Interactions, Parksville, Canada, september 2006

# E493S Shell structure and shape coexistence in neutron-rich Ar isotopes

M. Zielińska, A. Görgen, E. Clément, C. Dossat, J. Ljungvall, W. Korten, Ch.Theisen<sup>1</sup>  
A. Bürger<sup>2</sup> (Bonn)  
J. Iwanicki, P. Napiorkowski, D. Piętak, J. Srebrny, K. Wrzosek<sup>3</sup>  
G. Sletten<sup>4</sup>  
W. N. Catford<sup>5</sup>

- 1) CEA Saclay, DSM/DAPNIA/SPhN, F-91191 Gif-sur-Yvette, France
- 2) Helmholtz-Institut für Strahlen- und Kernphysik, Universität Bonn, D-53115 Bonn, Germany
- 3) Heavy Ion Laboratory, Warsaw University, Pl 02-097 Warsaw, Poland
- 4) The Niels Bohr Institute, Tandem Accelerator Laboratory, DK-4000 Roskilde, Denmark
- 5) Department of Physics, University of Surrey, Surrey GU2 7XH, United Kingdom

Contact person: [andreas.goergen@cea.fr](mailto:andreas.goergen@cea.fr)

## 1. Key question and initial goals

The primary question addressed by the experiment is the possible weakening of the  $N=28$  shell closure in neutron-rich nuclei and, closely connected to that, the development of deformation and shape coexistence in these nuclei. The goals of the first experiment concerning  $^{44}\text{Ar}$  were to measure the transition strength to the first  $2^+$  state with high precision, determine the static quadrupole moment of the  $2^+$  state, identify the  $4^+$  and second  $2^+$  state unambiguously, and measure the matrix elements connecting these states. This multi-step Coulomb excitation experiment at safe energies below the Coulomb barrier is currently only possible at GANIL. The  $B(E2; 0^+ \rightarrow 2^+)$  value had been measured previously at intermediate energy at MSU [1]. The much more precise value that will be established in the low-energy measurement at GANIL represents also a test for the reliability of intermediate-energy experiments. Together with  $(p,p')$  scattering data from MSU [2], the GANIL experiment will furthermore result in a more precise value for the  $M_n/M_p$  ratio of neutron and proton matrix elements. A second part of the experiment to study the Coulomb excitation of  $^{46}\text{Ar}$  has been presented to the GANIL PAC but was not approved.

## 2. Experiment set-up

The  $^{44}\text{Ar}$  projectiles were Coulomb excited on  $^{208}\text{Pb}$  and  $^{109}\text{Ag}$  targets at two different beam energies. Gamma rays were detected in the EXOGAM array comprising 10 clover detectors (out of 12 that were requested); scattered projectiles and recoiling target nuclei were detected in a highly segmented annular double-sided silicon detector, which was equipped with 160 channels of TIARA electronics. The mounting of the EXOGAM detectors in G2 had to be performed in only three days due to their use in other experiments. This was achieved due to the strong commitment of the technical staff. The CSS1 and CSS2 cyclotrons provided the maximum  $^{48}\text{Ca}$  primary beam intensity on the SPIRAL target over the entire period of the experiment. The secondary  $^{44}\text{Ar}$  beam had the required intensity and was very stable. A good beam focus and minimization of beam satellites was required in order to limit direct beam impinging on the silicon detector. While this could not be avoided entirely, the machine operators were very efficient in providing a beam of sufficiently

high quality. A contamination of the beam with stable  $^{132}\text{Xe}$  was detected during the experiment. This contaminant complicates the data analysis, but will not compromise the main goals.

### 3. Results and achievements

The experiment was performed in April 2006. Data analysis is currently ongoing at Saclay. Preliminary spectra are shown in Fig. 1. Coulomb excitation on the  $^{208}\text{Pb}$  target populated the first  $2^+$  state in  $^{44}\text{Ar}$  and at least two higher-lying states. With the  $^{109}\text{Ag}$  target both projectile and target nuclei were excited, which can be used to normalize the excitation probability in  $^{44}\text{Ar}$  with the well-known transition strengths of  $^{109}\text{Ag}$ . Having two independent high-statistics measurements will allow extracting a very precise  $B(E2;0^+ \rightarrow 2^+)$  value. The level of statistics is sufficient to divide the data into several subsets corresponding to different ranges of scattering angles. The static quadrupole moment (including its sign) will be determined from the differential Coulomb excitation cross section. Having data on two different target materials gives additional constraints. Higher-lying states in  $^{44}\text{Ar}$  had been previously observed at GANIL after beta decay of  $^{44}\text{Cl}$ , but no firm assignments could be made [3]. At least two of these states are also populated in Coulomb excitation on the  $^{208}\text{Pb}$  target, and their excitation probabilities will allow spin and parity assignments.

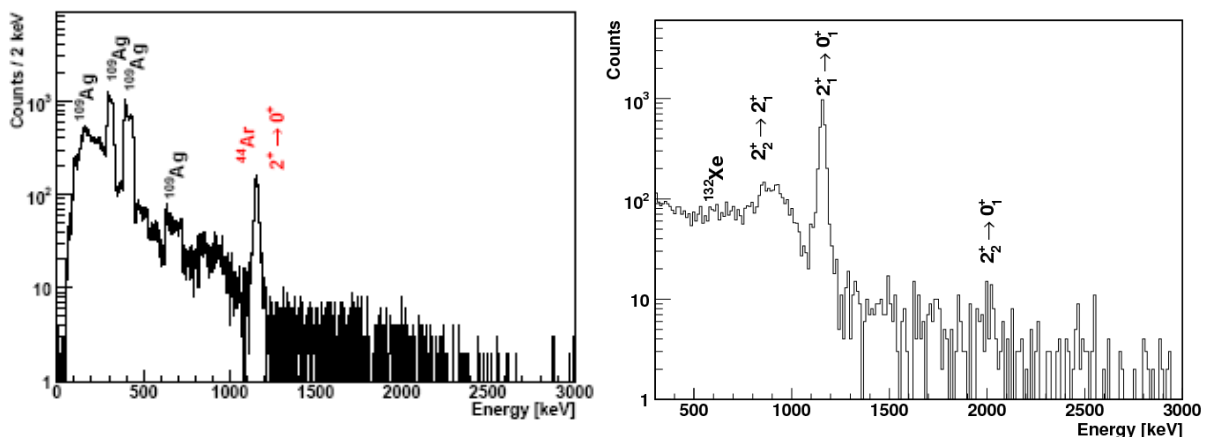


Figure 1: Left: Gamma-ray spectrum in coincidence with  $^{44}\text{Ar}$  projectiles scattered on a  $^{109}\text{Ag}$  target, corresponding to scattering angles of  $35^\circ < \theta_{\text{cm}} < 72^\circ$ . The  $2^+ \rightarrow 0^+$  transition is observed together with several transitions in  $^{109}\text{Ag}$ , which can be used for normalization. Right: Gamma-ray spectrum in coincidence with recoiling  $^{208}\text{Pb}$  target nuclei, corresponding to scattering angles of  $67^\circ < \theta_{\text{cm}} < 130^\circ$ . In addition to the  $2^+ \rightarrow 0^+$  transition, transitions from two higher-lying states in  $^{44}\text{Ar}$  are visible. Their spin assignments are preliminary.

### 4. Conclusion and perspective

Even though the data analysis is still in a preliminary stage, it is anticipated that the main goals of the experiment will be achieved. The static quadrupole moment of the  $2^+$  state will provide information on the prolate or oblate character of the deformation. Experimental matrix elements provide a stringent test for the theoretical description of the development of deformation in the  $N=28$  isotones, for example with configuration mixing calculations using the generator coordinate method based on

HFB mean-field states. Once the data analysis is further advanced and more definitive results can be presented, we plan to propose again the next step in this experimental program: the Coulomb excitation of  $^{46}\text{Ar}$  from SPIRAL.

## 5. [References](#)

- [1] H. Scheit et al., Phys. Rev. Lett. 77, 3967 (1996)
- [2] H. Scheit et al., Phys. Rev. C67, 014604 (2000)
- [3] J. Mrázek et al., Nucl. Phys. A734, E65 (2004)



# E494S Level density parameter determination for different isotopes

N. Le Neindre<sup>1,2</sup>

1) IPN Orsay, IN2P3-CNRS, Université Paris-Sud, F-91406 Orsay, France

2) Laboratoire de Physique Corpusculaire, IN2P3-CNRS, ISMRA, Université de Caen, F-14050 Caen, France

Contact person: [leneindre@lpccaen.in2p3.fr](mailto:leneindre@lpccaen.in2p3.fr)

## 1. Key question and initial goals

The advent of radioactive beams, coupled to judiciously chosen targets, allows to explore the properties of a large number of isotopes of compound nuclei of a given  $Z$ , and in correlation, to test the influence of the mass asymmetry of the entrance channel on the fusion cross section. The aim of this experiment is to explore the deexcitation properties and thus the evolution of the level density parameters of hot nuclei with  $N/Z$  when going from the proton drip line to stable nuclei. By using three different Ar beams ( $^{34, 36, 40}\text{Ar}$ ) with three different targets ( $^{58, 60, 64}\text{Ni}$ ) we want to produce five Pd isotopes ( $^{92, 94, 96, 100, 104}\text{Pd}$ ) at the same total excitation energy. For the very first time, thanks to the coupling of a  $4\pi$  multidetector (INDRA) with a spectrometer (VAMOS), complete information on the products emitted all along the de-excitation chain will be obtained. This gives very strong constraints on the statistical models for a better level density parameter determination.

## 2. Experimental set-up

We have coupled INDRA (for light charged particles identification) and the VAMOS spectrometer (for evaporation residue detection). The detection efficiency was maximized thanks to the  $4\pi$  angular coverage, which allows the use of low intensity beams. Indeed a  $4\pi$  multidetector works in all cases with low intensities  $\approx 10^7$  pps. Complete events (detection of the total charge of the incident system) will be selected, the charge and mass of the residue given by VAMOS and those of all light charged particles and fragments by INDRA. The multiplicity of the undetected neutrons will be obtained by mass difference. The  $4\pi$  angular acceptance allows differentiating more easily fusion reactions from deeply inelastic collisions.

We kept INDRA in its own reaction chamber and removing only the first three rings (angular acceptance  $7\text{-}176^\circ$ ) allowed to set the entrance of the first VAMOS quadrupole at  $\approx 130$  cm from the target. Different angular positions of the spectrometer have been set to cover the residue angular distribution ( $\approx 0\text{-}20^\circ$ ) and to avoid any bias of the relative weights of the different exit channels. VAMOS give the mass and the atomic number of the residue with a good accuracy. Concerning the residue charge state we have used a carbon foil of about  $70 \mu\text{g}/\text{cm}^2$  at a distance of about  $\approx 50$  cm from the target in order to reach the equilibrium charge state

distribution, independently of the compound nucleus production position within the target. The mechanical coupling between INDRA and VAMOS allows the rotation of VAMOS but has reduced the angular acceptance for the residue to  $\Delta\theta=\pm 2^\circ$ .

### **3. Results and achievements**

Our experiment was scheduled in April-May 2007. Already some tests concerning mainly the HARPEE ionisation chamber of VAMOS have been performed in March and September 2006 and also during the months preceding the experiment. Thanks to the huge work off all the Ganil staff, the mechanical coupling between INDRA and VAMOS was successfully working and we do not suffer from any technical problems. The expected program was fulfilled, either concerning the beams delivered and the targets we wanted to impinge. The statistics of events recorded during the measurements well agree with the one expected by the simulations and the predictions according to the general acceptance of the experimental set-up and the fusion-residue cross section. As a preliminary analysis, angular distributions for the fusion residue cross section events have been measured for all the reactions  $^{34}\text{Ar}+^{58}\text{Ni}$ ,  $^{36}\text{Ar}+^{58}\text{Ni}$ ,  $^{36}\text{Ar}+^{60}\text{Ni}$ ,  $^{40}\text{Ar}+^{60}\text{Ni}$  and  $^{40}\text{Ar}+^{64}\text{Ni}$ .

### **4. Conclusion and prospective**

This experiment offers for the very first time, to our knowledge, to fully measure and determine both the particles emitted all along the deexcitation chain and the residue, that follow the production of hot compound nuclei in heavy ion collisions. Moreover, by appropriate combination of targets and stable and radioactive beams, a wide variety of hot isotopes can be formed, relevant for level density parameter analysis. According to the results, we can foresee complementary experiments including other ( $^{33-46}\text{Ar}$ ) isotopes beams or/and different projectile/target combination. Furthermore for studying limiting temperature effects in those nuclei, a simple beam energy change is necessary, as it requires the same experimental set-up.

### **5. References**

- H. Lehr et al., Nucl. Phys. A415, 149 (1984)
- R. J. Charity et al., Phys. Rev. C67, 044611 (2003)
- Shlomo and Natowitz, Phys. Rev. C44, 2878 (1991)
- S.I. Al-Quraishi et al., Phys. Rev. C63, 065803 (2001)
- R.J. Charity and L.G. Sobotka, nucl-th/0405041
- G.A. Lalazissis et al., Nuclear Physics A679, 481 (2001)
- H. Gauvin et al., Phys. Lett. B58, 163 (1975)
- J.P. Coffin et al., Phys. Rev. C30, 539 (1984)

# E498S High Spin States in the $T_z=-3/2$ Nucleus $^{37}\text{Ca}$ – Mirror Symmetry at the Largest Values of Isospin

S.J. Williams, W. Gelletly, Zs. Podolyak, P.H. Regan, P.M. Walker<sup>1</sup>

J.N. Scheurer<sup>2</sup>

A. Algora, Zs. Dombrádi, J. Gál, J. Molnár, B.M. Nyakó, J. Timár, L. Zolnai<sup>3</sup>

K. Juhász<sup>4</sup>

A.M. Bruce<sup>5</sup>

G. de France<sup>6</sup>

J. Nyberg<sup>7</sup>

M. Palacz<sup>8</sup>

M.A. Bentley<sup>9</sup>

B. Rubio<sup>10</sup>.

1) Department of Physics, University of Surrey, Surrey GU2 7XH, United Kingdom

2) CEN Bordeaux-Gradignan, IN2P3-CNRS, Université de Bordeaux I, F-33170 Gradignan, France

3) Institute of Nuclear Research of the Hungarian Academy of Sciences, H-4026 Debrecen, Hungary

4) Faculty of Informatics, University of Debrecen, H-4032 Debrecen, Hungary

5) School of Engineering, University of Brighton, Brighton, BN2 4GJ, United Kingdom

6) GANIL, CEA/DSM - CNRS/IN2P3, BP 55027, F-14076 Caen Cedex 5, France

7) Department of Radiation Sciences, Uppsala University, Uppsala, Sweden

8) Heavy Ion Laboratory, Warsaw University, Warsaw, Poland

9) School of Chemistry and Physics, Keele University, Staffordshire, ST5 5BG, United Kingdom

10) IFIC, CSIC-Universidad de Valencia, E-46071 Valencia, Spain

Contact person: [s.williams@surrey.ac.uk](mailto:s.williams@surrey.ac.uk)

## 1. Key question and initial goals

This proposal aims to study high-spin states in the  $sd$ -shell nuclei  $^{37}\text{Ca}$  and  $^{37}\text{Cl}$ , which will represent the first study of a mirror pair of  $T=3/2$  states at high spin, and of high spin states in an isobaric quartet. The study of  $T=1/2$  states in the  $f7/2$ -shell has led to an understanding of the MED diagrams to an unprecedented level of detail [1-5], due in part to the concomitant increase in theoretical understanding of Coulomb effects provided by the full- $fp$  shell-model calculations in the region [6]. These studies have led to the understanding of the evolution of Coulomb effects, and thus nuclear structure effects, as a function of spin throughout the  $f7/2$ -shell. Phenomena such as the evolution of the one-body part of the Coulomb Matrix Elements due to nuclear shape-changes [2,5], the two-body part due to spatial correlations of the valence protons [1,3] and the observation of the so-called 'J=2 anomaly' [4,6] which may be due to a charge-symmetry breaking term have been observed and reproduced in the shell model calculations.

This proposal extends this study by moving to the  $sd$ -shell, and to greater values of isospin. This represents a significant challenge to our understanding, as the interaction between the different orbitals, and thus radial terms, will require a more detailed treatment of the one-body term. This term will also be affected due to the greater difference in isospin and thus bulk Coulomb terms. An open question is

whether the 'J=2 anomaly' will be observed, and whether it is a nuclear effect, and thus present in the entire nuclear chart, or a phenomenon unique to the f7/2-shell.

## **2. Experiment set-up**

The experiment was proposed to use a  $^{18}\text{Ne}$  beam at an energy of 60 MeV impinging upon a  $1\text{mg}/\text{cm}^2$   $^{24}\text{Mg}$  target. Gamma-rays from the decay of the compound nucleus were detected in EXOGAM. Identification of the reaction products was provided by the Neutron Wall and DIAMANT.  $^{37}\text{Ca}$  is produced via the  $(\alpha,n)$  channel, which can be cleanly selected by gating in offline analysis on the Neutron Wall and DIAMANT data.

## **3. Results and achievements**

The experiment was performed in the autumn of 2005, with 30 UTs of beam-time being awarded. The proposal required a beam current of  $10^7$  pps, which would result in  $3 \times 10^3$  identified alpha-n-gamma events during the experiment. Unfortunately, due to a lower production than initially quoted, and complications due to beam contamination, a beam current of only  $\sim 2 \times 10^5$  pps was provided. This would not have resulted in statistically significant numbers of identified  $^{37}\text{Ca}$  gamma-rays, and so a decision was taken to change the beam species to  $^{16}\text{O}$ . The focus of the experiment was thus moved to the nuclei  $^{38}\text{Ca}$  and  $^{37}\text{K}$ .  $^{38}\text{Ca}$  is an important nucleus for the study of MED effects in the *sd*-shell, as this nucleus provides the empirical *pp* (hole-hole) CME in this region.  $^{37}\text{K}$  is the  $T_z = -1/2$  member of the  $A=37$  isobaric quartet, and as in the case of  $^{38}\text{Ca}$ , has not been studied to high-spin. Many of the initial questions of the proposal can be answered through the study of these nuclei. A very significant data set was provided by this experiment, with over 300Gb of data being recorded.

## **4. Conclusion and perspective**

The data recorded in this experiment are being analysed at present. While the initial aim of the experiment was not achieved, the identification of high-spin states in  $^{37}\text{K}$  and  $^{38}\text{Ca}$  for the first time will answer many of the questions in the proposal.

## **5. References**

- [1] C. D. O'Leary et al., Phys. Rev. Lett. 79, 4349 (1997)
- [2] M. A. Bentley et al., Phys. Lett. B437, 243 (1998)
- [3] M. A. Bentley et al., Phys. Rev. C62, 051303(R) (2000)
- [4] S. J. Williams et al., Phys. Rev. C68, 011301(R) (2003)
- [5] S. M. Lenzi et al., Phys. Rev. Lett. 87, 122501 (2001)
- [6] A. P. Zuker et al., Phys. Rev. Lett. 89, 142502 (2002)

# E512 Laser Spectroscopic Determination of the $^8\text{He}$ Nuclear Charge Radius

P. Mueller<sup>1</sup>, I. A. Sulai<sup>1,2</sup>, A. C. C. Villari<sup>3</sup>, J. A. Alcántara-Núñez<sup>3</sup>, R. Alves-Condé<sup>3</sup>, K. Bailey<sup>1</sup>, G.W. F. Drake<sup>4</sup>, M. Dubois<sup>3</sup>, C. Eléon<sup>3</sup>, G. Gaubert<sup>3</sup>, R. J. Holt<sup>1</sup>, R.V.F. Janssens<sup>1</sup>, N. Lécresse<sup>3</sup>, Z.-T. Lu<sup>1,2</sup>, T. P. O'Connor<sup>1</sup>, M.-G. Saint-Laurent<sup>3</sup>, J.-C. Thomas<sup>3</sup>, and L.-B. Wang<sup>5</sup>

- 1) Physics Division, Argonne National Laboratory, Argonne, Illinois 60439, USA
- 2) Department of Physics and Enrico Fermi Institute, University of Chicago, Chicago, Illinois 60637, USA
- 3) GANIL, CEA/DSM - CNRS/IN2P3, BP 55027, F-14076 Caen Cedex 5, France
- 4) Physics Department, University of Windsor, Windsor, Ontario, Canada N9B 3P4
- 5) Los Alamos National Laboratory, Los Alamos, New Mexico 87545, USA

Contact person: [pmueller@anl.gov](mailto:pmueller@anl.gov)

## 1. Key question and initial goals

This experiment was aimed at a precision measurement of the nuclear charge radius of the neutron-rich isotope  $^8\text{He}$  ( $t_{1/2} = 0.1$  s) to test ab-initio calculations of light nuclei at the 1% level. These calculations provide quantitative predictions of nuclear properties based on empirical nucleon-nucleon and three-nucleon interactions [1,2]. In particular, the differences in charge radii in the helium isotopes are a sensitive probe of halo neutron correlations.

Experimentally, the change in charge radii is extracted from laser spectroscopic measurements of atomic isotope shifts in combination with precision atomic theory of helium. The  $^6\text{He}$  ( $t_{1/2} = 0.8$  s) nuclear charge radius had been measured previously using the same technique and apparatus at the Argonne ATLAS accelerator [3].

## 2. Experimental set-up

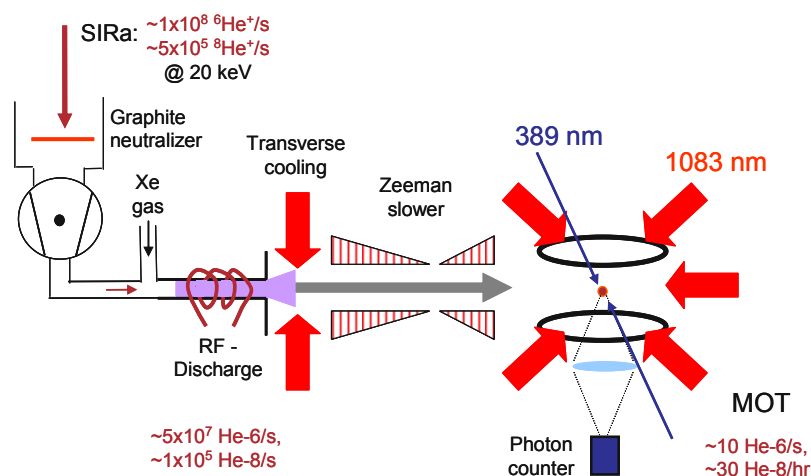


Figure 1: Schematic of the experimental set-up located at the SIRa beam-line. Observed rates of  $^6\text{He}$  and  $^8\text{He}$  are given for the ion beam, the atomic beam source and the magneto-optical trap, respectively.

The measurement was based on laser cooling and trapping of meta-stable helium atoms in a magneto-optical trap (MOT). The experimental setup is schematically shown in Fig. 1.  ${}^6\text{He}$  and  ${}^8\text{He}$  were produced from a primary beam of  ${}^{13}\text{C}$  at 75 A.MeV impinging on the SIRa graphite target and were delivered to the experiment as a mass separated, low-energy (20 keV) ion beam. Subsequently, the ions were neutralized on a hot graphite foil and transferred to a RF driven discharge region, which served as the atomic beam source for meta-stable helium atoms. Laser cooling and trapping was performed by infrared laser beams precisely tuned in frequency to an electronic transition of the respective isotope. The isotope shift measurement was performed on a transition in the near ultra-violet spectral region. Storage, cooling and spatial confinement provided by the MOT allowed for single atom detection and high resolution spectroscopy with one atom at a time. Trapping rates of around  $10 {}^6\text{He}$  atoms per second and  $30 {}^8\text{He}$  atoms per hour were achieved.

### 3. [Results and achievements](#)

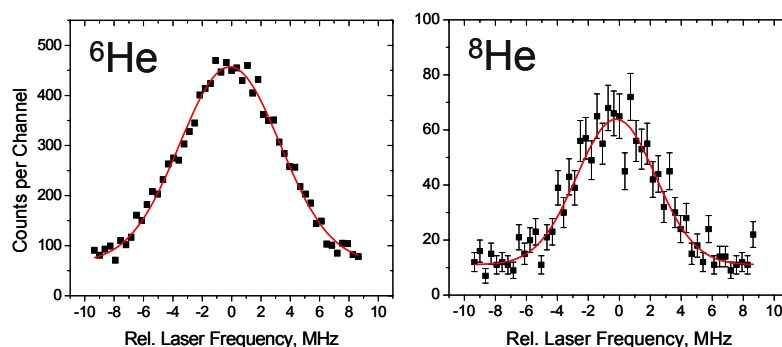


Figure 2: Sample spectra for  ${}^6\text{He}$  and  ${}^8\text{He}$  acquired over two minutes and two hours, respectively.

During seven days of on-line beam time in June 2007, a total of  $\sim 500$   ${}^8\text{He}$  atoms were captured in the MOT and the isotope shift between  ${}^4\text{He}$  and  ${}^8\text{He}$  could be measured to an uncertainty of 63 kHz, well within the goal of  $<80$  kHz set in the proposal. Based on this data, the rms nuclear charge radius of  ${}^8\text{He}$  was determined to be 1.929(26) fm. At the same time, reference measurements on  ${}^6\text{He}$  lead to a charge radius value of 2.068(11) fm in excellent agreement with the earlier result [3]. Sample spectra collected for  ${}^6\text{He}$  and  ${}^8\text{He}$  are shown in Fig. 2.

### 4. [Conclusion and prospective](#)

The reduction in nuclear charge radius going from  ${}^6\text{He}$  to  ${}^8\text{He}$  is an indication for a decrease in neutron correlation of the four excess halo neutrons in  ${}^8\text{He}$  as compared to the two strongly correlated halo neutrons in  ${}^6\text{He}$ . This leads to a more symmetric arrangement of the halo neutrons around the alpha-like core and correspondingly reduces the centre-of-mass motion of the core that carries the nuclear charge. The predictions by ab-initio

calculations were found to agree very well with these experimental observations. The final results of this experiment were published in PRL in December 2007 [4].

In conclusion, this experiment has led to a new precision measurement of nuclear ground state properties in light, neutron rich isotopes and now provides an excellent benchmark for nuclear theories. It also has demonstrated new possibilities for experiments at GANIL involving techniques of laser spectroscopy and neutral atom trapping.

## 5. [References](#)

- [1] S.C. Pieper, V.R. Pandharipande, R.B. Wiringa, and J. Carlson, Phys. Rev. C 64, 014001 (2001).
- [2] E. Caurier and P. Navrátil, Phys. Rev. C 73, 021302(R) (2006).
- [3] L.-B. Wang et al., Phys. Rev. Lett. 93, 142501 (2004).
- [4] P. Mueller et al., Phys. Rev. Lett. 99, 252501 (2007).



# E521S Measurement of $H(^{17}\text{Ne},p)^{17}\text{Ne}$ and $H(^{17}\text{Ne},3p)^{15}\text{O}$ reactions to study $^{18}\text{Na}$ , $^{17}\text{Ne}$ and $^{16}\text{F}$

F. de Oliveira Santos, C. Stodel, M.G. St Laurent, O. Sorlin, J-C Dalouzy, I. Stefan, S. Grévy, J. Mrazek, M. Lewitowicz<sup>1</sup>  
C. Borcea, R. Borcea, A. Buta, F. Negoita<sup>2</sup>  
M.G. Pellegriti<sup>3</sup>  
L. Achouri, J.C. Angelique<sup>4</sup>  
V. Lapoux, E. Berthoumieux<sup>5</sup>  
B. Blank et al. N. Smirnova<sup>6</sup>  
T. Davinson, P. Woods<sup>7</sup>  
D. Jenkins<sup>8</sup>  
G. Imbriani<sup>9</sup>

- 1) GANIL, CEA/DSM - CNRS/IN2P3, BP 55027, F-14076 Caen Cedex 5, France
- 2) Institute of Atomic Physics, P.O. Box MG6, Bucharest-Margurele, Romania
- 3) IPN Orsay, IN2P3-CNRS, Université Paris-Sud, F-91406 Orsay, France
- 4) Laboratoire de Physique Corpusculaire, IN2P3-CNRS, ISMRA et Université de Caen, F-14050 Caen, France
- 5) CEA Saclay, DSM/DAPNIA/SPhN, F-91191 Gif-sur-Yvette, France
- 6) CEN Bordeaux-Gradignan, IN2P3-CNRS, Université de Bordeaux I, F-33170 Gradignan, France
- 7) Department of Physics and Astronomy University of Edinburgh, Edinburgh EH9 3JZ, United Kingdom
- 8) Department of Physics, University of York, Heslington, York YO10 5DD, United Kingdom
- 9) INFN and Dipartimento di Scienze Fisiche, Mostra d' Oltremare, Pad 20, 80125 Napoli, Italy

Contact person: [oliveira@ganil.fr](mailto:oliveira@ganil.fr)

## 1. Key question and initial goals

a) To measure the unknown properties (mass excess, spin, width) of the ground state of  $^{18}\text{Na}$  ( $T_z=-2$ ).

b) To measure the unknown properties (excitation energies, spin and widths) of the low lying excited states in  $^{18}\text{Na}$  and to compare them with the measured properties of the mirror nucleus  $^{18}\text{N}$ .

c) To study the properties (excitation energies, spin, width, branching ratios) of the low-lying states in  $^{17}\text{Ne}$ . This nucleus is a borromean nucleus ( $^{17}\text{Ne} = ^{15}\text{O} + 2p$ ).

d) To search for two-proton emissions from  $^{17}\text{Ne}^*$  and measure the angular distribution of the protons. We want to search for a predicted simultaneous two-proton ( $^2\text{He}$ ) contribution in the two-proton events.

e) There are several astrophysical aspects in the study of  $^{17}\text{Ne}$  (see E442S).

## 2. Experiment set-up

We want to measure the resonant elastic scattering reaction  $H(^{17}\text{Ne},p)^{17}\text{Ne}$  at low energy ( $E \sim 2 \text{ A.MeV}$ ). We used this kind of measurement with several beams (see E400S and E442S for example). This measurement will allow us to measure very precisely (better than 4 keV) the properties (mass excess, excitation energies, spin, widths) of the low-lying states of  $^{18}\text{Na}$  including the ground state.

We also want to measure the inelastic scattering reaction  $H(^{17}\text{Ne},p')^{17}\text{Ne}^*$  with a  $^{17}\text{Ne}$  beam accelerated at higher energy ( $E \sim 5 \text{ A.MeV}$ ). The measurement of the energy of  $p'$  protons will give the position of the low-lying states in  $^{17}\text{Ne}$ . The excited states in  $^{17}\text{Ne}$  may decay in flight by gamma or 2-protons emission. We want to measure the protons with a strip silicon detector. A peculiarity of the method is the 'focusing effect' obtained by the inverse kinematics, which increases drastically the efficiency to detect the charged particles at forward angles. Moreover, we want to measure the angular distribution of the protons. This measurement should constrain spin assignments. In case of  $^2\text{He}$  emission, we may see evidences in the energies or in the angular distribution for the two protons.

### **3. Results and achievements**

Not yet scheduled

### **4. Conclusion and prospective**

Not yet measured

### **5. References**

Tours Symposium on Nuclear Physics VI, Tours 2006, AIP Conference Proceedings 891, to be published  
I. Stefan, PhD thesis, Univ. Caen/Basse-Normandie, 2006, GANIL T 06 02

# E528S Study of the correlations in ${}^6\text{He}$ using nuclear break-up on ${}^{208}\text{Pb}$

M. Assie, D. Beaumel, Y. Blumenfeld, M. Chabot, H. Iwasaki, C. Monrozeau, C. Petrache, J.-A. Scarpaci, F. Skaza, T. Tuna<sup>1</sup>  
A. Chatterjee, D. Lacroix<sup>2</sup>  
J.C. Angélique<sup>3</sup>  
D. Bazin<sup>4</sup>  
M. Fallot<sup>5</sup>  
W. Catford<sup>6</sup>  
D. Mengoni<sup>7</sup>  
J. Nyberg<sup>8</sup>

- 1) IPN Orsay, IN2P3-CNRS, Université Paris-Sud, F-91406 Orsay, France
- 2) GANIL, CEA/DSM - CNRS/IN2P3, BP 55027, F-14076 Caen Cedex 5, France
- 3) Laboratoire de Physique Corpusculaire, IN2P3-CNRS, ISMRA, Université de Caen, F-14050 Caen, France
- 4) NSCL Cyclotron Laboratory, MSU, MI 48824-1321, USA
- 5) SUBATECH, F-44070 Nantes, France
- 6) Department of Physics, University of Surrey, Surrey GU2 7XH, United Kingdom
- 7) University of Camerino, I-62032 Camerino, Italy
- 8) Department of Radiation Sciences, Uppsala University, Uppsala, Sweden

Contact person: [scarpaci@ipno.in2p3.fr](mailto:scarpaci@ipno.in2p3.fr)

## 1. Key question and initial goals

${}^6\text{He}$  is an archetype of three-body problem where the core is surrounded by two correlated neutrons. In the ground state of  ${}^6\text{He}$ , two configurations are predicted to be dominant [1]: a di-neutron configuration where the two neutrons are close to each other, and a cigar configuration where the two neutrons are on opposite side with respect to the core.

These correlations have been investigated by two different reaction mechanisms, namely transfer and Coulomb break-up. On the one hand, recent transfer reaction [2] indicated a dominance of di-neutron configuration. On the other hand, Coulomb break-up studies at 240 A.MeV for  ${}^6\text{He}$  on a lead target showed important final interactions between n-n and  ${}^5\text{He}$ -n. Another experiment [3] done at GANIL measured neutrons emitted in the forward direction in coincidence with  ${}^4\text{He}$ . The “neutron interferometry” method was proposed to differentiate sequential from simultaneous break-up and the relative distance found between the two neutrons ( $\sim 7.7$  fm) seem to indicate a cigar like configuration.

To investigate this issue, we have proposed to use nuclear break-up as reaction mechanism for  ${}^6\text{He}$  on lead, in inverse kinematics using the 20 A.MeV beam from SPIRAL. In the di-neutron configuration, the two neutrons participate to the nuclear break-up so that they will be detected at large angle but with a small relative angle. On the other hand, in the cigar configuration, only one of the neutrons is involved in the nuclear break-up of the projectile while the other neutron will be emitted at low angle, as  ${}^5\text{He}$  is not bound. This

is the reason why the relative angular distribution of the two neutrons emitted is expected to reveal the correlations inside the nucleus.

## 2. Experiment set-up

Using a 20 A.MeV  ${}^6\text{He}$  beam impinging on a  $10\text{mg}/\text{cm}^2$   ${}^{208}\text{Pb}$  target, the nuclear break-up of  ${}^6\text{He}$  was studied.

The  $\alpha$  particles were detected using the CD annular silicon-stripped detector coupled with an annular SiLi detector for particle identification. Neutrons were also detected, in coincidence with a charged particle in the CD detector, using the Neutron Wall at low angles and EDEN at large angles.

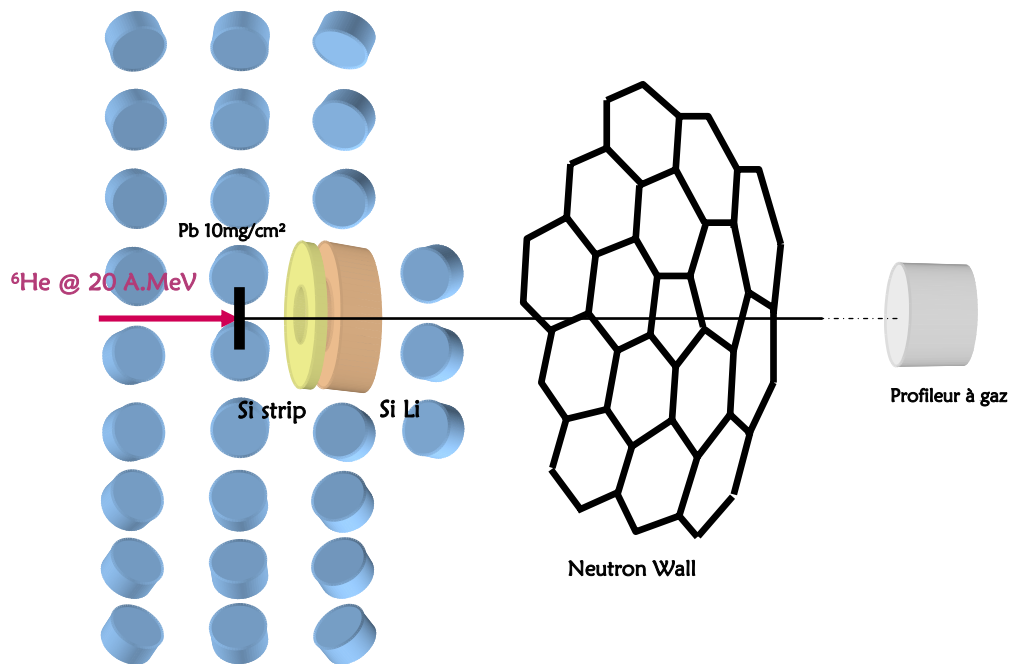


Figure 1: Experimental set-up

## 3. Preliminary results

Preliminary relative angular distribution of two neutrons in coincidence with an  $\alpha$  particle in the CD detector is represented on Fig. 1. The data have been corrected from cross-talk effects in the Neutron Wall. Its effect has been estimated at 30 % of the events using the  ${}^{12}\text{C}$  runs.

These results still need to be corrected from the acceptance of our detectors and also need to be compared with a non-correlated distribution. The analysis is under process.

## 4. Conclusion and prospective

The correlated and uncorrelated distribution in relative angle of the neutrons enables to calculate the correlation function, which will be

comparable to theoretical calculations. These calculations including two-body correlations beyond mean-field are under process.

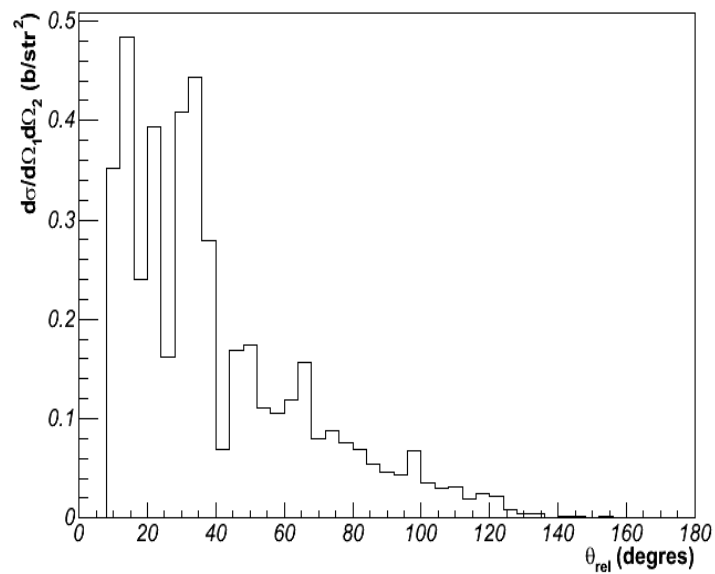


Figure 2: Relative Angular distribution of two neutrons corrected from possible crosstalk events

## 5. [References](#)

- [1] M.V. Zhukov et al., Phys. Rep. 231, 151 (1993)
- [2] D.T. Khoa et al., Phys. Lett. B595 (2004)
- [3] F.M. Marquès et al., Phys. Rev. C64, 061301 R (2001)



## C. Publication list



## I. Experiment and theory

### 2008

#### **Structure of the $N = 27$ isotones derived from the $^{44}\text{Ar}(d, p)^{45}\text{Ar}$ reaction**

L. Gaudefroy, O. Sorlin, F. Nowacki, D. Beaumel, Y. Blumenfeld, Z. Dombrádi, S. Fortier, S. Franchoo, S. Grévy, F. Hammache, K. W. Kemper, K. L. Kratz, M. G. St. Laurent, S. M. Lukyanov, L. Nalpas, A. N. Ostrowski, Yu.-E. Penionzhkevich, E. C. Pollacco, P. Roussel, P. Roussel-Chomaz, D. Sohler, M. Stanoiu, and E. Tryggestad, *Physical Review C* **78**, 034307 (2008)

#### **1n and 2n Transfer With the Borromean Nucleus $^6\text{He}$ Near the Coulomb Barrier**

A. Chatterjee, A. Navin, A. Shrivastava, S. Bhattacharyya, M. Rejmund, N. Keeley, V. Nanal, J. Nyberg, R. G. Pillay, K. Ramachandran, I. Stefan, D. Bazin, D. Beaumel, Y. Blumenfeld, G. de France, D. Gupta, M. Labiche, A. Lemasson, R. Lemmon, R. Raabe, J. A. Scarpaci, C. Simenel and C. Timis, *Physical Review Letters* **101**, 032701 (2008)

#### **Nuclear structure at the proton drip line: Advances with nuclear decay studies**

B. Blank, and M.J.G. Borge, *Progress in Particle and Nuclear Physics* **60**, 403 (2008)

#### **From Ge(Li) detectors to gamma-ray tracking arrays-50 years of gamma spectroscopy with germanium detectors**

J. Eberth and J. Simpson, *Progress in Particle and Nuclear Physics* **60**, 283 (2008)

#### **Status of the LPCTrap facility at GANIL**

F. Duval, A. Méry, G. Ban, D. Durand, X. Fléchar, M. Labalme, E. Liénard, F. Mauger, O. Naviliat-Cuncic, D. Rodríguez-Rubiales and J.C. Thomas, *Nuclear Instruments and Methods in Physics Research Section B266*, 4537 (2008)

#### **MAYA: An active target detector for the study of extremely exotic nuclei**

H. Savajols, C.E. Demonchy, W. Mittig, M. Caamano, M. Chartier, D. Cortina-Gil, A. Gillibert, T. Roger, P. Roussel-Chomaz and I. Tanihata, *Nuclear Instruments and Methods in Physics Research Section B266*, 4583 (2008)

#### **Étude des corrélations dans la dissociation de $^8\text{He}$**

B. Laurent, Ph.D. thesis, Université de Caen Basse-Normandie, Laboratoire de Physique Corpusculaire de Caen, 2008

### 2007

#### **Nuclear Charge Radius of $^8\text{He}$**

P. Mueller, I. A. Sulai, A. C. C. Villari, J. A. Alcántara-Núñez, R. Alves-Condé, K. Bailey, G. W. F. Drake, M. Dubois, C. Eléon, G. Gaubert, R. J. Holt, R. V. F. Janssens, N. Lecesne, Z.-T. Lu, T. P. O'Connor, M.-G. Saint-Laurent, J.-C. Thomas and L.-B. Wang, *Physical Review Letters* **99**, 252501 (2007)

#### **Comment on "Reduction of the spin-orbit splittings at the $n=28$ shell closure"**

L. Gaudefroy, O. Sorlin, D. Beaumel, Y. Blumenfeld, Z. Dombrádi, S. Fortier, S. Franchoo, M. Gélín, J. Gibelin, S. Grévy, F. Hammache, F. Ibrahim, K. W. Kemper, K.-L. Kratz, S. M. Lukyanov, C. Monrozeau, L. Nalpas, F. Nowacki, A. N. Ostrowski, T. Otsuka, Yu.-E. Penionzhkevich, J. Piekarewicz, E. C. Pollacco, P. Roussel-Chomaz, E. Rich, J. A. Scarpaci, M. G. Saint-Laurent, D. Sohler, M. Stanoiu, T. Suzuki, E. Tryggestad, and D. Verney, *Physical Review Letters* **99**, 099202 (2007)

### **Resonance State in $^7\text{H}$**

M. Caamaño, D. Cortina-Gil, W. Mittig, H. Savajols, M. Chartier, C. E. Demonchy, B. Fernández, M. B. Gómez Hornillos, A. Gillibert, B. Jurado, O. Kiselev, R. Lemmon, A. Obertelli, F. Rejmund, M. Rejmund, P. Roussel-Chomaz, and R. Wolski, *Physical Review Letters* **99**, 062502 (2007)

### **Probing the $^8\text{He}$ ground state via the $^8\text{He}(p,t)^6\text{He}$ reaction**

N. Keeley, F. Skaza, V. Lapoux, N. Alamanos, F. Auger, D. Beaumel, E. Becheva, Y. Blumenfeld, F. Delaunay, A. Drouart, A. Gillibert, L. Giot, K.W. Kemper, L. Nalpas, A. Pakou, E.C. Pollacco, R. Raabe, I. P. Roussel-Chomaz, K. Rusek, J.-A. Scarpaci, J.-L. Sida, S. Stepantsov and R. Wolski, *Physics Letters B* **646**, 222 (2007)

### **Shape coexistence in neutron-deficient krypton isotopes**

E. Clément, A. Gørgen, W. Korten, E. Bouchez, A. Chatillon, J.-P. Delaroche, M. Girod, H. Goutte, A. Hürstel, Y. Le Coz, A. Obertelli, S. Péru, Ch. Theisen, J. N. Wilson, M. Zielińska, C. Andreoiu, F. Becker, P. A. Butler, J. M. Casandjian, W. N. Catford, T. Czosnyka, G. de France, J. Gerl, R.-D. Herzberg, J. Iwanicki, D. G. Jenkins, G. D. Jones, P. J. Napiorkowski, G. Sletten and C. N. Timis, *Physical Review C* **75**, 054313 (2007)

### **Single particle structure of exotic nuclei with transfer reactions**

B. Fernández-Domínguez, R.C. Lemmon, C. Timis, M. Labiche, W.N. Catford, M. Chartier, N.I. Ashwood, N. Amzal, T.D. Baldwin, M. Burns, L. Caballero, R. Chapman, N. Curtis, G. de France, M. Freer, W. Gelletly, X. Liang, N.A. Orr, S.D. Pain, V.P.E. Pucknell, M. Rejmund, B. Rubio, H. Savajols, O. Sorlin, K. Spohr, C. Thiesen and D.D. Warner, *Progress in Particle and Nuclear Physics* **59**, 389 (2007)

### **Fusion and direct reactions of halo nuclei at energies around the Coulomb barrier**

N. Keeley, R. Raabe, N. Alamanos, J.-L. Sida, *Progress in Particle and Nuclear Physics* **59**, 579 (2007)

### **Low-lying states and structure of the exotic $^8\text{He}$ via direct reactions on the proton**

F. Skaza, V. Lapoux, N. Keeley, N. Alamanos, F. Auger, D. Beaumel, E. Becheva, Y. Blumenfeld, F. Delaunay, A. Drouart, A. Gillibert, L. Giot, E. Khan, L. Nalpas, A. Pakou, E. Pollacco, R. Raabe, P. Roussel-Chomaz, K. Rusek, J.-A. Scarpaci, J.-L. Sida, S. Stepantsov and R. Wolski, *Nuclear Physics A* **788**, 260 (2007)

### **SPIRAL at GANIL: Latest Results and Plans for the Future**

A. C. C. Villari, C. Eleon, R. Alves-Condé, J.C. Angelique, C. Barué, C. Canet, M. Dubois, M. Dupuis, J.L. Flambard, G. Gaubert, P. Jardin, N. Lecesne, P. Leherissier, F. Lemagnen, R. Leroy, L. Maunoury, J.Y. Pacquet, F. Pellemoine, M.G. Saint-Laurent, C. Stodel and J.-C. Thomas, *Nuclear Physics A* **787**, 126c (2007)

### **The LPCTrap facility for in-trap decay experiments**

D. Rodríguez, G. Ban, D. Durand, F. Duval, X. Fléchar, M. Herbane, E. Liénard, F. Mauger, A. Méry, O. Naviliat-Cuncic and J. -C. Thomas, *Hyperfine Interactions* **174**, 15 (2007)

### **MAYA: An active-target detector for binary reactions with exotic beams**

C.E. Demonchy, M. Caamaño, H. Wang, W. Mittig, P. Roussel-Chomaz, H. Savajols, M. Chartier, D. Cortina-Gil, A. Fomichev, G. Frémont, P. Gangnant, A. Gillibert, L. Giot, M.S. Golovkov, B. Jurado, J.F. Libin, A. Obertelli, E. Pollaco, A. Rodin, Ch. Spitaels, S. Stepantsov, G. Ter-Akopian and R. Wolski, *Nuclear Instruments and Methods in Physics Research Section A* **583**, 341 (2007)

#### **MAYA, a gaseous active target**

C.E. Demonchy, W. Mittig, H. Savajols, P. Roussel-Chomaz, M. Chartier, B. Jurado, L. Giot, D. Cortina-Gil, M. Caamaño, G. Ter-Akopian, A. Fomichev, A. Rodin, M.S. Golovkov, S. Stepantsov, A. Gillibert, E. Pollaco, A. Obertelli, H. Wang, *Nuclear Instruments and Methods in Physics Research Section A* **573**, 145 (2007)

#### **The search for $^7\text{H}$**

M. Caamaño, D. Cortina-Gil, W. Mittig, H. Savajols, M. Chartier, C. E. Demonchy, B. Fernández, A. Gillibert, M. B. Gómez-Hornillos, B. Jurado, O. Kiselev, R. Lemmon, A. Obertelli, F. Rejmund, M. Rejmund, P. Roussel-Chomaz and R. Wolski, *The European Physical Journal - Special Topics* **150**, 9 (2007)

#### **In-beam $\gamma$ spectroscopy using DIC with a radioactive Ne beam**

G. Benzoni, F. Azaiez, S. Leoni, S. Battacharyya, R. Borcea, A. Bracco, L. Corradi, D. Curien, G. De France, Zs. Dombrádi, E. Fioretto, S. Franchoo, S. Grevy, F. Ibrahim, S. Iulian, G. Mukherjee, A. Navin, G. Pollarolo, N. Redon, P. H. Regan, M. Rejmund, C. Schmitt, G. Sletten, D. Sohler, M. Stanoiu, S. Szilner and D. Verney, *The European Physical Journal - Special Topics* **150**, 83 (2007)

#### **Shape coexistence in $^{74}\text{Kr}$ and $^{76}\text{Kr}$**

A. Görgen, E. Clément, W. Korten, E. Bouchez, A. Chatillon, A. Hürstel, Y. Le Coz, Ch. Theisen, J. N. Wilson, M. Zielinska, C. Andreoiu, F. Becker, P. Butler, J. M. Casandjian, W. N. Catford, T. Czosnyka, G. de France, J. Gerl, R.-D. Herzberg, J. Iwanicki, D. G. Jenkins, G. D. Jones, P. J. Napiorkowski, G. Sletten and C. Timis, *The European Physical Journal - Special Topics* **150**, 117 (2007)

#### **Study of $N = 16$ for Ne isotopes**

A. Gillibert, A. Obertelli, N. Alamanos, M. Alvarez, F. Auger, R. Dayras, A. Drouart, G. de France, B. Jurado, N. Keeley, V. Lapoux, W. Mittig, X. Mougeot, L. Nalpas, A. Pakou, N. Patronis, E. Pollaco, F. Rejmund, M. Rejmund, P. Roussel-Chomaz, H. Savajols, F. Skaza and Ch. Theisen, *The European Physical Journal - Special Topics* **150**, 161 (2007)

#### **Search for tensor couplings in the weak interaction**

A. Méry, G. Ban, J. Blicke, D. Durand, F. Duval, X. Fléchar, M. Herbane, M. Labalme, Y. Lemièrre, E. Liénard, F. Mauger, O. Naviliat-Cuncic, D. Rodríguez and J. C. Thomas, *The European Physical Journal - Special Topics* **150**, 385 (2007)

#### **The LPCTrap facility: A transparent Paul Trap for the search of exotic couplings in the beta decay of radioactive $^6\text{He}^+$ ions**

X. Fléchar, G. Ban, J. Blicke, D. Durand, F. Duval, M. Herbane, M. Labalme, Y. Lemièrre, E. Liénard, F. Mauger, A. Méry, O. Naviliat-Cuncic, J.-C. Thomas and D. Rodríguez, *J. Phys., Conf. Ser.* **58**, 431 (2007)

#### **Etude de la structure des noyaux non liés $^{7,9}\text{He}$ et $^{10}\text{Li}$**

H. Al Falou, Ph.D. thesis, Université de Caen Basse-Normandie, Laboratoire de Physique Corpusculaire de Caen, 2007

### **Reduction of the spin-orbit splittings at the N=28 shell closure**

L. Gaudefroy, O. Sorlin, D. Beaumel, Y. Blumenfeld, Z. Dombrádi, S. Fortier, S. Franchoo, M. Gélín, J. Gibelin, S. Grévy, F. Hammache, F. Ibrahim, K. W. Kemper, K.-L. Kratz, S. M. Lukyanov, C. Monrozeau, L. Nalpas, F. Nowacki, A. N. Ostrowski, T. Otsuka, Yu.-E. Penionzhkevich, J. Piekarewicz, E. C. Pollacco, P. Roussel-Chomaz, E. Rich, J. A. Scarpaci, M. G. Saint-Laurent, D. Sohler, M. Stanoiu, T. Suzuki, E. Tryggestad, and D. Verney, *Physical Review Letters* **97**, 092501 (2006)

### **Experimental evidence for subshell closure in $^8\text{He}$ and indication of a resonant state in $^7\text{He}$ below 1 MeV**

F. Skaza, V. Lapoux, N. Keeley, N. Alamanos, E. C. Pollacco, F. Auger, A. Drouart, A. Gillibert, D. Beaumel, E. Becheva, Y. Blumenfeld, F. Delaunay, L. Giot, K. W. Kemper, L. Nalpas, A. Obertelli, A. Pakou, R. Raabe, P. Roussel-Chomaz, J.-L. Sida, J.-A. Scarpaci, S. Stepantsov, and R. Wolski, *Physical Review C* **73**, 044301 (2006)

### **Shell gap reduction in neutron-rich N=17 nuclei**

A. Obertelli, A. Gillibert, N. Alamanos, M. Alvarez, F. Auger, R. Dayras, A. Drouart, G. de France, B. Jurado, N. Keeley, V. Lapoux, W. Mittig, X. Mougeot, L. Nalpas, A. Pakou, N. Patronis, E.C. Pollacco, F. Rejmund, M. Rejmund, P. Roussel-Chomaz, H. Savajols, F. Skaza and Ch. Theisen, *Physics Letters B* **633**, 33 (2006)

### **Study of the N = 28 shell closure in the Ar isotopic chain - A SPIRAL experiment for nuclear astrophysics**

L. Gaudefroy, O. Sorlin, D. Beaumel, Y. Blumenfeld, Z. Dombrádi, S. Fortier, S. Franchoo, M. Gélín, J. Gibelin, S. Grévy, F. Hammache, F. Ibrahim, K. Kemper, K. L. Kratz, S. M. Lukyanov, C. Monrozeau, L. Nalpas, F. Nowacki, A. N. Ostrowski, Yu. -E. Penionzhkevich, E. Pollacco, P. Roussel-Chomaz, E. Rich, J. A. Scarpaci, M. G. St. Laurent, T. Rauscher, D. Sohler, M. Stanoiu, E. Tryggestad and D. Verney, *European Physical Journal A* **27**, 309 (2006)

### **Probing the maximally deformed light rare-earth region around the drip-line nucleus $^{130}\text{Sm}$**

M. Petri, E.S. Paul, P.J. Nolan, A.J. Boston, R.J. Cooper, M.R. Dimmock, S. Gros, B.M. McGuirk, H.C. Scraggs, G. Turk, B. Rossé, M. Meyer, N. Redon, Ch. Schmitt, O. Stézowski, D. Guinet, Ph. Lantesse, G. De France, S. Bhattachasya, G. Mukherjee, F. Rejmund, M. Rejmund, H. Savajols, J. N. Scheurer, A. Astier, I. Deloncle, A. Prévost, B.M. Nyakó, J. Gál, J. Molnár, J. Timár, L. Zolnai, K. Juhász, V.F.E. Pucknell, R. Wadsworth, P. Joshi, G. La Rana, R. Moro, M. Trotta, E. Vardaci, G. Hackman and G. Ball, *Phys. Scr.* **T125**, 214 (2006)

### **The LPCTrap experiment: measurement of the $\beta$ - $\nu$ angular correlation in $^6\text{He}$ using a transparent Paul trap**

E. Liénard, G. Ban, J. Blicq, D. Durand, F. Duval, X. Fléchar, M. Herbane, M. Labalme, Y. Lemièrre, F. Mauger, A. Méry, O. Naviliat-Cuncic, D. Rodríguez and J. C. Thomas, *Hyperfine Interactions* **172**, 29 (2006)

### **The LPCTrap facility: A novel transparent Paul trap for high-precision experiments**

D. Rodríguez, A. Méry, G. Ban, J. Brégeault, G. Darius, D. Durand, X. Fléchar, M. Herbane, M. Labalme, E. Liénard, F. Mauger, Y. Merrer, O. Naviliat-Cuncic, J.C. Thomas, C. Vandamme, *Nuclear Instruments and Methods in Physics Research Section A* **565**, 876 (2006)

### **A cryogenic target for direct reaction studies with exotic beams**

P. Dolégiéviez, A. Gillibert, W. Mittig, X. Mougeot, A. Obertelli, F. de Oliveira, M. Ozille, Ph. Robillard, P. Roussel-Chomaz, H. Savajols, *Nuclear Instruments and Methods in Physics Research Section A* **564**, 32 (2006)

## **Spectroscopie par diffusion élastique résonante de $^{15}\text{O}$ et nouveau chemin de réaction dans le cycle CNO**

G.I. Stefan, Ph.D. thesis, Université de Caen Basse-Normandie, GANIL T 06 02, Caen, 2006

## **Détection $\gamma$ et faisceaux radioactifs : recherche de noyaux exotiques très déformés**

B. Rossé, Ph.D. thesis, Université Claude Bernard – Lyon I, Institut de Physique Nucléaire de Lyon, 2006

## **Etude de la coexistence de formes dans les isotopes légers du krypton et du sélénium par excitation Coulombienne de faisceaux radioactifs**

E. Clément, Ph.D. thesis, Université Paris XI, DAPNIA-06-05-T, 2006

## **Production and characterization of the $^7\text{H}$ resonance,**

M. Caamaño Fresco, Ph.D. thesis, Universidade de Santiago de Compostela, 2006

## **2005**

### **Important pickup coupling effect on $^8\text{He}(p,p)$ elastic scattering**

F. Skazaa, N. Keeley, V. Lapoux, N. Alamanos, F. Auger, D. Beaumel, E. Becheva, Y. Blumenfeld, F. Delaunay, A. Drouart, A. Gillibert, L. Giot, K.W. Kemper, R.S. Mackintosh, L. Nalpas, A. Pakou, E.C. Pollacco, R. Raabe, I. P. Roussel-Chomaz, J.-A. Scarpaci, J.-L. Sida, S. Stepantsov and R. Wolski, *Physics Letters B* **619**, 82 (2005)

### **Study of $^{19}\text{Na}$ at SPIRAL**

F. de Oliveira Santos, P. Himpe, M. Lewitowicz, I. Stefan, N. Smirnova, N. L. Achouri, J. C. Angélique, C. Angulo, L. Axelsson, D. Baiborodin, F. Becker, M. Bellegui, E. Berthoumieux, B. Blank, C. Borcea, A. Cassimi, J. M. Daugas, G. de France, F. Dembinski, C. E. Demonchy, Z. Dlouhy, P. Dolégiéviez, C. Donzaud, G. Georgiev, L. Giot, S. Grévy, D. Guillemaud Mueller, V. Lapoux, E. Liénard, M. J. Lopez Jimenez, K. Markenroth, I. Matea, W. Mittig, F. Negoita, G. Neyens, N. Orr, F. Pougheon, P. Roussel Chomaz, M. G. Saint Laurent, F. Sarazin, H. Savajols, M. Sawicka, O. Sorlin, M. Stanoiu, C. Stodel, G. Thiamova, D. Verney and A. C. C. Villari, *European Physical Journal A* **24**, 237 (2005)

### **Study of $^{45}\text{Ar}$ through (d,p) reaction at SPIRAL**

L. Gaudefroy, O. Sorlin, D. Beaumel, Y. Blumenfeld, Z. Dombrádi, S. Fortier, S. Franchoo, M. Gélín, J. Gibelin, S. Grévy, F. Hammache, F. Ibrahim, K. Kemper, K.L. Kratz, S.M. Lukyanov, C. Monrozeau, L. Nalpas, F. Nowacki, A.N. Ostrowski, Y.-E. Penionzhkevich, E. Pollaco, P. Roussel-Chomaz, E. Rich, J.A. Scarpaci, M.G. St Laurent, D. Sohler, M. Stanoiu, E. Trygggestadt and D. Verney, *Journal of Physics G* **31**, S1623 (2005)

### **Nucleon transfer via (d,p) using TIARA with $^{24}\text{Ne}$ radioactive beam**

W.N. Catford, C.N. Timis, R.C. Lemmon, M. Labiche, N.A. Orr, L. Caballero, R. Chapman, M. Freer, M. Chartier, H. Savajols, M. Rejmund, N. Amzal, N.I. Ashwood, T.D. Baldwin, Burns M., N. Curtis, G. De France, W. Gelletly, X. Liang, S.D. Pain, V.P.E. Pucknell, B. Rubio, O. Sorlin, K. Spohr, C. Thiesen, D.D. Warner, *Journal of Physics G* **31**, S1655 (2005)

### **Spectroscopy of $^{212}\text{Po}$ and $^{213}\text{At}$ using a $^8\text{He}$ radioactive beam and EXOGAM**

A.B. Garnsworthy, N.J. Thompson, Z. Podolyák, P.M. Walker, S. Williams, G. Dracoulis, G. De France, G.J. Lane, K. Andgren, A.M. Bruce, A.P. Byrne, W.N. Catford, B. Cederwall, G.A. Jones, B. Mcguirk, S. Mandal, E.S. Paul, V. Pucknell, N. Redon, B. Rosse, R.J. Senior and G. Sletten, *Journal of Physics G* **31**, S1851 (2005)

### **Mass measurements with the CIME cyclotron at GANIL**

M.B.G. Hornillos, M. Chartier, W. Mittig, B. Blank, F. Chautard, C. E. Demonchy, A. Gillibert, B. Jacquot, B. Jurado, N. Lécèsne, A. L'Épine-Szily, N.A. Orr, P. Roussel-Chomaz, H. Savajols and A. C. C. Villari, *Journal of Physics G* **31**, S1869 (2005)

**Reactions induced beyond the dripline at low energy by secondary beams**

W. Mittig, C.E. Demonchy, H. Wang, P. Roussel-Chomaz, B. Jurado, M. Gélín, H. Savajols, A. Fomichev, A. Rodin, A. Gillibert, A. Obertelli, M.D. Cortina-Gil, M. Caamano, M. Chartier, *European Physical Journal A* **25**, 263 (2005)

**First experiments on transfer with radioactive beams using the TIARA array**

W.N. Catford, R. C. Lemmon, M. Labiche, C.N. Timis, N.A. Orr, L. Caballero, R. Chapman, M. Chartier, M. Rejmund, H. Savajols and the TIARA Collaboration, *European Physical Journal A* **25**, 245 (2005)

**Reactions induced beyond the dripline at low energy by secondary beams**

W. Mittig, C. E. Demonchy, H. Wang, P. Roussel-Chomaz, B. Jurado, M. Gelin, H. Savajols, A. Fomichev, A. Rodin, A. Gillibert, A. Obertelli, M. D. Cortina-Gil, M. Caama no, M. Chartier and R. Wolski, *European Physical Journal A* **25**, 263 (2005)

**Multineutron clusters - Perspectives to create nuclei 100% neutron-rich**

M. Marqués Moreno, *European Physical Journal A* **25**, 311 (2005)

**The LPCTrap for the measurement of the  $\beta$ - $\nu$  correlation in  ${}^6\text{He}$**

D. Rodríguez, A. Méry, G. Darius, M. Herbane, G. Ban, P. Delahaye, D. Durand, X. Fléchar, M. Labalme, E. Liénard, F. Mauger and O. Naviliat-Cuncic, *European Physical Journal A* **25**, 705 (2005)

**Measurement of the beta-neutrino angular correlation in nuclear beta-decay**

G. Ban, G. Darius, P. Delahaye, D. Durand, X. Fléchar, M. Herbane, M. Labalme, E. Liénard, F. Mauger, A. Méry, O. Naviliat-Cuncic, and D. Rodríguez, *Nuclear Physics A* **752**, 67c (2005)

**La fermeture de sous-couche N = 16**

A. Obertelli, Ph.D. thesis, Université Paris XI, DAPNIA -05-09-T, 2005

**Etude de la fermeture de couche N=28 : implication astrophysique. Spectroscopie  $\beta\gamma$  de noyaux riches en neutrons**

L. Gaudefroy, Ph.D. thesis, Université Paris XI, IPNO-T-05-07, 2005

**Le tétraneutron: mythe ou réalité ? Nouvelle analyse à partir de la cassure de  ${}^8\text{He}$  sur cible de carbone**

V. Bouchat, Ph.D. thesis, Université Libre de Bruxelles, 2005

## 2004

**Direct and compound reactions induced by unstable helium beams near the Coulomb barrier**

A. Navin, V. Tripathi, Y. Blumenfeld, V. Nanal, C. Simenel, J. M. Casandjian, G. de France, R. Raabe, D. Bazin, A. Chatterjee, M. Dasgupta, S. Kailas, R. C. Lemmon, K. Mahata, R. G. Pillay, E. C. Pollacco, K. Ramachandran, M. Rejmund, A. Shrivastava, J.-L. Sida, and E. Tryggestad, *Physical Review C* **70**, 044601 (2004)

**Physics with SPIRAL and SPIRAL 2 status of the EURISOL project**

M. Lewitowicz, *Nuclear Physics A* **734**, 645 (2004)

## Physics opportunities with SPIRAL and SPIRAL 2

M. Lewitowicz, *Nuclear Physics A* 746, 118 (2004)

**Etude de réactions et d'états isobariques analogues dans le système  $^8\text{He}+p$ , à basse énergie, à l'aide de la cible active MAYA**, C.-E. DEMONCHY, Ph.D. thesis, Université de Caen Basse-Normandie, GANIL T 03 06, Caen, 2004

**Structure du noyau exotique  $^8\text{He}$  par les réactions directes  $^8\text{He}(p,p')^8\text{He}$ ,  $^8\text{He}(p,d)^7\text{He}$  et  $^8\text{He}(p,t)^6\text{He}$**

F. Skaza, Ph.D. thesis, Université Paris XI, DAPNIA -04-13-T, 2004

## 2003

### Gamma-ray spectroscopy studies at GANIL: Status and perspectives

G. de France, *European Physical Journal A* 20, 59 (2003)

### First radioactive beam Coulomb excitation experiments on SPIRAL

E. Bouchez, A. Chatillon, A. Huerstel, W. Korten, Y. Le Coz, Ch. Theisen, J.M. Casandjian, G. de France, F. Becker, J. Gerl, T. Czosnyka, J. Iwanicki, M. Zielinska, P. Butler, R. Herzberg, D. Jenkins, G. Jones, G. Sletten, W. Catford, C. Timis, *Acta Physica Polonica B* 34, 2443 (2003)

### $\gamma$ -ray spectroscopy with a $^8\text{He}$ beam

Zs. Podolyák, P. M. Walker, H. Mach, G. de France, G. Sletten, F. Azaiez, J. M. Casandjian, B. Cederwall, D. M. Cullen, Zs. Dombrádi, G. D. Dracoulis, L. M. Fraile, S. Franchoo, H. Fynbo, M. Górski, Y. Kopatch, G. J. Lane, S. Mandal, L. Milechina, J. Molnár, C. O'Leary, W. Plocienniko, V. Pucknell, P. Raddonn, N. Redonq, E. Ruchowskao, M. Stanoiuc, O. Tengblad, C. Wheldon and R. Wood, *Nuclear Instruments and Methods in Physics Research Section A* 511, 354 (2003)

### First results at SPIRAL-GANIL

A. C. C. Villari and the SPIRAL group, *Nuclear Instruments and Methods in Physics Research B* 204, 31 (2003)

### Structure of light exotic nuclei $^6,8\text{He}$ and $^{10,11}\text{C}$ from $(p,p')$ reactions

V. Lapoux, N. Alamanos, F. Auger, A. Drouart, A. Gillibert, C. Jouanne, G. Lobo, L. Nalpas, A. Obertelli, E. Pollacco, R. Raabe, F. Skaza, J.-L. Sida, D. Beaumel, E. Becheva, Y. Blumenfeld, F. Delaunay, L. Giot, E. Khan, A. Lagoyannis, A. Musumarra, P. Navrátil, A. Pakou, P. Roussel-Chomaz, H. Savajols, J. -A. Scarpaci, S. Stepantsov, R. Wolski and T. Zerguerras, *Nuclear Physics A* 722, c49 (2003)

### Spectroscopy of drip-line nuclei with fast and slow radioactive nuclear beams at the GANIL/SPIRAL facility

Marek Lewitowicz, *Nuclear Physics A* 722, c67 (2003)

### SPIRAL - a new radioactive beam facility

M. Lieuvin, *Nukleonika* 48, S149 (2003)

### Recherche de grandes déformations nucléaires dans des noyaux exotiques en spin et en isospin à l'aide des multidétecteurs gamma EUROBALL IV et EXOGAM

Prévost A., Ph.D. thesis, Université Claude Bernard - Lyon I, Institut de Physique Nucléaire de Lyon, 2003

## 2002

### **What is next after SPIRAL at GANIL?**

D. Ridikas, W. Mittig and A. C. C. Villari, *Nuclear Physics A* **701**, 343c (2002)

## 2001

### **Radioactive beams in France**

A.C. Mueller, *Progress in Particle and Nuclear Physics* **46**, 359 (2001)

## 1998

### **The spiral project at GANIL and future opportunities**

W. Mittig, *Journal of Physics G* **24**, 1131 (1998)

## 1997

### **News from the SPIRAL project at GANIL**

A. C. C. Villari and the SPIRAL group, *Nuclear Physics A* **616**, 21c (1997)

## II. Beam development

2008

### **Measurement of the Ar diffusion coefficient in graphite at high temperature by the ISOL method**

C. Eléon, P. Jardin, J.C. Thomas, M.G. Saint-Laurent, C. Huet-Equilbec, R. Alvès-Condé, J.C. Angélique, D. Boilley, J. Cornell, M. Dubois, H. Franberg, G. Gaubert, B. Jacquot, U. Köster, R. Leroy, L. Maunoury, N. Orr, J.Y. Pacquet, F. Pellemoine, C. Stodel, M. Turrion, *Nuclear Instruments and Methods in Physics Research Section B266, 4284 (2008) – Proceedings of the XV<sup>th</sup> International Conference on Electromagnetic Isotope Separators and Techniques Related to their Applications, EMIS 2007, Deauville, France, 2007*

### **Set-up for systematic measurements of diffusion of atoms from ISOL targets**

P. Jardin, M.G. Saint-Laurent, F. Durantel, C. Eléon, C. Huet-Equilbec, R. Alvès Condé, J. Cornell, G. Gaubert, J.Y. Pacquet, F. Pellemoine and M. Ozille, *Nuclear Instruments and Methods in Physics Research Section B266, 4322 (2008) – Proceedings of the XV<sup>th</sup> International Conference on Electromagnetic Isotope Separators and Techniques Related to their Applications, EMIS 2007, Deauville, France, 2007*

### **Development of a surface ionization source for the production of radioactive alkali ion beams in SPIRAL**

C. Eléon, P. Jardin, G. Gaubert, M.-G. Saint-Laurent, J. Alcántara-Núñez, R. Alvès Condé, C. Barué, D. Boilley, J. Cornell, P. Delahaye, M. Dubois, B. Jacquot, P. Leherissier, R. Leroy, G. Lhersonneau, M. Marie-Jeanne, L. Maunoury, J.Y. Pacquet, F. Pellemoine, C. Pierret, J.C. Thomas and A. C. C. Villari, *Nuclear Instruments and Methods in Physics Research Section B266, 4362 (2008) – Proceedings of the XV<sup>th</sup> International Conference on Electromagnetic Isotope Separators and Techniques Related to their Applications, EMIS 2007, France, Deauville, 2007*

### **Status report of stable and radioactive ion beam production at GANIL**

G. Gaubert, C. Barué, C. Canet, J. C. Cornell, M. Dubois, M. Dupuis, C. Eleon, J. L. Flambard, R. Frigot, P. Jardin, C. Leboucher, N. Lecesne, P. Leherissier, F. Lemagnen, R. Leroy and J. Y. Pacquet, *Review of Scientific Instruments 79, 02A309 (2008) - Proceedings of the 12<sup>th</sup> International Conference on Ion Sources, Jeju, Korea, 2007*

### **Development of a 1+/N+ setup for the production of multicharged radioactive alkali ions in SPIRAL**

C. Eléon, G. Gaubert, P. Jardin, M.-G. Saint-Laurent, J. Alcantara, R. Alvès Condé, C. Barué, D. Boilley, J. C. Cornell, P. Delahaye, M. Dubois, B. Jacquot, P. Leherissier, R. Leroy, G. Lhersonneau, M. Marie-Jeanne, L. Maunoury, J.-Y. Pacquet, F. Pellemoine, C. Pierret, J. C. Thomas and A. C. C. Villari, *Review of Scientific Instruments 79, 02A904 (2008) - Proceedings of the 12<sup>th</sup> International Conference on Ion Sources, Jeju, Korea, 2007*

### **Preliminary results of the ion extraction simulations applied to the MONO1000 and SUPERSHYPIE electron cyclotron resonance ion sources**

C. Pierret, L. Maunoury, S. Biri, J. Y. Pacquet, O. Tuske, and O. Delferriere

## 2007

### **ECR Ion Sources for Radioactive Ion Beam Production**

P. Jardin, C. Canet, J. C. Cornell, M. Dupuis, C. Eleon, J.L. Flambard, G. Gaubert, N. Lecesne, P. Leherissier, F. Lemagnen, R. Leroy, J.Y. Pacquet, M.G. Saint Laurent, and A. C. C. Villari, *High Energy Physics and Nuclear Physics 31, 206 (2007)*

### **Recherche et développement concernant la production d'ions radioactifs dans le cadre de SPIRAL**

C. Eléon, Ph.D. thesis, Université de Caen Basse-Normandie, GANIL T 07 04, 2007

## 2006

### **Direct 10 GHz HF feed-through plasma device with the NANOGAN III ion source for SPIRAL**

G. Gaubert, C. Barue, C. Canet, M. Dubois, M. Dupuis, C. Eleon, J.L. Flambard, P. Jardin, N. Lecesne, P. Leherissier, F. Lemagnen, R. Leroy, J.Y. Pacquet, M.G. Saint-Laurent and A. C. C. Villari., *Review of Scientific Instruments 77, 03A326 (2006) - Proceedings of the 11<sup>th</sup> International Conference on Ion Sources, Caen, France, 2005*

### **Direct $1^+$ to $n^+$ method for production of radioactive alkaline ions.**

C. Eleon, O. Tuske, G. Gaubert, J.Y. Pacquet, M. Dubois, M.G. Saint Laurent, P. Jardin, J. Cornell and R. Leroy, *Review of Scientific Instruments 77, 03A704 (2006) - Proceedings of the 11<sup>th</sup> International Conference on Ion Sources, Caen, France, 2005*

### **Total efficiency of an ISOL production system based on an ECRIS associated with a carbon target: The case of SPIRAL I**

P. Jardin, W. Farabolini, C. Eleon, M. Dubois, G. Gaubert, J.C. Cornell, N. Lecesne, R. Leroy, J.Y. Pacquet and M.G. Saint Laurent, *Review of Scientific Instruments 77, 03A707 (2006) - Proceedings of the 11<sup>th</sup> International Conference on Ion Sources, Caen, France, 2005*

### **Purification of radioactive neutron-rich argon beams using an ion source in charge breeding mode**

T. Fritioff, J. Cederkäll, L. Weissman, C. J. Barton, K. A. Connell, D. Duniec, O. Kester, T. Lamy, T. Nilsson, P. Jardin, P. Sortais, G. Tranströmer and ISOLDE Collaboration and IS397 Collaboration, *Nuclear Instruments and Methods in Physics Research Section A 556, 31 (2006)*

## 2005

### **MONOBOB: A radiation-hard and efficient 2.45-GHz ECRIS dedicated to radioactive ion production**

C. Huet-Equilbec, P. Jardin, P. Gorel, J.-Y. Pacquet, G. Gaubert, J. Cornell, M. Dubois, N. Lecesne and R. Leroy, *Nuclear Instruments and Methods in Physics Research Section B 240, 752 (2005)*

### **ISOL beams of neutron-rich oxygen isotopes**

U. Köster, O. Arndt, U. C. Bergmann, R. Catherall, J. Cederkäll, I. Dillmann, M. Dubois, F. Durantel, L. Fraile, S. Franchoo, G. Gaubert, L. Gaudefroy, O. Hallmann, C. Huet-Equilbec, B.

Jacquot, P. Jardin, K. L. Kratz, N. Lecesne, R. Leroy, A. Lopez, L. Maunoury, J. Y. Pacquet, B. Pfeiffer, M. G. Saint-Laurent, C. Stodel, A. C. C. Villari and L. Weissman, *European Physical Journal A* 25, 729 (2005)

## 2004

### **Atom-to-ion transformation time in singly charged ECRISs**

P. Jardin, W. Farabolini, G. Gaubert, J. Y. Pacquet, J. Cornell, F. Durantel, C. Huet-Equibec, N. Lecesne, R. Leroy, M. G. Saint Laurent, C. Barué, C. Canet, M. Dubois, M. Dupuis, J. -L. Flambard, P. Leherissier, F. Lemagnen, O. Tuske and A. C. C. Villari, *Nuclear Instruments and Methods in Physics Research B* 225, 374 (2004)

### **Visible light spectrometry measurements for studying an ECRIS plasma and especially applied to the MONO1001 ion source**

O. Tuske, L. Maunoury, J.-Y. Pacquet, C. Barué, M. Dubois, G. Gaubert, P. Jardin, N. Lecesne, P. Leherissier, F. Lemagnen, R. Leroy, M.-G. Saint-Laurent, and A. C. C. Villari, *Review of Scientific Instruments* 75, 1529 (2004) - *Proceedings of the 10<sup>th</sup> International Conference on Ion Sources, JINR, Dubna, Russia, 2003*

### **Radioactive ion beam production at GANIL: Status and perspectives**

R. Leroy, *Review of Scientific Instruments* 75, 1601 (2004) - *Proceedings of the 10<sup>th</sup> International Conference on Ion Sources, JINR, Dubna, Russia, 2003*

### **Latest Results Obtained At Ganil With New Target-Source Systems Dedicated To Radioactive Ion Production**

P. Jardin, M.G. Saint-Laurent, W. Farabolini, G. Gaubert, J.C. Angélique, J.C. Cornell, M. Dubois, S. Gibouin, N. Lecesne, R. Leroy, L. Maunoury, J.Y. Pacquet, F. Pellemoine, C. Stodel, O. Tuske, D. Verney, A. C. C. Villari, C. Barue, C. Canet, M. Dupuis and F. Durantel, *Review of Scientific Instruments* 75, 1617 (2004) - *Proceedings of the 10<sup>th</sup> International Conference on Ion Sources, JINR, Dubna, Russia, 2003*

## 2003

### **MINIMONO: An ultra compact permanent magnet ion source for singly charged ions**

G. Gaubert, C. Barué, C. Canet, J. Cornell, M. Dupuis, W. Farabolini, J.-L. Flambard, P. Gorel, P. Jardin, N. Lecesne, P. Leherissier, F. Lemagnen, R. Leroy, J.-Y. Pacquet, M.G. Saint Laurent and A. C. C. Villari, *Review of Scientific Instruments* 74, 956 (2003)

### **Efficiency and production yield measurements of radioactive O, N and F for the spiral facility**

S. Gibouin, A. C. C. Villari, J. C. Angélique, O. Bajeat, F. Bocage, J. M. Casandjian, S. Essabaa, G. Gaubert, Y. Huguet, A. Joinet, P. Jardin, S. Kandri, A. Khouaja, F. Landre-Pellemoine, C. Lau, N. Lecesne, H. Lefort, R. Leroy, C. Marry, L. Maunoury, D. Nayak, J. Y. Pacquet, M. G. Saint-Laurent and C. Stodel, *Nuclear Instruments and Methods in Physics Research Section B* 204, 240 (2003) – *Proceedings of the 14<sup>th</sup> International Conference on Electromagnetic Isotope Separators and Techniques Related to their Applications, Victoria, B.C. Canada, 2002*

### **Optimization of ECR singly-charged ion sources for the radioactive ion beam production**

P. Jardin, W. Farabolini, G. Gaubert, J.Y. Pacquet, T. Drobert, J. Cornell, C. Barue, C. Canet, M. Dupuis, J.-L. Flambard, N. Lecesne, P. Leherissier, F. Lemagnen and R. Leroy, *Nuclear Instruments and Methods in Physics Research B* 204, 377 (2003) – *Proceedings of the 14<sup>th</sup>*

*International Conference on Electromagnetic Isotope Separators and Techniques Related to their Applications, Victoria, B.C. Canada, 2002*

**Contributions à l'étude de la production de faisceaux radioactifs par la méthode ISOL**

S. Gibouin, Ph.D. thesis, Université de Caen Basse-Normandie, GANIL T 03 02, 2003

## 2002

**Ion source developments for RNB production at SPIRAL/GANIL**

A. C. C. Villari, C. Barué, G. Gaubert, S. Gibouin, Y. Huguet, P. Jardin, S. Kandri-Rody, F. Landré-Pellemoine, N. Lecesne, R. Leroy, M. Lewitowicz, C. Marry, L. Maunoury, J. Y. Pacquet, J. P. Rataud, M. G. Saint-Laurent, C. Stodel, J. C. Angélique, N. A. Orr and R. Lichtenthäler, *Nuclear Physics A 701, 476c (2002)*

**Recent results at the SIRa test bench: Diffusion properties of carbon graphite and B4C targets**

F. Landré-Pellemoine, J. C. Angélique, O. Bajeat, C. Barué, R. Bennett, F. Clapier, M. Ducourtieux, G. Gaubert, S. Gibouin, Y. Huguet, P. Jardin, S. Kandri-Rody, C. Lau, N. Lecesne, R. Leroy, M. Lewitowicz, R. Lichtenthäler, C. Marry, L. Maunoury, J. Obert, N. A. Orr, J. Y. Pacquet, M. G. Saint-Laurent, C. Stodel, J. P. Rataud and A. C. C. Villari, *Nuclear Physics A 701, 491c (2002)*

**MONO1000: A simple and efficient 2.45GHz ECRIS using a new magnetic structure concept**

P. Jardin, C. Barué, C. Canet, M. Dupuis, J.L. Flambard, G. Gaubert, N. Lecesne, P. Lehérisier, F. Lemagnen, R. Leroy, J.-Y. Pacquet, F. Pellemoine, J.-P. Rataud, M.G. Saint-Laurent and A. C. C. Villari, *Review of Scientific Instruments 73, 789 (2002)*

**Ion source development at GANIL for radioactive beams and high charge state ions**

R. Leroy, C. Barué, C. Canet, M. Dupuis, J-L. Flambard, G. Gaubert, S. Gibouin, Y. Huguet, P. Jardin, N. Lecesne, P. Lehérisier, F. Lemagnen, L. Maunoury, J.-Y. Pacquet, F. Pellemoine-Landré, J-P. Rataud, M. G. Saint-Laurent, and A. C. C. Villari, *Review of Scientific Instruments 73, 711 (2002)*

## 2001

**RNB production at SPIRAL/GANIL**

A. C. C. Villari, F. Pellemoine-, C. Barué, G. Gaubert, S. Gibouin, Y. Huguet, P. Jardin, S. Kandri Rody, N. Lecesne, R. Leroy, M. Lewitowicz, C. Marry, L. Maunoury, J.-Y. Pacquet, J.-P. Rataud, M.-G. Saint-Laurent, C. Stodel, O. Bajeat, J.-C. Angélique and N.A. Orr, *AIP-Conference-Proceedings no.576, 254 (2001)*

**The accelerated ISOL technique and the SPIRAL project**

A. C. C. Villari and the SPIRAL group, *Nuclear Physics A 693, 465 (2001)*

**Temperature simulations of high power graphite targets for heavy ions**

L. Maunoury, O. Bajeat, F. Landre-Pellemoine, R. Lichtenthäler and A. C. C. Villari, *Nuclear Instruments and Methods in Physics Research B 184, 441 (2001)*

**Production de faisceaux d'ions radioactifs par la méthode ISOL pour SPIRAL**

F. Landré-Pellemoine, Ph.D. thesis, Université de Caen Basse-Normandie, GANIL T 01 03, 2001

## 2000

### **RNB production at SPIRAL/GANIL**

A. C. C. Villari, F. Pellemoine-, C. Barué, G. Gaubert, S. Gibouin, Y. Huguet, P. Jardin, S. Kandri Rody, N. Lecesne, R. Leroy, M. Lewitowicz, C. Marry, L. Maunoury, J.-Y. Pacquet, J.-P. Rataud, M.-G. Saint-Laurent, C. Stodel, O. Bajeat, J.-C. Angelique and N.A. Orr, *Proceedings of CAARI 2000, Denton, Texas, USA (2000)*

### **Développement d'un système d'identification pour SPIRAL et test d'une cible d'uranium liquide dans le cadre du projet PARRNe**

S. Kandri Rody, Thèse de la Faculté des sciences de El Jadida, GANIL T 00 04, 2000

## 1999

### **Ion source developments for stable and radioactive ion beams at GANIL**

R. Leroy, C. Barué, N. Lecesne, G. Gaubert, Y. Huguet, P. Jardin, J.Y. Pacquet, A. C. C. Villari, D. Lecler and T. Been, *Proceedings of the 14th Int. Workshop on ECR Sources, CERN, Geneva, Switzerland, 3-6 May 1999*

### **The first target ion source system for the SPIRAL project: results of the on line tests**

R. Leroy, J.-C. Angelique, O. Bajeat, P. Bertrand, B. Blank, M. Ducourtieux, P. Foury, G. Gaubert, Y. Huguet, S. Kandri Rody, P. Jardin, N. Lecesne, A. Lepine, M. Lewitowicz, C. Marry, L. Maunoury, J. Obert, N.A. Orr, J.-Y. Pacquet, J. Proust, J.-C. Putaux, M.-G. Saint-Laurent-, P. Sortais and A. C. C. Villari, *Proceedings of the Fifteenth International Conference on Cyclotrons and their Applications. IOP Publishing, Bristol, UK, 366 (1999)*

### **SHyPIE: a new source for on line production of multicharged radioactive condensable ion beams**

N. Lecesne, J.-C. Angélique, B. Blank, F. Clapier, M. Ducourtieux, P. Foury, G. Gaubert, Y. Huguet, S. Kandri Rody, P. Jardin, A. Lepine, R. Leroy, M. Lewitowicz, C. Marry, L. Maunoury, J. Obert, N.A. Orr, J.-Y. Pacquet, N. Pauwels, J. Proust, J.-C. Putaux, E. Robert, M.G. Saint-Laurent, D. Seron, P. Sortais and A. C. C. Villari, *Proceedings of the Fifteenth International Conference on Cyclotrons and their Applications. IOP Publishing, Bristol, UK, 362 (1999)*

### **The linear buncher of SPIRAL Beam test of a prototype**

A. Chabert, Ch. Ricaud, L. Boy, B. Monsanglant and W. Le Coz, *Nuclear Instruments and Methods in Physics Research Section A 423, 7 (1999)*

## 1998

### **A simulation of the temperature distribution in the SPIRAL target**

R. Lichtenthäler, P. Foury, J. C. Angelique, P. Bertrand, B. Blank, O. Bajeat, L. Boy, M. Ducourtieux, P. Jardin, N. Lecesne, A. Lépine-Szily, M. Lewitowicz, C. F. Liang, M. Loiselet, H. Lefort, R. Leroy, J. Mandin, C. Marry, L. Maunoury, J. Obert, N. Orr, J. Y. Pacquet, J. C. Putaux, G. Ryckewaert, E. Robert, M. G. Saint-Laurent, P. Sortais, M. Toulemonde, I. Tirrel and A. C. C. Villari, *Nuclear Instruments and Methods in Physics Research B 140, 415 (1998)*

### **The spiral project at GANIL and future opportunities**

W. Mittig, *Journal of Physics G 24, 1131 (1998)*

### **Constraints due to the production of radioactive ion beams in the SPIRAL project**

R. Leroy, Y. Huguet, P. Jardin, C. Marry, J.-Y. Pacquet and A. C. C. Villari, *Review of Scientific Instruments* **69**, 758 (1998)

### **Production de faisceaux d'ions radioactifs multichargés pour SPIRAL : études et réalisation du premier ensemble cible-source**

L. Maunoury, Ph.D. thesis, Université de Caen Basse-Normandie, GANIL T 98 01, 1998

## **1997**

### **ECR development for accelerated radioactive ion beams**

A. C. C. Villari, *Nuclear Instruments and Methods in Physics Research B* **126**, 35 (1997)

### **Graphite target for the SPIRAL project**

J.C. Putaux, P. Bertrand, M. Ducourtieux, A. Ferro, P. Foury, O. Kaitasov, L. Kotfila, N. Lecesne, R. Leroy, C.F. Liang, M. Loiselet, J. Mandin, L. Maunoury, A.C. Mueller, J. Obert, J.Y. Pacquet, N. Pauwels, J.C. Potier, J. Proust, E. Robert, J.Y. Pacquet, N. Pauwelsa, J.C. Potiera, J. Prousta, E. Robertc, M.O. Ruaultb, G. Ryckewaertd, P. Sortaisc, M. Toulemondec and A. C. C. Villari, *Nuclear Instruments and Methods in Physics Research Section B* **126**, 113 (1997)

### **A new method for measuring the absolute efficiency of isotope separation on-line systems**

N. Lecesne, A. C. C. Villari, J.C. Angélique, P. Bertrand, B. Blank, F. Clapier, F. De Las Heras, M. Ducourtieux, P. Foury, P. Jardin, A. Joubert, A. Lépine-Szily, R. Leroy, M. Lewitowicz, C.F. Liang, J. Mandin, C. Marry, L. Maunoury, J. Obert, N.A. Orr, J.Y. Pacquet, P. Paris, J.C. Potier, J. Proust, J.C. Putaux, E. Robert, M.G. Saint-Laurent and P. Sortais, *Nuclear Instruments and Methods in Physics Research Section B* **126**, 141 (1997)

### **Tuning methods for the SPIRAL facility**

L. Boy, A. Chabert, Ch. Ricaud and B. Launé, *Nuclear Instruments and Methods in Physics Research Section A* **400**, 1 (1997)

### **Nanogan II 14.5 GHz: a compact ECRIS for on line production of multi-charged radioactive ion beams for SPIRAL**

L. Maunoury, A. C. C. Villari, J.C. Angélique, F. Clapier, G. Dhilly, G. di Bartolo, M. Ducourtieux, T. Ethvignot, P. Jardin, N. Lecesne, R. Leroy, M. Lewitowicz, C.F. Liang, R. Lichtenthäler, C. Marry, J. Obert, N.A. Orr, J.Y. Pacquet, N. Pauwels, J.C. Putaux, E. Robert, M.G. Saint Laurent, P. Sortais and O. Tengblad, *Proceedings of the 18<sup>th</sup> Int. Workshop on ECR Ion Sources, February 26-28, College Station, Texas USA* (1997)

### **Etude de la production d'ions radioactifs multichargés en ligne**

N. Lecesne, Ph.D. thesis, Université de Caen Basse-Normandie, GANIL T 97 08, 1997

### **Problèmes posés par l'accélération d'ions radioactifs dans le projet SPIRAL. Réglage et stabilisation de l'accélérateur**

L. Boy, Ph.D. thesis, Université Pierre et Marie Curie - Paris VI, GANIL T 97 04, 1997

## **1996**

### **Radioactive Ion Beam Production Tests for SPIRAL**

N. Lecesne, J.C. Angélique, B. Blank, F. Clapier, M. Ducourtieux, P. Foury, Y. Huguet, P. Jardin, A. Lépine, R. Leroy, M. Lewitowicz, C.F. Liang, J. Mandin, C. Marry, L. Maunoury, J. Obert, N.A.

Orr, J.Y. Pacquet, P. Paris, J. Proust, J.C. Putaux, E. Robert, M.G. Saint Laurent, P. Sortais and A. C. C. Villari, *Nuclear Instruments and Methods in Physics Research B* **107**, 41 (1996)

**Extraction studies on ECR Ion Sources**

R. Leroy, J. Mandin, P. Bertrand, N. Lecesne, J. Y. Pacquet, E. Robert, P. Sortais, and A. C. C. Villari, *Review of Scientific Instruments* **67**, 1350 (1996)

## 1995

**Application to the SPIRAL project at GANIL of a new kind of large acceptance mass separator**

B. Bru, A. Chabert and Ch. Ricaud, *Nuclear Instruments and Methods in Physics Research Section A* **363** (1995) 105-113

**Radioactive ion beams at SPIRAL**

A. C. C. Villari, J. C. Angelique, B. Blank, F. Clapier, J. M. Deligne, M. Ducourtieux, P. Foury, A. Joubert, N. Lecesne, A. Lépine, R. Leroy, M. Lewitowicz, C. F. Liang, J. Mandin, C. Marry, L. Maunoury, J. Mercier, J. Obert, N. A. Orr, J. Y. Pacquet, P. Paris, J. C. Potier, J. Proust, J. C. Putaux, E. Robert, M. G. Saint-Laurent, P. Sortais, M. Lieuvin and the SPIRAL group, *Nuclear Physics A* **588**, 267c (1995)

**LIONS: a new set of Fortran90 codes for the SPIRAL project at GANIL**

P. Bertrand, *Nuclear Instruments and Methods in Physics Research Section A* **363**, 211 (1995)

## 1992

**ECRIS development for an on line isotopic separator at GANIL**

P. Bricault, P. Sortais, M. Bisch, P. Leherissier, R. Leroy, J. Y. Pacquet, and J. P. Rataud, *Review of Scientific Instruments* **63**, 2494 (1992)





**Contributors:**

*F. Azaiez, D. Beaumel, B. Blank, W. Catford, F. Chautard, S. Gales, G. Gaubert, A. Görge, S. Fortier, V. Lapoux, R.C. Lemmon, N. Le Neindre, O. Lopez, W. Mittig, P. Mueller, O. Naviliat-Cuncic, A. Navin, P.J. Nolan, A. Obertelli, F. de Oliveira Santos, P. Roussel-Chomaz, H. Savajols, J.-A. Scarpaci, O. Sorlin, J.-C. Thomas, P.M. Walker, J.-P. Wieleczo and S.J. Williams*